# The role of complement system-related genes in synapse formation and specificity in the olivo-cerebellar network

Keerthana Mahesh Iyer

Université Pierre et Marie Curie

École Doctorale Cerveaux Cognition Comportement

Centre Interdisciplinaire de Recherche en Biologie, Collège de France

# The role of complement system-related genes in synapse formation and specificity in the olivo-cerebellar network

Par Keerthana IYER

Thèse de doctorat de neuroscience

Dirigée par le Dr. Fekrije SELIMI

Présentée et soutenue publiquement le 16 septembre 2015

Devant un jury composé de :

| | |
|---|---|
| Dr. Alain CHÉDOTAL | *Président* |
| Dr. Jean-Louis BESSEREAU | *Rapporteur* |
| Dr. Fabrice ANGO | *Rapporteur* |
| Dr. Ann LOHOF | *Examinateur* |
| Dr. Claudia RACCA | *Examinateur* |
| Dr. Fekrije SELIMI | *Directeur de thèse* |

## ACKNOWLEDGEMENTS

First and foremost I would like to thank my thesis advisor, Dr. Fekrije Selimi for her continuous support, optimism and encouragement. Her tough-as-nails personality and ”out of the box” thinking approach to science made it incredibly inspiring to have her as my mentor. It would not have been possible to complete this project without her enthusiasm and unique insights into my data. Her advice on all things scientific and otherwise will go a long way with me.

I would like to thank Dr. Alain Chédotal, Dr. Jean-Louis Bessereau, Dr. Fabrice Ango, Dr. Ann Lohof and Dr. Claudia Racca, for agreeing to be a part of my thesis committee and, for some of them, traveling to Paris for my defense.

Many thanks to all the current and former members of the Selimi lab – Alessia, Séverine, Inès, Mélanie, Maëva and Vanessa – for your precious help with experiments, discussions, thesis proofreading, and of course, your friendship, daily laughs, and for making my PhD experience so memorable and rewarding.

Thanks to the ENP International PhD program for giving me the opportunity to gain a strong foothold in the Paris neuroscience fraternity, and to interact with and learn from several eminent researchers in the field. Conducting my research in the heart of Paris with monthly ENP social events made it easier to deal with the stresses and frustrations that come with a PhD.

A big thank you to all the collaborators – Dr. Marion Wassef for effortlessly teaching me the very challenging inferior olive injection in neonatal mice, Dr. Philippe Isope for help with the electrophysiology experiments, and Dr. Andrea Dumoulin for her tireless collaboration in maintaining and providing the Susd4 KO mice. Thank you to all the imaging, administrative and animal facility staff at the CIRB and also the animal facilities at INCI, Strasbourg and ENS, Paris. Their efforts were invaluable and crucial to our research especially in crunch situations during paper publishing.

Special mention to all the members of the Fleischmann lab and Verlhac lab, it has been a pleasure sharing workspace (and many apéros) with such fun, quirky and dynamic colleagues. Thanks to my fellow ENPers and Parisian friends for the great conversations, friendship and good times. Lastly, I want to thank my family and friends overseas for helping me keep it real. A very special thanks to my mum and dad who have been my most enthusiastic and encouraging supporters from the beginning. And finally, thank you Peter for your love, support and for keeping me grounded.

*"Unfortunately, nature seems unaware of our intellectual need for convenience and unity, and very often takes delight in complication and diversity." Santiago Ramón y Cajal, 1906*

# TABLE OF CONTENTS

## LIST OF FIGURES AND TABLES

## Introduction

## Results

**- 1 -**



**- 3 -**

# LIST OF ABBREVIATIONS

**ABP :** Androgen-binding protein
**AChR :** Acetylcholine receptor
**ADAM :** A Disintegrin And Metalloproteinase
**AIS :** Axon Initial Segment
**AMOP :** Adhesion-associated domain in MUC4 and Other Proteins
**AMPA :** Alpha-amino-3-hydroxy-5-methyl-4-isoxazolepropionic acid
**AP :** Alkaline phosphatase
**APC :** Antigen presenting cell
**ATP :** Adenosine triphosphate
**AZ :** Active zone
**B2M :** Beta-2-microglobulin
**BacTRAP :** Bacterial artificial chromosome Translating Ribosome Affinity Purification
**BAI :** Brain angiogenesis inhibitor
**BBB :** Blood-brain barrier
**BC :** Basket cell
**BCIP :** 5-bromo-4-chloro-3-indolyl-phosphate
**BCR :** B-cell receptor
**BDNF :** Brain derived neurotrophic factor
**BG :** Bergmann glia
**C1QL :** C1Q-like
**CaBP :** Calbindin
**CAM :** Cell adhesion molecule
**CAMK :** $Ca^{2+}$/calmodulin-dependent protein kinase
**CBLN :** Cerebellin
**CCL :** Chemokine (C-C motif) ligand
**CCP :** Complement control protein
**CF :** Climbing fiber
**CHL1 :** Close Homolog of L1
**CNS :** Central nervous system
**CR :** Complement receptor
**CREB :** Cyclic AMP response element-binding protein
**CRF :** Corticotrophin Releasing Factor
**CRP :** C-reactive protein
**CSMD :** CUB and sushi multiple domains protein
**CSPG :** Chondroitin sulphate proteoglycans
**CTSB :** Cysteine protease cathepsin B
**CUB :** Complement C1r/C1s, Uegf, Bmp1
**DAF :** Decay accelerating factor
**DAO :** Dorsal accessory olive
**DAPI** : 4',6-diamidino-2-phenylindole
**DCN :** Deep cerebellar nuclei
**DCV :** Dense-core vesicle
**DG :** Dentate gyrus
**DIV :** Days in vitro
**DNA :** Deoxyribonucleic acid
**ECD :** Extracellular domain
**ECN :** External cuneate nucleus
**EGF :** Epidermal growth factor-like domain
**EGL :** External granular layer
**ELK :** ETS domain-containing protein
**ELMO :** Engulfment and cell motility 1
**EPH :** Ephrin
**EPSC :** Excitatory postsynaptic currents

**FGF :** Fibroblast growth factor
**GABA :** Gamma-aminobutyric acid
**GAPDH :** GlycerAldehyde 3-Phosphate DeHydrogenase
**GC :** Granule cell
**GCP :** Granule cell precursors
**GFP :** Green fluorescent protein
**GluR :** Glutamate receptor
**GluRδ2 :** Glutamate receptor delta 2
**GO :** Gene Ontology
**GPCR :** G-protein coupled receptors
**GPS :** GPCR-Proteolysis Site
**GRIP :** Glutamate receptor-interacting protein
**GuK :** Guanylate kinase domain
**HA :** HemAgglutinin
**HEK :** Human Embryonic Kidney cell line
**IFN :** Interferon
**IGL :** Internal granular layer
**IgSF :** Immunoglobulin superfamily
**IL :** Interleukin
**IL-1RAP :** Interleukin-1 receptor accessory protein
**ION :** Inferior Olivary Neuron
**IP :** Immunoprecipitate
**IPL :** Inner plexiform layer
**IPSC :** Inhibitory postsynaptic current
**IZ :** Intermediate zone
**KEGG :** Kyoto Encyclopedia of Genes and Genomes
**KIF :** Kinesin superfamily
**KO :** Knockout
**L1CAM :** L1 family of cell adhesion molecules
**LGN :** Lateral geniculate nucleus
**LNS :** Laminin, NRXN, sex-hormone-binding globulin domains
**LRRTM :** Leucine rich repeat transmembrane protein
**LTD :** Long term depression
**LTP :** Long term potentiation
**MAGUK :** Membrane-associated guanylate kinases
**MAO :** Medial accessory olive
**MAPK :** Mitogen activated protein kinase
**MASP :** Mannose-binding lectin (MBL)-associated serine protease
**MBL :** Mannose-binding lectin
**MF :** Mossy fiber
**mGluR:** Metabotropic Glutamate Receptor
**MHC :** Major histocompatibility complex
**MSB :** Multisynaptic boutons
**NARP :** Neuronal activity related pentraxin
**NBT :** Nitro blue tetrazolium
**NCAM :** Neural cell adhesion molecule
**NECL :** Nectin-like
**Nfasc :** Neurofascin
**NK :** Natural killer
**NKCC :** Na-K-Cl cotransporter
**NLGN :** Neuroligin
**NMDA :** N-Methyl-D-aspartic acid
**NMJ :** NeuroMuscular Junction
**NPTX :** Neuronal pentraxin
**NRXN :** Neurexin

**NSB :** Nonsynaptic boutons
**NT :** Neurotrophin
**NTD :** N-terminal domain
**OD :** Ocular dominance
**PAJ :** Puncta adherentia junctions
**PAMPs :** Pathogen-associated molecular patterns
**PBS :** Phosphate buffer saline
**PC :** Purkinje cell
**PDGF :** Platelet-derived growth factor
**PDZ :** Post synaptic density protein (PSD95), Drosophila disc large tumor suppressor (Dlg1), and zonula occludens-1 protein (zo-1)
**PF :** Parallel fiber
**PFA :** Paraformaldehyde
**PICK :** Protein kinase C, alpha (PRKCA)-binding protein
**Pir :** Paired immunoglobulin-like
**PN :** Pontine nuclei
**PO :** Principal olive
**PPD :** Paired pulse depression
**PPF :** Paired pulse facilitation
**PRR :** Pattern-recognition receptors
**PSA :** Polysialic acid
**PSD :** Postsynaptic density
**PTP :** Protein-tyrosine phosphatase
**PTV :** Piccolo transport vesicles
**PTZ :** Pentylentetrazole
**Pv :** Parvalbumin
**Rac1 :** Ras-related C3 botulinum toxin substrate 1
**RCA :** Regulators of Complement Activation
**RGC :** Retinal ganglion cells
**RL :** Rhombic lip
**RNA :** Ribonucleic acid
**RTqPCR :** Real-Time Quantitative Reverse Transcription PCR
**SAM :** Sterile alpha motifs
**SAP :** Serum amyloid P component
**SB :** Somatomedin-B
**SC :** Stellate cell
**SEMA :** Semaphorin
**SER :** Smooth endoplasmic reticulum
**SEZ :** Seizure-related protein
**SH3 :** Src homology 3 domain
**SJ :** Synaptic junction
**SL :** Stratum lucidum
**SLM :** Stratum lacunosum-moleculare
**SLY :** Lymphocyte signaling adaptor protein domain
**SNAP :** Soluble NSF-attachment proteins / Synaptosomal-associated protein
**SNARE :** SNAP (Soluble NSF Attachment Protein) Receptor
**SO :** Stratum oriens
**Sp5 :** Spinal trigeminal nuclei
**SP :** Signal peptide
**SR :** Stratum radiatum
**SRPX2 :** X-linked sushi repeat containing protein
**S-SCAM :** Synaptic scaffolding molecule
**SSB :** Single synaptic boutons
**STV :** Synaptic vesicle protein transport vesicles
**SUSD :** Sushi domain containing protein

**SynCAM :** Synaptic cell adhesion molecule
**TAP :** Transporter associated with Antigen Processing
**TARP :** Transmembrane AMPA receptor regulatory proteins
**TCR :** T-cell receptor
**TEM :** Tetraspanin-enriched microdomains
**TGF :** Transforming growth factor
**TH :** Thalamus
**TLRs :** Toll-like receptors
**TM :** Transmembrane
**TNF :** Tumour necrosis factor
**Trk :** Tyrosine kinase
**TSR :** Thrombospondin repeat
**UB :** Unbound
**uPAR :** GPI-anchored plasminogen activator receptor
**VDCC :** Voltage-dependent $Ca^{2+}$ channel
**VGluT1 :** Vesicular glutamate transporter 1
**VGluT2 :** Vesicular glutamate transporter 2
**VIAAT :** Vesicular inhibitory amino acid transporter
**VL :** Ventrolateral thalamic nucleus
**VPM :** Ventroposterior medial nucleus of the thalamus
**VTA :** Ventral tegmental area
**VWD :** Von Willebrand factor type D domain mutant
**VZ :** Ventricular zone
**WT :** Wild type

# ABSTRACT

Multiple mechanisms are used by the nervous system to ensure specific synaptic connectivity between different afferents and a given target neuron. Target recognition by the presynaptic afferent is one such mechanism that has been implicated in the generation of synaptic specificity. Depending on the neuronal population and synapse type, the molecules and signaling pathways involved in this process are likely to vary. Thus, for each synapse type, a specific combination of molecules might exist at the pre- and postsynaptic sites. To test this hypothesis, I used the olivo-cerebellar network as a model system where two excitatory synapses are formed on the same target neuron. Distinct non-overlapping territories on the Purkinje cell are innervated by two excitatory afferents, the Parallel fibers from granule cells and the Climbing fibers from inferior olivary neurons. First, to identify differences at the presynaptic level, in particular specific proteins that might contribute to synapse specificity, I compared the gene expression profiles of the inferior olivary neurons and granule cells. Second, to test if these differences in the input cell populations control the specificity of the two corresponding synapses, I changed the identity of the input cell population either by loss of expression of a specific gene or misexpression in the wrong input. Using gene expression profiling, I found that the inferior olivary neurons express a greater diversity of membrane and secreted proteins belonging to immune system-related pathways. Moreover, a specific combination of complement-related genes are differentially expressed between the inferior olivary neurons and granule cells. Among these, I identified the functional roles of two novel candidate genes specifically expressed by inferior olivary neurons in regulating different aspects of Climbing Fiber/Purkinje cell synaptogenesis. Secreted C1Q-related protein C1QL1 plays an instructive role in specifying Climbing fiber innervation territory on Purkinje cells while membrane-bound complement control-related protein SUSD4 ensures the acquisition of proper functional properties of Climbing fiber synapses and their long-term stability. Thus, different proteins related to the complement system promote different characteristics during synaptogenesis and neural circuit development. Given that C1Q-related CBLN1 promotes Parallel fiber synaptogenesis, these results show that different members of the C1Q family are important determinants of the identity and specific connectivity of each excitatory synapse in the cerebellar cortex. These results provide novel insights into the “chemoaffinity code” that controls subcellular specificity at each synapse type during the formation of neural circuits. Since defects in synapse formation and function are hallmarks of autism and schizophrenia, dissecting the molecular basis of synapse specificity in neural circuits will improve our understanding of the pathophysiology of such neurodevelopmental disorders.

# INTRODUCTION

# 1. Synaptic organization in the brain

The synapse is the fundamental structural and functional unit for the generation of neural circuits in the brain. Synapse formation is a highly precise and tightly regulated process that involves a connection between the pre- and postsynaptic neurons. Neurotransmitters are released by synaptic vesicle exocytosis at the active zone of a presynaptic nerve terminal. This neurotransmitter signal is received by the postsynaptic side of the synapse which translates it into electrical and biochemical changes in the postsynaptic cell. Both the structural and functional development of a synapse is equally important for the proper formation and maintenance of neural circuits. The assembly and maturation of a synapse require the coordination of many cellular and molecular biological events including cytoskeletal rearrangements and recruitment of pre- and postsynaptic proteins. The refinement of the generated circuit is brought about by activity-dependent changes to the strength of synaptic transmission and elimination of inappropriate synaptic connections. Proper synapse formation and elimination are necessary for cognitive function, learning and memory in the mature brain. In this chapter, I will first describe the structural and molecular components of a synapse, followed by the cellular and molecular mechanisms involved in the assembly of a synapse.

## 1.1 Structural and molecular anatomy of a synapse

Since the late 1950s, the ultrastructural features of individual synapses have been studied extensively using snap-shots obtained via electron microscopy (Gray, 1959). As illustrated in Figure 1, two types of synapses exist within the brain based on the ultrastructural characteristics of the presynaptic (vesicle-bearing) and postsynaptic partners (length of apposed membrane, membrane thickenings and synaptic cleft) (Gray, 1959). Type 1 or asymmetric synapses, which are excitatory in function, predominate and account for about 80% of the total population of synapses. Most asymmetric synapses in the central nervous system occur between an axon and a dendritic spine. The axon terminals of asymmetric synapses contain spherical synaptic vesicles. The synaptic junction has a wide cleft and an obvious thickened postsynaptic density. Besides dendritic spines, the postsynaptic elements of such synapses also include dendritic shafts and the cell bodies of inhibitory neurons. In contrast, Type 2 or symmetric synapses, which are inhibitory in function, are less common and occur primarily on neuronal cell bodies, proximal dendritic shafts and axon initial segments (Knott et al., 2002; Wilson et al., 1983). Symmetric synapses involve axons that contain clusters of vesicles that are predominantly

flattened or elongated in their appearance. In addition, the synaptic cleft of symmetric synapses is narrower than at excitatory synapses, and the postsynaptic density is smaller and less prominent.

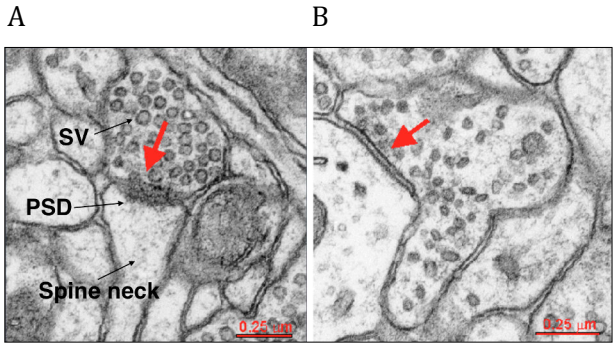


**Figure 1. Ultrastructure of asymmetric and symmetric synapses**

Asymmetric synapse (excitatory) **(A)** and symmetric synapse (inhibitory) **(B)** in mouse hippocampus as viewed by electron microscopy. Arrow points to the synapse from the presynaptic side. SV, synaptic vesicle; PSD, postsynaptic density

### 1.1.1 Presynaptic Components

#### *Axonal Boutons*

Axonal boutons are the axon terminals through which synaptic contacts are made by the axon on another neuron. Typical single synaptic boutons (SSB) have a single postsynaptic partner, while multisynaptic boutons (MSB) have more than one postsynaptic partner, and nonsynaptic boutons (NSB) contain vesicles but have no postsynaptic partners. For example, in the cerebellar cortex, axons form a variety of synapses. Cerebellar granule cells give rise to a single Parallel fiber, which divides and makes axospinous synapses with numerous Purkinje cell dendritic spines. Most of these are SSBs. In contrast, MSBs are formed by a single Climbing fiber originating from the inferior olivary neurons and forming numerous synaptic contacts along the proximal dendritic shaft of a single Purkinje cell (Palay & Chan-Palay, 1974; Xu-Friedman et al., 2001). In addition, specialized contacts on the dendrites of cerebellar granule cells are termed “synaptic glomeruli” where each glomerulus is characterized by an exceptionally large presynaptic bouton synapsing with multiple postsynaptic dendrites. In the hippocampus, mossy fiber axons arising from granule cells of the dentate gyrus terminate on the proximal dendrites of CA3 pyramidal cells as very large presynaptic boutons, each synapsing with multiple dendritic spines.

***The Active Zone***

The active zone (AZ) is a specialized region on the presynaptic plasma membrane where synaptic vesicles are docked and primed for release, and is in alignment with the postsynaptic density (Landis et al., 1988). In electron micrographs, the AZ is recognized by the increased electron density of the presynaptic membrane in this region. Associated with the AZ are cytoplasmic "dense projections", structures organized into presynaptic grids and, at some synapses (for example retinal photoreceptors synapses, cochlear hair cell afferent synapses), they form a specialized synaptic ribbon (Logiudice et al., 2009). The complex network of filaments in the AZ likely changes dimensions during release, enabling its role in vesicle mobilization and release (Fernandez-Busnadiego et al., 2010).

Active zones are composed of an evolutionarily conserved protein complex containing as core constituents RIM, Munc13, RIM-BP, a-liprin, and ELKS proteins (Figure 2). RIM proteins are the central organizers of the AZ that tether $Ca^{2+}$ channels along with RIM-BP to the docked vesicles to allow fast synchronous excitation. Munc13 mediates vesicle priming and docks synaptic vesicles for exocytosis. The RIM/Munc13/RIM-BP core complex recruits vesicles and $Ca^{2+}$ channels to AZ. This complex forms a dense protein network in the presynaptic cytomatrix and positions the active zone exactly opposite to postsynaptic specializations. ELKs modulate the functioning of these $Ca^{2+}$ channels and liprins interact with receptor tyrosine phosphatases called LARs, which are involved in AZ assembly. In addition to these five core active zone proteins, two large homologous proteins, namely piccolo and bassoon, act as a presynaptic skeleton and are associated with vesicle clustering in AZs in vertebrates (Dieck et al., 1998; Fenster et al., 1999; Limbach et al., 2011; Serra-Pages et al., 1998). In invertebrates, proteins related to *C.elegans* SYD-1 are important for the assembly of AZs (Hallam et al., 2002; Owald et al., 2010; Patel et al., 2006). Plasma membrane SNARE proteins syntaxin, SNAP-25 and Munc18 that are core components of the synaptic vesicle fusion machinery for exocytosis (Reviewed in (Südhof & Rothman, 2009)) are not enriched in AZs but distributed all over the plasma membrane. Other membrane proteins localized in the AZ include P/Q- (Cav2.1) and N-type $Ca^{2+}$ channels (Cav2.2), group III metabotropic glutamate receptors and cell adhesion molecules (See section 1.2.2.3). A schematic illustration of the molecular composition of the active zone is provided in Figure 2.

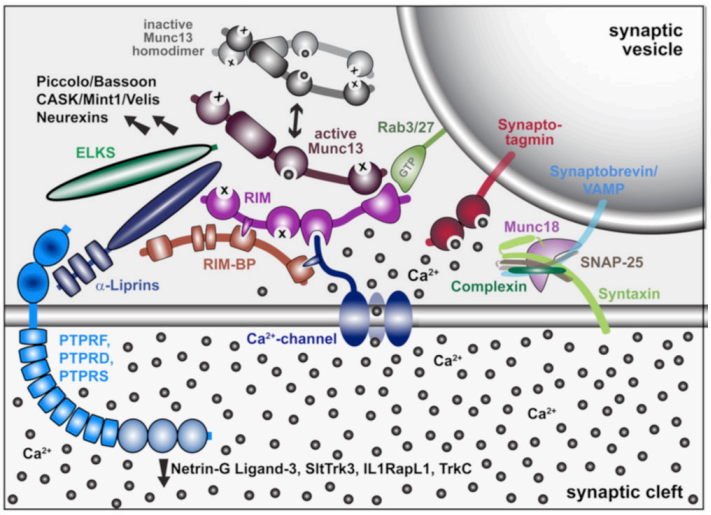


**Figure 2. The presynaptic active zone** *(From Sudhof 2012)*. Details see text.

***Vesicles in Axonal Boutons***

Within presynaptic boutons, the neurotransmitter is located in vesicles, about 35 nm in diameter (Harris & Sultan, 1995). During neurotransmission, the vesicles make contact and dock with the presynaptic membrane at the AZ and release the neurotransmitter into the synaptic cleft. After neurotransmission, the vesicles reduce in size and the vesicular membrane is recycled via clathrin-mediated endocytosis (Clayton & Cousin, 2009). Larger "dense core vesicles" (DCV), greater than 80 nm in diameter, are also present in some presynaptic boutons, and contain neuropeptides and aminergic neurotransmitters that modulate brain development and synaptic transmission (Bauerfeind et al., 1995). DCVs are lost from presynaptic axonal boutons during rapid synaptogenesis in the mature hippocampus, suggesting that DCVs are used to generate the AZ sites during synaptogenesis (Reviewed in (Ahmari & Smith, 2002); (Sorra et al., 2006)). Synaptic vesicle proteins constitute a diverse group of colocalized proteins: monotopic membrane proteins (Eg. Synapsin), proteins inserted into the plasma membrane through post-translational modifications (Eg. Rab and cysteine proteins) and proteins with multiple transmembrane regions (Eg. Synaptophysins, neurotransmitter transporters, components of the proton pump) (Reviewed in (Sudhof, 1995)). The direct regulation of molecular motor protein activity by synaptic vesicle proteins contributes to the trafficking of synaptic cargo. For example, the Rab3 guanine nucleotide exchange factor, DENN/MADD, functions as an adaptor between kinesin-3 and GTP-Rab3–containing synaptic vesicles to promote the trafficking of synaptic vesicles in the axon (Niwa et al., 2008).

### 1.1.2 Postsynaptic Components

The postsynaptic membrane at each synaptic terminal is the first place where information is processed as it converges on the dendrite. The postsynaptic membrane is covered with neurotransmitter receptors, which detect variations in neurotransmitter concentration. Below the postsynaptic membrane, the cytoplasm is occupied by a complex network of proteins, the postsynaptic density, which modulates the strength of synaptic transmission. The postsynaptic side of excitatory synapses differs from inhibitory synapses not only in their content of neurotransmitter receptors but also in their morphology, molecular composition and organization.

#### *1.1.2.1 Excitatory synapses*

**Dendritic spines**

Dendritic spines are tiny specialized actin-rich neuronal protrusions, each of which receives input typically from one excitatory synapse (Fifkova & Delay, 1982; Matus et al., 1982). Dendritic spines vary greatly in their dimensions, not only across brain regions but also along the short segments of a single dendrite. For example, spines along Purkinje cell dendrites, which synapse in the molecular layer with Parallel fibers, all have a similar "lollipop" shape with a bulbous head on a constricted neck. In contrast, dendritic spines in hippocampus are much more variable in shape; even neighboring spines can vary from an immature "filopodia-like" shape to a mature mushroom shape (Reviewed in (Yuste & Bonhoeffer, 2004)). In both regions, the size of the spine head correlates well with the number of presynaptic vesicles.

Particularly common in larger spines is a structure known as the spine apparatus, an organelle characterized by stacks of smooth endoplasmic reticulum (SER) membranes surrounded by densely staining material. The spine apparatus contains synaptopodin, an actin-binding protein, and it has been implicated in local calcium trafficking, and dendritic protein synthesis and post-translational processing (Reviewed in (Jedlicka et al., 2008)). The SER is arranged in laminae and performs a range of functions that promote synaptic transmission in dendrites, such as the regulation of calcium concentration within the dendrites, the trafficking of vesicles, and recycling spine membranes. Vesicles of 'coated' or smooth appearance are sometimes observed in spines and close to the synaptic membrane, consistent with roles in local membrane trafficking processes. Ribosomes are found in a subset of dendritic spines and function in the local translation of proteins in dendrites

((Steward & Schuman, 2003), reviewed in (Bramham & Wells, 2007)). Ribosomes can be bound to endoplasmic reticulum and synthesize local membrane proteins such as receptors, or they can be non-membrane bound and used to synthesize cytoplasmic proteins such as CaMKIIα and PSD-95 (Ostroff et al., 2002; Bourne et al., 2007). In addition, the distribution of ribosomes is variable between dendrites and is non-uniform, suggesting that different degrees of local protein synthesis occur along relatively short dendritic segments, which likely reflect local regions of synaptic growth and plasticity. Other components found in dendritic spines include mitochondria, which are required for generation of ATP, regulation of calcium levels and synaptic plasticity (MacAskill et al., 2010), as well as microtubules, which are crucial for trafficking organelles such as SER and vesicles, as well as for the trafficking of certain proteins and mRNAs. A mushroom-shaped spine containing various organelles is depicted in Figure 3.

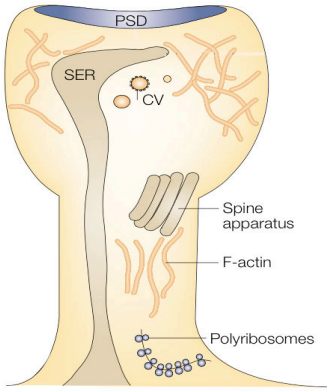


**Figure 3. Structure of the dendritic spine**

PSD, postsynaptic density; SER, smooth endoplasmic reticulum; CV, coated vesicles. *(Adapted from Hering and Sheng, 2001).* Details see text.

### Postsynaptic density

The most prominent postsynaptic component of excitatory synapses is the postsynaptic density (PSD), which appears as a fuzzy electron-dense structure extending about 35–50 nm into the cytoplasm beneath the plasma membrane at asymmetric synapses (Landis & Reese, 1983). The surface area of the PSD correlates with spine head volume and the total number of presynaptic vesicles and vesicles docked at the AZ (Harris & Stevens, 1988). A biochemical analysis of isolated PSD showed that it has a molecular weight of about 1 billion Daltons, and that there are hundreds of different proteins present (Chen et al., 2005; Sheng & Hoogenraad, 2007). Subsequent work has shown the PSD contains a variety of receptors, scaffolding proteins, and signaling complexes involved in synaptic transmission and plasticity (Reviewed in (Sheng & Kim, 2011)). The PSD is

apposed to the postsynaptic membrane, is in tight registry with the presynaptic AZ (Gulley & Reese, 1981; Landis & Reese, 1983), and has a direct role in facilitating trans-synaptic interactions.

Excitatory synapses are characterized by a very prominent PSD in the postsynaptic membrane. The exterior face of the PSD is rich in neurotransmitter receptors and trans-synaptic adhesion molecules inserted within the plasma membrane. Beneath the receptors resides a dense matrix of proteins, including scaffold, cytoskeletal-reorganizing and downstream signaling molecules (Figure 4). Ionotropic glutamate receptors, namely NMDA-, AMPA-, kainate and delta receptors concentrate in the plasma membrane at the PSD (Reviewed in (Ottersen & Landsend, 1997)(Nusser, 2000; Darstein et al., 2003)). AMPA receptors, composed of subunits GluA1-4, are responsible for the bulk of fast excitatory synaptic transmission throughout the Central Nervous System (CNS) and their modulation underlies much of the plasticity of excitatory transmission in the brain. Increasing the postsynaptic response to a stimulus is achieved either through increasing the number of AMPA receptors at the postsynaptic surface or by increasing the single channel conductance of the receptors expressed. This is shown to be the basis of long term potentiation (LTP) mechanisms (Reviewed in (Benke et al., 1998)). The trans-synaptic adhesion molecules inserted in the excitatory postsynaptic membrane are discussed in Section 1.2.2.3. The structural "core" of the PSD is made up of multidomain scaffold proteins (Chen et al., 2008). The most well characterized groups of scaffold proteins are the PSD-95 family of MAGUK proteins, including PSD-95, PSD-93, SAP102, and SAP97, and the Shank family of proteins including Shank1, Shank2 and Shank3 (Reviewed in (Kim & Sheng, 2004; Feng & Zhang, 2009)). MAGUKs contain several PDZ domains, an SH3 domain, and a guanylate kinase domain. Shank proteins contain multiple putative protein interaction domains, including ankyrin repeats, the SH3 domain, the PDZ domain, the proline-rich domain and the SAM domain. The scaffold proteins concentrate in a zone 10–20 nm inside the plasma membrane and are uniformly distributed tangentially along the synaptic membrane, except for SAP97, which concentrates at the edge of the synapse (Sans et al., 2000; Valtschanoff et al., 2000). Other multi-PDZ proteins, GRIP, ABP and TARPs concentrate at the PSD and play a role in AMPAR trafficking (Srivastava et al., 1998; Wyszynski et al., 1999; Chen et al., 2000). Using quantum dots to track the lateral movement of glutamate receptors, it has been shown that AMPA receptors coming into the synapse by lateral diffusion are already tied to stargazin, a TARP family protein, forming nanocomplexes that diffuse together in the neuronal membrane (Bats et al., 2007). Thus

stargazin, through its PDZ-binding domain, and not the GluR2 C-terminal PDZ domain, serves to stabilize AMPA receptors at synapses via an interaction with PSD95. The single PDZ-domain protein PICK1, also implicated in AMPAR trafficking, is located mainly in the cytoplasmic portion of the PSD (Haglerød et al., 2009). The Shank family of scaffold proteins lies on the cytoplasmic side of the PSD and bind to the Homer family (associated with metabotropic glutamate receptors) (Naisbitt et al., 1999; Petralia et al., 2005). The intermediate zone of the PSD contains MAGUK and Shank interacting proteins. Other PSD matrix proteins include those involved in downstream signaling (Reviewed in (Kennedy, 2000)) such as the calcium calmodulin-dependent kinase II (Cam-KII)(Wyszynski et al., 2002), protein phosphatases (Muly et al., 2004; Bordelon, 2005), proteins linked to the actin cytoskeleton (Morales & Fifkova, 1989; Korobova & Svitkina, 2010), and voltage gated potassium channels (Lörincz et al., 2002; Notomi & Shigemoto, 2004; Burkhalter et al., 2006; Kulik, 2006; Puente et al., 2010). A schematic illustration of the molecular composition of the excitatory PSD is provided in Figure 4.

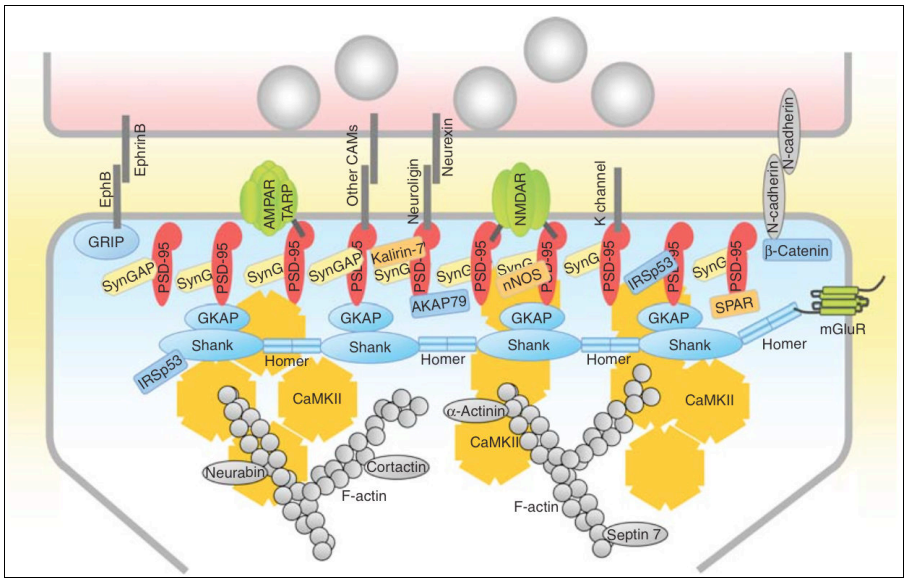


**Figure 4. Molecular organization of the postsynaptic density of an excitatory synapse** *(From Sheng and Kim, 2011).* Details see text.

### *1.1.2.2 Inhibitory synapses*

#### Postsynaptic specialization

There are two main classes of neurotransmitter receptors at central inhibitory synapses $GABA_A$ and glycine receptors. Compared to excitatory synapses, relatively few

intracellular proteins have been linked to inhibitory synapses. The best-known inhibitory postsynaptic protein is gephyrin, which is linked to both GABAergic and glycinergic synapses (Danglot et al., 2003). Gephyrin is critical for glycine receptor clustering, but appears less important for $GABA_A$ receptor clustering (Kneussel et al., 2001). Gephyrin can form multimers resulting in a hexagonal lattice, and thus may function as a postsynaptic scaffold through which $GABA_A$ /glycine receptors functionally interact with gephyrin-associated proteins. Actin-associated proteins Profilin and Mena/VASP link gephyrin to actin filaments (Neuhoff et al., 2005). Gephyrin-associated dynein light chains have been implicated in motor-dependent transport of the gephyrin-receptor complex along microtubules/actin filaments. The trans-synaptic adhesion molecules inserted in the inhibitory postsynaptic membrane are discussed in Section 1.2.2.3. A schematic illustration of the molecular composition of the inhibitory PSD is provided in Figure 5.

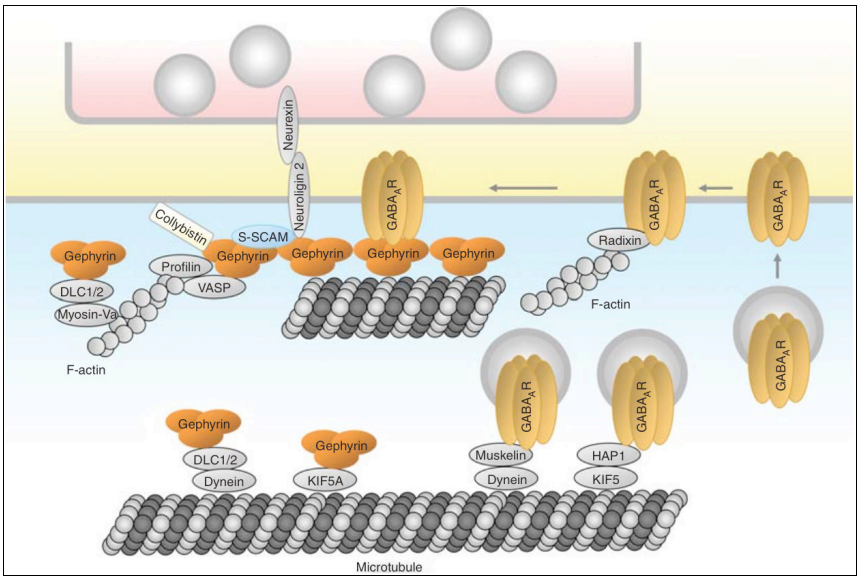


**Figure 5. Molecular organization of the postsynaptic specialization of an inhibitory synapse** *(From Sheng and Kim, 2011).* Details see text.

### 1.1.3 The Synaptic Cleft

The synaptic cleft is a widening of about 20 nm in the apposition between the presynaptic axon and its postsynaptic partner. Ultrastructural work on quick-frozen hydrated material shows that this widening is not really a space, but is instead packed with electron-dense material (Lučić et al., 2005; Zuber et al., 2005). The synaptic cleft contains extracellular matrix proteins and carbohydrate-containing material such as reelin,

chondroitin sulphate proteoglycans (CSPGs) and laminins (Reviewed in (Dityatev et al., 2010)). Some of the protein material found in the synaptic cleft also represents the extracellular domains of synaptic receptor-ligand protein complexes that directly link presynaptic active zones and postsynaptic densities. These receptor-ligand protein complexes engage in bidirectional signaling at the synaptic cleft to coordinate the differentiation of pre- and postsynaptic membrane specializations (See section 1.2.2.3).

## 1.2 Stages of synapse formation

CNS synaptogenesis occurs in a series of steps beginning with the stabilization of initial axo-dendritic contacts, followed by the recruitment of pre- and postsynaptic protein precursors, and finally the maturation of the synapse and the activity-dependent regulation of its molecular composition and function. The process of synapse formation explained in this section has been described previously in reviews by (Scheiffele, 2003; Waites et al., 2005; Fox & Umemori, 2006; McAllister, 2007).

### 1.2.1 Axon target recognition

At the beginning of synapse specification, a guidance mechanism is required to ensure that the correct target is recognized and to allow multiple axons from different brain regions to grow into their respective target fields and synapse with the correct cell type. This mechanism is mediated primarily by a prominent group of target-derived molecules known to guide axonal growth cones into their target brain regions. These include classic guidance molecule families such as netrins, semaphorins, and ephrinA (Tessier-Lavigne, 1995; Pascual et al., 2004). A second group of target-derived axon-priming molecules include members of the Wnt and FGF families. These molecules promote the maturation of both target neurons and incoming axons in preparation for synaptogenesis. They induce regional axon arborization and/or accumulation of recycling synaptic vesicles in innervating axons (Reviewed in (Scheiffele, 2003)).

Additional recognition between incoming axons and their target region is promoted by several classes of cell adhesion molecules (CAMs), of which prominent candidates include members of the cadherin and protocadherin families of calcium-dependent CAMs (Reviewed in (Shapiro & Colman, 1999)(Takai et al., 2003)). Cadherins are localized at pre- and postsynaptic plasma membranes in a variety of synaptic types, and have been observed in distinct and complementary expression patterns with respect to subgroups of neurons and their targets, a feature typically found in axon guidance molecules. For

example, barrel field pyramidal cells and septal granule cells in the somatosensory cortex, together with their corresponding thalamic inputs, express N-cadherin and cadherin-8, respectively (Gil et al., 2002). Similarly, genetic studies in the *Drosophila* visual system indicate that protocadherins are involved in axon target recognition between photoreceptor growth cones and the lamina (Lee et al., 2003).

### 1.2.2 Synapse formation

#### *1.2.2.1 Membrane trafficking in presynaptic assembly*

Once the axons and dendrites have been specified, the neurons continue to differentiate by entering the phase of synapse formation. Most synaptic material required for this process is synthesized in the cell body of neurons and transported to synapses by microtubule-based molecular motors before and during synaptogenesis (Bresler et al., 2004) (Figure 6). One important group of structures that requires microtubule transport to the synaptic membrane are the synaptic vesicle precursors, which eventually give rise to mature synaptic vesicles. In young neurons, two types of presynaptic precursors are present - piccolo transport vesicles (PTVs) and synaptic vesicle protein transport vesicles (STVs) (Zhai et al., 2001; Sabo et al., 2006). PTVs carry the AZ proteins Piccolo and Bassoon as well as other proteins that mediate synaptic vesicle exocytosis, including Munc13, Munc18, syntaxin, and snap25 (Zhai et al., 2001). These precursors are assembled in the trans-Golgi network and are transported via Golgi-derived vesicles (Shapira et al., 2003). In contrast, synaptic vesicle proteins like VAMP2/synaptobrevin II, synapsin, synaptotagmin are transported in heterogeneous STVs (Zhai et al., 2001). Once the PTVs or STVs arrive at the appropriate destination, they are unloaded in a regulated fashion and distributed throughout the synaptic boutons. A schematic illustration of this process is provided in Figures 6 and 7. Although microtubule-mediated transport is critical for long-range trafficking, actin-based mechanisms are required to organize local protein complexes in subcellular domains. F-actin is one prominent component that helps to initiate the presynaptic assembly process. F-actin levels are up-regulated in newly forming synapses compared with mature synapses (Zhang & Benson, 2002), and it has been observed that depolymerization of F-actin in young hippocampal neuronal cultures results in a reduction in the size and number of synapses (Zhang & Benson, 2001). F-actin has also been implicated in many steps of synapse assembly and function of which one proposed role is that it acts as a scaffold for other presynaptic proteins (Sankaranarayanan et al., 2003).

Overall, these studies show that long-range axonal transport of synaptic components is a necessary step for presynaptic formation and maintenance. F-actin, on the other hand, is important in initiating and stabilizing the site of presynaptic assembly and for recruiting other presynaptic proteins.

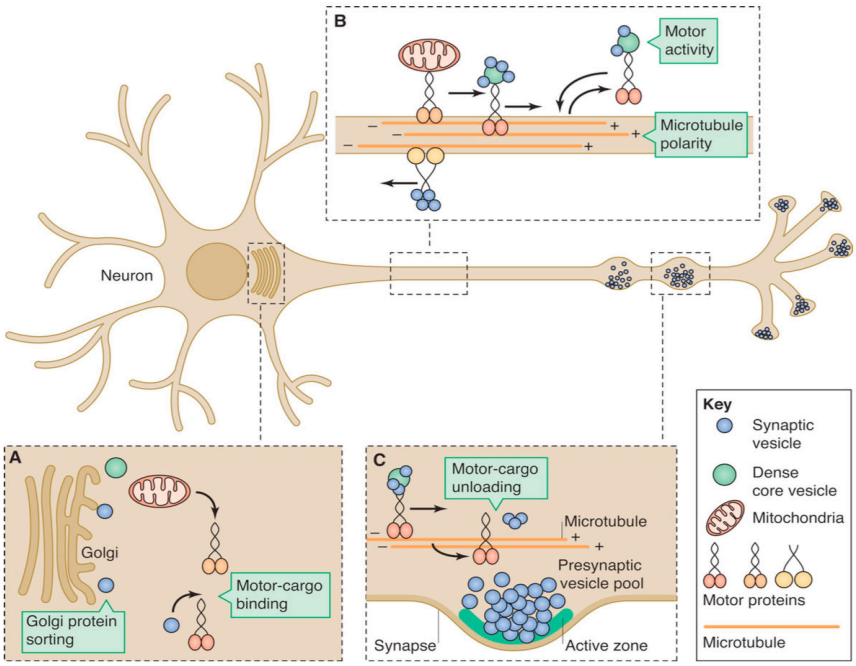


**Figure 6. Transport of presynaptic components** *(From Chia et al., 2013).* Details see text.

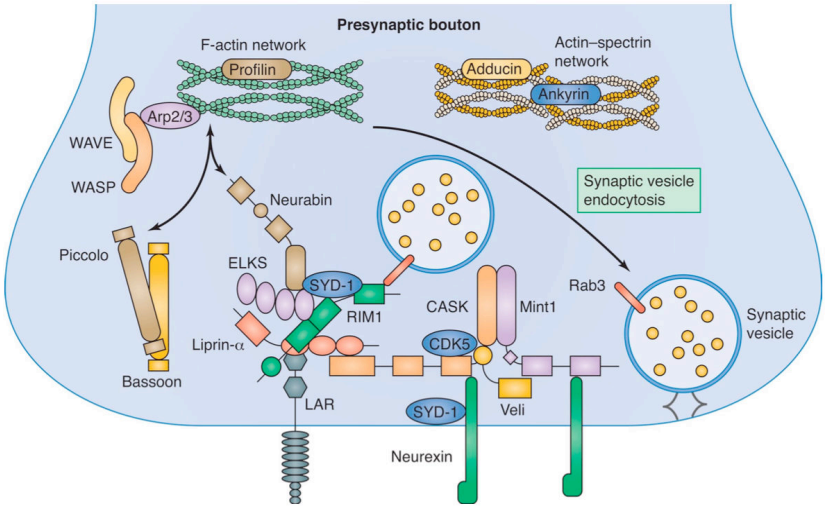


**Figure 7. Presynaptic assembly** *(From Chia 2013).* Details see text.

### *1.2.2.2 Membrane trafficking in postsynaptic assembly*

One of the most critical events in synaptogenesis of glutamatergic synapses is the recruitment of ionotropic glutamate receptors which are already present within dendrites before synapses are formed (Craig et al., 1993; Gerrow et al., 2006). Similar to presynaptic STVs, NMDA receptors (NMDARs) are transported in discrete transport packets that move within dendrites bidirectionally (Washbourne et al., 2002; Washbourne et al., 2004). Finally, these discrete, mobile transport packets are recruited to axo-dendritic contacts as one of the first events during synapse formation (Washbourne et al., 2002). Transport along microtubule filaments is mediated by motor proteins of the kinesin superfamily (KIFs), whereas transport along actin filaments is carried out by motor proteins of the myosin family. PDZ scaffolds on the surface of cargo vesicles can act as 'receptors' for molecular motors by binding to specific kinesins and myosins. For example, the PDZ domains of PSD-95, SAP97 and S-SCAM interact directly with the C terminus of KIF1B, a kinesin motor (Mok et al., 2002). The GluR2/3-binding protein GRIP interacts directly with conventional kinesin (KIF5) and this association is important for the targeting of AMPA receptors to dendrites (Setou et al., 2002). Tetraspanin membrane protein stargazin is recruited to synapses by PSD-95 where it induces the surface expression and synaptic accumulation of AMPARs through the interaction of the stargazin C terminus with the PDZ domains of PSD-95 (Chen et al., 2000). A schematic illustration of this process is provided in Figure 8.

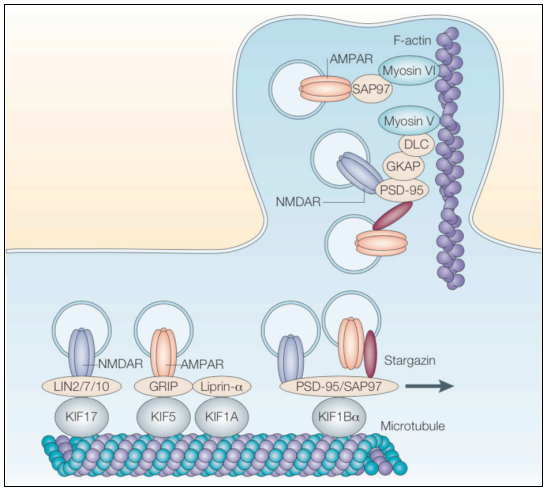


**Figure 8. Trafficking of protein complexes at the postsynaptic membrane** *(From Kim and Sheng, 2004).* Details see text.

### *1.2.2.3 Trans-synaptic signaling*

Once the pre- and postsynaptic components are assembled, signaling molecules at the membranes engage in bidirectional signaling to coordinate the differentiation of pre- and postsynaptic membrane specializations. Also called synaptic organizing proteins, they are mainly transmembrane adhesion complexes that bind *in trans* across the synaptic cleft, and secreted factors (Figure 9). Different adhesion molecules are used at excitatory and inhibitory synapses (Figure 10). None of these molecules function individually; they cooperate with one another in the form of an interconnecting meshwork. These synaptic organizers coordinate the following processes during the initial steps of synaptic differentiation: the precise apposition of pre- and postsynaptic membranes to ensure efficient neurotransmission, the matching of presynaptic neurotransmitter with appropriate postsynaptic receptor, the generation of a sense of directionality to induce the fundamentally different structures of pre- and postsynaptic terminals, and lastly, the selective formation of appropriate synaptic contacts and destabilization of inappropriate mismatched contacts. In this section, I will describe both membrane-bound adhesion proteins and secreted factors that contribute to these processes.

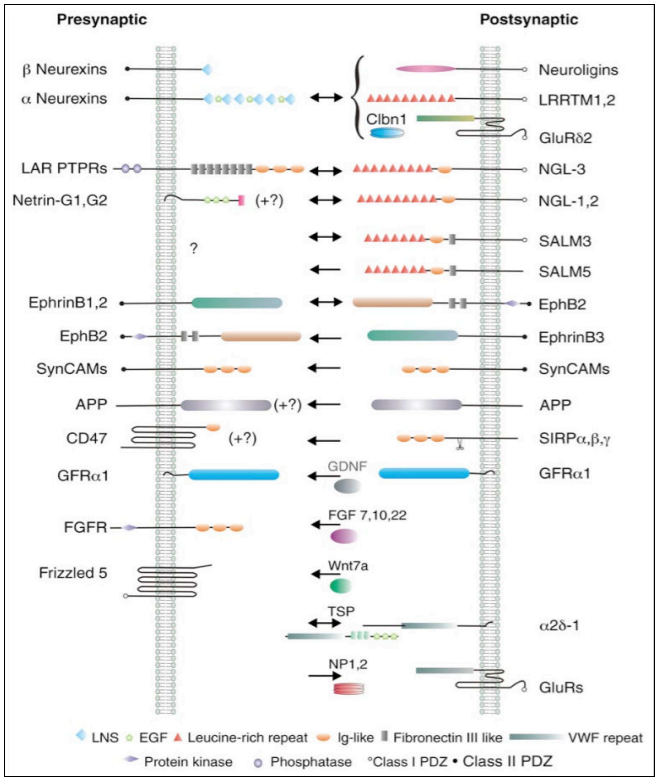


**Figure 9. Synaptogenic molecules that induce presynaptic or postsynaptic differentiation** *(From Siddiqui and Craig, 2011)*

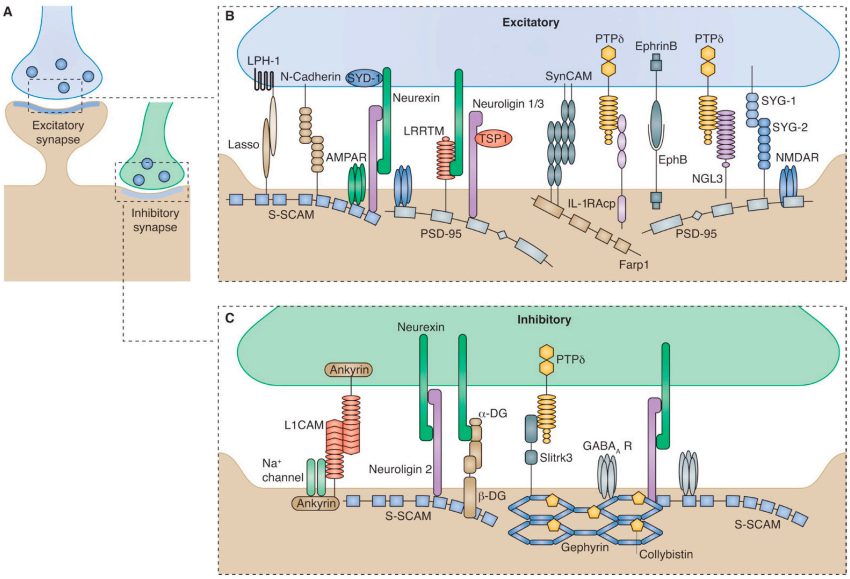


**Figure 10. Trans-synaptic signaling at excitatory and inhibitory synapses.**

Multiple pairs of trans-synaptic adhesion molecules organize synaptic differentiation and function on both pre- and postsynaptic sites. Neurexin-neuroligin signaling participates in both excitatory and inhibitory synaptogenesis LPH1, latrophilin 1; DG, dystroglycan; S-SCAM, synaptic scaffolding molecule; Lasso, LPH1-associated synaptic surface organizer; IL-1RAP, interleukin-1 receptor accessory protein. *(From Chia et al., 2013)*

### Neuroligins and Neurexins

A prototypic cleft-spanning synaptic organizing complex is the presynaptic Neurexin (NRXN) and postsynaptic Neuroligin (NLGN). The NRXN family consists of a large number of isoforms. In mice, three Neurexin genes are each transcribed from two alternative promoters resulting in six transcripts that generate the α- and β-NRXNs. From these transcripts, more than 1000 NRXN isoforms are generated by alternative splicing (Missler et al., 1998). As a result, NRXNs bind multiple, structurally diverse partners across the cleft. The four mammalian Neuroligins were the first characterized binding partners of Neurexin (Ichtchenko et al., 1995; 1996). Overexpression of NLGN in dissociated cerebellar or hippocampal cultures leads to the recruitment of NRXNs to cell-cell contact sites and results in a five-fold increase in the number of synaptic puncta (Dean et al., 2003). NLGN-NRXN interactions may be sufficient to induce presynaptic differentiation because expression of NLGN-1 in non-neuronal cells can trigger the assembly of functional presynaptic terminals in axons that contact these cells (Scheiffele et al., 2000).

NRXN-NLGN interactions participate in both glutamatergic and GABA-ergic synaptogenesis (Figure 10). NLGN-1 with an insert at its B splice site is the major

glutamatergic neuroligin and binds only β-NRXNs (Ushkaryov et al., 1992). NLGN-2 functions specifically at GABAergic synapses and binds all NRXNs (Ichtchenko et al., 1995). Interaction of α- but not β-NRXNs with dystroglycan, which is present along with NLGN-2 at a subset of mature GABAergic postsynaptic sites, may also contribute to the long-term stabilization of GABAergic synapses (Sugita et al., 2001; Levi et al., 2002). A recent study in invertebrates shows that NRXN-1 and NLGN-1 interact individually with MADD-4, an ADAMTS-like extracellular protein, at GABAergic postsynaptic neuromuscular junctions, and induce postsynaptic $GABA_A$ receptor clustering (Maro et al., 2015). Different glutamatergic synapses also express selective Neurexin variants (Figure 11). α- and β-NRXNs specifically lacking an insert at splice site 4 (-S4), interact with glutamatergic postsynaptic Leucine-rich repeat transmembrane neuronal proteins LRRTM1 and LRRTM2 (De Wit et al., 2009; Linhoff et al., 2009). LRRTM2 and NLGN-1 compete with similar affinity for β-NRXN (-S4) (Siddiqui et al., 2010). β-NRXN (+S4) binds with Cerebellin-1 (CBLN1), and together with GluRδ2 form a trans-synaptic triad that is essential for normal bidirectional Parallel fiber/Purkinje cell excitatory synaptogenesis (Uemura et al., 2010). Extracellularly, α-NRXNs have six LNS domains (laminin, NRXN, sex-hormone-binding globulin domains) with three intercalated epidermal growth factor (EGF)-like domains, whereas β-NRXNs have a single LNS domain. The extracellular domain of NLGNs consists largely of a region homologous to acetylcholinesterases, but the amino acids important for catalysis in acetylcholinesterases are not conserved in NLGNs (Ichtchenko et al., 1995). NLGNs and NRXNs both interact with cytoplasmic scaffolding molecules that may be mediators of their synaptic functions. The intracellular domain of NRXNs binds to class II PDZ domains that interacts with CASK, a MAGUK protein containing a $Ca^{2+}$/calmodulin-dependent protein kinase (CAMK) domain that is absent from other MAGUKs (Hata et al., 1996). CASK in turn interacts with intracellular adaptor proteins VELI and MINT to form a tight trimeric complex (Butz et al., 1998). The intracellular domain of NLGNs binds to class I PDZ domains such as those contained in PSD95 (Irie et al., 1997). PSD95 binds to intracellular adaptor proteins, and especially to GKAP (a protein that binds to the guanylate-kinase domain of PSD95), which, in turn, binds to Shank proteins (Reviewed in (Kim & Sheng, 2004)). PSD-95 has been shown to facilitate the assembly of multimeric complexes of other cell-surface molecules and may similarly induce clustering of NLGNs in the postsynaptic membrane (Reviewed in (Craven & Bredt, 1998)). NLGN activity depends on lateral clustering between individual NLGN molecules (Dean et al., 2003). Such lateral complexes of NLGN might induce clustering of NRXN in the presynaptic membrane and

thereby recruit scaffolding molecules, such as CASK, MINT, and CIPP, that can interact directly with the cytoplasmic tail of NRXNs (Biederer & Sudhof, 2000).

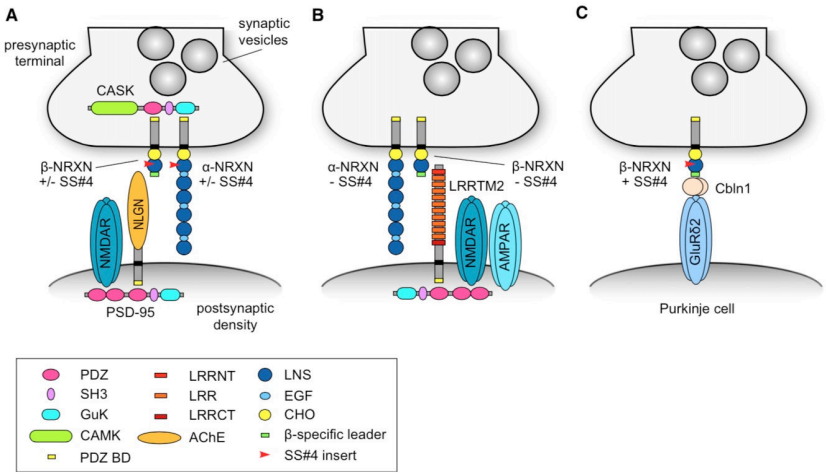


**Figure 11. Alternative splicing of Neurexin regulates specificity in neurexin-ligand trans-synaptic interactions.**

Schematic illustrating the interactions of different NRXN splice variants with NLGN **(A)**, LRRTM2 **(B)** and CBLN1 **(C)** at glutamatergic synapses. SS, splice site; GuK, guanylate kinase domain; CaMK, $Ca^{2+}$/calmodulin-dependent kinase domain; LRR, leucine-rich repeat; LRRNT and LRRCT, N-terminal and C-terminal LRR flanking domains; PDZ BD, PDZ binding domain; AChE, acetylcholinesterase homology domain; LNS, laminin/neurexin/sex-hormone-binding protein domain; EGF, epidermal growth factor-like domain; CHO, carbohydrate attachment sequence. *(From Williams et al., 2010)*

### Eph Receptors and Ephrins

EphB-receptor tyrosine kinases and their membrane-bound EphrinB ligands represent a second class of heterophilic signaling molecules at the synapse. Eph receptors have been well characterized as repulsive axon guidance molecules during earlier stages of nervous system development (Reviewed in (Flanagan & Vanderhaeghen, 1998)). Although receptors are found on axonal growth cones during the phase of axon guidance, they are restricted to dendrites in postnatal development (Henderson et al., 2001).

Several studies suggest an important postsynaptic function for EphB receptors in regulating the NMDA-receptor subunit NR1 via the extracellular domain (Dalva et al., 2000). Clustering of EphB receptors with recombinant EphrinB ligands strongly promotes this interaction in dissociated cortical neurons and leads to the generation of NR1 clusters at the cell surface. Furthermore, stimulation of cortical neurons over several days with clustered EphrinB ligands leads to a 1.5-fold increase in the number of pre- and

postsynaptic sites (Dalva et al., 2000). EphB2 knockout mice show a 40% reduction in the number of NR1-containing receptors in asymmetric synapses, which suggest that Ephrin-EphB2 interactions might regulate synaptic recruitment or retention of NMDA receptors (Henderson et al., 2001). In agreement with a reduction in the number of synaptically localized NR1 subunits, EphB2-deficient mice show reduced NMDA-mediated currents and reduced LTP at hippocampal CA1 and dentate gyrus synapses. Besides regulating NMDA receptor recruitment at synapses, EphB2 activation might also directly regulate NMDA-receptor function. Stimulation of dissociated cortical neurons with recombinant B-Ephrins leads to tyrosine phosphorylation of the modulatory subunit NR2B by src-kinases (Takasu et al., 2002). This phosphorylation event improves the calcium permeability of the NMDA receptor such that glutamate stimulation of cells results in increased calcium influx through the receptor and activation of CREB-dependent transcription (Takasu et al., 2002). These findings established a role for EphB receptors in postsynaptic signaling and function.

Ephrin-EphB signaling in neurons might also affect the presynaptic terminal. Mossy fiber LTP was blocked by extracellular addition of recombinant B-Ephrins to hippocampal slice cultures or by intracellular perfusion of the postsynaptic cell with reagents that block interactions with the EphB-receptor cytoplasmic domains (Contractor et al., 2002). This suggests that clustering of postsynaptic EphB receptors by cytoplasmic interactions might initiate a trans-synaptic signal by stimulating presynaptic Ephrins. These findings expand the synaptic function of Ephrin-EphB- signaling to NMDAR-independent forms of plasticity; however, it still remains to be shown whether Ephrins indeed localize to presynaptic terminals.

**Ig-Domain containing Proteins**

Several Ig-superfamily proteins have been implicated in synaptic interactions through heterophilic or homophilic cell adhesion. Members of this family contain one or several Ig-domains in their extracellular region that frequently bind to multiple ligands by calcium-independent interactions.

L1CAM family

The L1 family of cell adhesion molecules (L1CAMs) is a subfamily of the immunoglobulin superfamily of transmembrane receptors, comprised of four structurally related proteins: L1, Close Homolog of L1 (CHL1), Neural cell adhesion molecule (NCAM), and neurofascin. CHL1 and Neurofascin play a role in controlling the specific subcellular

localization of inhibitory synapses in the cerebellar cortex (See section 3.5.1). So in this section, I will describe only NCAM.

*NEURAL CELL ADHESION MOLECULE (NCAM)*

NCAM is found predominantly in growth cones (Brittis et al., 2002) with an important role in axon outgrowth. Earlier during development, NCAM is modified with high levels of polysialic acid (PSA), which reduces the adhesive interactions of NCAM (Pollerberg & Beck-Sickinger, 1993). After birth, this PSA-modification is strongly reduced resulting in an increase of adhesiveness once most neuronal circuits have formed. All axonal IgSF-CAMs including NCAM stimulate signalling pathways which induce the activation of the MAP kinase Erk; this activation is pivotal for the instructive role of these IgSF-CAMs in promoting axon growth and not for their adhesive properties (Schmid et al., 2000). NCAM-deficient mice have several brain abnormalities such as mis-orientation of hippocampal mossy fiber projections, defects in lamination and fasciculation, and a significant reduction in LTP (Cremer et al., 1997; Cremer et al., 1998). However, since NCAM is largely absent from mossy fiber terminals and is mostly detected at the axonal plasma membrane of fasciculating mossy fibers (Schuster et al., 2001), the reduction in LTP is not directly due to adhesive properties of NCAM. Therefore, NCAM appears to have more important functions during axon outgrowth and pathfinding, than during synapse formation.

SYNAPTIC CELL ADHESION MOLECULE (SynCAM)

SynCAM is a transmembrane protein containing three Ig-domains and an intracellular C-terminal PDZ-binding motif through which it interacts with CASK, a synaptic scaffolding molecule (Biederer et al., 2002; Samuels et al., 2007). Many of the molecules that interact with the C-terminus of SynCAM can interact with other synaptic factors, as is seen in the case of CASK that also binds to Neurexins and Syndecans (Hata et al., 1996). Overexpression of the cytoplasmic tail of SynCAM in neurons results in a decrease in the density of active terminals and slows the rate of synaptic vesicle exocytosis (Biederer et al., 2002). Conversely, similar to NLGN-expressing cells, expression of full-length SynCAM in non-neuronal cells induces synapse formation by co-cultured hippocampal neurons with normal release properties (Biederer et al., 2002). Furthermore, co-expression of the AMPA receptor subunit GluR2 with SynCAM yields proper glutamatergic transmission of these presynaptic terminals onto a non-neuronal cell (Biederer et al., 2002), demonstrating that

the presynaptic terminal is fully competent to release neurotransmitter. SynCAM and the NRXN-NLGN system show overlapping expression patterns in the CNS and may have partially redundant functions in the induction of presynaptic differentiation. Unlike NRXNs and NLGNs, however, SynCAM is expressed on both sides of the synapse and can homodimerize with itself to mediate synaptogenesis (Biederer et al., 2002). Whether either of these adhesion systems can also organize postsynaptic structures is not known. Because NRXN-NLGN interactions are heterophilic, they might precede the SynCAM interactions during the formation of synapses. Since NRXN and SynCAM both interact with CASK, nascent adhesion complexes containing NRXNs might therefore recruit SynCAM through a common scaffold.

SIDEKICKS

Sidekick-1 and -2 are two homophilic adhesion molecules that were identified in a screen for genes that are differentially expressed in subsets of neurons in the retina (Yamagata et al. 2002). The proteins have a similar domain structure consisting of six Ig-domains, 13 fibronectin type III repeats, a single transmembrane domain, and a C-terminal PDZ-binding motif. Despite these similarities, each Sidekick protein appears to form separate homophilic but not heterophilic complexes. Immunohistochemical analysis demonstrated that Sidekick-1 and -2 are expressed in different subsets of retinal neurons where they are strongly concentrated at synapses. Sidekicks and another IgSF adhesion molecule Dscam are expressed by retinal interneurons and retinal ganglion cells (RGC), and promote the lamina-specific targeting of retinal interneuron afferents on RGC dendrites (Yamagata & Sanes, 2008). Moreover, misexpression of Sidekick-1 or -2 in Sidekick-negative cells leads to aberrant termination of axons in the Sidekick-positive laminae, suggesting that the Sidekicks confer a lamina-specific identity on RGCs (Yamagata et al., 2002).

CADHERINS

The first class of molecules implicated in promoting axo-dendritic adhesion during synapse formation is the cadherins. Cadherins mediate the formation of junctional complexes in a wide variety of cells including epithelia, glia, and neurons. Initially, a group of about 30 “classical” cadherins had been identified, which are expressed in various tissues. Subsequently, additional members of the cadherin family were discovered that are termed protocadherins (Kohmura et al., 1998). “Classical” cadherins are the founding

members of the cadherin family. They are associated with the adherens junction and feature an amino-terminal extracellular region or ectodomain (EC) that is followed by a transmembrane anchor and a carboxy-terminal intracellular region. Classical cadherins have important functions in the structural assembly and reorganization of synaptic terminals, as well as for the selectivity of synapse formation during development. The N-terminal EC domain forms a dimerization interface in *trans* with the EC domain of a cadherin in the opposite membrane.

As mentioned in section 1.2.1, cadherins exhibit distinct yet complementary expression patterns with respect to subgroups of neurons and their targets. For example, cadherin-6 is expressed in functionally connected groups of neurons involved in audition (Bekirov et al., 2002). With regard to synapse formation, individual cadherins not only localize to the pre- and postsynaptic plasma membranes in a variety of synaptic types (Takai et al., 2003) but also are found at initial axo-dendritic contact sites (Benson & Tanaka, 1998). However, classical cadherins are not directly involved in triggering synapse formation. For example, introduction of N-cadherin blocking antibodies in the developing chick optic tectum causes RGC axons to overshoot their targets and form exuberant synapses but does not inhibit synapse formation per se (Inoue & Sanes, 1997). Similarly, axons originating from photoreceptor cells in the *Drosophila* ommaditium are mistargeted when they lack N-cadherin, but synapse formation itself is not disrupted (Lee et al., 2001). Thus, these data support a role for cadherins in target specification and perhaps stabilization of early synaptic contact sites.

A role for cadherins in the initial stages of synapse formation is supported by their rapid appearance at developing synapses (Benson & Tanaka, 1998) and by the decrease in excitatory synapse number caused by expression of a dominant-negative form of N-cadherin in developing neurons (Bozdagi et al., 2004). This effect of cadherins in promoting synapse assembly appears to depend on interactions with p120catenin, which enhances cadherin stability and mediates cadherin signaling to the Rho-family of GTPases to regulate cytoskeletal changes (Elia et al., 2006). This role for cadherin has led to the hypothesis that initial cadherin-based adhesion stabilizes transient, dynamic axo-dendritic contacts long enough to allow other classes of synaptogenic molecules to interact and activate intracellular cascades that recruit synaptic proteins (Togashi et al., 2002).

Classical cadherins have also been implicated in synaptic plasticity. In hippocampal slice cultures, LTP at Schaffer collateral–CA1 synapses is reduced by addition of antibodies directed against the extracellular domain of N- or E-cadherin (Tang et al., 1998). Another

study confirmed that L-LTP is accompanied by an increase in the number of synaptic puncta and requires new protein synthesis. Although the addition of anti-N-cadherin antibodies blocked L-LTP, it did not block the increase in the number of synaptic puncta. This suggests that new synaptic puncta assemble independently of N-cadherin, whether by de novo formation of synapses, splitting of existing synapses, or by the stabilization and enlargement of synapses that could not initially be detected. The role of classical cadherins in LTP suggests that cadherin-mediated adhesion might be modulated in response to cellular stimulation. Experiments in dissociated cultures of hippocampal neurons revealed that N-cadherin transiently disperses in response to massive presynaptic stimulation. Postsynaptic stimulation of NMDA receptors by direct application of glutamate, on the other hand, induced the formation of cadherin strand-dimers, a form that mediates increased adhesive interactions (Tanaka et al., 2000). In another study it was observed that overexpressed beta-catenin is recruited from dendritic shafts into spines in response to depolarization of hippocampal neurons (Murase et al., 2002). Recruitment of beta-catenin is likely to strengthen cadherin adhesiveness at the synapse.

NECTINS

Nectin-1, -2, -3, and -4 constitute a family of adhesion molecules with three extracellular Ig-domains. Nectins localize to the puncta adherentia junctions (PAJs) between nerve terminals and dendrites, and are not associated with the presynaptic active zone of mature synapses (Mizoguchi et al., 2002). This suggests that they are part of a different adhesion system than the one connecting presynaptic release sites and postsynaptic densities. The linkage of nectins to afadin, a cytoplasmic scaffold molecule, is needed for the localization of nectins to cell-cell junctions, and coupling of afadin to the actin cytoskeleton promotes the adhesive interactions mediated through nectins (Miyahara et al., 2000). The nectin-afadin complex co-localizes and cooperates with the cadherin-catenin complex to organize adherens junctions, and participates in synaptic formation, maintenance and remodeling (Figure 12). At the synapses between mossy fiber terminals and CA3 pyramidal cell dendrites in the hippocampus, Nectin-1 and Nectin-3 localize asymmetrically at the presynaptic and postsynaptic sides, respectively, of the plasma membranes of the PAJs and form hetero-*trans*-dimers (Mizoguchi et al., 2002). Afadin, N-cadherin and αN-catenin localize symmetrically at both sides. The N- cadherin/catenin system promotes synaptic differentiation, in cooperation with the Nectin-1-Nectin-3 hetero-*trans*-dimers, which determine the position and the size of synapses. *Cis*-dimers of

nectins mediate homophilic adhesion with nectins in the opposing membranes (in *trans*). In both nectin1$^{-/-}$ and nectin3$^{-/-}$ mutant mice, the number of PAJs at the mossy fiber-CA3 synapses are reduced with an abnormal mossy fiber trajectory (Honda et al., 2006). Further, in rat hippocampal neuron cultures, Nectin-1 and Nectin-3 display differential patterns of distribution: Nectin-1 preferentially localizes in axons than in dendrites, whereas Nectin-3 is equally present in axons and dendrites (Togashi et al., 2006). The heterophilic interaction between Nectin-1 and Nectin-3, together with the recruitment of N-cadherin/catenins, promotes the proper formation and stabilization of axo-dendritic synaptic contacts. Nectin-3 can also form heterophilic complexes with Nectin-2 (Satoh-Horikawa et al., 2000). Nectins transduce signals cooperatively with integrin $a_vb_3$, and regulate the formation of cell–cell junctions. *Cis*-interaction between nectins and PDGF receptor regulates its signaling for anti-apoptosis. Furthermore, Nectin-3 interacts in *trans* with nectin-like molecule-5 (Necl-5) and regulate cell movement and proliferation (Takai et al., 2003a).

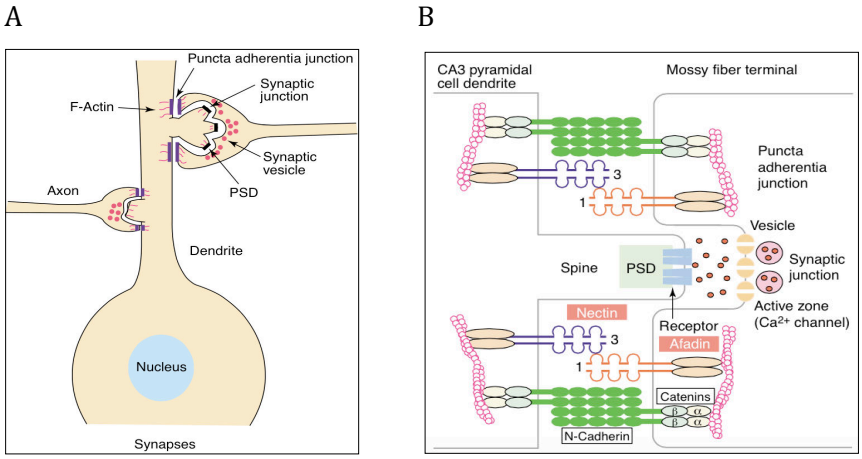


**Figure 12. Coordinated roles of nectin-afadin and cadherin-catenin systems in synapse organization**

**(A)** Schematic illustrating synaptic and puncta adherentia junctions **(B)** Organization of puncta adherentia junction at hippocampal mossy fiber-CA3 pyramidal cell synapse mediated by nectin-1, nectin-3, N-cadherin, catenins and afadin. Details see text. *(From Takai et al., 2003)*

### Secreted factors

In addition to adhesion proteins, the specific secretion of some factors contribute to synapse formation and specificity. In the invertebrate neuromuscular junction (NMJ), specific isoforms of Ce-Punctin/MADD-4, an ADAMTS-like secreted protein, are secreted by

cholinergic and GABAergic inputs and control the proper localization of corresponding synapses (Pinan-Lucarré et al., 2014). Two very recent studies describe the involvement of NRXN1 and NLGN1 in Ce-punctin mediated $GABA_AR$ localization. The short isoform of Ce-Punctin binds and clusters NLGN-1 postsynaptically at GABAergic synapses, and NLGN-1 in turn is indispensable for $GABA_AR$ clustering since NLGN-1 disruption causes a strong reduction of $GABA_AR$ localization (Tu et al., 2015). Ce-Punctin also binds and localizes UNC-40/DCC receptors in the postsynaptic membrane of NMJs, and this interaction promotes the recruitment of $GABA_AR$ by NLGN-1 (Tu et al., 2015). In another study, Ce-punctin is shown to interact with NRXN-1 (Maro et al., 2015). Although NRXN-1 does not influence the clustering of $GABA_ARs$ by NLGN-1, the absence of NRXN-1 and Ce-Punctin lead to an impairment of NLGN-1 and $GABA_AR$ clustering and synaptic transmission (Maro et al., 2015).

Proteins belonging to and related to the immune system have also emerged as important secreted synaptic organizers. These include immune system molecules like the complement proteins C1q and C3, as well as complement-related proteins related such as the C1q family, proteins containing the Complement Control Protein (CCP) or sushi domain and neuronal pentraxins (NARPs). Their mechanisms of action are described in sections 2.2 and 2.3.

Growth factors and neurotrophic factors comprise one class of secreted synaptogenic proteins. BDNF and Neurotophin-3 (NT-3) promote synaptogenesis through activation of their tyrosine kinase receptors TrkB and TrkC, respectively (Reviewed in (Poo, 2001)). Fibroblast Growth Factor-22 (FGF22) induces vesicle clustering in cultured motoneurons (Umemori et al., 2004). FGF22 and FGF7 selectively mediate synaptic vesicle clustering and not active zone formation or postsynaptic differentiation (Terauchi et al., 2010). In addition to neuronally derived synaptogenic factors, glial-derived factors may also regulate the timing of synapse formation. Two glial-derived factors shown to promote synapse formation include cholesterol bound to apolipoprotein E (Mauch et al., 2001) and thrombospondin-1 (Ullian et al., 2004). Thrombospondins (TSPs) are secreted by immature astrocytes and induce the formation of ultrastructurally normal synapses that are presynaptically functional but lack postsynaptic AMPA receptors (Christopherson et al., 2005). Wnts are another class of secreted factors that promote synaptogenesis. Wnt7a is involved transiently in cerebellar glomerular development *in vivo* (Hall et al., 2000) by a mechanism involving Dishevelled (Ahmad-Annuar et al., 2006).

#### *1.2.2.4 Synapse specificity*

Proper function of neural circuits not only requires that synapses be made with the correct target cell but also at the correct subcellular location within the target cell. Subcellular location is important since the relative strength and position of a synapse affects how much influence it has on the generation of action potentials.

The subcellular targeting of inhibitory neurons has been well studied in the cerebellar cortex where two inhibitory afferents, the stellate cells and basket cells, innervate distinct subcellular regions on the Purkinje cells. Adhesion proteins from the L1 Ig subfamily have been shown to control the specific subcellular localization of each inhibitory synapse on Purkinje cells (Ango et al., 2004; 2008)(See section 3.5.1). Moreover, in the case of stellate cells, proper targeting of stellate axons to Purkinje dendrites and synapse formation is mediated by Bergmann glial fibers that act as an intermediate scaffold guiding the stellate axons along the Purkinje cell dendritic arbor. Taken together, these studies on GABAergic innervation of Purkinje cells indicate that cell surface molecules regulate subcellular synaptic specificity both by mediating direct hemophilic adhesion between axon and dendrite as well as by providing an intermediate target to facilitate local connectivity.

The subcellular specificity of excitatory synapses has been studied in the hippocampus, where the axon guidance family semaphorins play an important role in the segregation of different classes of excitatory inputs along the dendritic regions of CA3 neurons (Figure 13). In the CA3 region, the main bundle of dentate gyrus (DG) axons or mossy fibers synapse only with the most proximal dendrites of CA3 neurons. In mice lacking the semaphorin co-receptors Plexin-A2 or Plexin-A4, the mossy fibers grow and synapse in ectopic synaptic zones (Figure 13). In Plexin-A2 mutant mice the mossy fibers grow in the pyramidal zone containing CA3 cell bodies and in Plexin-A4 mutant mice mossy fibers grow too far into distal layers of the CA3 (Suto et al., 2007). Interestingly, despite its hippocampal expression, Sema6A knockout mice do not have any defects in the main mossy fiber projection (Sahay et al., 2003; Suto et al., 2007). Nonetheless, Sema6A repels mossy fibers *in vitro* and Sema6A interacts genetically with Plexin-A2 to rescue the mossy fiber defect in those mice. This suggests that Sema6A in the distal CA3 layers act as a repellant signal for mossy fibers expressing Plexin-A4 and that Plexin-A2 in the proximal mossy fiber layer counteracts and attenuates the local Sema6A repulsive signal to allow mossy fibers into this zone (Suto et al., 2007). Further, these semaphorin/plexin

interactions are necessary only for the lamina-restricted synapse innervation, and not for synapse formation per se.

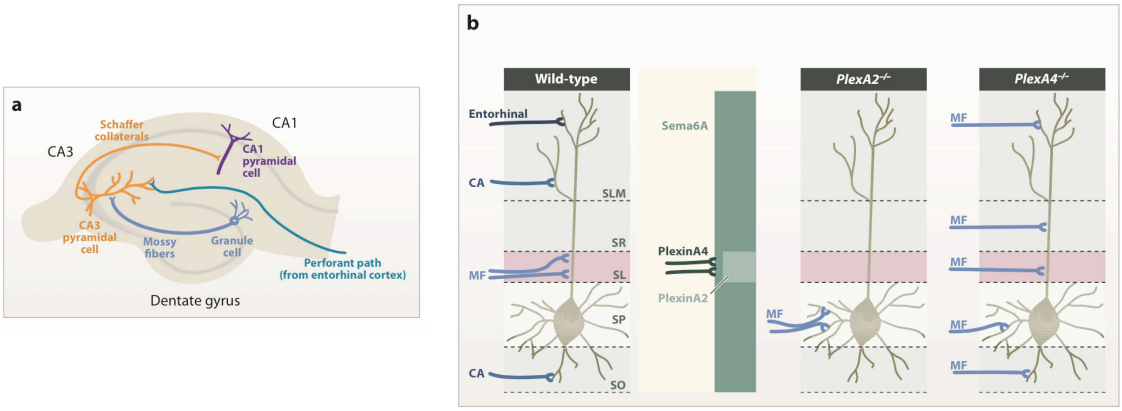


**Figure 13. Lamina-specific innervation of hippocampal neurons by distinct inputs**

**(A)** Apical dendrites of pyramidal cells in CA1 and CA3 and of granule cells in the dentate gyrus receive inputs from distinct sources on discrete dendritic segments. **(B)** In CA3 axons from entorhinal cortex, commisural/associational afferents (CA), and dentate gyrus [mossy fibers (MF)] innervate distinct dendritic segments in the stratum lacunosum-moleculare (SLM), stratum radiatum (SR), stratum lucidum (SL), and stratum oriens (SO) as shown. Genetic studies suggest that it sends a repellent signal to MF axons that express its receptor, plexin-A4. Expression of another receptor, plexin-A2, in the SL attenuates this signal, however, allowing MFs to synapse on proximal dendrites. *(From Sanes and Yamagata, 2009)*

As described earlier, neuroligins are involved in selective GABAergic versus glutamatergic postsynaptic differentiation. Given the evidence for a role of NLGN-1 in ciliary ganglion cholinergic synaptogenesis (Conroy et al., 2007), the roles of NLGNs may be even broader. In the CNS, NLGN-2 localizes specifically to GABAergic synapses (Graf et al., 2004; Varoqueaux et al., 2004), NLGN-1 localizes selectively to glutamatergic synapses (Song et al., 1999), and individual knockout mice exhibit selective deficits in GABAergic/glycinergic or glutamatergic transmission, respectively (Chubykin et al., 2007; Poulopoulos et al., 2009). Yet the phenotype of the NLGN-1,2,3 triple knockout mice is more severe than any of the single knockouts (Varoqueaux et al., 2006). NLGNs 1–3 are co-expressed in almost all neurons, yet only the triple knockouts are neonatally lethal, indicating that there is a large degree of functional redundancy among NLGNs. Moreover, electrophysiological and morphological analyses reveal that knocking out all three genes affects only synapse maturation and function, rather than synapse formation and density (Varoqueaux et al., 2006). Thus, the molecular diversity and functional redundancy correlates with the idea that a single unique ligand-receptor couple does probably not

specify each type of synapse. Instead, different types of synapses are likely to be regulated by distinct combinations of molecules that confer specificity and functional synaptic identity.

### 1.2.3 Synapse maturation

The maturation of a synapse is a prolonged event in contrast to its relatively rapid initial assembly. It is the phase during which the fate of an assembled synapse gets decided. Connections with functional signaling get stabilized, whereas emerging nascent connections that lack compatible trans-synaptic signaling systems get eliminated.

#### *Synapse stabilization*

Synapse stabilization is evidenced by maturation of the ultrastructure, including changes in the synapse location, size and postsynaptic form, and maturation of the synaptic electrophysiological properties (Bolshakov & Siegelbaum, 1995; Tovar & Westbrook, 1999; Mohrmann et al., 2003). A change of physical location is an important event in the stabilization of some types of synapses such as glutamatergic synapses. These synapses are initially formed on dendritic filopodia and dendrite shafts, but later they are primarily located on dendritic spines (Ziv & Smith, 1996; Fiala et al., 1998). Another important change in synapse stabilization is an increase in size of the synapse, which occurs in a coordinated fashion between the pre- and postsynaptic sites. It has been observed that the correlation of the size of different components is maintained including for bouton volume, number of total synaptic vesicles, docked vesicles, AZ area, postsynaptic density area, and spine head volume (Harris & Stevens, 1989; Schikorski & Stevens, 1997). This coordinated increase in size suggests that the area and/or volume of the pre- and postsynaptic partner sites are replete with trans-synaptic signaling by cell-adhesion complexes or other secreted factors.

Perhaps the most dramatic maturational change in synapses is the change in postsynaptic morphology. In the case of glutamatergic synapses, they initially form on filopodia or dendrite shafts, which are long, thin structures that have a short half-life of several minutes. But these structures develop over time into dendritic spines, which are typically shorter structures with a bulbous head, branched features and longer half-life of days or more (Grutzendler et al., 2002). Conversion of shaft synapses into spine synapses has also been inferred on the basis of the percentage of synapses of different morphological classes in the developing hippocampus (Fiala et al., 1998). Dendritic spine morphogenesis

is regulated by numerous mechanisms including cell adhesion via the cadherin, syndecan, and ephrin systems. These in turn signal through proteins that regulate Rho and Ras family GTPases, actin-binding proteins, and calcium regulatory mechanisms (Reviewed in (Hering & Sheng, 2001)).

The functional properties of synapses also change with maturation, and typically involve changes to the postsynaptic receptors. Changes in receptor subunit composition have been reported to occur during synapse maturation. For example, the NR2B subunit is initially incorporated into synaptic NMDA receptors but is partially replaced by NR2A subunits (Tovar & Westbrook, 1999). Another change that occurs during synapse maturation is the appearance of "silent synapses". These synapses contain NMDA receptors but show a great variability in the number of surface AMPA receptors, which lead to a reduction in AMPA current (Nusser et al., 1998). It is possible that silent synapses arise from changes in modes of vesicle fusion that activate NMDA receptors but fail to activate AMPA receptors (Choi et al., 2000). Another possibility is the presence of non-activated NMDA receptors, which may prevent the recruitment and insertion of AMPA receptors in the postsynaptic plasma membrane (Cottrell et al., 2000).

Overall, synaptic maturation consists of synapses growing larger and the amount of pre- and postsynaptic protein increasing considerably. So far, only the core components of the synapse including the SVs, presynaptic AZ, postsynaptic receptors, and directly associated scaffolding proteins, have been examined for the time-course of their recruitment to nascent synapses. It is not clear how the remaining, extremely large number of proteins, are recruited to nascent synapses. Some of these proteins might be added to the synapse only at later stages of synaptic maturation. For example, AMPARs and their associated scaffolding proteins appear to be part of a second wave of protein recruitment to nascent synapses that may serve to stabilize the synapse and mediate synaptic plasticity (Song & Huganir, 2002; Malenka, 2003).

***Activity-dependent synapse regulation***

Most synaptogenesis occurs during early postnatal development, but synapses can also form in the mature brain. At both stages, it is commonly observed that neuronal activity modulates arbor growth and synapse formation. During development, for example, activity-dependent pruning of synapses underlies the formation of ocular dominance columns in the visual cortex (Shatz & Stryker, 1978; Mataga et al., 2004)(See Section 2.2.1), refinement of the facial barreloid map in the somatosensory cortex by whisker-dependent

neural activity (Takeuchi et al., 2014) and innervation of muscles by neurons originating in the spinal cord (Lichtman & Colman, 2000). Evidence that activity regulates synapse formation and elimination between mature neurons has come from studies in the rodent barrel cortex that receives sensory input from the whiskers. New dendritic spines appear transiently and disappear over a period of weeks, and upon sensory deprivation, the new transient dendritic protrusions do not get stabilized (Trachtenberg et al., 2002). These studies reveal that synapses between mature neurons can be formed and eliminated rapidly and that activity regulates these processes.

However, in some other cases, neuronal activity is not required for synapse formation during development (Verhage et al., 2000). For example, in hippocampal cultures, synaptogenesis occurs normally in the presence of glutamate receptor blockers that prevent action potentials (Rao & Craig, 1997). In some systems, activity is only one of the determinants of synapse elimination. For example, the elimination of Climbing fiber synapses on Purkinje cells occurs in two phases – the early phase (postnatal day P7-11 in mouse) depends on Climbing fiber activity, whereas the late phase (postnatal day P12-17 in mouse) depends on the heterosynaptic competition between Climbing fibers and Parallel fibers (Crepel, 1982; Hashimoto & Kano, 2005)(See section 3.4.2). In addition, it has been reported that activity modulates the removal of inappropriate or ineffective connections in order to fine-tune networks. This is best illustrated in the retinogeniculate system where microglia and complement system molecules C1q and C3 promote synapse elimination in an activity-dependent manner (Stevens et al., 2007; Schafer et al., 2012) (See Section 2.2.2). In this case, neural activity serves to improve the precision of synaptic connectivity.

### 1.2.4 Synaptic plasticity

In mature neurons, the PSD composition undergoes continual molecular turnover under basal conditions and shows larger changes in response to activity (Inoue & Okabe, 2003). Proteins of the PSD turn over in large part by continuous exchange with counterparts outside of the PSD. PSD-95, for example, is dynamically exchanged between neighboring PSDs in cortical neurons *in vivo* (Gray et al., 2006). Among the most dynamic proteins in PSDs are the AMPA-type glutamate receptors, which show rapid lateral diffusion in and out of the postsynaptic membrane. Regulated AMPA receptor insertion into, and removal from, the PSD are major mechanisms underlying the strengthening and weakening of synaptic transmission (Reviewed in (Shepherd & Huganir, 2007; Lüscher &

Malenka, 2011)). The first transmembrane protein found to interact with AMPA receptors was stargazin (Chen et al., 2000), which is mutated in epileptic stargazer mice (Letts et al., 1998). In addition to absence epilepsy, stargazer mice show cerebellar ataxia (Noebels et al., 1990). In stargazer granule cells *in vitro*, the expression of AMPA receptor protein subunits GluR2 and GluR4 is largely maintained, but these receptors are not delivered to the cell surface. PDZ domain interactions with stargazin mediate synaptic clustering of AMPA receptors (Chen et al., 2000). The family of stargazin-related transmembrane AMPA receptor regulatory proteins (TARPs) function as AMPAR auxiliary subunits and specifically cluster at the PSD together with AMPA receptors (Tomita et al., 2003) (Reviewed in (Jackson & Nicoll, 2011)). A remaining question is how the structural organization of the PSD is altered to enable AMPA receptor incorporation and removal during LTP and LTD. It is likely that remodeling of the actin cytoskeleton and regulated proteolysis of PSD components are crucial for synaptic rearrangements underlying plasticity (Reviewed in (Cingolani & Goda, 2008; Bingol & Sheng, 2011)).

PSD composition can also be rapidly modified by post-translational modification mechanisms including protein phosphorylation, palmitoylation, ubiquitination, and proteasome-mediated protein degradation. Phosphorylation of PSD-95 on Ser-295, mediated by JNK1, promotes localization of PSD-95 in the PSD (Kim et al., 2007), whereas PSD-95 phosphorylation on Ser-73 by CaMKIIa mobilizes PSD-95 (Steiner et al., 2008). Palmitoylation of PSD-95 favors its synaptic localization (El-Husseini et al., 2002). Activity-dependent degradation of synaptic proteins, which is required for LTP and LTD as well as learning and memory (Colledge et al., 2003; Fonseca et al., 2006), may be aided by the rapid redistribution of proteasomes to postsynaptic sites following synaptic stimulation (Bingol & Schuman, 2006).

PSD composition also changes over a time period of hours to days during synaptic scaling, which is a homeostatic adjustment of synaptic strength in response to long-term alterations in activity (Turrigiano, 2008). In addition to compensatory changes in synaptic AMPA receptor content, chronic elevation of synaptic activity leads to large-scale changes in PSD composition, because of ubiquitination and proteasome-mediated degradation of GKAP and Shank scaffolds (Ehlers, 2003). PSD-95, which docks AMPA receptors at excitatory synapses via TARPs and whose synaptic content changes by neuronal activity, is required for homeostatic synaptic scaling (Sun & Turrigiano, 2011).

## 2. Immune system proteins in the brain

Many proteins initially identified in the immune system are also expressed in the developing and adult nervous system, affecting a variety of processes during the formation and refinement of neural circuits. In the healthy nervous system, immune system molecules play roles in neurogenesis, neuronal migration, axon guidance, synapse formation, activity-dependent refinement of circuits, and synaptic plasticity (Reviewed in (Boulanger, 2009; Carpentier & Palmer, 2009)). These functions for immune molecules during neural development are also effected during pathological states where the immune system mediates chronic inflammatory responses in neurodevelopmental disorders like autism spectrum disorders and schizophrenia (Reviewed in (Monji et al., 2009; Estes & McAllister, 2015)).

Recent studies have highlighted the roles for molecules mediating the crosstalk between the innate and adaptive immune responses in the establishment, function, and modification of synaptic connections (Reviewed in (Garay & McAllister, 2010)). These molecules include molecules of the major histocompatibility complex class I (MHC-I) family (Eg. β2m, TAP), molecules belonging to and related to the complement system (Eg. C1q, C3, pentraxins), and proinflammatory cytokines (Eg. TNFα, IL-6). In this chapter, I will first give a brief account of the innate and adaptive immune systems and how they work together. Then, I will describe immune system molecules known to play a role in neural development. Finally I will highlight the known roles of complement system-related proteins in synaptogenesis.

### 2.1 Bridging the innate and adaptive immune responses

The vertebrate immune system consists of two lines of defense – the innate immune system, and the adaptive immune system (Reviewed in (Vivier & Malissen, 2005)). The innate immune system consists of the complement cascade and phagocytes, and produces a rapid non-specific response to a variety of molecules like damaged self cells, apoptotic cells, pathogens and immune complexes (Ag/Ab). These foreign pathogens or damaged self molecules are then presented by the phagocytes to the adaptive immune system, which is composed of highly specialized lymphoid cells called B and T-lymphocytes. The adaptive response is characterized by its ability to create immunological memory that enables a stronger and more rapid response upon subsequent exposure to the same pathogen.

The first line of defense, the innate immune response, begins with the identification of foreign cells by proteins called pattern-recognition receptors (PRRs), such as Toll-like

receptors (TLRs) and NOD-like receptors, which recognize pathogen-associated molecular patterns (PAMPs) present on a variety of pathogens (Reviewed in (Janeway & Medzhitov, 2002; Akira et al., 2006)). Apoptotic or damaged self cells are recognized by soluble PRRs, such as complement proteins (C1Q), mannose-binding protein (MBP), and acute phase reactants, such as C-reactive protein (CRP). This recognition is followed by the activation of the complement system, both the classical (through C1q) and the lectin pathways (through MBP), and amplification via the alternative pathway (through C3 hydrolysis). The activation of the complement cascade results in pathogen endocytosis by antigen presenting cells (APC) such as macrophages, dendritic cells and natural killer cells, which in turn provide an inflammatory cytokine stimulus to activate the second line of defense, the adaptive system T-cell and B-cell signaling (Reviewed in (Gordon, 2002; O'Shea & Murray, 2008)). The T-cells lyse the pathogens, release more cytokines and induce activated antigen-specific B-cells to differentiate into either plasma cells for antibody secretion or memory cells. Thus, as illustrated in Figure 14, the complement system and cytokines provide a link between innate and adaptive immunity functions, leading to an augmentation of the immune response and buildup of immunological memory (Reviewed in (Carroll, 2004)). Further, it appears that parallels can be drawn between the immune response and circuit formation in the nervous system, both characterized by a primary recognition process followed by a switch to specific responses in a distinct, cell type-specific manner.

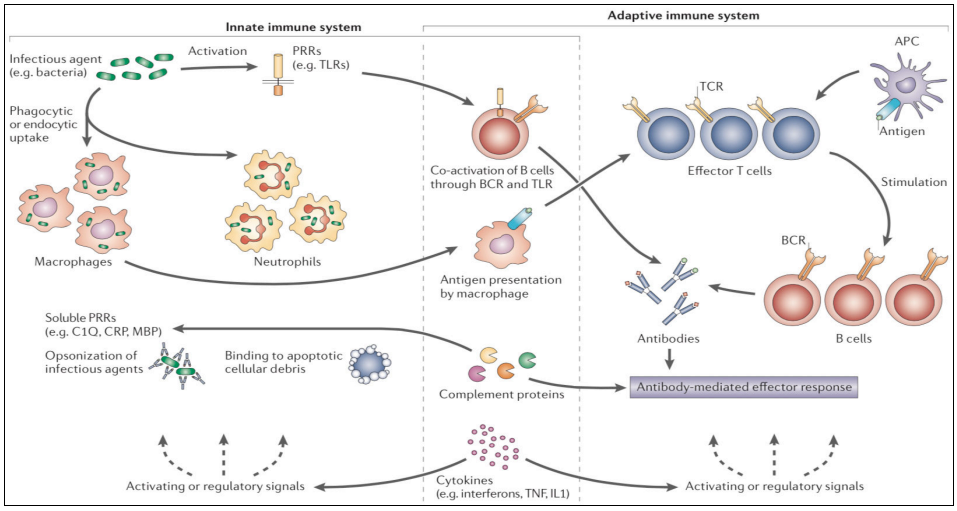


**Figure 14. Intersection between innate and adaptive immune systems**

Innate system regulation of adaptive immunity is mediated by complement proteins, phagocytes and cytokines. PRR, pattern recognition receptor; TLR, Toll like receptor; BCR, B-cell receptor; TCR, T-cell receptor; APC, antigen presenting cell *(From Gregersen and Behrens, 2006)*

## 2.2 Role of immune system molecules in the development of functional neural circuits

Initially, immune molecules were thought to cross the blood-brain barrier (BBB) and infiltrate the brain only in case of neural insult or trauma. However, several recent studies have shown that besides immune infiltration during stress and injury, immune molecules are also expressed in the healthy brain, albeit at significantly lower levels than in the immune system (Giulian et al., 1988; Corriveau et al., 1998; Barnabé-Heider et al., 2005). In the CNS, the main types of cells that express immune molecules are microglia, astrocytes or neurons. The main classes of immune molecules whose functions have been described in the brain are the MHC-I family, the complement system and cytokines. The MHC-I and complement cascade proteins are found in the healthy brain, particularly during development, and play a role in synapse pruning and refinement of neural circuits (Boulanger & Shatz, 2004; Stephan et al., 2012). Cytokines play a versatile role in the CNS, and mediate neurogenesis, synapse formation and response to injury in both healthy and pathological states (Boulanger, 2009; Deverman & Patterson, 2009; Carpentier & Palmer, 2009). A simplified schematic of the main immune molecules with roles in the CNS is shown in Figure 15.

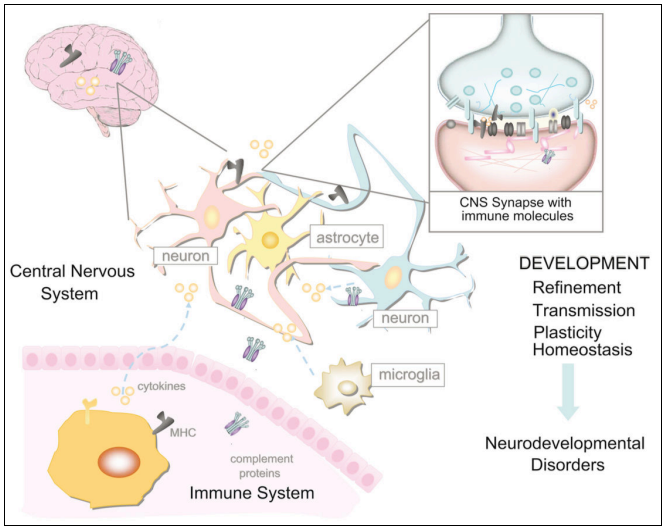


**Figure 15. Neuro-immune crosstalk**

Immune molecules like MHC-I, cytokines and complement are expressed during normal brain development and have roles in synaptic refinement and plasticity. In neurodevelopmental disorders, microglia and astrocytes proliferate and perpetuate cellular and molecular responses to neuroinflammation that occurs when the nervous system is exposed to infection or trauma *(From Garay and McAllister, 2010)*

### 2.2.1 MHC-I molecules

MHC-I molecules are heterodimers that consist of two polypeptide chains, an α heavy chain and β2-microglobulin (β2m) (Reviewed in (Cresswell et al., 2005). In the immune system, MHC-I molecules distinguish self from non-self proteins. Their function is to process the peptides derived from non-self proteins and present them to cytotoxic T-cells with the help of the Transporter associated with Antigen Processing (TAP) complex (Figure 16)(Babbitt et al., 1985). The cytotoxic T cell containing glycoprotein CD8 recognizes and binds to the MHC-I/antigen complex via T-cell receptor (TCR)-CD3 zeta (ζ) complex (Mercep et al., 1988). In addition to TCRs, MHC-I molecules also bind to receptors on natural killer (NK) cells including (in mice) paired immunoglobulin-like (Pir) and Ly49 receptors to regulate NK-mediated lysis of target cells (Reviewed in (Long, 2008)).

In the CNS, MHC-I molecules are expressed by activated microglia and in neurons during development and in adulthood with roles in different neural circuits such as the retinogeniculate system and hippocampus. Receptors for MHC-I are also detected in the adult mammalian brain. These include the immunoglobulin-like receptor B (PIRB) (Syken et al., 2006), the killer cell immunoglobulin-like receptor-like (KIRL) receptor (Bryceson et al., 2005), and the T-cell receptor beta subunit (TCR-β) (Syken & Shatz, 2003).

The MHC-I molecules and receptors were the first immune-related molecules implicated in neural circuit development, in particular, development of the retinogeniculate system. Visual information is processed from the retina through Retinal Ganglion Cell (RGC) axons into the lateral geniculate nucleus (LGN) of the thalamus and from there up to the primary visual cortex. In binocular adult animals, axons carrying information from each eye segregate into eye-specific layers in the LGN and into eye-specific regions, called ocular dominance (OD) columns, in the visual cortex (Miller et al., 1989). In the mouse retinogeniculate system, activity-dependent large-scale synaptic pruning and consequent eye-specific segregation occur by P10, before the onset of vision (Godement et al., 1984). The normal adult mouse dorsal Lateral Geniculate Nucleus (dLGN) has a small layer that receives inputs from ganglion cells in the ipsilateral eye; inputs from the contralateral eye occupy the remainder of the dLGN. Fine-scale synaptic refinement follows till P30 during eye opening (Shatz & Sretavan, 1986; Campbell & Shatz, 1992). Deprivation of input from one eye occurs during a specific time early in development, termed a “critical period”, and causes a shift in the OD to represent inputs that favor the remaining eye, forming much wider segregation zones. This process is called OD plasticity (Reviewed in (Hensch, 2005)).

MHC-I and CD3ζ mRNA are highly expressed in the mouse dorsal LGN during the first two postnatal weeks, when large-scale synaptic pruning occurs, and in the RGC layer of the retina (Corriveau et al., 1998; Huh et al., 2000). MHC-I deficient mice like β2m$^{-/-}$ and TAP$^{-/-}$, as well as mice deficient in CD3ζ show defects in normal segregation of retinal inputs, resulting in an expanded ipsilateral projection area in the dLGN with ectopic clusters of inputs (Huh et al., 2000; Datwani et al., 2009)(Figure 16). Similarly, mice that lack the MHC-I isoforms H2-Kb and H2-Db (KbDb$^{-/-}$), exhibit defects in LGN refinement that mimic those found in β2m$^{-/-}$ mice (Huh et al., 2000; Datwani et al., 2009; Lee et al., 2014), reduced ocular dominance (OD) plasticity (Huh et al., 2000) and impaired LTD (Lee et al., 2014). The effects on synapse elimination, eye-specific retinal input segregation and LTD are rescued by the neuronal expression of H2-Db in KbDb$^{-/-}$ mice (Lee et al., 2014). In genetically engineered mice expressing an inactive form of PirB, the retinogeniculate refinement proceeds normally, but the critical period for OD plasticity is extended (Syken et al., 2006). These studies show that MHC-I is involved in the regulation of synaptic plasticity and activity-dependent remodeling of the retinogeniculate system.

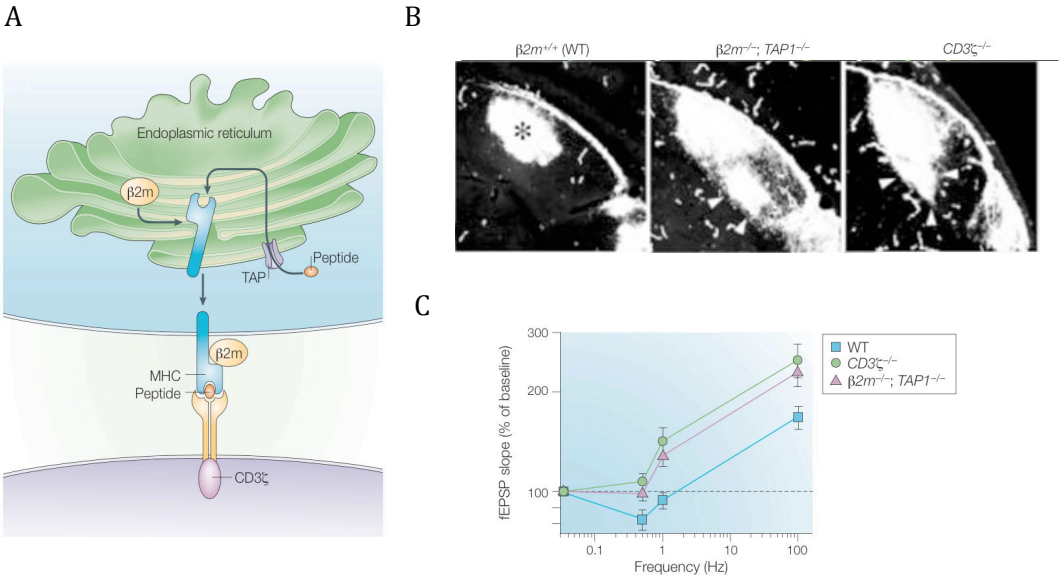


**Figure 16. MHC-I mediates synaptic refinement and plasticity**

**(A)** Schematic illustrating MHC class I antigen processing machinery. Intracellular non-self antigens are digested into small peptides. A specialized carrier, the transporter associated with antigen processing (TAP) complex, translocates the peptide into the endoplasmic reticulum (ER), allowing the antigen to bind MHC-I, which consists of an alpha (blue) and beta-2 microglobulin (β2m) chain. The assembled MHC-I complex and processed peptide fuse with the plasma membrane to insert the complex on the cell surface. MHC-I molecules present antigens to T-cell receptors, containing CD3 and zeta (ζ) chains, on CD8+ cytotoxic T cells. **(B)** Mice that are deficient for MHC-I genes β2m, TAP1 or CD3ζ fail to undergo

normal activity-dependent refinement of the developing visual projection. HRP injection in the eye results in anterograde labeling in the ipsilateral dLGN as shown by the white labeling in dark-field composites. Asterisks indicate labeled area, arrowheads indicate ectopic projections in mutants. **(C)** Enhanced hippocampal LTP in mice deficient either for cell surface MHC-I expression ($\beta 2m^{-/-}$ or $TAP^{-/-}$) or for CD3ζ, indicated by increased field EPSP (fEPSP) slopes in mutant mice. *(Adapted from Boulanger and Shatz, 2004)*

MHC-I expression was first demonstrated in different neuronal populations, usually after exposure of cultured hippocampal neurons to interferon gamma (IFN-γ) (Wong et al., 1984; Neumann et al., 1997). Subsequently, MHC-I was found to be expressed in developing and adult hippocampal pyramidal neurons (Neumann et al., 1997; Corriveau et al., 1998; Goddard et al., 2007). The MHC-I protein is enriched in synaptic fractions (Huh et al., 2000), and in hippocampal neurons *in vitro*, it is detected in dendrites, where it co-localizes with the postsynaptic marker PSD-95 (Goddard et al., 2007). MHC-I and CD3ζ are both expressed in the adult hippocampus as well, and required for normal activity-dependent synaptic plasticity in the hippocampus. In the hippocampus of adult CD3ζ, TAP and β2m mutants, NMDAR–dependent LTP is enhanced, and LTD is absent (Huh et al., 2000), indicating a role for MHC-I in regulating synaptic strength (Figure 16).

MHC-I is also found in other CNS neurons like the dorsal root ganglia neurons, brainstem motor neurons (Lidman et al., 1999; Loconto et al., 2003; Edstrom et al., 2004) and cerebellar Purkinje cells (Corriveau et al., 1998; McConnell et al., 2009). In the adult cerebellum, they do not mediate normal activity-dependent remodeling of Climbing fiber/Purkinje cell projections (Letellier et al., 2008). Instead they regulate synaptic plasticity and motor learning in the cerebellum. H2-Kb and H2-Db, are co-expressed by Purkinje cells (PCs) (McConnell et al., 2009). In the cerebellum of mice deficient for both H2-Kb and H2-Db ($KbDb^{-/-}$), there is a lower threshold for induction of LTD at Parallel fiber/Purkinje cell synapses and enhanced rotarod learning (Letellier et al., 2008; McConnell et al., 2009).

### 2.2.2 Complement system molecules

The complement system forms the first line of defense in the innate immune response. Upon pathogen recognition by C1q, both the classical (through C1q) and the lectin pathways (through MBP) get activated, and amplification of the complement effector response via the alternative pathway (through C3 hydrolysis) occurs.

Microglia in the CNS express high levels of complement component C1q, and complement receptors CR3 and CR5, which are necessary for inducing phagocytosis of

immune complexes. C1q and C3 are particularly highly localized to synapses in developing retina and dLGN in the developing brain during periods of synaptogenesis, and their expression decreases with age (Perry & O'Connor, 2008). In contrast, under pathological conditions such as glaucoma, C1q expression persists into adulthood (Stevens et al., 2007). In the retina, C1q protein is detected in the synaptic inner plexiform layer (IPL) of postnatal mouse retinas and in developing RGCs (Stevens et al., 2007). After MHC-I, a role for C1Q and C3 has also been shown during development of the retinogeniculate system. In contrast to microglia, which continue to express C1q in the mature brain, C1q expression in retinal neurons is developmentally restricted to the early postnatal period before P10. C1q and C3 are expressed in the dLGN with a peak at P5, and disappear by P30 (Stevens et al., 2007). Using knockout mice models, a role for C1q and C3 in synapse elimination has been demonstrated. In both $C1q^{-/-}$ and $C3^{-/-}$ mice, the retinal inputs fail to segregate into eye-specific territories starting at P10 (Figure 17). The dLGN remains binocularly innervated and this segregation defect is long lasting and sustained till P30. No defects are observed in axon guidance, early retinal activity or the number of RGCs (Stevens et al., 2007). This demonstrates that C1q is involved in the elimination of weaker retinal synapses during development in a manner analogous to its effector pathway in the immune system. C1q activates downstream C3, which in turn activates C3 receptors on microglia resident in the CNS. This induces phagocytosis of synapses “tagged” for elimination at the peak of the retinogeniculate pruning period (Schafer et al., 2012). Moreover, this engulfment is dependent upon neural activity and the microglia- specific phagocytic signaling pathway, complement receptor 3(CR3)/C3. Initially the astrocyte-derived factor that controlled C1q expression in the retina was unknown (Stevens et al., 2007). Subsequently, C1q was found to be induced by TGF-β, whose timing of expression in the retina coincided with that of C1q during the synaptic pruning period (Bialas & Stevens, 2013). Mice lacking TGF-β receptor II (TGFβRII) in retinal neurons had reduced C1q expression in RGCs and reduced synaptic localization of complement. These mice mimicked the C1q and C3 KO mice, showing reduced eye-specific segregation and microglia-mediated synapse elimination. Thus, complement components C1q and C3 are involved in activity-dependent refinement of retinogeniculate connections and control the topographic mapping of eye-specific inputs. A schematic illustration of complement-mediated synaptic elimination mechanism is provided in Figure 17.

A B

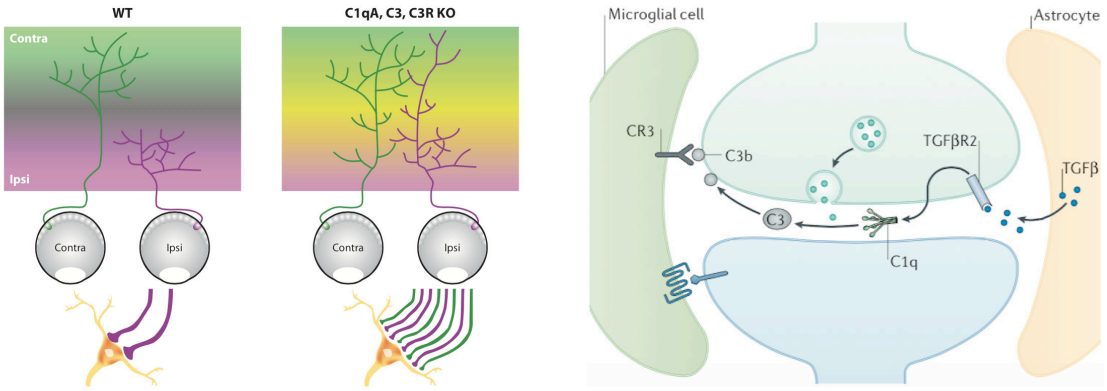


**Figure 17. Classical complement cascade proteins mediate synaptic refinement in the developing retinogeniculate system.**

**(A)** Sustained defects in C1q, C3, C3R knockout mice in eye-specific segregation of retinal ganglion cell (RGC) inputs (green, purple) in the dorsal lateral geniculate nucleus (dLGN) resulting in increased overlap (yellow region) of ipsilateral and contralateral RGC inputs *(From Stephan et al., 2012)* **(B)** Schematic illustrating the mechanism of complement-mediated synapse elimination. Astrocytes induce the secretion of C1q in neurons through TGF-β. C1q initiates the complement cascade, leading to cleavage of C3 into C3b, which binds to synaptic surfaces. Microglial expressed complement receptor 3 (CR3) recognizes tagged synapses and initiates synaptic pruning at a subset of complement-tagged synapses. *(From Estes and McAllister 2015)*

In the hippocampus, C1q is localized to a subset of inhibitory neurons (Stephan et al., 2013) and in hippocampal synapses, C1q is often colocalized with MHC-I molecules (Datwani et al., 2009). An increase in C1q level (up to 300-fold) is observed in the aging mouse brain, especially in some regions selectively vulnerable in neurodegenerative diseases such as the piriform cortex, substantia nigra, and hippocampus (Stephan et al., 2013). C3 is present only at very low levels in the adult and aging brain (Stephan et al., 2013). C1q expression in the aging brain also has effects on cognitive decline independent of synapse elimination (Stephan et al., 2013). Aged C1q-deficient mice do not show any alteration in dendritic spine or synapse number in the hippocampus, but exhibit significantly less cognitive and spatial memory decline in hippocampus-dependent behavior tests like the water maze and open field test compared with their wild-type littermates (Stephan et al., 2013). Adult C1q-deficient mice also exhibit enhanced activity-dependent long term synaptic potentiation in dentate gyrus synapses. This aging-dependent effect of C1q on hippocampal circuitry is independent of C3 as adult C3-deficient mice show a reduced LTP-phenotype in contrast to adult C1q-deficient mice

(Stephan et al., 2013). Furthermore, C3 plays a role in the regulation of the number and function of glutamatergic synapses in the hippocampus. Adult C3 KO mice have an increased number of functional CA3-CA1 glutamatergic synapses but reduced presynaptic glutamate release probability (Perez-Alcazar et al., 2014). C3 deficiency does not induce spontaneous epileptiform activity in the hippocampus, but results in enhanced hippocampus-dependent place and reversal learning ability, showing a negative effect of C3 on hippocampus-dependent cognitive performance (Perez-Alcazar et al., 2014).

### 2.2.3 Cytokines

In the immune system, pathogen recognition by the complement system induces antigen processing and signaling through MHC receptors and leads to the expression of multiple cytokine effectors. Local or autocrine cytokine secretion increases the sensitivity to the initial stimulus, the antigen-presenting cell (APC) displaying a peptide-MHC complex, to promote a pathogen-specific inflammatory response. Paracrine cytokine secretion promotes the recruitment and differentiation of T-cells and B-cells to augment the adaptive immune response (Reviewed in (Neumann et al., 1995)). Broadly speaking, there are two types of cytokine effector responses. When macrophages are triggered by pathogens alone, they mount an anti-inflammatory response that promotes cell proliferation, repair and apoptotic cell clearance. This elicits the production of corresponding anti-inflammatory cytokines which include Interleukins IL-4, IL-10, IL-11, IL-13, IL-1 receptor antagonist (IL-1ra), Interferon-α (IFNα) and transforming growth factor-β (TGF-β). Whereas, a more robust pro-inflammatory pathogen-clearance response is elicited when macrophages are triggered by pathogens and by cytokine Interferon-γ (IFN-γ) produced by lymphoid cells, generating pro-inflammatory cytokines like IL-1, IL-6, IL-12, IL-18, IFN-γ and tumour necrosis factor-α (TNF-α). The pro-inflammatory cytokine IFN-γ, in particular, is a versatile immunomodulator that is secreted by Natural Killer cells, activated T-cells and macrophages. It is the major factor that converts a macrophage into its “activated” state (Nathan et al., 1985).

The following major cytokines are expressed in the CNS: IL-1α, IL-1β, IL-4, IL-6, IL-10, IL-11, IL-13, IL-18, TNF-α, TGF-β, IL1-ra and CCL2 (Reviewed in (Bauer et al., 2007)). Pro-inflammatory cytokines TNF-α, IL-1β and IL-6 play a role in regulating excitatory and inhibitory synapse function by inserting AMPARs and removing $GABA_A$Rs from the synapse. Application of exogenous TNF-α to mature dissociated hippocampal neuron cultures or hippocampal slices induces a rapid increase in synaptic strength as indicated by

an increase in average mEPSC amplitude and frequency (Beattie et al., 2002; Stellwagen & Malenka, 2006). Given that TNF-α is a proinflammatory cytokine that regulates MHC-I expression, changes in MHC-I are likely to mediate the effect of TNF-α on plasticity.

In isolated spinal cord slices, TNF-α and IL-1β enhanced AMPA- or NMDA- induced excitatory currents, while IL-1β and IL-6 suppressed GABA- and glycine-induced inhibitory currents (Kawasaki et al., 2008). In dorsal root ganglion neurons, IL-6 enhances the function of the NA-K-Cl co-transporter NKCC1, thereby increasing intracellular chloride concentration (Pieraut et al., 2011). Another pro-inflammatory cytokine IFN-γ is found at neuronal synapses (Vikman et al., 1998), and in an IFN-γ knockout mouse model, the resulting decrease in MHC-I and β2m expression in spinal cord motor neurons leads to decreased synapse elimination of inhibitory inputs to the motor neurons (Victório et al., 2012).

In the developing mammalian visual cortex, TNF-α also mediates experience-dependent synapse plasticity. In wild type mice, visual deprivation of one eye leads to a reduction in the response of binocular neurons to one eye with a corresponding increase in response to the other eye. Mice deficient in TNF-α fail to exhibit this increase in response to the open eye following the normal initial loss of deprived-eye responses (Kaneko et al., 2008). Thus, TNF-α signaling regulates a homeostatic mechanism between these two non-competitive processes and mediates the strengthening of open eye inputs.

## 2.3 Complement-related proteins and their known roles in synaptogenesis

Complement proteins are part of the innate immune defense, which recognize foreign and damaged self cells to enhance phagocytosis and clearance. Besides this immune function, complement proteins and their downstream effector molecules like cytokines and MHC molecules also play roles in the development and refinement of neural circuits (See section 2.2). The complement system is tightly regulated by an array of molecules called Regulators of Complement Activation (RCA) in the cell membrane or extracellular matrix, which control the spontaneous activation of the complement cascade and prevent damage to tissues and autoimmunity (Reviewed in (Zipfel & Skerka, 2009)). Protein domains found in both complement and complement regulatory proteins are evolutionarily conserved and also found in many non-complement proteins, which in turn are referred to as complement-related proteins. For example, the gC1q signature domain of the complement target recognition C1q protein is also found in non-complement proteins like collagen VIII and precerebellin to name a few (Reviewed in (Ghai et al., 2007)). Pentraxins are fluid

phase pattern recognition molecules of the innate immune system that activate complement by binding C1q (Reviewed in (Bottazzi et al., 2010)). Their homologues, called neuronal pentraxins, are found secreted in the CNS (Schlimgen et al., 1995). The Complement Control Protein (CCP) or sushi domain found in complement regulators like Factor H and C4-binding protein are found in non-complement proteins like glycoproteins, X-linked seizure-related protein SRPX2, sushi domain containing SUSD proteins (Reviewed in (Reid & Day, 1989)). There is an increasing interest in the role of complement-related proteins in the development of neural circuits (Reviewed in (Yuzaki, 2008; Nakayama & Hama, 2011)). In this section, I will describe complement-related proteins that have been shown to mediate various aspects of neural development, focusing on their role in synaptogenesis.

### 2.3.1 C1q family

#### *Members*

C1q is the target recognition protein of the classical complement cascade in the innate immune response. The C-terminal globular C1q (gC1q) domain has also been identified in a variety of non-complement proteins that are together referred to as the C1q family. Since the gC1q domain is structurally similar to the tumor necrosis factor (TNF) homology domain of the multifunctional TNF family, these combined groups are also referred to as the C1q / TNF superfamily ((Shapiro & Scherer, 1998), Reviewed in (Kishore et al., 2004)). This family comprises of 32 proteins, and phylogenetic analysis suggests that the mouse C1q family can be divided into four groups: C1q, Emilin, Cerebellin (Cbln), C1q-like (C1ql) (Reviewed in (Yuzaki, 2008)) (Figure 18). C1qA, a target recognition protein of the classical complement pathway, and adiponectin, which is involved in sugar metabolism, belong to the C1q group (Yamauchi et al., 2001). The Emilin group contains the Emilin and Multimerin subfamilies, which are extracellular matrix proteins (Bressan et al., 1993; Hayward et al., 1995). The Cbln group is composed of the Cbln and C1q/TNF subfamilies, and the C1ql group contains only the C1ql subfamily (Reviewed in (Ghai et al., 2007)). The phylogenetic analysis of the amino acid conservation of the gC1q domain indicates that Cbln and C1ql subfamilies evolved differently from the rest of the C1q family proteins (Figure 18). Both the Cbln and the C1ql subfamilies are highly and predominantly expressed in the CNS.

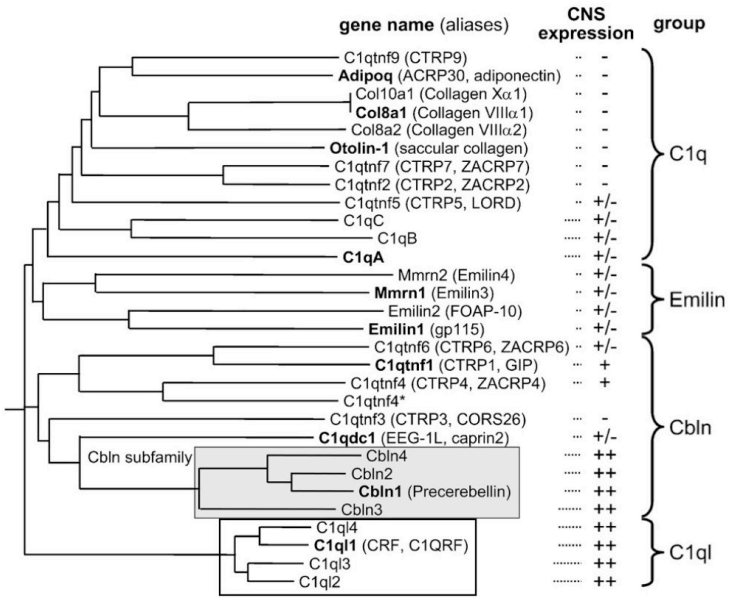


**Figure 18. Phylogenetic tree of mouse C1q family members**

ClustalW alignment of all mouse gC1q domain sequences with an indicated of their level of expression in the CNS. The Cbln and C1ql subfamilies are boxed to show their different evolution from the rest of the family. *(Adapted from Yuzaki 2008)*

***Structure***

Members of the C1q subfamily have a short N-terminal region (3–9 residues), a collagen region having 81 residues and a C-terminal globular (gC1q) domain of about 185 residues (Sellar et al., 1991; Kishore et al., 1998). The C1ql1 and Cbln subfamilies share structural similarity with the C1q subfamily, except that Cbln subfamily members lack the collagen domain (Figure 19). Crystal structure of the gC1q domain reveals that this domain is characterized by its ability to fold into a compact jelly-roll topology of five pairs of anti-parallel β-strands creating two β-sheets, generally referred to as the globular domain (gC1q) (Figure 19) (Gaboriaud et al., 2003). This gives the C1q molecule a bulbous shape made up of structural units, which combine in the tubular central portion (Reid & Porter, 1976). The gC1q domain of C1q and Cbln forms heteromeric trimers with each other, whereas other C1q family members like Emilin, Multimerin, collagen VIII, and Adipoq form homomeric trimers (Figure 19). The N-terminal collagen triple helix repeat and cysteine residues facilitate the formation of a higher order complex. The gC1q domain binds to various target proteins, such as pentraxins, immunoglobulins, lipopolysaccharides and phospholipids (Reid & Porter, 1976; Kishore et al., 1998).

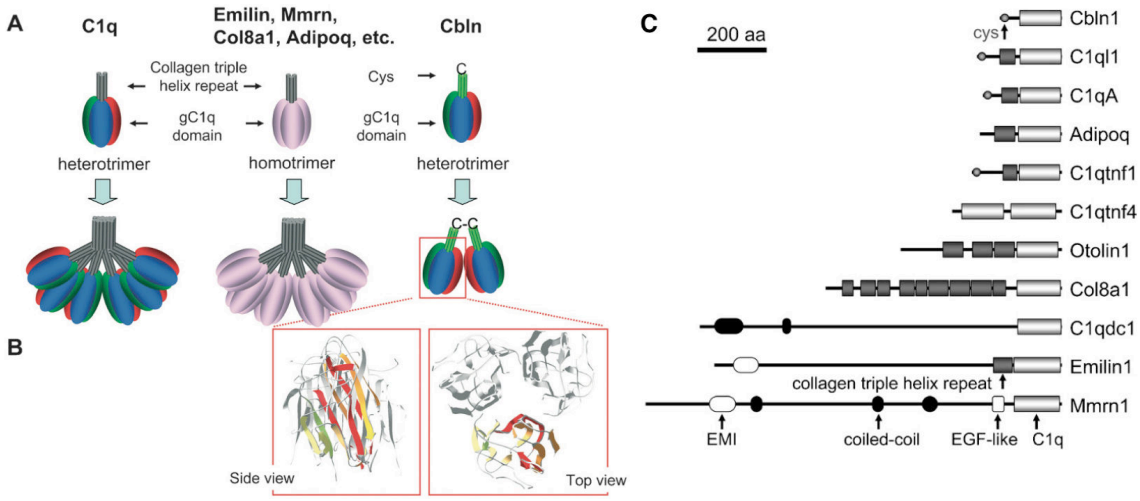


**Figure 19. Structural organization of the C1q family proteins**

**(A)** Heterotrimers formed by C1q and Cbln, homotrimers formed by other C1q family members. **(B)** Magnified view of a trimeric structural model of the gC1q domain of Cbln1 (C) Domain organization of representative C1q family members *(From Yuzaki 2008)*

Since I already outlined the role of C1q in synapse elimination (see section 2.2.2), in this section I will describe only the Cbln and C1ql1 subfamilies.

#### 2.3.1.1 Cbln subfamily

***Expression pattern***

The Cbln subfamily consists of four members, Cbln1–4; the full-length amino acid sequence is 71–86% identical to each other. In the adult brain, Cbln1 mRNA is highly expressed in cerebellar granule cells, certain thalamic nuclei, cortex and olfactory bulb (Morgan et al., 1988; Miura et al., 2006; Wei et al., 2007). Cbln2 expression is more widespread, being found in the olfactory bulb, thalamus, hypothalamus, cortex and colliculus. In contrast, the expression of Cbln3 and Cbln4 mRNAs is more restricted; Cbln3 is exclusively expressed in cerebellar granule cells, and Cbln4 expression is restricted to certain thalamic nuclei (Miura et al., 2006). During development, Cbln1, 2 and 4 mRNAs are expressed as early as embryonic day 13 and show transient up-regulation during the perinatal period. Whereas Cbln3 mRNA is first detected only on postnatal day 7 (Miura et al., 2006). Thus, distinct Cbln subtypes are expressed in various regions of developing and mature brains. All four Cbln members are secreted and form homomeric and heteromeric complexes with each other *in vitro* (Bao et al., 2005; Iijima et al., 2007).

***Functional roles***

Of the four Cblns, Cbln1 is the most functionally well-characterized protein. Secreted by cerebellar granule cells (Bao et al., 2005), it plays two crucial roles at Parallel fiber/Purkinje cell (PF/PC) synapses: it is indispensable for the assembly and maintenance of pre- and postsynaptic structures, and it contributes to the induction of long term depression at this synapse, a form of synaptic plasticity that underlies motor learning (Hirai et al., 2005). A detailed description of the molecular mechanism of PF/PC synapse formation mediated by Cbln1 is provided in Section 3.5.2. In brief, it acts as a bifunctional ligand that bridges the pre- and postsynaptic membranes by binding to β-neurexins on granule neurons and glutamate receptor δ2 (GluRδ2) on Purkinje cells, thereby stabilizing PF/PC synaptic contacts (Matsuda et al., 2010; Uemura et al., 2010). Cbln1 also undergoes transneuronal trafficking at synapses that do not contain GluRδ2 and is aggregated in Bergmann glia that also do not express GluRδ2 (Wei et al., 2009). Besides the cerebellum, the function of Cbln1 is characterized in the striatum. It is expressed in glutamatergic neurons of the parafascicular nucleus of the thalamus whose axons synapse onto dendrites of striatal medium spiny neurons (MSNs) (Wei et al., 2007; Kusnoor et al., 2010). Increased synaptic spine densities on the dendrites of MSNs are seen in the absence of Cbln1 (Kusnoor et al., 2010). Cbln1 also form heteromeric complexes with Cbln3 and they mutually regulate each other's degradation and secretion (Pang et al., 2000; Bao et al., 2006). However, unlike Cbln1, Cbln3 cannot form homomeric complexes and is secreted only when bound to Cbln1. This is evidenced by the fact that Cbln1-null mice lack both Cbln1 and Cbln3, whereas Cbln3-null mice lack Cbln3 but display a dramatic six-fold increase in Cbln1, indicating a stronger regulation of Cbln3 by Cbln1 (Bao et al., 2006). No functional roles of Cbln2 and Cbln4 have been described. However, distinct binding partners have been identified. Similar to Cbln1, Cbln2 binds to the S4-containing splice variants of α and β-NRXNs as well as to GluRδ1 and GluRδ2 (Wei et al., 2012). On the other hand, Cbln4 competes with netrin for binding to the netrin receptor, Deleted in Colorectal Cancer (DCC) (Wei et al., 2012; Haddick et al., 2014). Netrin-1-null mice exhibit dramatic neuroanatomical deficits, notably the absence of a corpus callosum, hippocampal commisure and pontine nucleus (Serafini et al., 1996). However, Cbln4-null mice do not phenocopy netrin-null mice (Wei et al., 2012), suggesting that Cbln4 does not exhibit a netrin-like function.

#### 2.3.1.2 C1ql subfamily

***Expression pattern***

The C1ql subfamily also consists of four members, C1ql1–4, among which C1ql1-3 are more predominantly expressed in the CNS. In the adult brain, C1ql1–3 mRNAs are strongly expressed in neurons in specific regions of the brain, with weak expression in glia-like structures (Iijima et al., 2010). C1ql1 mRNA is predominantly expressed in the inferior olivary neurons and transiently in the cerebellar external granular layer during development, whereas C1ql2 and C1ql3 are strongly expressed in the dentate gyrus of the hippocampus (Iijima et al., 2010). Although the C1ql1 and C1ql3 mRNAs are detected as early as embryonic age 13, the C1ql2 mRNA is observed only at later embryonic stages. All the C1ql subfamily proteins are secreted and form homomeric complexes (Iijima et al., 2010). They also form hexameric and higher-order complexes via their N-terminal cysteine residues.

***Functional roles***

In comparison to the Cbln subfamily, the functional roles of the C1ql subfamily are not well characterized. The adhesion G-Protein Coupled Receptor (GPCR) Brain Angiogenesis Inhibitor 3 (BAI3) has been found to interact with high affinity with all four C1ql proteins (Okajima et al., 2010; Bolliger et al., 2011). The gC1q domain of the C1ql protein binds to the extracellular thrombospondin-repeat (TSR) domain of BAI3. It is also shown that incubating primary hippocampal neurons with low concentrations of C1ql3 leads to a decrease in the density of excitatory synapses; this is blocked by the addition of a TSR-containing fragment of BAI3 (Bolliger et al., 2011). However, a very recent study identifies the complement C1r/C1s; Uegf, Bmp1 (CUB) domain of BAI3 as the mediator of its interaction with C1QL1 (Kakegawa et al., 2015). Both the CUB and TSR domains are highly conserved in evolution with roles in various neurodevelopmental processes. The CUB domain is found in many extracellular proteins associated with the plasma membrane and is implicated in many biological processes such as determining the dorsoventral axis, regulation of the complement system, angiogenesis, axon guidance, and the functioning of neurotransmitter receptors in the postsynaptic membrane (Reviewed in (Bork & Beckmann, 1993; Nakayama & Hama, 2011)). The TSR domains are found predominantly in large oligomeric extracellular matrix proteins. They mediate cell-cell and cell-matrix interactions by binding an array of membrane receptors, other extracellular matrix

proteins, and cytokines, with roles in cell adhesion, motility and proliferation. In the CNS, TSR proteins are also secreted by astrocytes and promote synaptogenesis (Christopherson et al., 2005). All these evidences provide insights into the potential functional roles of the C1ql proteins. Furthermore, analysis of the crystal structures of the globular C1q domains of C1QL1, C1QL2, and C1QL3 has revealed the presence of $Ca^{2+}$-binding sites, resembling ion channels, along the trimeric symmetry axis of both the C1QL1 and C1QL3 structures (Ressl et al., 2015). $Ca^{2+}$ binding through these sites confers a thermal stability upon the protein configuration of C1QL1 and C1QL3 proteins, both of which bind with similarly high affinity to $Ca^{2+}$, whereas C1QL2 crystallizes in an inactive, unbound state (Ressl et al., 2015). Compared with other gC1q domain proteins such as adiponectin and C1q, C1QL proteins have a more negative net electrostatic charge (Ressl et al., 2015). These unique properties may thus influence their specific binding to other proteins.

### 2.3.2 Neuronal pentraxins

#### *Members*

Neuronal pentraxins (NPTX) are immune-related molecules specific to the nervous system, with structural homology to immune system pentraxins such as C-reactive and acute-phase proteins which mark cells for degradation and phagocytosis (Whitehead et al., 1990; Schlimgen et al., 1995). They include NPTX1, NPTX2, NPTX3 and Neuronal Activity Related Pentraxin (NARP). They are released from pre- and postsynaptic neurons and form a high-molecular-weight complex at the synaptic junction (O'Brien et al., 1999; Fox & Umemori, 2006). NARP is expressed in several regions of the developing CNS with a prominent increase in the hippocampus and cortex during synaptogenesis (Tsui et al., 1996).

#### *Functional roles*

Neuronal pentraxins are secreted synaptic organizers and play roles in activity-dependent synaptogenesis and synaptic plasticity. In the hippocampus, NARP overexpression increases the number of excitatory synapses (O'Brien et al., 1999; Xu et al., 2003). Neuronal pentraxins NPTX1 and NPTX2 bind to the N-terminal domain of AMPARs and induce AMPAR clustering in neuronal and non-neuronal cells, and promote synaptogenesis (O'Brien et al., 1999; Sia et al., 2007). Through clustering of AMPAR subunit GluA4 in parvalbumin fast-spiking interneurons, NPTX2 maintains the inhibition/excitation balance in the hippocampus and makes it less susceptible to

epileptiform activity (Pelkey et al., 2015). Neuronal pentraxins have also been reported to bind C1q through their C-terminal domain (Stevens et al., 2007). Similar to mice deficient in C1q, mice that lack neuronal pentraxins exhibit defects in the eye-specific segregation of retinal ganglion cell projections to the dorsal lateral geniculate nucleus (Bjartmar et al., 2006). This suggests that C1q may modulate the interaction between neuronal pentraxins and the NTD of AMPA receptors at synapses (Perry & O'Connor, 2008). Thus, neuronal pentraxins possibly play a coordinated role with C1q during synapse development and complement-mediated synaptic pruning (Schematic in Figure 20).

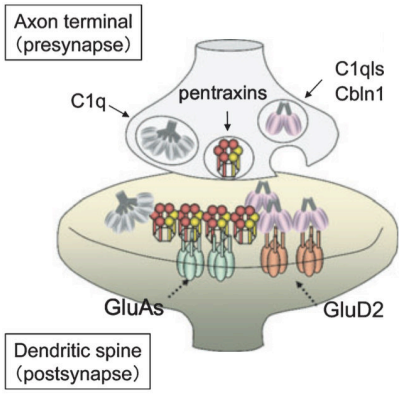


**Figure 20. Localization of C1q family and neuronal pentraxin proteins**

Schematic illustration of potential interaction between C1q and pentraxin molecules to mediate postsynaptic receptor clustering of GluAs *(From Yuzaki 2010)*

### 2.3.3 Complement control-related proteins

***Members***

This family is composed of proteins containing Complement Control Protein (CCP) domains, also referred to as the 'sushi domain' or the 'short consensus repeat' SCR. CCP domains have been identified in a variety of proteins involved in or related to the complement cascade, as well as non-complement proteins like cell adhesion molecules. Examples of complement and related proteins with CCP domains include the complement receptor CR1, the regulatory protein decay accelerating factor (DAF), complement protein C2, C-type lectin subfamily selectin and lectin-associated serine protease MASP-1. Non-complement proteins containing CCP domains include seizure-related X-linked SRPX2, complement-related SUSD protein family, blood coagulation factor XIIIb subunit, glycoproteins, interleukin-2 receptor, and haptoglobin 2, and murine seizure-related SEZ6 (Caras et al., 1987; Siegelman & Weissman, 1989; Reviewed in (Reid & Day, 1989)). Found in proteins from unicellular protozoan choanoflagellates to vertebrates, CCP domains are highly evolutionarily conserved and are likely to contribute to the diversity of cell signaling and adhesion protein families in multicellular organisms (King et al., 2003). Interestingly,

the complement system does not exist in *C.elegans*, suggesting that CCP-related proteins in vertebrates could also have non-immune related functions. The domain organization of some CCP-containing proteins across species in which they have been studied are illustrated in Figure 21.

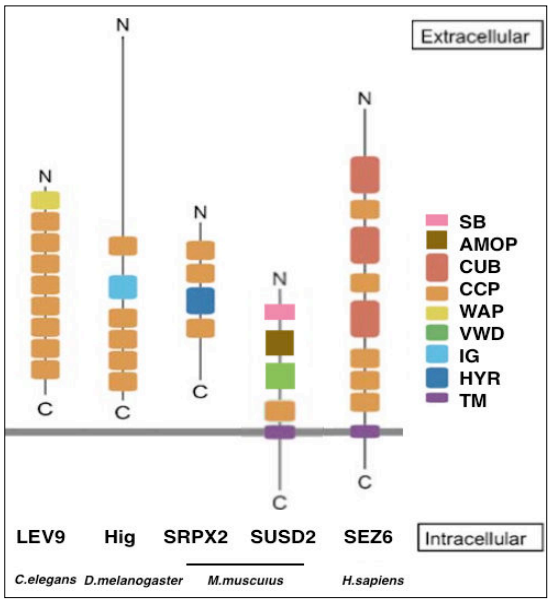


**Figure 21. CCP-containing proteins and their structural organization.**

SB, somatomedin-B; AMOP, Adhesion-associated domain in MUC4 and Other Proteins; CUB, complement C1r/C1s; Uegf, Bmp1 domain; CCP, complement control protein domain; WAP, whey acidic protein domain; VWD, von Willebrand factor type D domain mutant; IG, immunoglobulin domain; HYR, hyaline repeat; TM, transmembrane domain. *(Adapted from Nakayama and Hama, 2011)*

### *Structure*

Each CCP domain is an extracellular motif showing a compact globular structure. The three-dimensional structure of CCPs has been described as shown in Figure 22. About 60 amino acid hydrophobic residues characterized by tryptophan, glycine and proline form a core wrapped by β-sheets that are held together by the two conserved disulphide bonds formed between a consensus sequence including four cysteine residues (Reid & Day, 1989; Barlow et al., 1991; Chou & Heinrikson, 1997; Kirkitadze & Barlow, 2001). The CCP domain shares structural similarity with the CUB domain, also identified in components of the complement system. Each CUB domain also has a β-sheet folded core formed by 110 amino acid residues, held together by two disulphide bridges (Reviewed in (Bork, 1991; Bork & Beckmann, 1993)). Accordingly, there is a considerable overlap in the functional roles of proteins containing CUB or CCP domains, such as complement activation and neurotransmission (Reviewed in (Bork, 1991; Bork & Beckmann, 1993; Nakayama & Hama, 2011)).

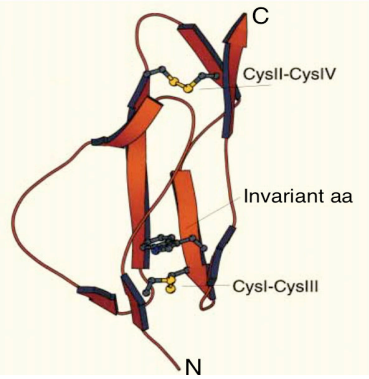


**Figure 22. Protein structure of the Complement Control Protein (CCP) motif**

The β-sheets (red block arrows) made up of invariant hydrophobic residues are held together via disulphide bridges (yellow) formed between cysteine residues. *(From Kirkitadze and Barlow, 2001)*

***Functional roles***

In vertebrates, CCP domain proteins were first identified to regulate complement activation. The role of CCP-containing complement proteins like C2, CR2 and DAF in regulating the complement cascade have been well characterized (Reviewed in (Ricklin et al., 2010)). Recent studies have highlighted roles for CCP-containing complement-related and non-complement proteins in neural development in both vertebrates and invertebrates. Some CCP-containing genes also have neuropsychiatric implications in humans – *Srpx2* and *Sez6* have been associated with epilepsy (Roll et al., 2006; Yu et al., 2006), *Csmd1/2* have been linked to schizophrenia (Håvik et al., 2011) and deletion of *Susd4* has been associated with Fryns syndrome (Shaffer et al., 2007), an autosomal recessive multiple congenital neurodevelopmental disorder in humans. In this section, I will describe CCP-containing genes across animal models identified to mediate different aspects of neural development.

### *2.3.3.1 Invertebrates*

**LEV-9**

Levamisole is a potent nematode-specific cholinergic agonist that causes muscle hypercontractions, paralysis and ultimately death at high concentrations (Lewis et al., 1980). Genetic screening for *C.elegans* mutants that exhibited low resistance to levamisole identified the *lev-9* gene that encodes a CCP-containing protein, and the *lev-10* gene that encodes a CUB domain-containing protein (Gally et al., 2004; Gendrel et al., 2009). LEV-10 is a transmembrane protein expressed in muscle cells and is specifically required for the localization of levamisole-sensitive acetylcholine receptors (AChRs) on muscle cell surfaces at neuromuscular junctions (NMJs) (Gally et al., 2004). LEV-9, secreted by muscle cells,

forms an extracellular scaffold by binding to the ectodomain of LEV-10, that is necessary to cluster AChRs at NMJs (Gendrel et al., 2009). At the NMJ, LEV-9 and LEV-10 are mutually interdependent for the proper localization and aggregation of postsynaptic L-AChRs at cholinergic synapses. LEV-9 contains eight CCP domains and a WAP (whey acidic protein) domain that is known to control cell proliferation ((Reviewed in (Bouchard et al., 2006)(Gendrel et al., 2009)). The receptor clustering role of LEV-9 is mediated by protein cleavage at a highly conserved sequence of residues present at the C-terminal, which acts as a limiting step in L-AChR clustering and neurotransmission (Briseno-Roa & Bessereau, 2014).

**Hig protein**

The Hig gene was identified by a genetic screen in adult Drosophila mutants that exhibited reduced locomotion (Hoshino et al., 1993). The inhibition of its expression at the precise embryonic mid-pupae period corresponding to synaptogenesis resulted in abnormal motor activity. Mutant larvae displayed uncoordinated movements, and both larvae and adults displayed reduced locomotion. Behavioral phenotypes in mutant larvae included uncoordinated muscle contractions and abnormally small forward movements than wild-type larvae when the head terminal was touched. High-frequency bursting activity was also recorded in thoracic muscles of the null mutants (Hoshino et al., 1996). The hig gene encodes a protein with four CCP domains that is secreted by the synaptic terminals and is localized to the nuclear membrane, endoplasmic reticulum, vesicles in the nerves, and a subset of synaptic clefts in the adult brain (Hoshino et al., 1996).

### *2.3.3.2 Vertebrates*

**Sushi domains on GABA receptors**

$GABA_B$ receptors are the G-protein-coupled metabotropic receptors that respond to the main inhibitory neurotransmitter in the brain, gamma-aminobutyric acid (GABA). They are expressed in almost all neurons of the brain, where they mediate slow inhibitory synaptic transmission and signal propagation by controlling the activity of voltage-gated calcium (Ca(v)) and potassium (K(ir)) channels (Reviewed in (Bettler, 2004)). $GABA_B$ receptors are similar in structure to and belong to the same receptor family as metabotropic glutamate receptors (Kaupmann et al., 1997). Functional $GABA_B$ receptors are formed by the heteromeric assembly of $GABA_B$-R1 with $GABA_B$-R2 subunits. The R1 subunit has two isoforms R1a and R1b. Accordingly, two receptor subtypes, $GABA_{B(1a,2)}$ and

$GABA_{B(1b,2)}$, are formed by the assembly of $GABA_{B1a}$ and $GABA_{B1b}$ subunits with $GABA_{B2}$ subunits (Schwenk et al., 2010). The R1a subunit is longer than R1b, and contains two CCP domains in the N terminus. The selective expression of CCP domains in R1a confers an axonal localization role to R1a. $GABA_{B1a}$ proteins are selectively trafficked into the axons of glutamatergic neurons, whereas both the $GABA_{B1a}$ and $GABA_{B1b}$ proteins traffic into the dendrites (Biermann et al., 2010). Furthermore, R1aR2 heteromers display increased cell surface stability compared with R1bR2 receptors in axons of cultured hippocampal neurons (Hannan et al., 2012). Both the CCP domains bring about this increased stability of R1aR2, since single CCP deletions cause the receptors to be internalized at the same rate as R1bR2 receptors (Hannan et al., 2012).

**Seizure-related SEZ6**

*Sez6* was first identified as a seizure-related gene following differential screening of mRNA from cortical neurons that were treated with pentylentetrazole (PTZ), a drug known to induce epileptic seizures (Shimizu-Nishikawa et al., 1995a). Variants of the *Sez6* gene are also found more frequently in a population of children with febrile seizures compared to controls, making *Sez6* a potential susceptibility gene for febrile seizures and epilepsies with complex inheritance (Yu et al., 2006; Mulley et al., 2011). *Sez6* gene encodes three isoforms of which two are transmembrane proteins with long extracellular domains and one is a secreted protein. The Sez6 protein consists of a threonine-rich domain, five CCP domains and three CUB domains (Shimizu-Nishikawa et al., 1995b). Sez6 knockout mice present deficits in spatial memory and motor performance, and display behaviors suggestive of depression and anxiety (Gunnersen et al., 2007). Functional analysis reveals that SEZ6 plays a role in promoting dendritic arborization and excitatory synaptogenesis (Gunnersen et al., 2007). Cultured cortical neurons from mice lacking *Sez6* display a reduction in excitatory synapse number, in dendritic spine density and PSD95 levels (Gunnersen et al., 2007). Moreover, the membrane-bound and secreted isoforms exert opposing effects when over-expressed in neurons cultured from *sez6*-null mice, with membrane-bound Sez-6 producing an anti-branching effect on dendrites leading to a decrease in neurite number. This effect on neuronal cell morphology and neurite branching occurs through the interaction of SEZ6 with Motopsin, a mental retardation gene that codes for a secreted serine protease containing adhesion protein domains (Mitsui et al., 2013). Motopsin is also known to cleave the presynaptic organizer agrin, a proteoglycan important for the formation and maintenance of excitatory synapses (Ksiazek et al., 2007; Stephan et al.,

2008), suggesting the possibility of a coordinated mechanism of action between SEZ6, motopsin and agrin.

**X-linked Sushi Repeat containing protein (SRPX2)**

SRPX2 is an X-linked gene encoding a secreted protein containing three CCP domains. It was first identified from a genetic screen in patients suffering from rolandic seizures and mental retardation (Roll et al., 2006), and has since been implicated in speech and cognitive development. Investigating the neural basis of speech led to the identification of the following functionally related SRPX2 interaction partners: a GPI-anchored plasminogen activator receptor called uPAR, the cysteine protease cathepsin B (CTSB) and the metalloproteinase ADAMTS4 (Royer-Zemmour et al., 2008). Since all these proteins form part of the extracellular proteolysis machinery, this suggests that SRPX2 is involved in the proteolytic remodeling of the extracellular matrix. This correlates with a role of SRPX2 in neural development, where it promotes neuronal migration and maturation in the cerebral cortex (Salmi et al., 2013). A transcriptional regulatory network was eventually discovered between transcription factor FoxP2 and the SRPX2/uPAR complex (Roll et al., 2010). FoxP2 inhibits the expression of this complex by interacting with the promoters of both SRPX2 and uPAR. This mechanism is also found to underlie the role of SRPX2 in synaptogenesis in the cerebral cortex (Sia et al., 2013). Cortical neurons cultured with SRPX2-conditioned medium show a preferential increase in excitatory synapse density with no change in inhibitory synapse density. FoxP2 regulates this excitatory synaptogenesis in cortical neurons by repressing SRPX2 levels through its transcriptional activity. Since mutations of the FoxP2 transcription factor also cause related disorders of speech processing and language (Lai et al., 2001), this suggests that FoxP2/SRPX2-mediated regulation of synaptogenesis could underlie the development of language-related neural circuitry, and that SRPX2 may be involved in the pathogenesis of language disorders.

**Sushi Domain Containing Protein 2 (SUSD2)**

This protein is one of four members (SUSD1-4) of the family of Sushi Domain Containing Proteins (SUSD). SUSD2 and SUSD3 have been implicated in cell adhesion, cell migration and tumorigenesis (Watson et al., 2013; Moy et al., 2014). In particular, SUSD2 has been identified as a cancer therapeutic target since it increases the invasion of breast cancer cells and contributes to a potential immune evasion mechanism by inducing

apoptosis of Jurkat T cells (Watson et al., 2013). In syngeneic mice tumor models, there is accelerated tumor formation, significant reduction of CD4 tumor infiltrating lymphocytes and decreased survival in mice with tumors expressing Susd2 (Watson et al., 2013). SUSD2 mediates this mechanism by interacting with and influencing the cell surface localization of galectin-1 (Watson et al., 2013), a secreted laminin-binding protein that promotes tumor immune evasion, angiogenesis, and metastasis (Reviewed in (Liu, 2000; Rabinovich, 2005)). Besides its identification as a tumor-reversing gene, so far, Susd2 is the only member of the SUSD family characterized to have a functional role in CNS development. Susd2 gene encodes two protein isoforms; one membrane-bound and one secreted protein, both of which contain one CCP domain. In hippocampal neuronal cultures, SUSD2 protein is localized on the soma, axon and dendrites, and preferentially promotes excitatory synaptogenesis (Nadjar et al., 2015). In developing neuronal cultures, knockdown of SUSD2 results in increased dendritic length but reduced axon length and branching (Nadjar et al., 2015). Since Susd2 has been shown to reduce the attachment of HeLA cells to the fibronectin extracellular matrix protein (Sugahara et al., 2007), the effect of SUSD2 on dendritic growth could be mediated by repulsive adhesive functions.

## 3. The olivo-cerebellar network as a model system to study synapse formation and specificity

The olivo-cerebellar network consists of the Inferior Olivary Neurons (ION) in the medulla, the cerebellar cortex and the deep cerebellar nuclei (DCN). The cerebellar cortex with its sophisticated and well-orchestrated microcircuitry is the main signaling processing center of the cerebellum or "little brain". The cerebellum, along with the ION, is primarily associated with motor learning, motor control and adaptive plasticity (Eccles, 1967; Ito, 1998; Welsh, 1998; Kandel, 2000). The cerebellum herein plays a modulatory rather than an executive role on motor output, by ensuring control over voluntary movements and balance (De Zeeuw et al., 2011). Functional imaging studies have demonstrated a role for the cerebellum in language, cognition and memory as well (Desmond & Fiez, 1998; Schmahmann, 1998; Leiner et al., 2002). The understanding of the cerebellar functions is largely made possible due to the dissection of the olivo-cerebellar synaptic connections and multiple levels of plasticity (Alba et al., 1994; De Zeeuw et al., 1998; Gao et al., 2012).

The long-range connectivity of inferior olivary afferent projections to its target, occurs in a highly organized manner, along the medio-lateral and antero-posterior axes of the cerebellum (Groenewegen & Voogd, 1977; Ruigrok & Voogd, 2000; Sugihara, 2005; Reeber et al., 2013). Elegant tracing and lesion experiments have demonstrated that Climbing fibers (CF) originating from different inferior olivary sub-nuclei terminate in distinct parasagittal bands in the cerebellum, forming longitudinal zones (Chan-Palay et al., 1977; Groenewegen & Voogd, 1977; Herrup & Kuemerle, 1997). This orderly olivo-cerebellar projection pattern is directed by biochemical cues on the Purkinje cells (PC) as well as axon guidance cues in the cerebellum (Wassef et al., 1985; 1992) (Chedotal et al., 1997; Sugihara, 2004). Once in the cerebellum, synaptic competition and refinement of Climbing fibers occur at the level of Purkinje cells, resulting in non-overlapping synaptic targeting and innervation (Hashimoto & Kano, 2003; Cesa & Strata, 2009). Thus, the specificity of olivo-cerebellar connections is generated at two levels – a broad topographic mapping of the olivary projections at the macro level and fine-tuning of synaptic connections at the micro level.

Two key constituents of the olivo-cerebellar network are established during cerebellar development: a highly specific laminar arrangement of cells in the cerebellar cortex, and an equally specific and uniform cellular microcircuitry. In this chapter, I will

first describe the functional and molecular organization of the cerebellum, followed by the cytoarchitecture, development and synaptic connectivity of the cerebellar cortex. Lastly, I will highlight the molecular mechanisms known to control synapse formation and specificity in the cerebellar cortex.

## 3.1 Functional organization of the cerebellum

The first theories of cerebellar function arose from the observation of clear motor impairments resulting from cerebellar lesions. The cerebellum integrates motor commands and sensory information to help coordinate movements. My description of cerebellar function in this section is based on the detailed explanation of the cerebellar circuit provided by the seminal work of Eccles, Ito and others (Eccles, 1967; Ito, 1982; Raymond et al., 1996). The cerebellum consists of the cerebellar cortex with a stereotyped foliation pattern and the white matter underneath which contains the output module of the cerebellum, the deep cerebellar nuclei (DCN). The DCN ascending efferents project to the cerebral cortex via the ventrolateral thalamus and the ventral tegmental area (Figure 23). The DCN modulate sensory input-driven movement and posture through their spinocerebellar descending efferents that project in reticulo-, vestibulo- and rubrospinal tracts (Also see Figure 29). The lateral cerebellar hemispheres are referred to as the cerebrocerebellum and receive input exclusively from the cerebral cortex via the pontine nucleus (PN). The cerebrocerebellum projects to the ventrolateral thalamus and the red nucleus, which in turn projects to the ION, ultimately providing feedback to the cerebellum. The part of the cerebellum that receives direct or indirect vestibular input is referred to as the vestibulocerebellum and controls eye and body reflexes following vestibular input. The cerebellum receives all its synaptic input from the precerebellar nuclei, whose fibers collaterally innervate the DCN. Thus, the precebellar system modulates cerebellar output directly and indirectly through the DCN. The precebellar nuclei consist of the dorsal nucleus of the spinal cord (Clarke's column) and various nuclei distributed throughout the brainstem that include the ION, the PN, the lateral reticular nucleus (LRN) and the external cuneate nucleus (ECN). The pons, located in the rostral part of the ventral brainstem, serves as a relay between the cortex and the cerebellum, and also receives reciprocal excitatory input from the cerebellar nuclei. The ION receives afferent input from the dorsal column nuclei, the spinal cord, various midbrain regions (red nucleus, superior colliculus and others), the cerebellar nuclei as well as the cerebral cortex. As illustrated in Figure 23, activity is thus integrated by two commissural loops in the olivo-cerebellar system: The

ION sends excitatory CF afferents to the Purkinje cells (PC) and the DCN. The PCs project inhibitory afferents onto the DCN, which in turn send inhibitory inputs to the ION among other target cells, completing the loop.

A B

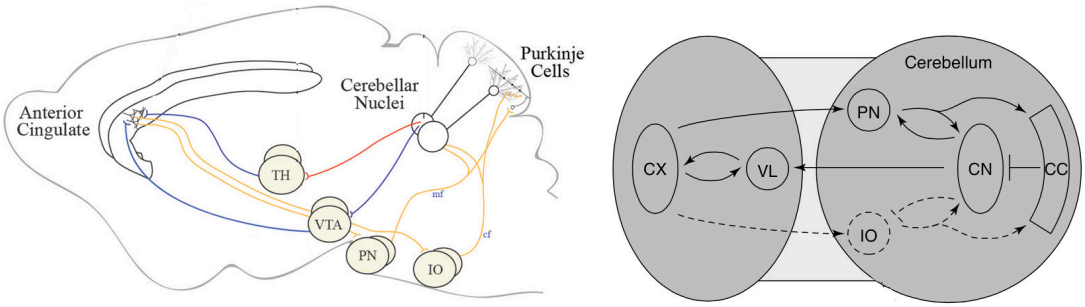


**Figure 23. Cerebellar connectivity in the brain**

**(A)** Schematic representation of the efferent cerebellar projections enabling cerebellar access to the cerebral cortex in a sagittal view. TH, thalamus; VTA, ventral tegmental area; PN, pontine nuclei; IO, inferior olive. *(Adapted from Parker et al., 2014)* **(B)** Schematic representation of excitatory and inhibitory connections between the cerebral cortex and cerebellum, including the two commissural loops in the olivo-cerebellar network between the inferior olivary neurons (IO), the deep cerebellar nuclei (CN) and Purkinje cells in the cerebellar cortex (CC). CX, cerebral cortex; VL, ventrolateral thalamus; PN, pontine nuclei; IO, inferior olive; CN, deep cerebellar nuclei; CC, cerebellar cortex *(From Schwarz and Thier, 1999)*

## 3.2 Molecular basis of olivo-cerebellar maps

The adult cerebellum has a stereotyped foliation pattern consisting of 10 folia or lobules. Each lobule is divided along the medio-lateral axis to form sagittal zones that are defined by the patterned expression of genes and proteins. One of the first demonstrations of a cerebellar striped expression pattern was shown by the distribution of 5'-nucleotidase enzyme activity in the cerebellar cortex (Scott, 1963). Subsequently Zebrin II, an antigen on the aldolase C protein, was identified to be expressed by alternating subsections of PCs (Brochu et al., 1990; Hawkes, 1992; Hawkes & Herrup, 1995). This biochemical distinction at the level of PCs is matched by CF innervation pattern. For example, a subset of CFs expressing Corticotrophin Releasing Factor (CRF) project and align with zebrin II positive Purkinje cell zones (Sawada et al., 2008) (Figure 24). Grafting experiments show that the zonal patterning of PCs occurs even before they receive CF afferents (Wassef et al., 1992). At a functional level, the release of glutamate and synchronous firing of CF inputs is shown

to be Purkinje cell zone-dependent, leading to a difference in synaptic plasticity between zones (Llinas & Sasaki, 1989; Blenkinsop & Lang, 2006; Paukert et al., 2010).

The first inferior olivary axons arrive in the developing cerebellum as Climbing fibers at E14/E15 and are already organized into a crude zonal map by E15/16 (Paradies & Eisenman, 1993). This corresponds to the beginning of expression of parasagittal markers by PCs (Wassef et al., 1985; Hashimoto & Mikoshiba, 2003). It was subsequently demonstrated that a molecular recognition between subsets of IONs and PCs ensures the appropriate targeting of inferior olivary axons onto Purkinje cell zones (Chédotal & Sotelo, 1992; Wassef et al., 1992). For example, members of the cadherin family were found to be markers of compartmentalization of the inferior olive, as well as expressed in Purkinje cell sagittal zones (Redies et al., 2011).

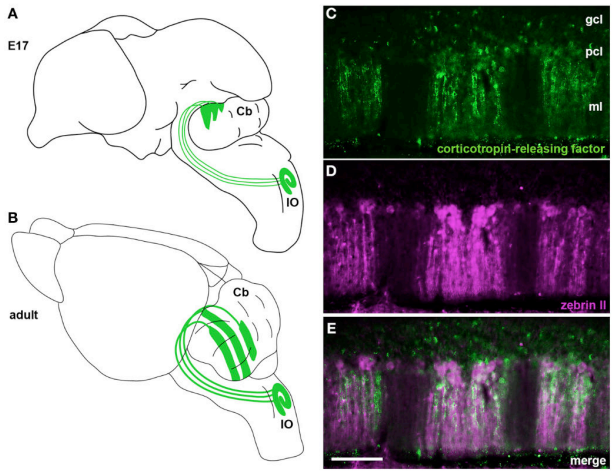


**Figure 24. Zonal pattern organization of olivo-cerebellar projections**

**(A)** Schematic illustrating climbing fiber projections from the inferior olive to the cerebellum at E17 **(B)** Subsequent delineation of climbing fibers into well-defined cerebellar Purkinje cell zones in the adult brain **(C-E)** Alignment of CRF expressing climbing fiber subsets with zebrin II expressing Purkinje cell zones *(From Reeber et al., 2013)*

## 3.3 Anatomical description of the olivo-cerebellar network

Having described the functional and topographic organization of the cerebellum, this section will now focus on the anatomy of the olivo-cerebellar network, including the generation and final positioning of different cell types in this system.

### 3.3.1 Cell populations

#### *Cerebellar cortex*

The cerebellar cortex is a well-organized trilaminar structure, and Cajal established its fundamental anatomical organization more than a century ago. The innermost granular layer predominantly contains tiny densely packed granule cells (GCs), the most numerous type of neuron in the brain (estimated at $3x10^{10}$ in humans), and interneurons like the unipolar brush cells, large Golgi cells and the Lugaro cells. The outermost molecular layer contains two types of interneurons, the stellate cells and basket cells, which are sparsely distributed. This layer also harbors the axons of the GCs and the elaborate PC dendritic arbor. In between these two layers lies the Purkinje cell monolayer that contains the large Purkinje cell bodies. Their axons project into the underlying white matter to the deep cerebellar nuclei or vestibular nuclei. They form the sole output of the cerebellar cortex and are therefore, the crucial cell type around which the cerebellar circuit is organized. Bergmann glia are astrocytes in the cerebellum with their cell bodies in the Purkinje cell layer and processes that extend into the molecular layer, terminating with bulbous end-feet in the pial surface. This trilaminar organization with different cell types is illustrated in Figure 25.

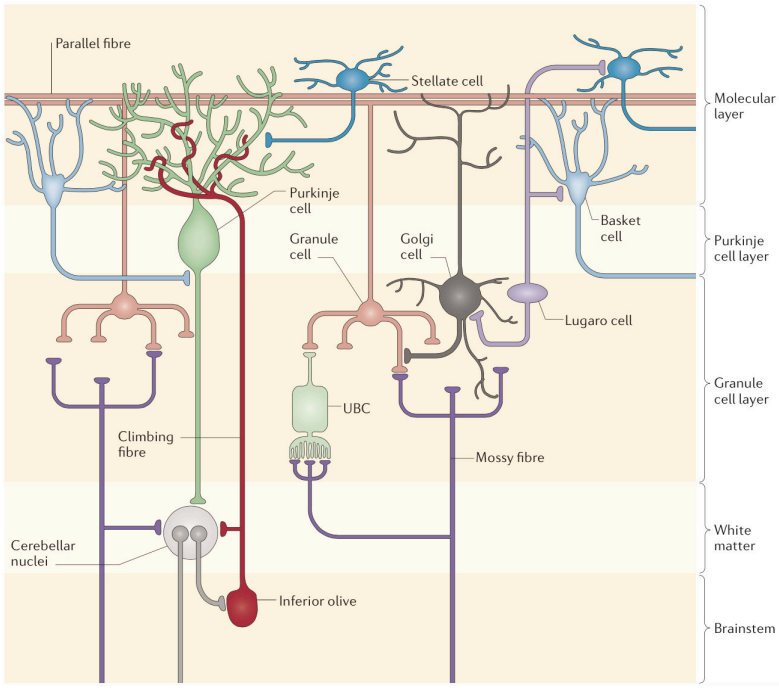


**Figure 25. Cell populations in the olivo-cerebellar network**

Illustration of different cell types in the trilaminar cerebellar cortex, with projections to and from the white matter and the brainstem *(From Cerminara et al., 2015)*

***Deep cerebellar nuclei (DCN)***

The deep cerebellar nuclei are the main output station of the cerebellum and comprise the dentate, interposed and fastigial subnuclei. They receive afferent inhibitory input from Purkinje cells and excitatory input from pre-cerebellar nuclei including the inferior olive and pontine nucleus. The output cells of DCN provide excitatory projections to their targets in the thalamus and brainstem, while a distinct group of GABAergic neurons in the DCN provide inhibitory inputs to the ION.

***Inferior olivary neurons (ION)***

The organization of the inferior olive in vertebrates was first documented in detail by Kooy in 1916. The ION resides in the medulla and consists of several sub-nuclei. The vertebrate ION is composed of three main sub-divisions: the medial accessory olive (MAO), the dorsal accessory olive (DAO) and the principal olive (PO) (Azizi & Woodward, 1987). Each sub-nucleus sends excitatory afferents that terminate within particular subsets of Purkinje cell lobules (Azizi & Woodward, 1987; Sotelo & Chedotal, 2005; Sawada et al., 2008; Reeber & Sillitoe, 2011). The MAO is composed of horizontal, vertical, and rostral lamellae. The horizontal lamella projects to a sagittal zone in the cerebellar vermal anterior lobe, the vertical lamella (further anatomically sub-divided into beta-nucleus, dorsal cap of Kooy, ventrolateral outgrowth, and dorsomedial cell column) projects to a sagittal zone in the posterior vermis and the flocculus, and the rostral lamella projects to the lateral cerebellum. The DAO is composed of two distinct lamellae, of which the dorsal part projects to the vermal anterior lobe and receives afferents from the spinal cord, whereas the ventral part projects to a sagittal zone in the intermediate cerebellum and receives afferents primarily from dorsal column nuclei. The PO also contains two lamellae, each of which projects to a specific sagittal strip in the lateral cerebellum.

### 3.3.2 Neurogenesis and migration of main cell populations

During early development in the mouse, the anterior neural tube is divided into three vesicles: the forebrain (prosencephalon), midbrain (mesencephalon) and the hindbrain (rhombencephalon). The germinative neuroepithelium in the dorsolateral rim of the hindbrain proliferates and curves to form the so-called rhombic lip. The cerebellum originates from the rostral part of the rhombic lip, referred to as the metencephalon (Hallonet & Le Douarin, 1993). The rhombic lip symmetrically develops towards the dorsal midline and merges in the rostro-caudal axis to form a transverse thickening called the

cerebellar plate, which eventually forms the roof of the 4th ventricle (Hatten & Heintz, 1995; Wang & Zoghbi, 2001). The 4th ventricle is located dorsally spanning most of the medulla in the anterior-posterior extent up until above the pontine nucleus. During development, its sidewalls are formed by the cerebellar peduncles. In mice, the development of the cerebellar cortex begins around the tenth embryonic day (E10).

Two proliferative zones of the presumptive cerebellum arise from the 4th ventricle - the cerebellar ventricular zone (VZ) from the floor of the 4th ventricle, and the external granular layer (EGL) from the roof of the 4th ventricle (Figure 26). The VZ lies at the junction of the midbrain and metencephalon. It gives rise to the DCN around E10-E12, Purkinje cells around E11-E13, Golgi cells around E16-E17, and finally the stellate and basket cells during the first two postnatal weeks (Uzman, 1960; Zhang & Goldman, 1996). The progenitors of the DCN are the first to migrate from E10 towards the dorsal rostral cerebellar surface before translocating into deeper regions (Altman & Bayer, 1985a; 1985b) (Bourrat & Sotelo, 1986). The Purkinje cell progenitors migrate along radial glial cells extending from the VZ to the pial surface and by E13, they accumulate in multiple layers in the cerebellum, organized into clusters expressing specific markers (Herrup & Kuemerle, 1997; Armstrong & Hawkes, 2000). They eventually form a monolayer soon after birth, and through changes in their cell adhesion properties, (Howell et al., 1997; Gallagher et al., 1998; Gilmore & Herrup, 2000) the clusters disperse to form parasagittal bands of cells.

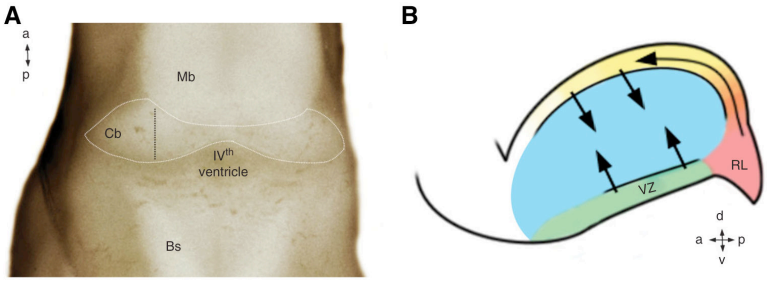


**Figure 26. Cerebellar proliferative zones**

**(A)** Dorsal view of the cerebellum at embryonic day 12 (E12). The white line outlines the cerebellum, the black line represents the sagittal section shown on the right. Mb, midbrain; Cb, cerebellum; Bs, brainstem **(B)** The two germinal zones in the cerebellar primordium (blue), the ventricular zone (green) and rhombic lip (pink). Neuronal migratory pathways are represented with arrows. Neurons arising from the verntricular zone migrate radially whereas rhombic lip-derived neurons migrate tangentially and then radially. VZ, ventricular zone; RL, rhombic lip. *(From White and Sillitoe, 2013)*

The EGL originates from the most rostral part of the rhombic lip and gives rise to the granule cell progenitors around E13. GC precursors migrate from the ependymal cells to the outer surface of the rhombic lip and tangentially accumulate in the EGL. Here, they proliferate, form processes that contact the Bergmann glia and migrate radially through the molecular layer (ML) to reach the internal granular layer (IGL) where they complete their differentiation during the first 3 postnatal weeks (Hatten & Heintz, 1995; Hatten et al., 1997)(Figure 27).

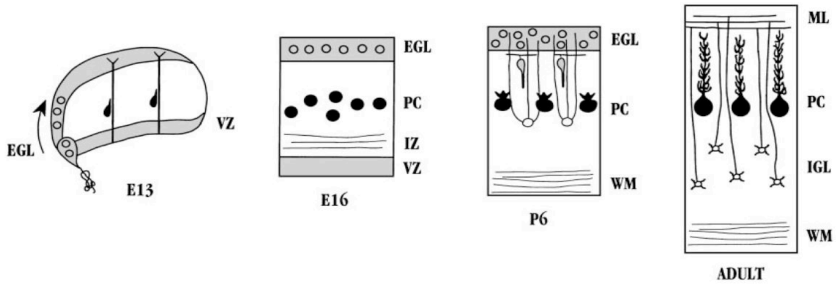


**Figure 27. Neuronal migration in the cerebellar cortex**

The Purkinje cell precursors migrate from the ventricular zone (VZ) to the intermediate zone (IZ) and eventually form the layer of Purkinje cells (PC). The granule cell precursors migrate to the surface of the rhombic lip and constitute the external granular layer (EGL). The granule cells then differentiate to form the parallel fibers, and migrate along the Bergman glia through the Purkinje cell layer to finally reside in the internal granular layer (IGL) *(From Hatten, 1999)*

In addition to the various cerebellar cells, the caudal part of the rhombic lip gives rise to the pontine nuclei and the inferior olivary neurons. Similar to the timing of origin of PCs, the olivary neurons arise around E10-11 near the roof of the 4$^{th}$ ventricle. Unlike other pre-cerebellar nuclei, they migrate from the rhombic lip to the medulla through a circumferential path and stop before crossing the floor plate at E14-E16 to form their characteristic laminated pattern of nuclear distribution (Altman & Bayer, 1987)(Bourrat & Sotelo, 1988; 1991). Around the same time as the arrest of migration and settling of IONs adjacent to the floor plate, inferior olivary axons are projected to Purkinje cell clusters in the cerebellum (Chédotal & Sotelo, 1992; Wassef et al., 1992). Other pre-cerebellar nuclei, such as the pontine (PN), lateral reticular nucleus (LRN) and external cuneate nucleus (ECN) neurons, migrate superficially from the rhombic lip in a tangential manner. The cell bodies of LRN and ECN neurons cross the midline to establish ipsilateral mossy fiber projections onto cerebellar GCs, whereas the cell bodies of most PN neurons stop at the midline and only their axons project to the contralateral cerebellum (Figure 28).

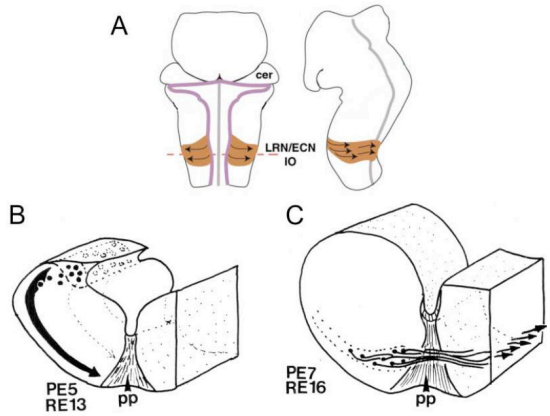


**Figure 28. Schematic representations of inferior olivary neuron migration**

**(A)** dorsal and latero-ventral views **(B, C)** transverse view. The neurons leave the rhombic lip and migrate into the sub-marginal area on the outskirts of the neural tube (A, B; arrows) and toward the floor plate (pp). Once in the floor plate, they stop but continue to migrate to develop their axons to the contralateral side (C). ECN, external cuneatus nucleus; IO, inferior olive; LRN, lateral reticular nucleus *(From Bourrat, 1992; Marillat et al., 2004.)*

The inhibitory interneurons basket and stellate cells are derived from dividing progenitors in the postnatal cerebellar white matter. These progenitors migrate into the cerebellar cortex in the first two postnatal weeks as simple unipolar cells until they reach the ML. The cell bodies of BCs and SCs are found in the lower and upper parts of the ML respectively.

## 3.4 Synaptic connectivity in the olivo-cerebellar network

In this section, I shall focus on the afferent excitatory and inhibitory inputs of the deep cerebellar nuclei and Purkinje cells, followed by a description of the developmental profile of Purkinje cell synaptic connectivity.

### 3.4.1 Deep cerebellar nuclei connectivity

These nuclei receive inhibitory inputs from Purkinje cells and excitatory inputs from Mossy fiber and Climbing fiber pathways (described in the following section). All outputs from the cerebellum originate from the DCN. There are four deep cerebellar nuclei and their anatomical locations correspond to the cerebellar cortex regions from which they receive input (Figure 29).

The fastigial nucleus is the most medially located of the cerebellar nuclei. It receives input from the vermis and from cerebellar afferents that carry vestibular, proximal somatosensory, auditory, and visual information. It projects to the vestibular nuclei and the reticular formation.

The interposed nuclei comprise the emboliform nucleus and the globose nucleus. They are situated lateral to the fastigial nucleus. They receive input from the intermediate

zone and from cerebellar afferents that carry spinal, proximal somatosensory, auditory, and visual information. They project to the contralateral red nucleus.

The dentate nucleus is the largest of the cerebellar nuclei, located lateral to the interposed nuclei. It receives input from the lateral hemisphere and from cerebellar afferents that carry information from the cerebral cortex (via the pontine nuclei). It projects to the contralateral red nucleus and the ventrolateral (VL) thalamic nucleus.

The vestibular nuclei are located outside the cerebellum, in the medulla. Hence, they are not strictly cerebellar nuclei, but they are considered to be functionally equivalent to the cerebellar nuclei because their connectivity patterns are identical to the cerebellar nuclei. The vestibular nuclei receive input from the flocculonodular lobe and from the vestibular labyrinth. They project to various motor nuclei and originate the vestibulospinal tracts.

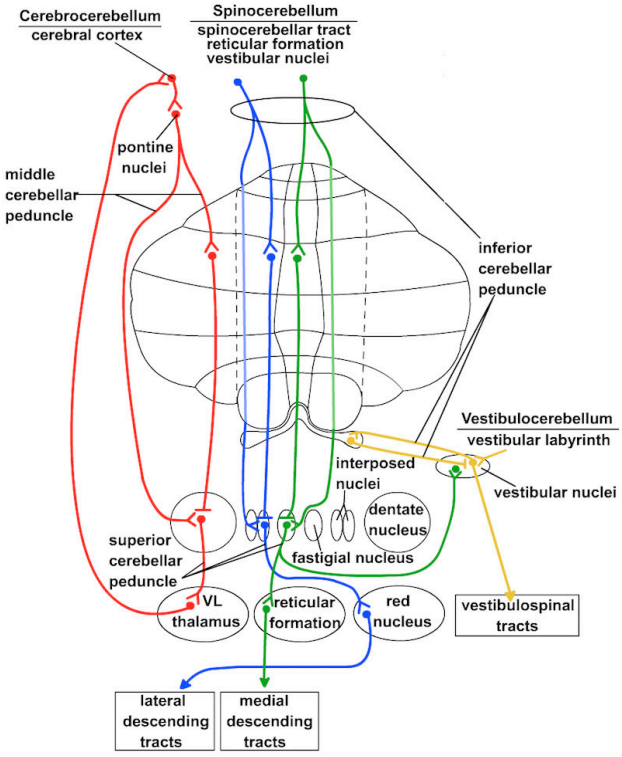


**Figure 29. Output pathways of the Deep Cerebellar Nuclei.** Details see text.

### 3.4.2 Purkinje cell connectivity

The two main types of excitatory inputs come from the Mossy fibers and Climbing fibers, while the inhibitory inputs come from stellate cells, basket cells and Golgi interneurons.

***Inhibitory synapses***

The excitatory synapse network is overlaid by inhibitory interneurons resident in the cerebellar molecular layer. The Purkinje cell receives its GABAergic inputs from the stellate cells and basket cells on different subcellular compartments (Figure 30A). About 10 stellate cells innervate 1 Purkinje cell, and form close to 1500 synapses per Purkinje cell (Korbo et al., 1993). On the other hand, 5-7 basket cells contact a single Purkinje cell and form "pinceau" synapses on PC Axon Initial Segment (AIS) (Somogyi & Hámori, 1975). A feedforward inhibition loop is formed between the basket cells, which receive excitatory stimulation from GC-Parallel fibers, and in turn inhibit Purkinje cells. This way, basket cells sharpen the time window during which Purkinje cells can fire.

The Golgi cell has an elaborate dendritic arbor in the molecular layer. Golgi cells form GABAergic axo-dendritic synapses with the GCs and propagates a feedback inhibition loop with the Mossy fiber-Granule cell glomeruli. By inhibiting the excitatory input conveyed by MFs on GCs, the Golgi cell inhibits one of the two prime input information sources coming into the cerebellar circuitry.

The Purkinje cell is the sole output of the cerebellar cortex and projects inhibitory afferents from the cerebellar cortex to the cerebellar and vestibular nuclei. From these nuclei, projections are provided to the ION for inhibitory feedback and to other extracerebellar motor and thalamic nuclei for the control of motor behaviour and cognitive functions (Granit & Phillips, 1956).

***Excitatory synapses***

The cerebellum receives extensive sensory input, and it appears to use this input to guide movements in both a feedback and feedforward control manner. In its function as a feedforward controller, the Mossy fibers (MF) may provide information regarding the desired output from motor cortex and a representation of the actual sensory state at present. MFs convey such information as: what is the current load on the muscle (proprioceptors, somatosensory receptors), what other sensory information can predict a useful response (e.g., the tone in the eye blink conditioning), what are the desired movements (motor cortex). The error signal is believed to be conveyed by the Climbing fiber (CF) inputs, which are especially active when an unexpected event occurs, such as when a greater load than expected is placed on a muscle. When the desired motor output is not achieved, the CFs signal this error and trigger a calcium spike in the Purkinje cell. The influx of calcium changes the connection strengths between Parallel fibers (PF) and

Purkinje cells, providing a teaching signal such that the cerebellum is more likely to produce the correct movement the next time the output is desired.

The CFs ascend from the ION in the medulla, traverse the pons, and enter the cerebellum through the inferior cerebellar peduncle and cerebellar white matter. In the cerebellum, they form glutamatergic synapses on PCs and DCN. Each mature PC receives input from a single CF, whereas each inferior olivary neuron sends CF afferents to about seven PCs (Schild, 1970). Each CF contacts clusters of 2-6 thorny spines on the PC proximal dendrites, ultimately forming about 250-300 synapses on each PC. In the CNS, this 1:1 PC:CF connectivity is unique to the CFs (Figure 30). The terminals of the CFs in the cerebellar cortex are arranged topographically; the axons of clusters of olivary neurons terminate in parasagittal zones that extend across the cerebellar lobules.

The MFs arising from the DCN, pontine nuclei and medulla spinalis terminate as exceptionally large rosette-shaped glomeruli on dendrites of the GCs in the granular layer. Each branch of a MF entering the granular layer produces from 20 to 50 or more rosettes (Albus, 1971). Most of the MF inputs are excitatory, except those arising from the DCN (Kandel, 2000). The GCs in turn project excitatory PFs, which branch into bidirectional T-shaped afferents to form glutamatergic synapses on PC distal dendrites, as well as dendrites of the inhibitory interneurons, the stellate cells and basket cells. Each Purkinje cell receives about 150,000-200,000 PF synapses on the more numerous and dense spines on its distal dendrites (Napper & Harvey, 1988) (Figure 30B).

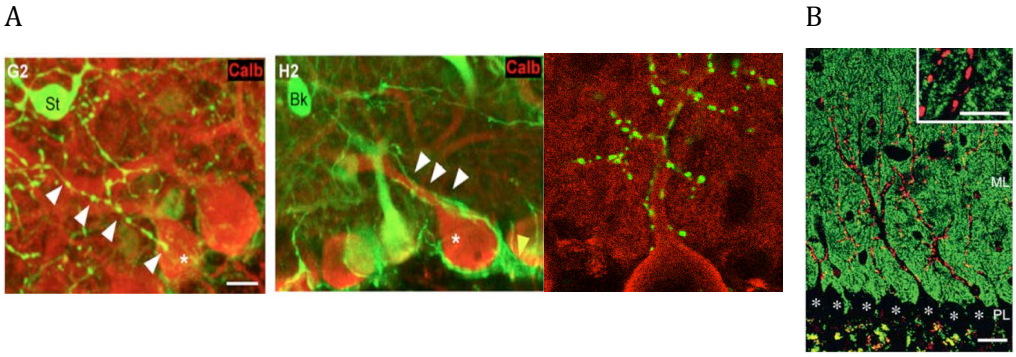


**Figure 30. Synaptic connections on cerebellar Purkinje cells**

**(A)** From left to right: Inhibitory stellate axons (green) are beaded (white arrowheads) and innervate Purkinje cell dendrites (red with asterisk). Inhibitory basket axons (green) are smooth (white arrowheads) and form pinceau synapses on Purkinje cell Axon Initial Segment (AIS) (yellow arrowhead) *(From Ango et al., 2008).* Excitatory climbing fibers (green) innervate Purkinje cell proximal dendrite (red). Scale bars, 20µm. **(B)** Excitatory afferents innervating Purkinje cells (asterisk) on distinct territories. Climbing fibers (red) innervate proximal dendrites. Parallel fibers (green) innervate distal dendrites. Scale bars, 20µm; 10µm (inset) *(From Miyazaki et al., 2003)*

### 3.4.3 Developmental timeline of synaptic connections on Purkinje cells

***Inhibitory synapses***

During development, basket cell axons are considered to be the first known GABAergic fibers to contact Purkinje cells (Yan & Ribak, 1998). Basket cells and stellate cells migrate through the Inner Granular layer (IGL) and Purkinje cell layer (PCL) to enter the molecular layer (ML) during the period of P6-P14 (Cameron et al., 2009). After entering the ML, basket cells and stellate cells sequentially exhibit four distinct phases of migration (Cameron et al., 2009). First, the cells migrate radially from the bottom of the ML to the top (Phase I). Second, the cells turn at the top, change their orientation and migrate tangentially in a rostro-caudal direction, with an occasional reversal of the direction of migration (Phase II). Third, the cells turn and migrate radially within the ML while repeatedly extending and withdrawing the leading processes (Phase III). Fourth, the cells turn at the middle and migrate tangentially, while extending several dendrite-like processes after having completely withdrawn the leading process (Phase IV) (Cameron et al., 2009). Finally, the cells stop, complete their migration and acquire their synaptic innervation territories. The Basket cells first contact PCs on their soma around P7, then cross the PCL reaching the axon initial segment (AIS) around P12 as thin terminals, and subsequently crowd around the AIS forming "pinceau" synapses around P16-18. Stellate cell axons send ascending and descending collaterals in the ML between P16–18, which further branch into a more elaborate axonal network in the following 2 weeks (Weisheit et al., 2006; Sotelo, 2007) (Figure 31).

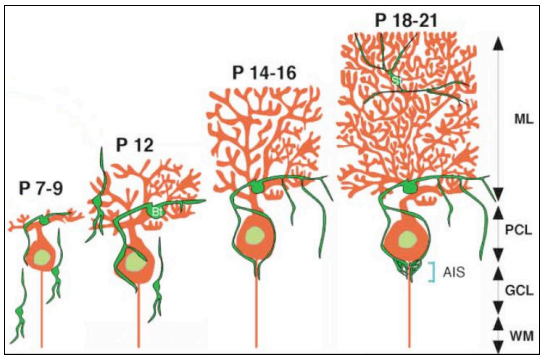


**Figure 31. Development of inhibitory basket and stellate synapses**

Schematic illustrating the formation of "pinceau" synapses by basket cells (Bt) on Purkinje cell Axon Initial Segment (AIS), and synaptic collaterals by stellate cells (St). ML, molecular layer; PCL, Purkinje cell layer; GCL, Granule cell layer; WM, white matter. *(From Ango et al., 2004)*

*Excitatory synapses*

**Climbing fiber development**

The first inferior olivary axons arrive in the developing cerebellum at ~embryonic day (E) 14/15 in the mouse (Paradies & Eisenman, 1993). Inferior olivary axons split into an average of six to seven CFs in the cerebellum that synapse onto PCs in the same sagittal plane (Sugihara et al., 2001). In the first "creeper stage" around P0-P3, CFs are thin and form transient synapses on immature PC dendrites (Chedotal & Sotelo, 1993; Sugihara, 2005; Watanabe & Kano, 2011). Between P3-5, the "pericellular nest" stage is characterized by each PC soma being innervated by more than five different CFs, which form a plexus on the lower part of the PC somata (Crepel et al., 1976; Mason et al., 1990; Chedotal & Sotelo, 1993). Between P6-P9, CFs are progressively displaced onto the apical portion of PC somata and developing dendrites, and this is called the "capuchon stage". From P9 onwards, as the PC dendritic arbors develop, the CFs leave their perisomatic and capuchon positions to occupy peridendritic positions, referred to as the "dendritic stage" (Chédotal & Sotelo, 1992). During this period, CFs translocate up the PC dendrite to find their ultimate location within the basal two thirds of the molecular layer by P21 (Crepel et al., 1976; Mariani & Changeux, 1981; Hashimoto & Kano, 2005; Watanabe & Kano, 2011). The different stages of CF innervation are illustrated in Figure 32.

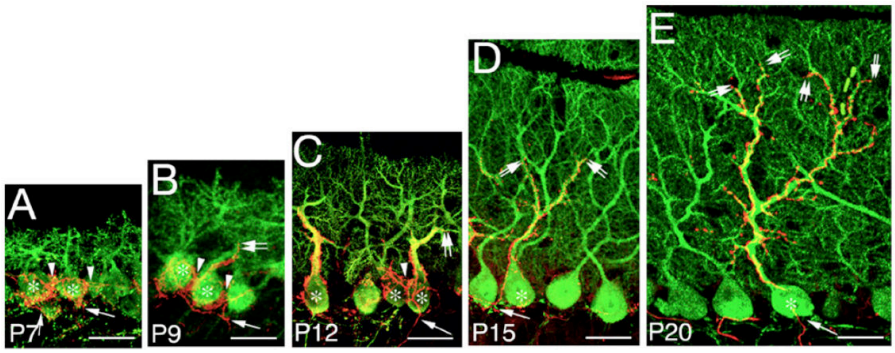


**Figure 32. Developmental profile of Climbing fiber innervation from perisomatic nest stage to peridendritic stage**

**(A-E)** Fluorescent labeling of CFs with anterograde tracer biotinylated dextran amine (red) and PCs with calbindin antibody (green) at different developmental stages. PCs are marked with white asterisks. Arrowheads point to perisomatic innervation, arrows point to dendritic innervation. *(From Hashimoto et al., 2009)*

The monoinnervation of adult CFs onto PCs is achieved through massive pruning of CFs during postnatal development. Until P3, CF-mediated excitatory postsynaptic currents (EPSCs) recorded in PCs have similar amplitudes, indicating similar synaptic strengths of

the multiple innervating CFs. In the second postnatal week, the functional differentiation of multiple CFs into a single 'winner' CF and 'loser' CFs occurs as is evidenced by one large EPSC and a few small EPSCs (Hashimoto & Kano, 2003). After the strengthening of a single "winner" CF, pruning and perisomatic synapse elimination occur in two distinct phases: the early phase (~P7–11), which is independent of PF synapses and the late phase (~P12–17), which depends on activity between PFs and PCs (Crepel, 1982; Watanabe & Kano, 2011)(Figure 33). CF activity leading to $Ca^{2+}$ influx through the P/Q-type voltage-dependent $Ca^{2+}$ channel (VDCC) in PCs triggers selective strengthening of single CF inputs. This promotes dendritic translocation of the strengthened CFs, and drives the early phase of CF synapse elimination. In contrast, the late phase of CF elimination is mediated by PF/PC synapses through two mechanisms. First, trans-synaptic interaction of presynaptic NRXN and postsynaptic GluRδ2 via CBLN1 (see section 3.5.2) consolidate structural connectivity of PF/PC synapses at distal dendrites, which eventually restrict CF innervation to proximal dendrites. Second, neural activities transmitted along the MF/GC-PF/PC pathway activate the mGluR1-PLCβ4-PKCγ signaling cascade in PCs and drives non-selective elimination of perisomatic synapses. (Kashiwabuchi et al., 1995; Hashimoto et al., 2009b; Watanabe & Kano, 2011). There has been considerable debate about the key sequential events of dendritic translocation and CF elimination. It has long been shown that spontaneous activity determines the "winner" CF that eventually undergoes dendritic translocation (Hashimoto et al., 2009a). However, a recent study claims that dendritic translocation precedes selective CF strengthening, and is the determinant of the "winner" CF (Carrillo et al., 2013).

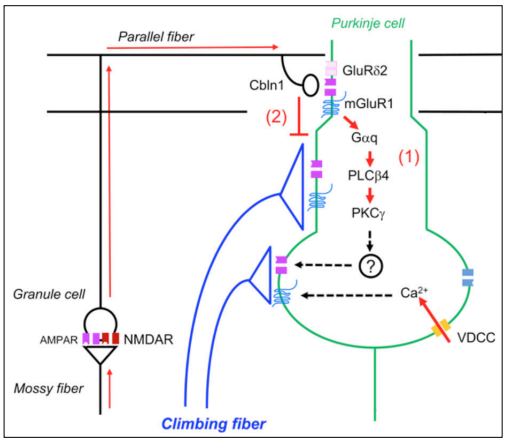


**Figure 33. Mechanisms underlying Climbing fiber synapse elimination**

The early phase is dependent on $Ca^{2+}$ influx through the VDCC. The late-phase is dependent on heterosynaptic interactions between CF and PF synapses. **(1)** Neural activity along the

MF-GC-PF pathway activates mGluR1 and downstream signaling cascades at PF/PC spines. **(2)** Stabilization of PF/PC synapses on spines of distal dendrites through Cbln1-GluRδ2 of PCs restrict the innervation sites of CFs to proximal dendrites. *(Adapted from Hashimoto and Kano, 2013)*

**Parallel fiber development**

In the developing cerebellum, granule cell migration and axon outgrowth is a key step toward establishing proper Parallel fiber connections with Purkinje cells (Figure 34). By E15, GC precursors occupy the External Granular Layer (EGL) in the cerebellum (Rakic, 1971; Hatten & Heintz, 1995). After clonal expansion in the EGL, GC precursors produce postmitotic GCs. Between P0-P3, these GCs tangentially migrate at the EGL-ML border, and have two long horizontal processes coming out from opposite sides of the soma (Rakic, 1971; Rakic & Sidman, 1973; Edmondson & Hatten, 1987). At the same time, they start to extend a vertical process from the ventral side of the soma into the ML. Then, the nucleus and surrounding cytoplasm of the GC soma enter into the short vertical process descending into the ML (Jiang et al., 2008). After the somal translocation within the vertically oriented leading process, the GC soma radially migrate toward the bottom of the ML and the horizontal processes divide in a "T" pattern in the ML to transform into oppositely directed immature PFs (Komuro et al., 2001; Kumada et al., 2009). During the second and third postnatal weeks, migration of the bulk of GCs takes place, giving rise to millions of PFs, which grow orthogonally across PCs. The development of PFs is accompanied by the formation of thin distal branches of the PC dendritic arborization. Activation of PF ''beams'' by MF afferents may play a role in coordinating the activity of PCs in the successive longitudinal compartments (Reviewed in (Thach et al., 1992)). Immature PFs form junctions with the dendritic shafts of PCs during postnatal development (Altman, 1972; 1973)(Landis & Sidman, 1978), but in adult animals the PFs form synaptic junctions exclusively on PC dendritic spines (Landis & Reese, 1974; Palay & Chan-Palay, 1974; Landis, 1987).

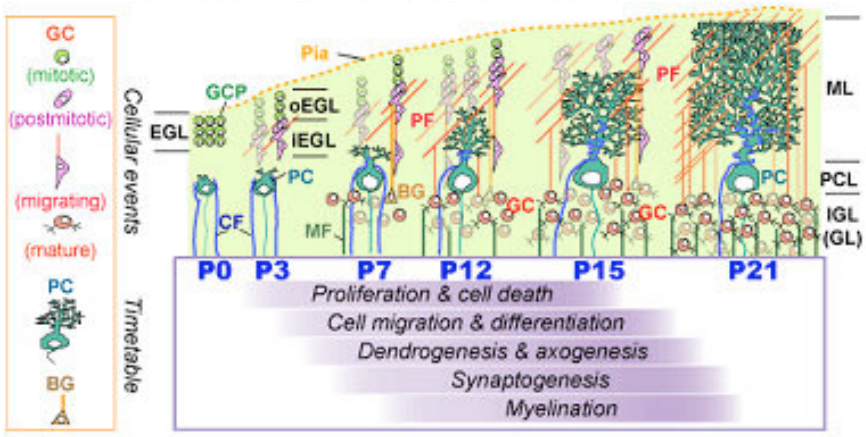


**Figure 34. Development of Parallel fibers in the cerebellum**

Postmitotic Granule cells migrate from the external granular layer towards the bottom of the molecular layer and initiate T-shaped neurite outgrowth at the EGL-ML interface which transforms into oppositely directed immature parallel fibers. From P7 onwards, Parallel fiber synaptogenesis occurs in tandem with the bulk of granule cell migration and Purkinje cell dendritic arborization. EGL, external granular layer; ML, molecular layer; PCL, Purkinje cell layer; IGL, internal granular layer; GCP, granule cell precursor; CF, climbing fiber; PF, parallel fiber; GC, granule cell; PC, Purkinje cell

## 3.5 Molecules regulating synapse specificity in the olivo-cerebellar network

As described above, PCs are innervated by different inputs synapsing onto different subcellular parts of their target. This makes PCs an interesting model to address questions of synaptic specificity in a subcellular compartmentalized manner. They receive two types of excitatory inputs (Parallel fibers from Granule cells and Climbing fibers from Inferior Olivary Neurons) and two types of inhibitory inputs (from basket cells and stellate cells in the molecular layer), which form synapses on distinct and non-overlapping territories (Figure 35). The excitatory PFs innervate the slender spines on PC distal dendrites, whereas CFs innervate thorny spines on PC proximal dendrites. The inhibitory basket cells majorly rank around the axon initial segment (AIS) forming “pinceau” synapses, whereas stellate cells’ axons target the PC dendritic shaft. Significant progress has already been made in dissecting the molecular mechanisms governing the specificity of the innervation pattern of inhibitory synapses on PCs. Using cell type specific promoters, BAC transgenic mice and known synapse-specific markers, the subcellular localization of the inhibitory synapses has been shown to be regulated by adhesion proteins from the L1 Ig subfamily (Ango et al., 2004; 2008). In case of excitatory synapse specificity, only the PF synapse identity and specificity has been shown to be regulated by members of the complement C1Q-related family (Miura et al., 2009; Matsuda et al., 2010). The PF/PC protein profile has

also been determined at its postsynaptic density using a combination of affinity purified synaptosome preparations and mass spectrometry analysis (Selimi et al., 2009). On the other hand, the mechanisms that direct the innervation of Purkinje cells by climbing fibers have yet to be understood.

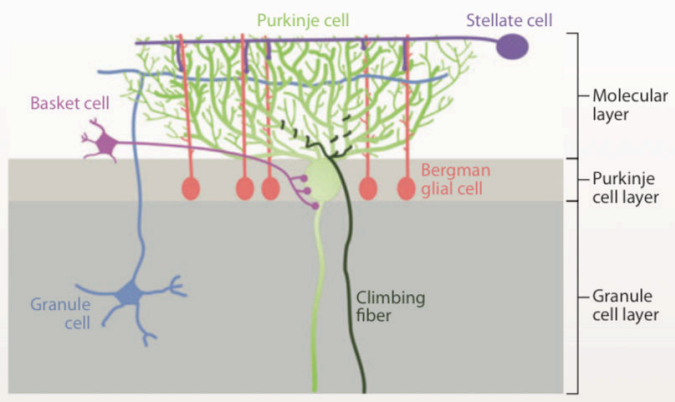


**Figure 35. Distinct synaptic innervation territories of excitatory and inhibitory afferents on Purkinje cells** *(From Sanes and Yamagata, 2009)*

### 3.5.1 Specificity at the inhibitory synapses

***Basket cell/Purkinje cell synapse***

Basket cells are the only cell type in the cerebellum to target the axon initial segment (AIS) of PCs for synaptic innervation. The AIS, where action potentials are initiated, have a high density of voltage-gated channels along with specialized anchoring proteins needed for action potential generation (Ogawa & Rasband, 2008). AnkyrinG is one such membrane adaptor protein known to be concentrated at the Purkinje AIS (Jenkins & Bennett, 2001). The L1 family of cell adhesion molecules (L1CAMs) is a subfamily of the immunoglobulin superfamily of transmembrane receptors, comprised of four structurally related proteins: L1, Close Homolog of L1 (CHL1), Neural cell adhesion molecule (NCAM), and neurofascin (Nfasc). Neurofascin is the only member of the L1CAM family known to be localized at the PC-AIS (Davis et al., 1997). The most conserved feature of L1CAMs is their ability to interact with the actin cytoskeletal adapter protein ankyrin (Davis & Bennett, 1994). Ango et al. investigated whether this interaction at the PC-AIS controls basket cell synapse formation. They showed that the restricted innervation of basket cells at the PC-AIS is indeed controlled by an alternatively spliced form of neurofascin, namely neurofascin-186 (NF-186) in an ankyrinG-dependent manner (Ango et al., 2004).

NF186, is shown to be expressed in a gradient form in PCs. It is highly concentrated in the PC-AIS and adjoining PC soma, with a gradual decrease towards the distal part of the

PC dendrite. This gradient was found to exist even before PCs receive GABAergic innervation from Basket cells. The AIS-restricted localization of NF186 depends on the binding of its cytoplasmic domain with ankyrinG. In the absence of ankyrinG, the AIS-centric gradient of NF186 is disrupted; it is now uniformly distributed along the PC axon-soma membrane (Figure 36A). This affects the directionality of incoming basket axons and as a result, they are mistargeted to distal locations. They are intact but extend beyond the AIS, and are smaller and thinner with aberrant morphology. Moreover, they fail to form normal pinceau synapses along the ectopic NF186 distribution. Thus, NF186, anchored by ankyrinG, plays a role in promoting axon growth, axon targeting as well as basket synapse formation. A schematic illustration of this mechanism is provided in Figure 36B.

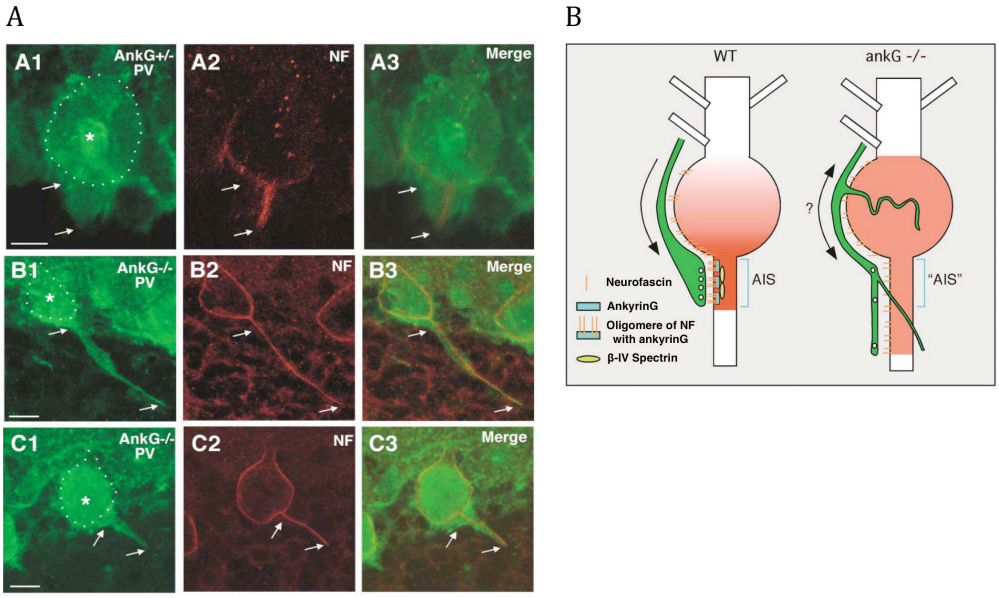


**Figure 36. Mistargeted basket axons follow ectopic Neurofascin localization in the absence of AnkyrinG**

**(A)** Double labeling of Purkinje cell (Parvalbumin in green) and NF186 (red) in P21 heterozygous control mice (A1-A3) and AnkyrinG knockout mice (B1-C3). Asterisks indicate PC soma. Arrows indicate AIS. **(B)** Schematic illustrating basket cell innervation at PC-AIS in the presence and absence of NF186 subcellular gradient *(From Ango et al., 2004)*

### *Stellate cell/Purkinje cell synapse*

The stellate cells project their beaded axons as straight ascending and descending collaterals in the molecular layer. They abruptly cut across multiple PC dendrites at sharp angles, and innervate PC dendrites. This stereotyped pattern of innervation has been shown to be controlled by another member of the L1CAM family, Close Homologue of L1

(CHL1), that is localized to Bergmann glial (BG) fibers and stellate cell somata (Ango et al., 2008). BG appear in the cerebellum even before PCs and as described by Ramon y Cajal in 1911, their fibers intercalate between the dendritic trees of successive PCs (De Blas, 1984; Altman, 1997). They are known to play an important role in the migration of GCs and PCs (Rakic, 1971). In case of stellate cells, the BG fibers are shown to act as a scaffold and mediate an axon guidance mechanism.

Stellate axons and BG fibers are closely apposed to each other. Stellate axons follow migrating BG fibers to reach the PC dendrites and form synapses preferentially at the BG-PC intersections (Ango et al., 2008)(Figure 37). The L1CAM member CHL1 is distributed in a radial pattern similar to BG fibers and this co-localization exists even before stellate cells make synaptic contacts. In the absence of CHL1, stellate axons no longer associate with BG fibers. Their morphology is abnormal, characterized by thinner wavy axons, and they lose directionality. A schematic illustration of these phenotypes is provided in Figure 37. The synapses made by these aberrant axons on PC dendrites have reduced density and stability, eventually resulting in atrophy of the axon terminals (Ango et al., 2008). The specificity of the action of CHL1 is confirmed by the presence of intact basket synapses at the PC-AIS. Thus, the localization of adhesion molecule CHL1 in BG fibers and stellate cells is needed for the proper axon targeting, as well as formation and stability of stellate synapses.

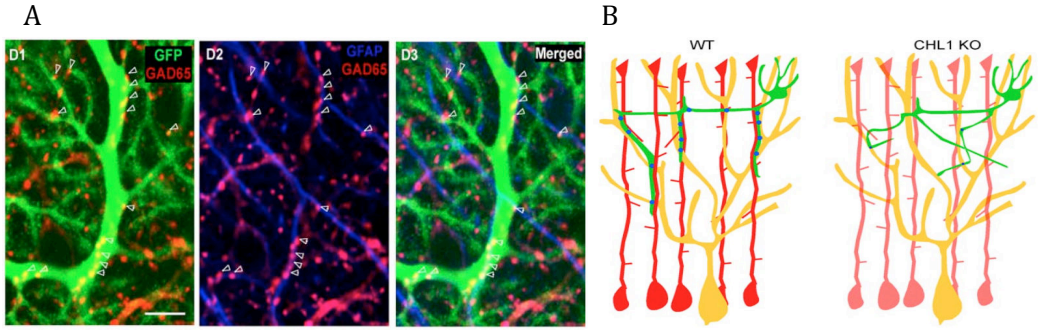


**Figure 37. Formation of stellate synapses at the intersection between Purkinje Cell dendrites and Bergmann Glial fibers**

**(A)** Triple labeling of GABAergic boutons (red), BG fibers (blue), and Purkinje dendrite (Pv-GFP green) in P44 wild type mice. **(B)** Schematic illustrating aberrant stellate synapses in the absence of CHL-1. Stellate axons (green) no longer associate with Bergmann glia fibers (red) along Purkinje dendrites (yellow) in CHL-/- mice (right) *(From Ango et al., 2008)*

Apart from L1CAMs, the formation and specificity of stellate cell synapses are also determined by postsynaptic $GABA_A$ receptors containing the α1 subunit on PCs. Deletion of

the α1 subunit gene in a knockout mouse model results in the absence of functional synaptic $GABA_A$ receptors on PCs and an associated loss of GABAergic transmission (Kralic et al., 2005; Fritschy et al., 2006). Despite this, only the inhibitory stellate cell synapses on PC dendrites are selectively impaired while the perisomatic inhibitory basket cell synapses are retained with normal symmetric synapse morphology (Fritschy et al., 2006). Moreover, the 75% of the stellate cell terminals in the molecular layer of the mutant mice form uncharacteristic large asymmetric synapses on several PC spines that contain GluRδ2, which is selectively located at the PF PSD (Figure 38). This implies the role of $GABA_A$ receptors in conferring a synapse identity to stellate cells. The differential alteration of inhibitory synapses formed by stellate and basket cells onto PCs, appears only in adult mutant mice; GABAergic terminals form normally during development at P10 and P14. This suggests that the absence of $GABA_A$ receptor-mediated neurotransmission affects only the maturation and not formation of stellate cell terminals in the molecular layer.

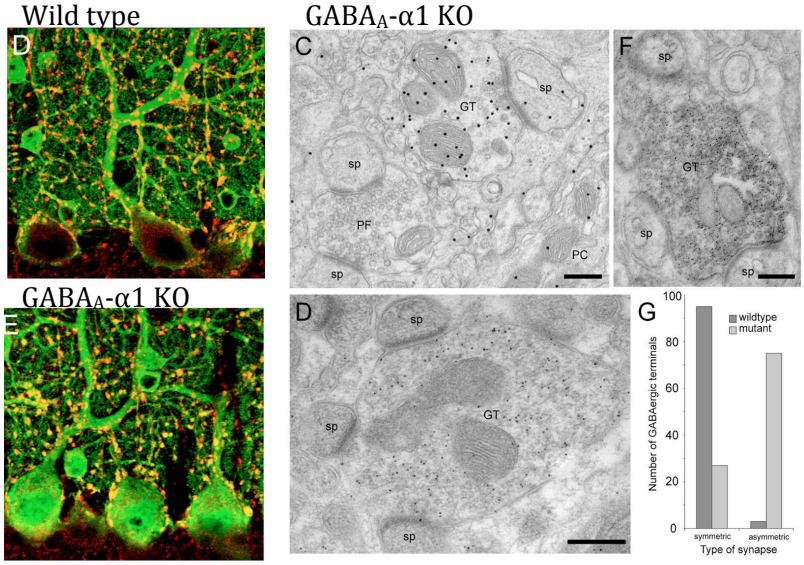


**Figure 38. GABA ionotropic receptors in stellate cell synapse identity and maintenance**

**(Left)** Double immunostaining for parvalbumin to label Purkinje cell dendrites (green) and vesicular inhibitory amino acid transporter (VIAAT), a postsynaptic GABA synapse-specific marker (red) in adult wild type and $GABA_A$-α1 KO mice, showing larger VIAAT positive GABA terminals (yellow) in mutant mice **(Right)** Immunogold labeling of GABA (C), VIAAT (D) and immunoperoxidase staining for parvalbumin (F) in the molecular layer of $GABA_A$-α1 KO mice illustrating formation of asymmetric GABA terminals with PC spines. Scale bars, 300nm. GT, GABAergic terminal; sp, PC spine. *(From Fritschy et al., 2006)*

### 3.5.2 Specificity at the excitatory synapses

#### *Parallel fiber/Purkinje cell (PF/PC) synapse*

Glutamate receptor delta 2 (GluRδ2) was initially identified as an orphan receptor subunit selectively expressed in cerebellar PCs (Araki et al., 1993). Mice that lack GluRδ2 suffer from ataxia and exhibit the following defects at the synaptic level: PC distal dendrites lack synaptic contact with PF terminals thus generating free spines, and the remaining PF synapses exhibit an impairment of LTD resulting in motor learning deficits (Takeuchi et al., 2005). Furthermore, RNAi had a similar LTD-like effect (Hirano et al., 1994; Uemura et al., 2010). In addition, the lack of PF synaptic contact leads to CF invasion of PF territory and the formation of ectopic CF synapses on distal dendrites. Mismatched synapses are formed more on proximal dendrites, characterized by a longer PSD length than the active zone (Hashimoto et al., 2001; Ichikawa et al., 2002; Uemura et al., 2007). A schematic illustration of these phenotypes is provided in Figure 39A. The PF/PC synapse morphological and functional phenotypes can be rescued by the reintroduction of full-length GluRδ2. However GluRδ2 that lacks the N-terminal domain (NTD) only restores LTD (Kakegawa et al., 2009). GluRδ2 interacts intracellularly with PDZ-domain containing proteins like PSD93 and PTPMEG (Yuzaki, 2003) and extracellularly with the extracellular domain (ECD) of Neurexin-1beta (NRXN1β) containing splice segment S4 expressed in the cerebellum via cerebellin 1 (CBLN1) (Uemura et al., 2010).

A B

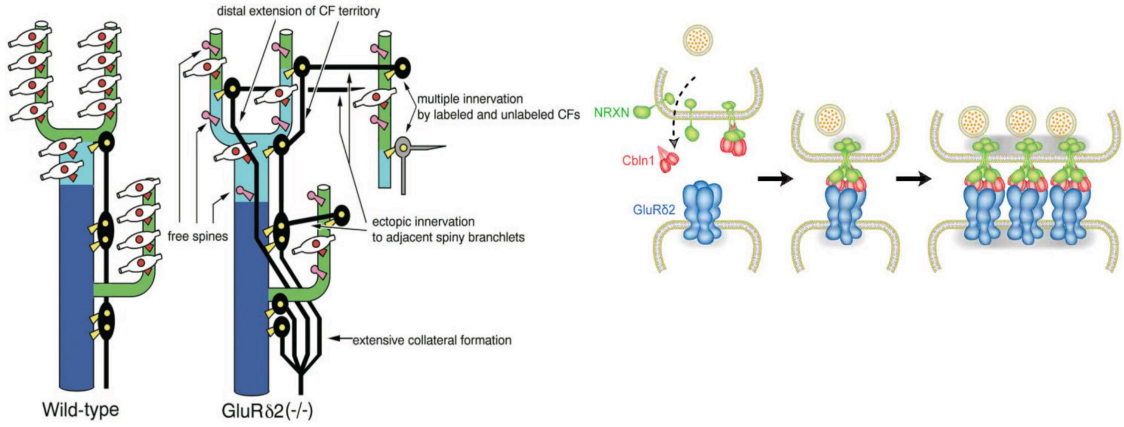


**Figure 39. Molecular mechanism of Parallel fiber/Purkinje cell synapse formation**

**(A)** Schematic illustrating the summary of CF and PF phenotypes in the GluRδ2 knockout mouse *(From Ichikawa et al., 2002)* **(B)** Schematic illustrating the formation of PF synapse by GluRδ2 by clustering four NRXNs through triad formation *(From Mishina et al., 2012)*

CBLNs were identified in rat cerebellar crude synaptosome fractions about 30 years ago (Slemmon et al., 1984). A reduction of CBLN in weaver mice was the first indication that GC migration and innervation of PCs played a role in controlling the expression of this protein (Morgan et al., 1988). There are four CBLN proteins, of which CBLN1 and CBLN3 are selectively expressed in the cerebellum (Miura et al., 2006), and CBLN1 is secreted by GCs. Related to the C1q and TNF families, CBLNs are post-translationally modified (glycosylated). They are then secreted and assemble as a trimer through their globular C1q domain (Kishore et al., 2004). The functional roles of CBLN1 were demonstrated in knockout (KO) and conditional deletion models (Hirai et al., 2005; Yuzaki, 2008; Uemura et al., 2010). The CBLN1 KO phenotype closely resembles the GluRδ2 KO phenotype at the synaptic morphological and functional levels. Loss of CBLN1 in the KO mice leads to ataxia, reduced number of PF terminals, diminished LTD, free spines in the distal dendrites, mismatched spines in the proximal dendrites and ectopic CF synapses in PF territory (Hirai et al., 2005). This suggested the interaction between presynaptic CBLN1 and postsynaptic GluRδ2 (Hirai et al., 2005; Matsuda et al., 2010; Uemura et al., 2010).

Subsequent *in vitro* experiments demonstrated a bidirectional role for CBLN1 at the PF/PC synapse. CBLN1 secreted at the synaptic cleft binds postsynaptically to the N-terminal domain (NTD) of GluRδ2, and this interaction affinity increases in a CBLN1-dependent manner (Matsuda et al., 2010). Moreover, the interaction of GluRδ2 with NRXN1β occurs only in the presence of CBLN1 (Uemura et al., 2010). At the PF/PC synapse, CBLN1 plays the following roles: it induces presynaptic terminals and postsynaptic GluRδ2 clusters, it induces clustering of other postsynaptic receptors in the presence of GluRδ2 (Matsuda et al., 2010), and it stimulates the maturation of presynaptic boutons to match the size of the PSD (Ito-Ishida et al., 2012). GluRδ2 induces presynaptic differentiation by interacting with NRXN1β through CBLN1 in the form of a synaptogenic triad (Lee et al., 2012). This triad consists of one molecule of tetrameric GluRδ2, two molecules of hexameric CBLN1 and four molecules of monomeric NRXN. A schematic illustration of this mechanism is provided in Figure 39B.

CBLN3 is co-expressed with CBLN1 in cerebellar granule cells (Pang et al., 2000; Hirai et al., 2005; Miura et al., 2006). This co-expression is necessary for the trafficking and secretion of CBLN1 after exiting the endoplasmic reticulum (Iijima et al., 2007). CBLN3 has also been shown to colocalize with CBLN1 at the synaptic cleft of PF/PC synapses (Miura et al., 2009) but there has been no direct evidence for the functional role of CBLN3 in PF/PC synaptogenesis.

### *Climbing fiber/Purkinje cell (CF/PC) synapse*

Unlike PF synapses, the molecular mechanisms regulating the formation and specific connectivity of CF synapses are not well understood. As described earlier, during the late phase of CF elimination, PF/PC synapse formation and stabilization in Purkinje cell distal dendrites play a role in restricting CF innervation to proximal dendrites. GluRδ2 is expressed by both the PF/PC and CF/PC synapses during development, and becomes restricted to the PF/PC synapses after P14 (Zhao et al., 1998). Multiple CFs contact PCs on their somata, and surplus redundant CFs are eventually eliminated until a 1:1 connectivity is established by the end of the third postnatal week (Crepel et al., 1976). Initially, GluRδ2 was thought to play a role in this elimination process during development. Studies involving mutant mice models showed that the targeted disruption of GluRδ2 led to persistent multiple CF innervation of PCs and ataxia (Kashiwabuchi et al., 1995; Ichikawa et al., 2002). Multiple CFs also persist in mGluR1 KO mice models but they do not invade the distal dendrites of PCs, normally innervated by PFs (Hashimoto et al., 2001). In contrast, the loss of GluRδ2 leads to reduced PF/PC synapse density and a consequent ectopic invasion of CFs into PF territory (Uemura et al., 2007)(Figure 40). This led to the speculation that GluRδ2 is needed not only to stabilize PF/PC synapses, but also to restrict CF/PC synapse innervation territory. However, pharmacological and lesion studies invalidate this. Upon blocking CF activity by tetrodotoxin, a large number of new spines appear on the proximal PC dendrites (Rossi & Strata, 1995; Bravin et al., 1999). Moreover, in the absence of CF activity, GluRδ2 appears in the postsynaptic densities of the proximal dendritic spines, which then lose their contact with CFs and become ectopically innervated by PFs (Morando et al., 2001). When the CF blockade is removed, CFs transiently reinnervate the proximal spines expressing GluRδ2. This is also observed during the reinnervation period following an inferior olivary lesion (Cesa et al., 2003). Thus, while GluRδ2 and activity play a role in the heterosynaptic competition between PFs and CFs and maintenance of their respective innervation territories, the molecular cues that play an instructive role in defining CF innervation territory remain elusive.

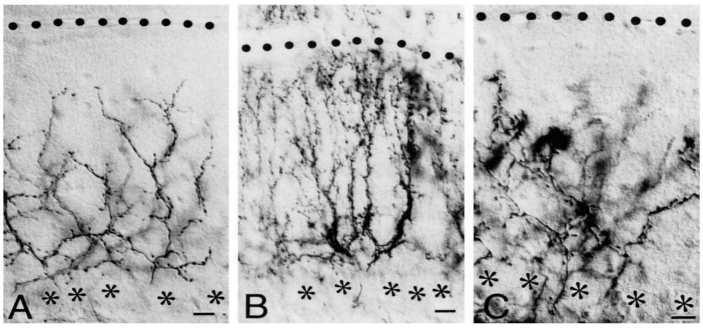


**Figure 40. Aberrant Climbing fiber/Purkinje cell synapse morphology in the absence of receptors GluRδ2 and mGluR1**

Anterogradely labeled CFs showing **(A)** Normal morphology in proximal dendrites of wild-type mice **(B)** Distal invasion of PF territory by CFs in GluRδ2 mutant mice **(C)** Lack of CF elimination and persistence of multiple innervation in CF territory in mGluR1 mutant mice. Dotted lines indicate the pial surface of the molecular layer. Asterisks indicate PC somata. *(From Hashitomo et al., 2001)*

# RESULTS

## 1. The two excitatory inputs targeting the Purkinje cell have distinct gene expression profiles

### Introduction

Molecules engage in trans-synaptic signaling to play a key role in the assembly and identity of a synapse in both vertebrate and invertebrate systems. A number of membrane and secreted adhesion proteins have been shown to function as synaptic organizers, such as the transmembrane cadherins, neuroligins, leucine-rich repeat proteins (LRRTM) as well as the secreted WNTs, cerebellins and pentraxins (Dalva et al., 2007; Shen & Scheiffele, 2010). In some cases, the same molecule is found at different synapse types, with different interacting partners. For example, presynaptic neurexins interact with postsynaptic neuroligins 1/3 and LRRTM proteins at excitatory synapses, and with neuroligin 2 at inhibitory synapses (Südhof, 2008; Linhoff et al., 2009). Given this molecular diversity, it is likely that no two synapses harbour the exact same combination of molecules. This has been postulated 40 years ago, as the "chemoaffinity hypothesis" by Sperry (Sperry, 1963), positing that different combinations of molecules encode the specificity of neuronal connections, implying the existence of a ''molecular synaptic code.''

Using the olivo-cerebellar network as a model system, we test the hypothesis that two excitatory synapses formed on the same target neuron are defined by a unique combination of molecules. The cerebellar Purkinje cells (PC) receive two inhibitory inputs (from stellate cells and basket cells) and two excitatory inputs (Parallel fibers from granule cells and Climbing fibers from inferior olivary neurons). The specific synaptic targeting of the two inhibitory inputs has already been shown to be established by members of the L1CAM subfamily (Ango et al., 2004; 2008). Whereas the molecular mechanisms underlying the specific synaptic targeting of the two excitatory inputs have yet to be understood. Moreover, unlike the Parallel fiber synapse, until very recently, nothing was known about the molecules that regulate the formation and specificity of the Climbing fiber/Purkinje cell (CF/PC) synapse.

To investigate whether each PC excitatory afferent expresses a unique combination of proteins that could contribute to synapse identity, I first compared the gene expression profiles of the Inferior Olivary Neurons (ION) and Granule Cells (GC). Through this comparison, I identified biological pathways enriched at each input cell population. Second, to determine whether these pathways are developmentally regulated, I selected a few candidate genes from the most enriched pathways to characterize their expression pattern

in the developing olivocerebellar network. Finally, using the gene expression data, I selected a few candidate genes that could potentially control the formation and specificity of the CF/PC synapse.

The comparative analysis of gene expression profiles of the ION and GC in adult mice revealed differences in terms of differentially enriched genes and biological pathways. The IONs express a higher percentage of genes coding for membrane and secreted proteins while the GCs express a higher percentage of genes coding for nuclear proteins and transcription factors. Immune system-related pathways are significantly enriched in the ION compared to GCs. In particular, genes related to the complement cascade are differentially expressed in the ION and GCs. The timing and pattern of expression of these complement-related genes in the ION and GC in the developing olivo-cerebellar network indeed match with the timing of formation of excitatory synapses on their target PCs. These results suggest that the specific connectivity of the two excitatory synapses could indeed be due to differences at the presynaptic level, and complement system-related molecules differentially expressed by the presynaptic cell populations could contribute to the identity of the two excitatory synapses.

## Experimental procedures

### *BacTRAP experiments and scheme for global comparison of ION and GC gene lists*

To obtain the genetic profiles of the two input cell populations, the ION and GCs, we employed the bacterial artificial chromosome Translating Ribosome Affinity Purification (bacTRAP) approach (Doyle et al., 2008; Heiman et al., 2008). Using cell-type specific promoters, separate transgenic mouse lines were generated for the specific expression of a GFP-fusion protein in the ION and GC. The fusion protein was obtained by tagging eGFP to the N-terminal of the large subunit ribosomal protein L10a. The polysomes that contained the eGFP-L10a transgene were then immunoprecipitated from each mouse line using beads coated with anti-GFP antibody. This step allowed the immunoaffinity purification of translating mRNAs from the ION and GC, which formed the IP fraction of each cell population. The polysomes that did not contain the eGFP-L10a transgene formed the unbound fraction (UB) of the immunoprecipitation and indicated the genes expressed in the dissected region as a whole (brainstem or cerebellum). For microarray analysis, immunoaffinity purified translating mRNAs were amplified and labeled using the GeneChip Expression 3' Amplification 2-Cycle cDNA Synthesis Kit (Affymetrix) and hybridized to

GeneChip Mouse Genome 430 2.0 microarrays (Affymetrix) according to manufacturers' protocols.

The GC gene expression profile had already been described using NeuroD1 bacTRAP transgenic mouse line, already generated and maintained by the Heintz laboratory at Rockefeller University (Doyle et al., 2008). The ION transcriptome was obtained from two bacTRAP transgenic mouse lines using two different promoters S100a10 and Cdk6 (Figure 1A). The previously described S100a10 mouse line (Schmidt et al., 2012) drove GFP-L10a expression in the entire ION, but also labeled other brainstem neurons like the hypoglossal nucleus and dorsal motor nucleus of the vagus nerve. In contrast, GFP-L10a expression using the Cdk6 BAC driver was restricted to the ION, but targeted only specific sub-nuclei of the ION, namely the medial accessory olive (MAO), the dorsal accessory olive (DAO) and the dorsal part of the principal accessory olive (PAO) (Figure 1A). This Cdk6-driven expression pattern was consistent with previous GENSAT reports (http://www.gensat.org). Therefore, genes commonly enriched in both s100a10 and cdk6 were chosen for functional and pathway analyses. This increased the stringency of probing for ION-specific genes and eliminating background expression from the brainstem.

Two criteria were simultaneously considered to obtain a list of genes enriched specifically in the ION and GC. First, the gene expression in the immunoprecipitated cell type (IP) and the dissected tissue sample (UB) was compared, generating an IP/UB ratio. Second, the gene expression in the two immunoprecipitated cell types was compared, generating an IP/IP ratio. A different threshold was applied to select genes from each of these comparisons. A lower threshold (≥ -1.5) was applied to the IP/UB comparison since this ratio represented a baseline level of gene expression, and was used to select genes with a high level of expression and high degree of specificity in the ION compared to other cell types in the brainstem. In contrast, a higher threshold (≥ 5) was applied to the IP/IP comparison since it was critical to obtain a high level of input cell specificity of gene expression. Using these criteria, common genes were selected between the IP/IP and IP/UB comparisons and constituted the final gene list for each cell type. From each of these ION and GC final gene lists, genes with a microarray threshold ≥ 5 were shortlisted and compared with each other to identify genes that were specifically enriched in each cell population. This scheme of sequential comparison is illustrated in Figure 1B.

***Bioinformatics-aided analysis of ION and GC gene lists***

To get an idea of which functional groups are enriched in the ION and GC gene lists, functional classification and clustering of ION and GC-specific genes were first performed using DAVID (Database for Annotation, Visualization and Integrated Discovery) Functional Annotation Clustering tool (http://david.abcc.ncifcrf. gov/) (Dennis et al., 2003; Huang et al., 2008). The probe set description provided by Affymetrix was used by this tool to add annotations to the submitted gene list. Unannotated genes, which were anyway included in the output, were then manually annotated. The SP_PIR_KEYWORDS functional annotation category was selected to generate a clustered chart report of annotation terms. Genes with functionally related annotations are clustered into groups according to the group enrichment score. The enrichment score is calculated as the geometric mean of all the enrichment P-values of each annotation term in the group. Second, to further investigate key pathways linked to these enriched genes, gene classification was done using the KEGG pathway map on the DAVID software, and the PANTHER tool for gene classification (http://www.pantherdb.org/) (Mi et al., 2013). Since PANTHER is part of the GO reference genome project, the Gene Ontology (GO) terms are used for gene classification. Genes which code for a protein involved in more than one biological pathway are classified according to 2 ontology terms, hence resulting in the same gene appearing in two different classes of biological processes. Third, in order to find expression regulators of genes enriched in the ION and GC, I applied the « Find Subnetworks Enriched with Selected Entities » algorithm in Pathway Studio 11.0.5 (Nikitin et al., 2003). The p-value of each enriched sub-network depends on the overlap of the sub-network with the input entities list calculated by Fisher's exact test.

***RTqPCR***

For RTqPCR, RNA samples were obtained from mixed cerebellar cultures using the RNeasy Mini kit (QIAGEN, Hilden, Germany), cDNA were amplified using the SuperScript® VILO™ cDNA Synthesis kit (Life technologies, Paisley, UK) according to manufacturer's instructions. Quantitative PCRs were done using the TaqMan Universal Master Mix II with UNG (Applied Biosystems, Courtaboeuf, France) and the following TaqMan probes: Nrxn3 (#4448892_Mm04279482_m1), Il16 (#4448892_Mm00516039_m1), Ppp3ca (#4448892_Mm01317678_m1), Nck1 (#4448892_Mm00834053_m1), Crtam (#4448892_Mm00490300_m1), Ifngr2 (#4448892_Mm00492626_m1), B2m (#4448892_Mm00437762_m1), H2-Aa (#4331182_Mm00439211_m1), Ifi27l1

(#4331182_Mm00835449_g1), Ifitm1 (#4448892_Mm00850040_g1), Cbln1 (#4448892_Mm01247194_g1), Cbln3 (#4448892_Mm00490772_g1), Cbln4 (#4448892_Mm00558663_m1), C3 (#4448892_Mm00437838_m1), C1ql1 (#4448892_Mm00657289_m1), Susd4 (#4331182_Mm01312134_m1), Rpl13a (#4331182_Mm01612986_gH).

***In situ hybridization***

For Susd4, fresh frozen sections of 20µm thickness were prepared from mouse brains at postnatal day 0 (P0), P7 and P21 using a cryostat. The riboprobes were used at a final concentration of 0.05 µg/µL, and hybridization was done overnight at a temperature of 72°C. The anti-digoxigenin-AP antibody was used at a dilution of 1/5000. Alkaline phosphatase detection was done using BCIP/NBT colorimetric revelation. For Cbln1, Cbln4, C1ql1, in situ hybridization was performed using a previously described protocol with a few modifications (Bally-Cuif et al., 1992). PFA-fixed freely floating vibratome sections were obtained (100 µm thickness) from mouse brains at postnatal day 0 (P0), P7 and P21. The riboprobes were used at a final concentration of 2 µg/µL. The proteinase K (10µg/mL) treatment was given for 30 seconds for P0 and P7 brain sections, and 10 minutes for P21 brain sections. The anti-digoxigenin-AP antibody was used at a dilution of 1/2000. The probe sequences corresponded to the following nucleotide residues for the indicated mouse cDNA: 641-1200 bp for C1ql1 (NM_011795.2), 287-1064 bp for Susd4 (NM_144796.4), 716–1702 bp for Cbln1 (NM_019626.3), 1609-2405bp for Cbln4 (NM_175631.3). Images were acquired using a brightfield microscope (Leica DMRB) using 10x objective (pixel size 670 nm).

**Results**

***High diversity of differentially expressed genes coding for membrane and secreted proteins in the ION and nuclear proteins in the GC***

The gene expression profiles for all the major cerebellar cell types, including granule cells and Purkinje cells, have already been described using the bacTRAP method (Doyle et al., 2008). Our laboratory generated the ION gene expression profile. The microarray gene expression data specific to the ION and GC were analyzed using the GeneSpringGX software (Version 11.5). The cdk6 promoter drives the expression of the eGFP-L10a transgene in a more specific and restricted manner in the ION compared to s100a10. Accordingly there were more genes identified from the s100a10 cell line. To decrease the number of false

positives, gene lists from both the s100a10 and Cdk6 cell lines were pooled. 598 and 401 genes were specifically enriched in the ION and GC populations respectively. First, I confirmed that known markers of the ION and GC, such as VGluT2 and VGluT1 respectively, were specifically enriched in the corresponding cell populations (Figure 1C).

Then, I proceeded with the functional classification of the ION and GC gene lists using the DAVID functional annotation clustering tool. This tool identified 151 functionally annotated clusters from the ION gene list and 109 clusters from the GC gene list. Among these, the top 10 annotation clusters are listed in Table 1. Differentially expressed genes coding for membrane, secreted and nuclear proteins are found both in the ION and GC. However the IONs are more complex in the diversity of genes (250 genes) coding for membrane and secreted proteins while the GCs are more complex in the diversity of genes (142 genes) coding for nuclear proteins (Figure 2A). Given that many membrane and secreted adhesion molecules are already known to regulate synaptogenesis and control synapse specificity through their protein interaction domains (Shen & Scheiffele, 2010), we were particularly interested in the genes coding for membrane and secreted proteins differentially expressed between the ION and GC.

The IONs express about three times as many genes coding for membrane and secreted proteins compared to GCs. Among 250 ION-specific genes coding for membrane and secreted proteins, two categories are predominantly enriched – 30 genes coding for cell adhesion molecules and 70 genes coding for immune system-related molecules. (Figure 2B).

A large diversity of cell adhesion molecules is found in the ION. Various protein families such as nectins (Eg. PVRL2), cadherins (Eg. CDH9, CDH13), protein tyrosine phosphatase receptors (Eg. PTPRN, PTPRO), immunoglobulin superfamily (Eg. IgSF3), ephrins (Eg. EPHA4, EFNA3), lectins (Eg. LGALS3, MBL2), ADAM family of metalloproteases (Eg. ADAM11, ADAM23), leucine-rich repeat proteins (Eg. LGI2, LRFN5) and Adhesion G-protein coupled receptors (Eg. BAI1, GPR123, EGFL7) are expressed by the ION. In contrast, among 74 GC-specific genes coding for membrane and secreted proteins, only 5 genes encode cell adhesion molecules. These include members of the neurexin (Eg. NRXN3), cadherin (Eg. CDH15), lectin (Eg. CLEC10A), syndecan (Eg. SDC1) and integrin (Eg. ITGAV) families (Figure 2B). Table 2 lists all the cell adhesion molecules found specifically in the ION and GC with their corresponding microarray fold change values in the s100a10 and cdk6 mouse lines. Most of the ION-specific immune system related genes are those directly involved in the complement cascade (Eg. C3, MASP1), those related to the

complement cascade (Eg. C1Q/TNFα family of secreted proteins), and cytokine signaling pathways (Eg. members of the PDGF, IFN, IL and chemokine families).

Thus, the comparative analysis of gene expression profiles of the ION and GC in adult mice revealed that the two cell populations are fundamentally different in terms of the expression of genes and that the ION is more complex in the diversity of genes encoding membrane and secreted proteins.

***Immune system-related processes are enriched in the ION compared to GCs***

To investigate key pathways linked to genes specifically enriched in the ION and GC, gene classification was done using the KEGG pathway map on the DAVID software and the PANTHER tool. Both the bioinformatics tools confirmed that both the ION and GC are enriched with immune system-related genes, albeit with a 2.5-fold higher representation in the ION compared to GC (Figure 3A). These include genes coding for both innate and adaptive immunity-related pathways. This result included two main features. First, both the ION and GC are specifically enriched with different immune system-related genes belonging to the same biological processes, such as cell adhesion (as mentioned in the previous section) and complement system-related processes. I will describe this result further in the next section. Second, different immune system-related processes are uniquely prevalent in each cell population. Due to the relatively lower number of immune system-related genes in the GC population, there is no major over-representation of any particular signaling pathway. The GC-specific immune system genes belong to pathways related to T-cell activation, B-cell activation, cytokine inflammatory responses and Wnt signaling (Figure 3B). The Sub-Network Enrichment Analysis by Pathway Studio revealed a significant number of these genes to be regulated by the anti-inflammatory cytokine TGFB1 and MAPK (Figure 4A). In the ION, there is a striking enrichment of cytokine inflammatory responses in particular (Figure 3B). These include genes encoding chemokines, hematopoietins, and members of the PDGF, IFN, IL and TNF families. A significant number of these cytokine signaling genes belong to the IFNγ signaling pathway. These include inhibitors of IFNγ (Eg. IL10RB, IFNGR2, TGFBR2, TGFBI) as well as downstream signaling molecules of IFNγ like chemokines and MHC molecules (Eg. TAPBP, B2M, CCL5, H2A-A). This was further validated by the Pathway Studio analysis, which identified pro-inflammatory cytokines TNF and IFNγ as the top two expression regulators of the ION-specific immune system-related genes (Figure 4B). Table 3 lists the immune system-related

genes enriched in the ION and GC with their corresponding microarray fold change values in the s100a10 and cdk6 mouse lines.

Since the bacTRAP microarray data were representative of gene expression in the adult olivocerebellar network, online expression databases were consulted to confirm the adult expression pattern and to check for developmental expression pattern. The expression data of a few immune system-related genes in both the ION and GC-specific lists are available in the developing and adult mouse brain in two major in situ hybridization databases online, the GENSAT/Brain Gene Expression Map (http://www.ncbi.nlm.nih.gov/projects/gensat/; http://www.stjudebgem.org/) and Allen Brain Atlas (http://www.brain-map.org). For example, the expression of ION-specific *Htr5b* is detected at the mRNA level in the ION starting from embryonic stage E13.5. In case of some other genes, like the GC-specific *Nrxn3* for example, only the adult mouse expression data is available online. Thus, to supplement this online expression data, we performed RTqPCR analysis to check the expression pattern in the developing olivo-cerebellar network. I selected a few genes belonging to the GC-enriched T-cell and ION-enriched IFNγ signaling pathways and characterized their expression in mouse cerebellar and brainstem extracts at different ages. In the first postnatal week, the cerebellar Purkinje cells are contacted only by Climbing fibers from the ION. The second and third postnatal weeks are characterized by the specific establishment of synaptic connectivity by the Climbing fibers and GC-originating Parallel fibers on Purkinje cells. Accordingly, we observed that the expression of GC-specific genes in cerebellar extracts is low during the first postnatal week and sharply increases starting at P7 (Figure 4A). This developmental expression pattern was seen to correlate with the in situ hybridization data available online for select genes. For example, the online data for *Il16* reveals an especially strong expression in the GCs at P14 and adult compared to earlier developmental stages. Likewise, RTqPCR analysis detects a peak in *Il16* expression in cerebellar extracts at P14 after which it plateaus till adulthood, and no expression is detected in brainstem extracts. Similar to *Il16*, the expression of *Crtam* and *Nck1* increases in cerebellar extracts starting at P7, and is not detected in brainstem extracts. In situ hybridization data online reveals the expression of *Ppp3ca* and *Nrxn*3 in the adult mouse brain to be strong in the cerebellum as well as faint in the brainstem. Accordingly, RTqPCR analysis detects the expression of *Nrxn3* and *Ppp3ca* in cerebellar extracts with an increase at P7 reaching high levels at P14 and adulthood, and in brainstem extracts throughout development. In contrast, none of the five selected ION-specific genes have developmental expression data available online. In the adult mouse

brain, in situ hybridization data online reveals expression of *B2m* in the ION, and *Ifngr2* in the ION and PCs. RTqPCR analysis corresponds to this pattern in the case of *Ifngr2*, as expression is detected at comparable levels in both the adult cerebellar and brainstem extracts. In the case of *B2m*, its expression in brainstem extracts is detected as early as E17, with a steady increase starting at P0 till adulthood. Its expression is also detected in cerebellar extracts, with an increase starting at P0, reaching comparable levels of expression in adulthood as in the brainstem. Online expression data for *Ifitm1, Ifi27l1* and *H2-Aa* are either unavailable or inconclusive. RTqPCR analysis reveals that their expression levels in the brainstem and cerebellar extracts are relatively low throughout development. Small peaks in expression are detected for *Ifitm1* at P0 and *Ifi27l1* in adulthood.

In case of some selected genes, these results confirmed the reliability of our screening approach, and showed that the expression of some immune system-related genes in the ION and GC populations matched with the developmental synaptogenesis timeline in the olivocerebellar network. However, since the RTqPCR analysis was performed using cerebellar and brainstem extracts, additional data from in situ hybridization experiments will confirm whether the RTqPCR gene expression profile in the brainstem and cerebellum is due to cell-specific expression in Purkinje cells or other neurons in the brainstem respectively. Together, these approaches would provide more robust data to identify bona fide candidate genes.

***Complement-related genes are developmentally regulated in the olivo-cerebellar network***

The role of some immune system-related molecules in CNS development and synaptogenesis has been established. Proteins of the complement cascade such as C3 and C1Q, as well as MHC-I molecules play a role in promoting synapse elimination in the developing retinogeniculate pathway (Corriveau et al., 1998; Stevens et al., 2007). Moreover, in the olivo-cerebellar network, the role of complement C1Q-related molecules CBLN1 and CBLN3 in controlling PF/PC synaptogenesis is well established (Miura et al., 2009; Matsuda et al., 2010). As mentioned earlier, our comparative analysis of gene expression profiles in adult mice revealed that the ION and GC differentially expressed genes related to the complement cascade (Figure 5A). GCs expressed C1Q-related proteins CBLN1 and CBLN3. IONs expressed C1Q-related protein CBLN4, C1Q-like subfamily member C1QL1, complement protein C3, and complement control protein SUSD4. We thus reasoned that this differential combination of complement-related molecules expressed in

the ION and GC could contribute to the specific connectivity of their corresponding synapses.

Similar to the systematic screening approach described in the previous section, I combined expression data available online with RTqPCR experiments in mouse brainstem and cerebellar extracts (Figure 5B), and in situ hybridization experiments at different ages (Figure 5C). This allowed me to determine cell-specific gene expression patterns in the developing olivo-cerebellar network and check whether the timing and pattern of gene expression was in agreement with the timing of synaptogenesis. Parallel fiber synaptogenesis occurs in the cerebellum during the second and third postnatal weeks (Sotelo, 1990). Accordingly, RTqPCR analysis revealed that the expression of GC-specific genes *Cbln1* and *Cbln3* in cerebellar extracts began to increase at P7 till they peaked in adulthood. In contrast, in the brainstem extracts, *Cbln1* was present at a much lower level than in the cerebellum, which gradually decreased further with age. *Cbln3* was absent in the brainstem at all ages. In situ hybridization data for all four cerebellin genes in the developing mouse brain have already been published (Miura et al., 2006). We confirmed this with in situ hybridization experiments in the laboratory. Analysis on P0, P7 and adult sections confirmed that the expression of *Cbln1* was restricted to the GCs in adulthood and during development. Faint expression of *Cbln1* in the ION was detected at P0 and P7 but not in adulthood, similar to what was observed by RTqPCR (Figure 5B, C).

Climbing fiber synaptogenesis begins before Parallel fiber synaptogenesis, around postnatal day 0-2. Before P7, multiple CFs innervate the PC soma. Around P7, synapse elimination begins and a single CF proceeds to establish its innervation territory on Purkinje cell dendrites (Crepel et al., 1976; Watanabe & Kano, 2011). Accordingly, RTqPCR analysis revealed complement-related genes found using our screen to be expressed in the brainstem with an increase P0 onwards and a peak at P7; *C3* was the only gene whose expression was undetected in the brainstem at all ages. Online in situ hybridization data from Allen Brain Atlas (http://mouse.brain-map.org) confirmed this in the adult mouse brain, with very faint expression of *C3* in the ION. The overall expression of *Cbln4* was low in the RTqPCR brainstem extracts during the first postnatal week with a small peak at P7 and then decreasing in adulthood. In situ expression data confirmed this, with faint *Cbln4* expression detected in the ION only at P0 and P7. The RTqPCR expression of *C1ql1* also peaked at P7 in the brainstem extract and plateaued till adulthood. In situ hybridization confirmed that *C1ql1* was strongly expressed by the ION at all ages P0, P7 and adulthood. This correlated with previously published expression data (Iijima et al., 2010). *Susd4*

expression also peaked in the RTqPCR brainstem extract at P7 and plateaued thereon. In the cerebellar extract, *Susd4* expression was found to increase P7 onwards at a rate such that in adulthood, it reached comparable levels as in the brainstem. In situ hybridization revealed *Susd4* expression in the ION and other brainstem neurons at all ages. In the cerebellum, its expression was specific to the PCs at all ages. This correlated with the identification of SUSD4 in a previously generated adult Purkinje cell transcriptome (Doyle et al., 2008) (Figure 5B, C). This analysis revealed the developmentally regulated expression pattern of complement-related genes in the olivo-cerebellar network and allowed us to select candidate genes to analyze their potential roles in synaptogenesis.

**Conclusion**

The results described so far demonstrate that a different combination of complement-related genes is expressed at each excitatory input cell population, the ION and GC. The gene expression data (collectively obtained from bacTRAP analysis, RTqPCR analysis and in situ hybridization) confirm that the timing and pattern of complement-related gene expression in the ION and GC are in agreement with the developmental timeline of synaptogenesis corresponding to each input. Taken together, this data provides insights into candidate genes that could be potentially analyzed for their functional roles in synaptogenesis. Secretion of the complement-related protein CBLN1 by GCs is indispensable for the formation and specificity of the PF/PC synapse (Matsuda et al., 2010). So we hypothesized that this class of proteins could play a role at the CF/PC synapse as well.

Of all the ION-specific genes, C3 expression is either low or undetected in the ION during development and in adulthood. Despite a high microarray fold increase for CBLN4 in the adult ION compared to GCs, expression analysis in the developing mouse brain reveals a low expression pattern in the ION. The microarray gene expression data showed that C1QL1 had a very high fold increase (>1200) in the ION compared to GCs, making it one of the top five most highly enriched genes in the ION (Figure 5A). It also had a high fold increase (>60) in the IP-ION compared to UB-ION fraction. This indicates the ION-specific expression of C1QL1 in the brainstem and an extremely high input-specificity in the ION compared to GCs. This, combined with the specific and consistent expression of C1QL1 in the developing ION, strongly suggest the potential involvement of C1QL1 in regulating CF/PC synaptogenesis. In contrast to C1QL1, SUSD4 had a lower microarray fold increase >10 in the ION compared to GCs and fold increase >2 compared to the UB-ION fraction.

Despite this, SUSD4 is an interesting candidate, since its expression is high in the brainstem during the developmental stages of CF/PC synaptogenesis, and it is also expressed by cerebellar Purkinje cells, the postsynaptic site of CF synapses. Moreover, SUSD4 has been shown to interact with the globular C1Q domain *in vitro* (Holmquist et al., 2013). Taken together, this strongly suggests a role for SUSD4 in CF/PC synaptogenesis, possibly in coordination with C1QL1.

**References**


Ango, F., di Cristo, G., Higashiyama, H., Bennett, V., Wu, P., & Huang, Z. J. (2004). Ankyrin-Based Subcellular Gradient of Neurofascin, an Immunoglobulin Family Protein, Directs GABAergic Innervation at Purkinje Axon Initial Segment. *Cell*, *119*(2), 257–272.

Ango, F., Wu, C., Van der Want, J. J., Wu, P., Schachner, M., & Huang, Z. J. (2008). Bergmann Glia and the Recognition Molecule CHL1 Organize GABAergic Axons and Direct Innervation of Purkinje Cell Dendrites. *PLoS Biology*, *6*(4), 739–756.

Bally-Cuif, L., Alvarado-Mallart, R. M., Darnell, D. K., & Wassef, M. (1992). Relationship between Wnt-1 and En-2 expression domains during early development of normal and ectopic met-mesencephalon. *Development*, *115*(4), 999–1009.

Corriveau, R. A., Huh, G. S., & Shatz, C. J. (1998). *Regulation of class I MHC gene expression in the developing and mature CNS by neural activity. Neuron, 21*(3), 505–520.

Crepel, F., Mariani, J., & Delhaye-Bouchaud, N. (1976). Evidence for a multiple innervation of purkinje cells by climbing fibers in the immature rat cerebellum. *Journal of Neurobiology*, *7*(6), 567–578.

Dalva, M. B., McClelland, A. C., & Kayser, M. S. (2007). Cell adhesion molecules: signalling functions at the synapse. *Nature Reviews Neuroscience*, *8*(3), 206–220.

Dennis, G., Sherman, B. T., Hosack, D. A., Yang, J., Gao, W., Lane, H., & Lempicki, R. A. (2003). DAVID: Database for Annotation, Visualization, and Integrated Discovery. *Genome Biology*, *4*(9), R60.

Doyle, J. P., Dougherty, J. D., Heiman, M., Schmidt, E. F., Stevens, T. R., Ma, G., Bupp, S., Shrestha, P., et al. (2008). Application of a Translational Profiling Approach for the Comparative Analysis of CNS Cell Types. *Cell*, *135*(4), 749–762.

Heiman, M., Schaefer, A., Gong, S., Peterson, J. D., Day, M., Ramsey, K. E., Suárez-Fariñas, M., Schwarz, C., et al. (2008). A Translational Profiling Approach for the Molecular Characterization of CNS Cell Types. *Cell*, *135*(4), 738–748.

Holmquist, E., Okroj, M., Nodin, B., Jirstrom, K., & Blom, A. M. (2013). Sushi domain-containing protein 4 (SUSD4) inhibits complement by disrupting the formation of the classical C3 convertase. *The FASEB Journal*, *27*(6), 2355–2366.

Huang, D. W., Sherman, B. T., & Lempicki, R. A. (2008). Systematic and integrative analysis of large gene lists using DAVID bioinformatics resources. *Nature Protocols*, *4*(1), 44–57.

Iijima, T., Miura, E., Watanabe, M., & Yuzaki, M. (2010). Distinct expression of C1q-like family mRNAs in mouse brain and biochemical characterization of their encoded proteins. *European Journal of Neuroscience*, *31*(9), 1606–1615.

Linhoff, M. W., Laurén, J., Cassidy, R. M., Dobie, F. A., Takahashi, H., Nygaard, H. B., Airaksinen, M. S., Strittmatter, S. M., & Craig, A. M. (2009). An Unbiased Expression Screen for Synaptogenic Proteins Identifies the LRRTM Protein Family as Synaptic Organizers. *Neuron*, *61*(5), 734–749.

Matsuda, K., Miura, E., Miyazaki, T., Kakegawa, W., Emi, K., Narumi, S., Fukazawa, Y., Ito-Ishida, A., et al. (2010). Cbln1 Is a Ligand for an Orphan Glutamate Receptor 2, a Bidirectional Synapse Organizer. *Science*, *328*(5976), 363–368.

Mi, H., Muruganujan, A., Casagrande, J. T., & Thomas, P. D. (2013). Large-scale gene function analysis with the PANTHER classification system. *Nature Protocols*, *8*(8), 1551–1566.

Miura, E., Iijima, T., Yuzaki, M., & Watanabe, M. (2006). Distinct expression of Cbln family mRNAs in developing and adult mouse brains. *European Journal of Neuroscience*, *24*(3), 750–760.

Miura, E., Matsuda, K., Morgan, J. I., Yuzaki, M., & Watanabe, M. (2009). Cbln1 accumulates and colocalizes with Cbln3 and GluRδ2 at parallel fiber-Purkinje cell synapses in the mouse cerebellum. *European Journal of Neuroscience*, *29*(4), 693–706.

Nikitin, A., Egorov, S., Daraselia, N., & Mazo, I. (2003). Pathway studio - the analysis and navigation of molecular networks. *Bioinformatics*, *19*(16), 2155–2157.

Schmidt, E. F., Warner-Schmidt, J. L., Otopalik, B. G., Pickett, S. B., Greengard, P., & Heintz, N. (2012). Identification of the Cortical Neurons that Mediate Antidepressant Responses. *Cell*, *149*(5), 1152–1163.

Shen, K., & Scheiffele, P. (2010). Genetics and Cell Biology of Building Specific Synaptic Connectivity. *Annual Review of Neuroscience*, *33*(1), 473–507.

Sotelo, C. (1990). Cerebellar synaptogenesis: what we can learn from mutant mice. *The Journal of Experimental Biology*, *153*, 225–249.

Sperry, R. W. (1963). Chemoaffinity in the orderly growth of nerve fiber patterns and connections. *Proceedings of the National Academy of Sciences U S A*, *50*, 703–710.

Stevens, B., Allen, N. J., Vazquez, L. E., Howell, G. R., Christopherson, K. S., Nouri, N., Micheva, K. D., Mehalow, A. K., et al. (2007). The Classical Complement Cascade Mediates CNS Synapse Elimination. *Cell*, *131*(6), 1164–1178.

Südhof, T. C. (2008). Neuroligins and neurexins link synaptic function to cognitive disease. *Nature*, *455*(7215), 903–911.

Watanabe, M., & Kano, M. (2011). Climbing fiber synapse elimination in cerebellar Purkinje cells. *European Journal of Neuroscience*, *34*(10), 1697–1710.

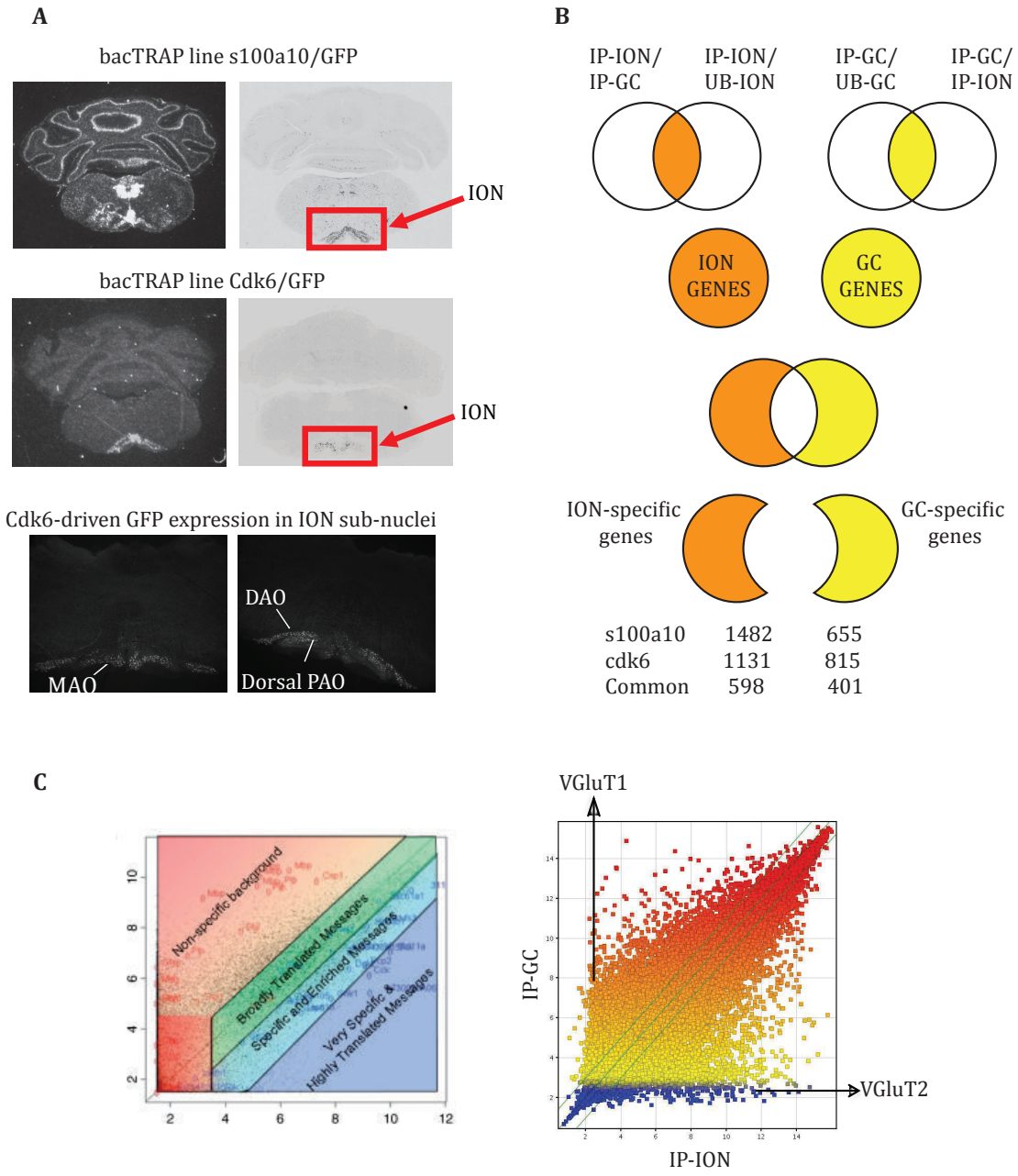


**Figure 1. Comparison of the Inferior Olivary Neurons and Granule Cell transcriptomes**
**(A)** S100a10 and Cdk6 transgenic mouse lines expressing eGFP-L10a in the ION (red rectangle) and used for the pulldown of translating mRNAs from the ION. ION sub-nuclei that express eGFP-L10a under Cdk6 BAC promoter. MAO, medial accessory olive ; DAO, dorsal accessory olive ; PAO, principal accessory olive. **(B)** Scheme of systematic comparison to obtain genes specific to the ION and GC. This was done for each line, s100a10 and cdk6, followed by a common pool of genes found in both. **(C)** GeneSpring scatterplot to represent genes specifically enriched in GC and ION. Positive controls Vesicular Glutamate Transporter 1 (VGluT1) and Vesicular Glutamate Transporter 2 (VGluT2) were found in GC and ION respectively.

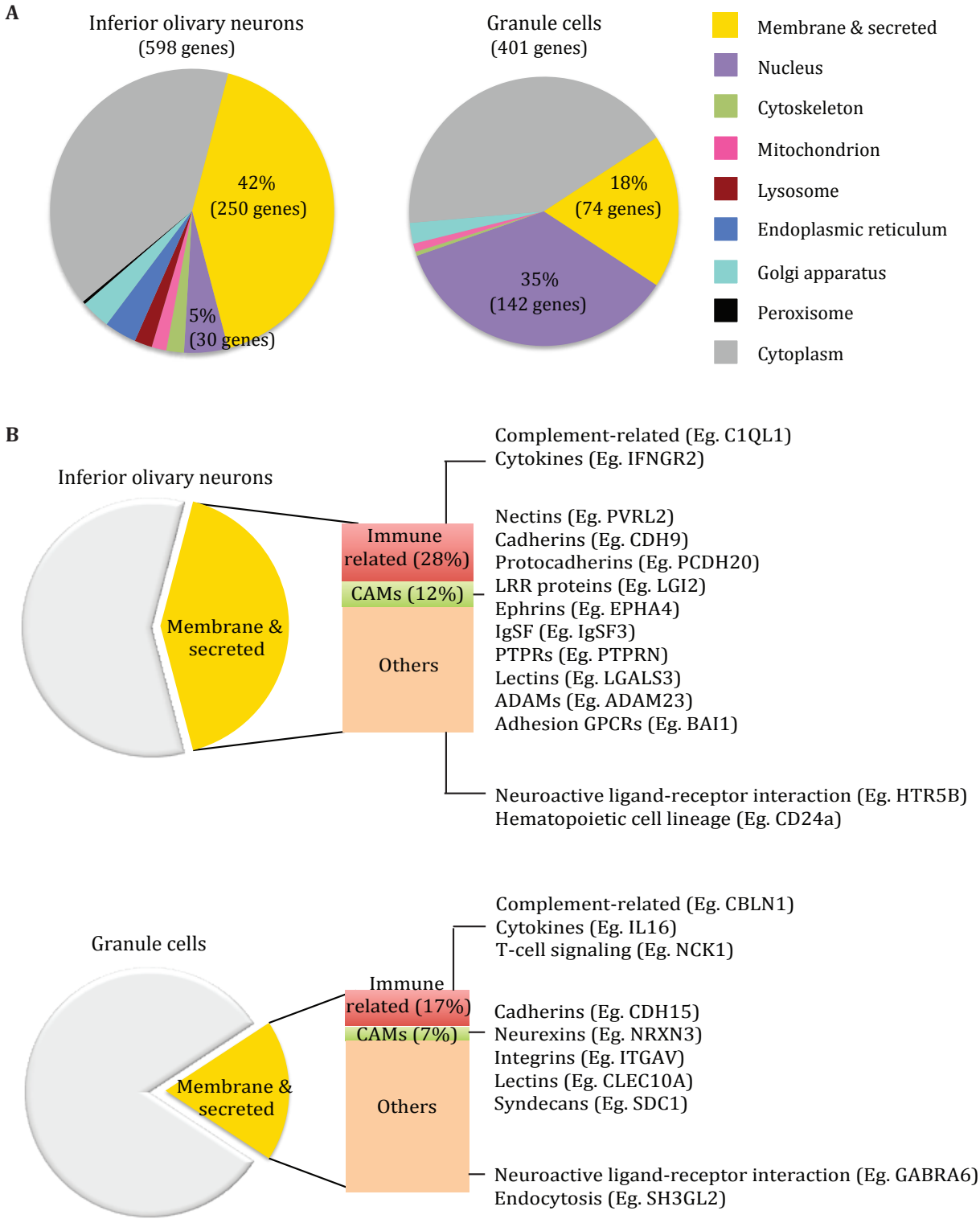


**Figure 2. High diversity of genes coding for membrane and secreted proteins in ION compared to GC**
**(A)** Classification of ION and GC specific genes according to sub-cellular localization based on DAVID Functional Annotation Clustering **(B)** Molecular diversity of membrane and secreted proteins in ION and GC


**Figure 3. Immune system-related processes are enriched in the ION compared to GCs**
**(A)** Classification of ION and GC specific genes according to biological processes based on PANTHER classification system **(B)** Diversity of pathways in ION and GC-specific immune system related genes

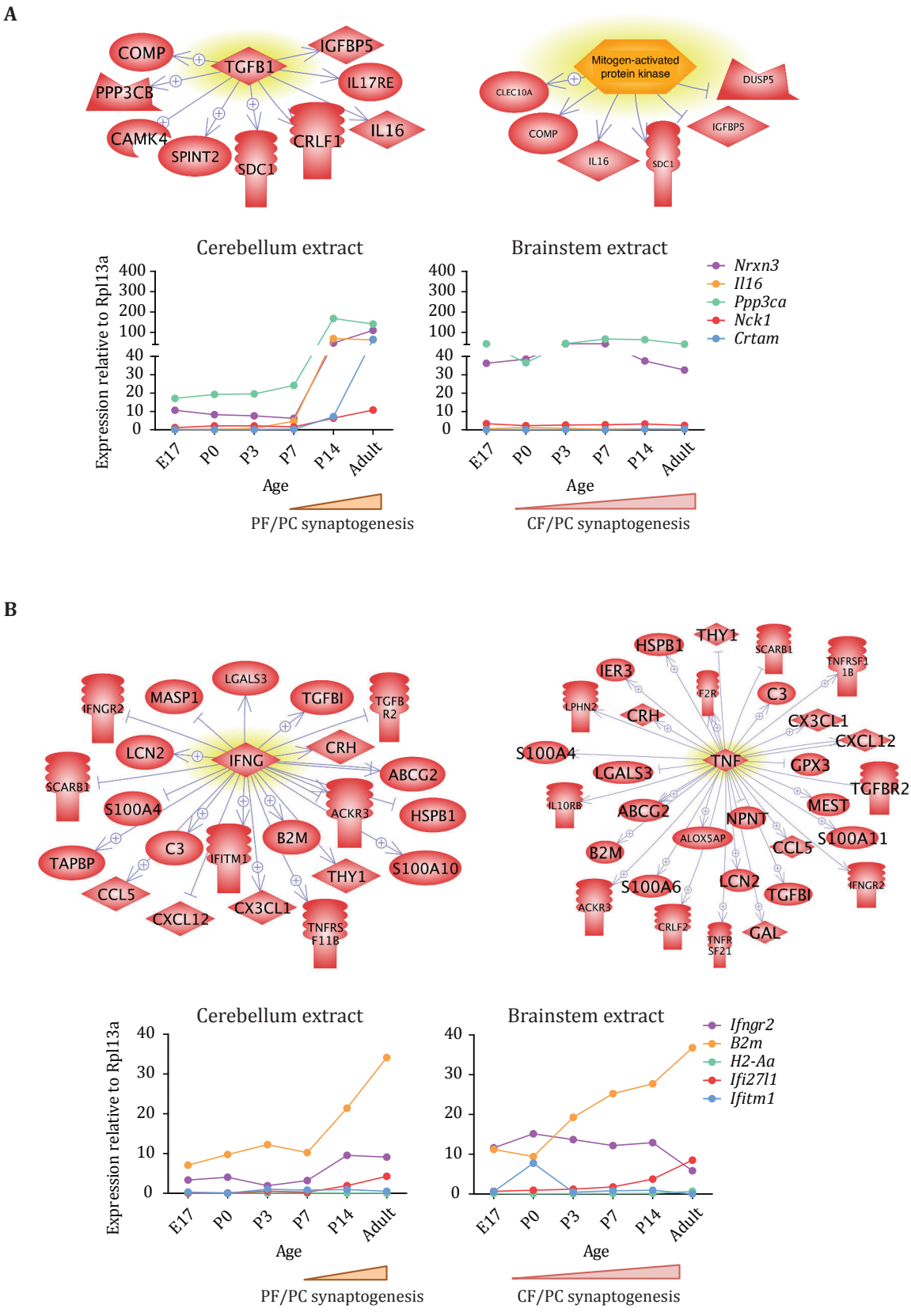
A
COMP
TGFB1
IGFBP5
PPP3CB
IL17RE
CAMK4
SPINT2
SDC1
CRLF1
IL16
Mitogen-activated protein kinase
CLEC10A
DUSP5
COMP
IGFBP5
IL16
SDC1
Cerebellum extract
Brainstem extract
Expression relative to Rpl13a
Nrxn3
Il16
Ppp3ca
Nck1
Crtam
E17
P0
P3
P7
P14
Adult
Age
PF/PC synaptogenesis
CF/PC synaptogenesis
B
IFNGR2
MASP1
LGALS3
TGFBI
TGFBR2
LCN2
IFNG
CRH
ABCG2
SCARB1
S100A4
ACKR3
HSPB1
C3
IFITM1
B2M
TAPBP
THY1
S100A10
CCL5
CXCL12
CX3CL1
TNFRSF11B
THY1
HSPB1
SCARB1
TNFRSF1 1B
IER3
F2R
C3
LPHN2
CRH
CX3CL1
CXCL12
S100A4
TNF
GPX3
LGALS3
TGFBR2
IL10RB
ABCG2
MEST
NPNT
ALOX5AP
S100A11
B2M
CCL5
S100A6
LCN2
TGFBI
IFNGR2
ACKR3
CRLF2
TNFRSF21
GAL
Ifngr2
B2m
H2-Aa
Ifi27l1
Ifitm1

**Figure 4**

**Figure 4. Expression of immune system-related genes in the olivo-cerebellar network matches with the developmental timeline of excitatory synaptogenesis**

**(A)** Pathway Studio analysis showing 9 out of 24 GC-specific immune system-related genes regulated by TGFB1 (p-value= 5.78E-4) and 6 genes regulated by MAPK (p-value= 4.32E-3). Genes are indicated as red ovals, and regulation events are displayed with arrows and documented by literature citations. Expression of select GC-specific T-cell signaling genes at different stages of mouse brain development using quantitative RT-PCR on extracts from brainstem and cerebellum (E17: embryonic day 17; P0 to P14: postnatal day 0 to 14). Expression levels are normalized to the RPL13A gene. N=3 samples per stage. Tgfb1, Transforming Growth Factor 1; MAPK, Mitogen activated protein kinase; *Nrxn3*, Neurexin 3; *Il16*, Interleukin 16; *Ppp3ca*, protein phosphatase 3, catalytic subunit, alpha isoform; *Nck1*, non-catalytic region of tyrosine kinase adaptor protein 1; *Crtam*, cytotoxic and regulatory T cell molecule **(B)** Pathway Studio analysis showing 31 out of 94 ION-specific immune system-related genes regulated by TNF (p-value= 1.82E-9) and 22 genes regulated by IFNγ (p-value= 3.55E-8). Genes are indicated as red ovals, and regulation events are displayed with arrows and documented by literature citations. Expression of select ION-specific IFNγ signaling genes at different stages of mouse brain development using quantitative RT-PCR on extracts from brainstem and cerebellum (E17: embryonic day 17; P0 to P14: postnatal day 0 to 14). Expression levels are normalized to the RPL13A gene. N=3 samples per stage. Tnf, Tumor Necrosis Factor; Ifnγ; Interferon gamma; *Ifngr2*, Interferon gamma receptor 2; *B2m*, beta-2 microglobulin; *H2-Aa*, histocompatibility 2, class II antigen A, alpha; *Ifi27l1*, interferon, alpha-inducible protein 27 like 1; *Ifitm1*, interferon induced transmembrane protein 1

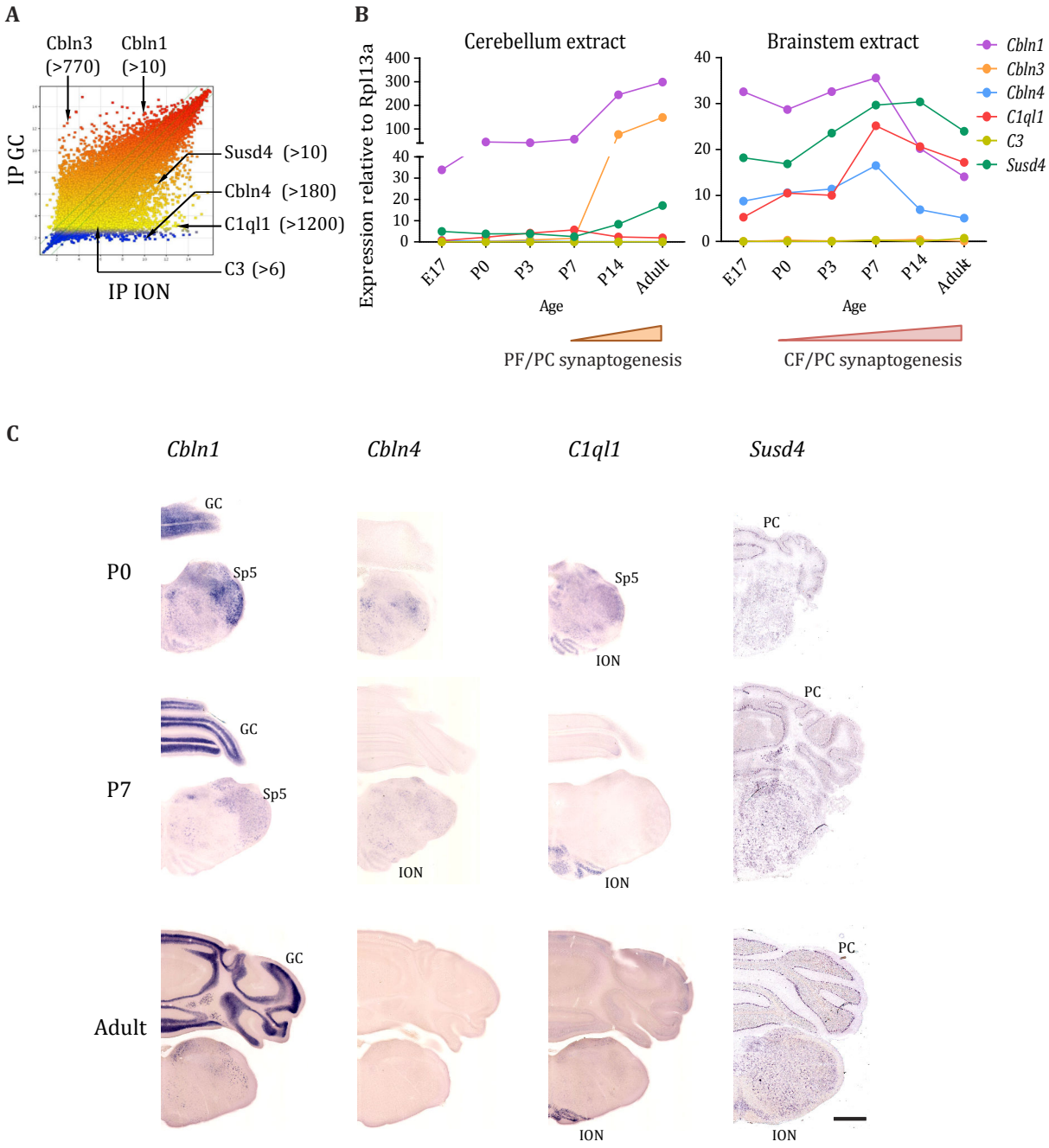


**Figure 5. Characterization of complement-related proteins during development in the olivo-cerebellar network**

**(A)** Scatter plot analysis of microarray data, representing differentially expressed complement-related genes with corresponding fold change in the ION and GC **(B)** Expression of complement-related genes at different stages of mouse brain development using quantitative RT-PCR on extracts from brainstem and cerebellum (E17: embryonic day 17; P0 to P14: postnatal day 0 to 14). Expression levels are normalized to the RPL13A gene. N=3 samples per stage. C1ql1, complement component 1, q subcomponent-like 1; Cbln1, cerebellin 1; Cbln3, cerebellin 3; Cbln4, cerebellin 4; C3, complement component 3; Susd4; sushi domain containing protein, 4 **(C)** In situ hybridization experiments were performed using probes specific for Cbln1, C1ql1, Cbln4, Susd4 on coronal sections of mouse brain taken at postnatal day 0, 7 and adult. IO, inferior olive; GC, Granule cell; Sp5, spinal trigeminal nuclei; PC, Purkinje cell. Scale bars, 500µm; each scale bar applies to the whole column.

**Table 1. Top 10 annotation clusters identified in Inferior Olivary Neurons and Granule cells by DAVID Functional Annotation Clustering Tool**

| Annotation cluster | Representative Annotation terms: ION (151 clusters) | Enrichment score |
|---|---|---|
| 1 | Integral to membrane | 4,89 |
| 2 | Extracellular region | 4,21 |
| 3 | Lysosome | 4 |
| 4 | Angiogenesis | 2,85 |
| 5 | Lipid biosynthesis | 2,45 |
| 6 | Magnesium, manganese ion binding | 2,17 |
| 7 | Protein dimerization | 2,11 |
| 8 | Oxidation reduction | 2,1 |
| 9 | Inflammatory response | 2,01 |
| 10 | Polysaccharide metabolic process | 2 |

| Annotation cluster | Representative Annotation terms: GC (109 clusters) | Enrichment score |
|---|---|---|
| 1 | Nucleus, transcription regulation | 7,31 |
| 2 | Nucleoplasm | 5,62 |
| 3 | Metal ion binding | 5,35 |
| 4 | Synapse, cell junction | 3,27 |
| 5 | Nuclear chromatin | 3,12 |
| 6 | Synaptic transmission, cell signaling | 3,08 |
| 7 | Chromatin organization | 2,89 |
| 8 | Positive regulation of transcription | 2,62 |
| 9 | Cytoskeleton | 2,4 |
| 10 | Zinc finger region | 2,39 |

**Table 2. Cell Adhesion Molecules differentially expressed in Inferior Olivary Neurons and Granule Cells**

| Gene symbol | Gene name: ION list | Fold change in cdk6 | | Fold change in s100a10 | |
|---|---|---|---|---|---|
| | | IP ION vs IP GC | IP ION vs UB ION | IP ION vs IP GC | IP ION vs UB ION |
| GPR123 | G protein-coupled receptor 123 | 762,1 | 25,3 | 312,6 | 3,6 |
| LGI2 | Leucine-rich repeat LGI family, member 2 | 421,3 | 9,4 | 67,0 | 1,1 |
| GPR64 | G protein-coupled receptor 64 | 364,6 | 9,7 | 170,5 | 1,7 |
| AJAP1 | Adherens junction associated protein 1 | 295,4 | 5,8 | 193,5 | 2,9 |
| PTPRO | Protein tyrosine phosphatase, receptor type, O | 92,4 | 4,0 | 125,0 | 1,2 |
| PLXDC1 | Plexin domain containing 1 | 91,7 | 3,1 | 305,7 | 4,8 |
| CNTNAP2 | Contactin associated protein-like 2 | 77,7 | 4,2 | 43,1 | 2,4 |
| MBL2 | Mannose-binding lectin (protein C) 2 | 71,5 | 7,7 | 116,4 | 5,7 |
| GJD2 | Gap junction protein, delta 2 | 60,0 | 9,6 | 23,8 | 2,3 |
| PVRL2 | Poliovirus receptor-related 2 | 44,8 | 13,1 | 11,8 | 6,7 |
| NRCAM | Neuron-glia-CAM-related cell adhesion molecule | 33,8 | 4,9 | 14,4 | 1,2 |
| IGSF3 | Immunoglobulin superfamily 3 | 30,4 | 2,2 | 16,1 | 1,0 |
| MASP1 | Mannan-binding lectin serine peptidase 1 | 29,4 | 5,9 | 9,8 | 2,2 |
| ADAM11 | A disintegrin and metallopeptidase domain 11 | 26,7 | 9,7 | 6,5 | 3,1 |
| SEMA4F | Semaphorin 4F | 22,5 | 13,7 | 5,9 | 3,0 |
| ADAM23 | A disintegrin and metallopeptidase domain 23 | 22,3 | 2,6 | 10,1 | 3,8 |
| EPHA4 | Eph receptor A4 | 21,2 | -1,1 | 22,9 | -1,4 |
| LGALS3 | Lectin, galactose binding, soluble 3 | 21,0 | 5,4 | 51,7 | 5,1 |
| BAI1 | Brain-specific angiogenesis inhibitor 1 | 19,8 | 1,6 | 9,2 | -1,0 |
| SEMA4A | Semaphorin 4A | 18,1 | 1,3 | 24,9 | -1,0 |
| EGFL7 | EGF-like domain 7 | 17,8 | 2,5 | 39,8 | 4,5 |
| CDH9 | Cadherin 9 | 17,2 | 1,4 | 23,7 | 1,4 |
| PCDH20 | Protocadherin 20 | 16,1 | 3,1 | 38,9 | 1,8 |
| DNER | Delta/notch-like EGF-related receptor | 14,6 | 1,1 | 13,3 | -1,1 |
| PTPRN | Protein tyrosine phosphatase receptor type, N | 11,8 | 3,1 | 6,7 | 2,0 |
| TMEFF1 | Transmembrane protein with EGF-like and follistatin-like domains 1 | 11,2 | -1,1 | 6,5 | -1,4 |
| CDH13 | Cadherin 13 | 9,7 | 1,1 | 37,2 | 1,9 |
| LRFN5 | Leucine rich repeat and fibronectin type III domain containing 5 | 9,6 | 1,3 | 57,8 | 1,3 |
| EFNA3 | Ephrin A3 | 8,8 | 1,4 | 29,1 | 2,2 |
| GPR125 | G protein-coupled receptor 125 | 5,7 | 1,1 | 14,3 | 1,6 |

| Gene symbol | Gene name: GC list | Fold change in cdk6 | | Fold change in s100a10 | |
|---|---|---|---|---|---|
| | | IP GC vs IP ION | IP GC vs UB GC | IP GC vs IP ION | IP GC vs UB GC |
| NRXN3 | Neurexin3 | 49,0 | 1,2 | 5,1 | 1,2 |
| SDC1 | Syndecan 1 | 11,1 | -1,6 | 7,0 | -1,6 |
| CLEC10A | C-type lectin domain family 10 member A | 10,9 | -3,7 | 33,2 | -3,7 |
| CDH15 | Cadherin 15 | 8,6 | -1,3 | 5,3 | -1,3 |
| ITGAV | Integrin alpha V | 6,7 | -1,1 | 7,5 | -1,1 |

**Table 3. Immune system-related pathways differentially expressed in Inferior Olivary Neurons and Granule Cells**

| Pathway | Gene symbol | Gene name: ION list | Fold change in cdk6 | | Fold change in s100a10 | |
|---|---|---|---|---|---|---|
| | | | IP ION vs IP GC | IP ION vs UB ION | IP ION vs IP GC | IP ION vs UB ION |
| Cytokine signaling | CXCR7 | Chemokine (C-X-C motif) receptor 7 | 182,1 | 14,7 | 33,2 | 2,5 |
| | CX3CL1 | Chemokine (C-X3-C motif) ligand 1 | 10,9 | 1,4 | 17,2 | 1,2 |
| | CRLF2 | Cytokine receptor-like factor 2 | 7,6 | 2,0 | 5,4 | 3,3 |
| | SOCS2 | Suppressor of cytokine signaling 2 | 52,9 | 3,0 | 29,3 | 3,3 |
| | VEGFB | Vascular endothelial growth factor B | 16,1 | 2,5 | 6,3 | 2,2 |
| | TNFRSF21 | Tumor necrosis factor receptor superfamily, member 21 | 69,1 | 1,1 | 228,1 | 1,8 |
| | TNFRSF11B | Tumor necrosis factor receptor superfamily, member 11b | 10,5 | 2,8 | 18,0 | 3,4 |
| | GAB2 | Growth factor receptor-associated-binding protein 2 | 60,7 | -1,0 | 76,3 | -1,0 |
| | MAPKAPK2 | MAP kinase-activated protein kinase 2 | 9,6 | 3,5 | 5,2 | 3,7 |
| | IL10RB | Interleukin 10 receptor, beta | 8,2 | 1,5 | 48,6 | 4,1 |
| | IFNGR2 | Interferon gamma receptor 2 | 97,2 | 3,9 | 13,9 | 4,8 |
| | TAPBP | TAP binding protein | 6,5 | 2,2 | 7,6 | 2,3 |
| | B2M | Beta-2 microglobulin | 152,9 | 2,5 | 47,1 | 1,6 |
| | CCL5 | Chemokine (C-C motif) ligand 5 | 72,8 | 28,6 | 10,7 | 15,8 |
| | H2-AA | Histocompatibility 2, class II antigen A, alpha | 59,1 | 14,5 | 45,7 | 10,0 |
| | IFI27L1 | Interferon, alpha-inducible protein 27 like 1 | 33,7 | -1,1 | 485,9 | 3,8 |
| | IFITM1 | Interferon induced transmembrane protein 1 | 2443,9 | 161,2 | 21,8 | 3,6 |
| | TGFBR2 | Transforming growth factor, beta receptor II | 13,7 | 1,8 | 11,4 | 1,1 |
| | TGBFI | Transforming growth factor, beta-induced | 78,6 | 3,6 | 32,9 | 1,5 |
| Complement cascade, complement-related | C3 | Complement component 3 | 6,5 | 1,8 | 6,8 | 1,3 |
| | F2R | Coagulation factor II (thrombin) receptor | 36,2 | -1,1 | 49,3 | 1,3 |
| | MASP1 | Mannan-binding lectin serine peptidase 1 | 29,4 | 5,9 | 9,8 | 2,2 |
| | MBL2 | Mannose-binding lectin (protein C) 2 | 71,5 | 7,7 | 116,4 | 5,7 |
| | LGALS3 | Lectin, galactose binding, soluble 3 | 21,0 | 5,4 | 51,7 | 5,1 |
| | B2M | Beta-2 microglobulin | 152,9 | 2,5 | 47,1 | 1,6 |
| | CBLN4 | Cerebellin4 | 182,7 | 3,4 | 94,2 | 1,4 |
| | C1QL1 | Complement component 1, q sub-component-like 1 | 1238,9 | 64,9 | 93,7 | 6,3 |
| | SUSD4 | Sushi domain containing protein 4 | 15,5 | 2,8 | 8,9 | 1,4 |

| Pathway | Gene symbol | Gene name: GC list | Fold change in cdk6 | | Fold change in s100a10 | |
|---|---|---|---|---|---|---|
| | | | IP GC vs IP ION | IP GC vs UB GC | IP GC vs IP ION | IP GC vs UB GC |
| T-cell receptor signaling | CRTAM | Cytotoxic and regulatory T cell molecule | 969,3 | -1,8 | 1526,1 | -1,8 |
| | NCK1 | Non-catalytic region of tyrosine kinase adaptor protein 1 | 26,0 | -1,5 | 7,2 | 1,4 |
| | PPP3CA | Protein phosphatase 3, catalytic subunit, alpha isoform | 65,1 | 1,3 | 5,0 | 1,2 |
| | PPP3CB | Protein phosphatase 3, catalytic subunit, beta isoform | 10,7 | -2,2 | 5,4 | -2,2 |
| | DNAJB6 | DnaJ (Hsp40) homolog, subfamily B, member 6 | 11,7 | -3,8 | 5,2 | -3,8 |
| | PAK7 | P21 (Cdc42/Rac)-activated kinase 7 | 21,8 | 1,2 | 31,9 | 1,2 |
| Cytokine signaling | CRLF1 | Cytokine receptor-like factor 1 | 5,8 | -2,2 | 5,7 | -2,2 |
| | IL16 | Interleukin 16 | 39,6 | -1,6 | 61,9 | -1,6 |
| | IL17RE | Interleukin 17 receptor E | 9,6 | -1,4 | 5,7 | -1,4 |
| Complement-related | CBLN1 | Cerebellin1 | 10,5 | 1,0 | 7,8 | 1,2 |
| | CBLN3 | Cerebellin3 | 773,0 | 1,2 | 829,1 | -1,2 |

## 2. The secreted protein C1QL1 and its receptor BAI3 control the synaptic connectivity of excitatory inputs converging on cerebellar Purkinje Cells

### - Preface -

Our comparative analysis of gene expression profiles in adult mice revealed that C1QL1 is one of the most specific and highly expressed genes in the adult ION (Part I – Figure 5). By in situ hybridization, I confirmed this specific expression of C1QL1 in the adult ION and also showed that it is expressed as early as embryonic age E17. These expression data correlate with previously published results (Iijima et al., 2010). C1QL1 has been shown to be a ligand of the adhesion-GPCR Brain Angiogenesis Inhibitor 3 (BAI3) and through this interaction, to inhibit synaptogenesis in cultured hippocampal neurons (Bolliger et al., 2011). BAI3 has been identified in biochemical fractions of postsynaptic densities in the forebrain (Collins et al., 2006) and in the cerebellum (Selimi et al., 2009). My in situ hybridization data illustrate that in the cerebellum, BAI3 is highly expressed in Purkinje cells starting from P0. Taken together, these expression patterns suggest a possible role for secreted C1QL1 and its postsynaptic receptor BAI3 in regulating the formation and stability of the Climbing Fiber/Purkinje Cell (CF/PC) synapse.

Studies from our group have demonstrated that the BAI3 receptor is crucial for different processes during the development of the olivo-cerebellar network. First, we identified the role of BAI3 in modulating Purkinje cell dendrite morphogenesis via the signaling pathway ELMO1/Rac1 (Lanoue et al., 2013)(See annexe). The *in vivo* knockdown of BAI3 in developing PCs led to a significant reduction in spine density in distal dendrites, normally innervated only by Parallel Fibers (PF). Its ligand C1QL1 is transiently expressed in the developing cerebellum, possibly by GC precursors (Iijima et al., 2010). Knockdown experiments in mixed cerebellar cultures showed that cerebellar C1QL1 could also regulate PC spinogenesis in a BAI3-dependent manner. Additionally, loss of BAI3 in PCs led to defects in excitatory synaptogenesis. In mixed cerebellar cultures, the knockdown of BAI3 showed a decrease in PF synapse maturation. A corresponding decrease in PF transmission was confirmed by electrophysiological recordings *in vivo*. Upon BAI3 knockdown in developing PCs *in vivo*, a significant decrease in CF synapse innervation territory, number and size were observed. This phenotype was accompanied by a reduction in CF transmission, shown by electrophysiological recordings. These results demonstrated that

BAI3 in Purkinje cells regulates dendritogenesis, spinogenesis and excitatory synaptogenesis of both the PF/PC and CF/PC synapses.

The ligand of BAI3, C1QL1, is specifically expressed by the ION in the adult brain, and shares structural similarities with PF/PC synapse-specific CBLN1 (Yuzaki, 2008). We thus hypothesized that akin to the CBLN1/GluRδ2 complex at the PF/PC synapse, the C1QL1/BAI3 complex played a role in CF/PC synapse formation and specificity. To test this, I used an *in vivo* knockdown approach to delete the expression of C1QL1 in the ION by injection of lentiviral particles driving shC1QL1. In collaboration with Dr. Marion Wassef at the ENS, I setup an injection technique to knockdown C1QL1 in the ION of neonatal mice at P4, just after the beginning of CF synaptogenesis (Crepel et al., 1976; Chédotal & Sotelo, 1992). Injection of the brainstem through the more accessible dorsal side of the skull is detrimental to the survival of the mice at this age. So I successfully standardized an injection technique involving a micro-surgery in the mouse throat region to access the brainstem from the ventral side and consistently target the ION. Using this challenging method, I was able to demonstrate that the loss of C1QL1 in the ION by knockdown leads to a significant reduction in the number of CF contacts made on PC dendrites, and in the extension of CF innervation. This is similar to the effect observed upon BAI3 knockdown in Purkinje cells. The morphological effects are partially rescued by the simultaneous transduction of the knockdown construct with a resistant C1QL1 construct. A reduction in CF synaptic transmission upon C1QL1 knockdown is also shown by electrophysiology. A smaller but significant decrease in the ability of CFs to undergo dendritic translocation is also observed at P9, the stage when translocation of the winning CF begins (Crepel, 1982; Chédotal & Sotelo, 1992; Hashimoto, 2009a). Since the *in vivo* injection site is located outside of the cerebellum, these results confirm the cell autonomous effect of C1QL1. To test whether the input-specific expression of C1QL1 in the ION is necessary for maintaining CF innervation territory, I then mis-expressed C1QL1 in the cerebellum during development by injecting lentiviral particles driving C1QL1 over-expression in the developing cerebellum at P7 *in vivo*. This leads to a significant reduction in the extent of CF innervation territory at P14, but does not cause ectopic invasion of CF territory by PFs. This confirmed that the ION-specific expression of C1QL1 is necessary for proper CF/PC synaptogenesis and maintenance of CF innervation territory, but is not sufficient to characterize CF synapse identity.

Thus, we show that proteins of the complement C1Q-related subfamily contribute to the identity of the two excitatory synapses formed on Purkinje cells. The specific

expression of C1QL1 and CBLN1 at the ION and GC respectively, is needed for proper formation and specificity of the corresponding synapses formed by these cell populations on their target Purkinje cells. This provides insights into the "chemoaffinity code" that controls subcellular specificity at each synapse type during the formation of neural circuits.

**- Article -**

## The secreted protein C1QL1 and its receptor BAI3 control the synaptic connectivity of excitatory inputs converging on cerebellar Purkinje Cells

Sigoillot S.M[1,2,3], Iyer K.[1,2,3], Binda F.[4], Gonzalez-Calvo I.[1,2,3,4], Talleur M.[1,2,3], Vodjdani G.[5], Isope P.[4], Selimi F.[1,2,3]

[1] Collège de France, Center for Interdisciplinary Research in Biology (CIRB), Paris, F-75005, France;

[2] CNRS, UMR 7241, Paris, F-75005, France; [3] INSERM, U1050, Paris, F-75005, France;

[4] Institut des Neurosciences Cellulaires et Intégratives, CNRS UPR 3212, Université de Strasbourg, Strasbourg, F-67084, France ;

[5] Neuroprotection du cerveau en développement (PROTECT), INSERM, UMR1141; Université Paris-Diderot, Sorbonne Paris-Cité, Paris, F-75019, France.

Article

Cell Reports

# The Secreted Protein C1QL1 and Its Receptor BAI3 Control the Synaptic Connectivity of Excitatory Inputs Converging on Cerebellar Purkinje Cells

## Graphical Abstract

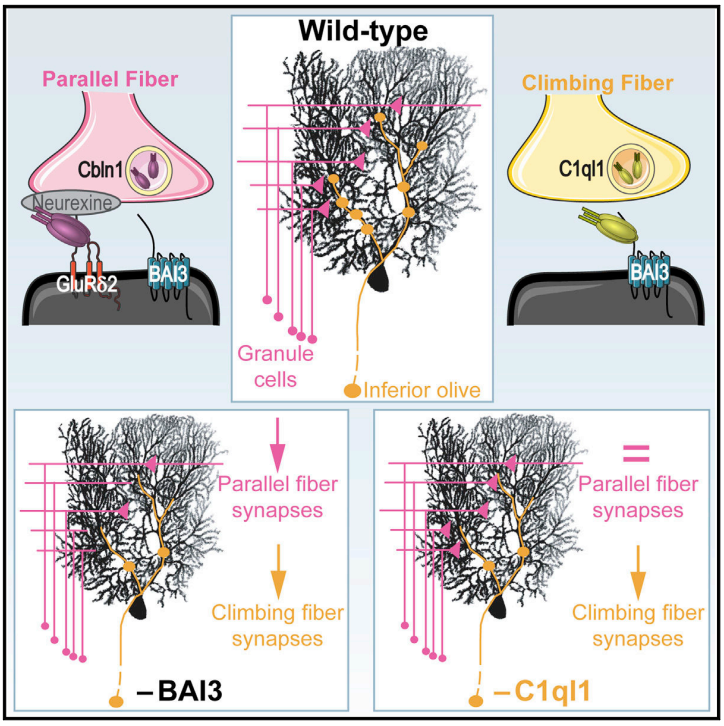


## Highlights

- C1QL and BAI3 proteins are highly expressed during synaptogenesis
- BAI3 promotes spinogenesis and excitatory synaptogenesis in Purkinje cells
- C1QL1 controls climbing fiber synaptogenesis and territory on Purkinje cells
- C1QL1's modulation of Purkinje cell spinogenesis is BAI3 dependent

## Authors

Séverine M. Sigoillot, Keerthana Iyer, ..., Philippe Isope, Fekrije Selimi

## Correspondence

fekrije.selimi@college-de-france.fr

## In Brief

Sigoillot et al. show that the adhesion-GPCR BAI3 and its ligand C1QL1 contribute to synapse specificity during development. The BAI3 receptor regulates synaptogenesis for both types of excitatory inputs on cerebellar Purkinje cells, whereas C1QL1 promotes proper synaptogenesis and innervation territory for only one type, the climbing fiber.

Sigoillot et al., 2015, Cell Reports *10*, 820–832
February 10, 2015 
http://dx.doi.org/10.1016/j.celrep.2015.01.034

CellPress

OPEN ACCESS
CellPress

Cell Reports
Article

# The Secreted Protein C1QL1 and Its Receptor BAI3 Control the Synaptic Connectivity of Excitatory Inputs Converging on Cerebellar Purkinje Cells

Séverine M. Sigoillot,[1] Keerthana Iyer,[1] Francesca Binda,[2] Inés González-Calvo,[1,2] Maëva Talleur,[1] Guilan Vodjdani,[3] Philippe Isope,[2] and Fekrije Selimi[1,*]
[1]Center for Interdisciplinary Research in Biology (CIRB), Collège de France; CNRS UMR 7241; and INSERM U1050, Paris 75005, France
[2]Institut des Neurosciences Cellulaires et Intégratives, CNRS UPR 3212, Université de Strasbourg, Strasbourg 67084, France
[3]Neuroprotection du Cerveau en Développement (PROTECT), INSERM, UMR1141, Université Paris-Diderot, Sorbonne Paris-Cité, Paris 75019, France
*Correspondence: fekrije.selimi@college-de-france.fr
http://dx.doi.org/10.1016/j.celrep.2015.01.034


## SUMMARY

**Precise patterns of connectivity are established by different types of afferents on a given target neuron, leading to well-defined and non-overlapping synaptic territories. What regulates the specific characteristics of each type of synapse, in terms of number, morphology, and subcellular localization, remains to be understood. Here, we show that the signaling pathway formed by the secreted complement C1Q-related protein C1QL1 and its receptor, the adhesion-GPCR brain angiogenesis inhibitor 3 (BAI3), controls the stereotyped pattern of connectivity established by excitatory afferents on cerebellar Purkinje cells. The BAI3 receptor modulates synaptogenesis of both parallel fiber and climbing fiber afferents. The restricted and timely expression of its ligand C1QL1 in inferior olivary neurons ensures the establishment of the proper synaptic territory for climbing fibers. Given the broad expression of C1QL and BAI proteins in the developing mouse brain, our study reveals a general mechanism contributing to the formation of a functional brain.**

## INTRODUCTION

In the nervous system, each type of neuron is connected to its afferents in a stereotyped pattern that is essential for the proper integration of information and brain function. A neuron can receive several convergent inputs from different neuronal populations with specific characteristics. The number and the subcellular localization of synapses from each afferent on a target neuron are determined by a complex developmental process that involves recognition, repulsion, elimination of supernumerary synapses, and/or guidance posts (Sanes and Yamagata, 2009; Shen and Scheiffele, 2010). How these precise patterns of connectivity are established is likely to vary depending on the neuronal population and remains a poorly understood question.

Several classes of adhesion proteins, such as cadherins, immunoglobulin-superfamily (IgSF) proteins, neuroligins, and leucine-rich repeats transmembrane (LRRTM) proteins, have been involved in synapse formation, maturation, and function (Shen and Scheiffele, 2010). In addition, secreted proteins, such as WNTs (Salinas, 2012), pentraxins (Sanes and Yamagata, 2009; Shen and Scheiffele, 2010; Sia et al., 2007), or CBLNs (Yuzaki, 2011), can regulate synapse formation and function, both in an anterograde and retrograde manner. This molecular diversity and functional redundancy is in agreement with the idea that a specific set of molecular pathways defines each combination of afferent-target neuron in the vertebrate brain (O'Rourke et al., 2012; Sperry, 1963).

Molecular signaling pathways regulate different aspects of synapse specificity. Adhesion proteins, such as IgSF members sidekicks in the retina (Yamagata and Sanes, 2008), can have an instructive role for the choice of the synaptic partners and also determine the balance of inhibitory versus excitatory connectivity, as illustrated by the studies of neuroligins (Südhof, 2008). Further specificity resides in the definition of non-overlapping territories for inhibitory and excitatory synapses on a given neuron. For example, Purkinje cells receive two types of excitatory inputs (parallel fibers from granule cells and climbing fibers from inferior olivary neurons) and two types of inhibitory inputs (from basket cells and stellate cells), which form synapses on separate and non-overlapping territories. Adhesion proteins from the L1 Ig subfamily have been shown to control the specific subcellular localization of each inhibitory synapse (Ango et al., 2004, 2008). A very recent study of Ce-Punctin, an ADAMTS-like secreted protein, in the invertebrate nervous system has shown that specific isoforms are secreted by cholinergic and inhibitory inputs and control the proper localization of corresponding synapses at the neuromuscular junction (Pinan-Lucarré et al., 2014). Thus, in addition to adhesion proteins, the specific secretion of some factors could play an important role in defining synapse specificity.

In the vertebrate brain, the complement C1Q-related proteins comprise several subfamilies: proteins related to the innate

immunity factor C1Q, some of which have been involved in synapse elimination (Stevens et al., 2007), CBLNs known for promoting synapse formation (Yuzaki, 2011), and the C1Q-like (C1QL) subfamily. Proteins of this last subclass were recently shown to be high-affinity binding partners of the adhesion G-protein-coupled receptor (GPCR) brain angiogenesis inhibitor 3 (BAI3) and to promote synapse elimination in cultured hippocampal neurons (Bolliger et al., 2011). Our understanding of the function of brain angiogenesis inhibitor receptors in synaptogenesis is limited. The BAI3 receptor has been identified in biochemical preparations of synapses both in the forebrain (Collins et al., 2006) and in the cerebellum (Selimi et al., 2009), and recently, BAI1 was shown to promote spinogenesis and synaptogenesis through its activation of RAC1 in cultured hippocampal neurons (Duman et al., 2013). Interestingly, the BAI proteins have been associated with several psychiatric symptoms by human genetic (DeRosse et al., 2008; Liao et al., 2012) or functional studies (Okajima et al., 2011) and could thus directly be involved in the synaptic defects found in these disorders. In the present study, we explored the role of the C1QL/BAI3 signaling pathway in the establishment of specific neuronal networks using a combination of expression and functional studies in the developing mouse brain. Our results show that the temporally and spatially controlled expression of C1QL1 and the presence of its receptor, the adhesion-GPCR BAI3, in target neurons are key determinants of excitatory synaptogenesis and innervation territories in the vertebrate brain.

## RESULTS

### The Spatiotemporal Expression Pattern of the C1QL Ligands and Their BAI3 Receptor Is in Agreement with a Role in Neuronal Circuit Formation

The adhesion-GPCR BAI3 has been found at excitatory synapses by biochemical purifications (Collins et al., 2006; Selimi et al., 2009). In transfected hippocampal neurons, BAI3 is highly enriched in spines and is found to colocalize with and surround clusters of the postsynaptic marker PSD95 using immunocytochemistry (Figure S1). Together with the fact that BAI receptors can modulate RAC1 activity, a major regulator of the actin cytoskeleton, in neurons (Duman et al., 2013; Lanoue et al., 2013), these data suggest a function for the BAI3 receptor in the control of synaptogenesis. To play this role, the timing and pattern of BAI3 expression should be in agreement with the timing of synaptogenesis. In situ hybridization experiments showed that *Bai3* mRNAs are highly expressed in the mouse brain during the first 2 postnatal weeks, in regions of intense synaptogenesis such as the hippocampus, cortex, and cerebellum (Figure 1A). In the cerebral cortex, a gradient of *Bai3* expression is observed with the highest level at postnatal day 0 (P0) in the deep layers and at P7 in the most superficial layer, reminiscent of the inside-out development of this structure. At these stages, *Bai3* is also expressed in the brainstem, in particular in the basilar pontine nucleus and the inferior olive, and in the cerebellum (Figure 1A). In the adult mouse brain, *Bai3* expression decreases in many regions, such as in the brainstem (assessed by qRT-PCR; Figure 1B) and becomes restricted to a few neuronal populations, such as cerebellar Purkinje cells, pyramidal cells in the hippocampus, and neurons in the cerebral cortex (Figures 1A and S2).

Secreted C1QL proteins of the C1Q complement family can bind the BAI3 receptor with high affinity (Bolliger et al., 2011) and could thus regulate its synaptic function. In situ hybridization experiments (Figure 1), in accordance with previously published data (Iijima et al., 2010), show that *C1ql* mRNAs, in particular *C1ql1* and *C1ql3*, are highly expressed during the first 2 postnatal weeks in various neuronal populations. *C1ql3* mRNA is found in the cortex, lateral amygdala, dentate gyrus, and deep cerebellar nuclei. *C1ql1* is very highly expressed in the inferior olive at all stages, including in the adult. It is also found at P0 and P7 in neurons of the hippocampus, cerebral cortex, and in few other neurons of the brainstem. By qRT-PCR, we also detected *C1ql1* expression in the cerebellum, with a peak at P7 at a level that is 5-fold less than in the brainstem. This transient cerebellar expression is in agreement with previous in situ hybridization data that showed expression of *C1ql1* in the external granular layer of the developing cerebellum (Iijima et al., 2010).

This expression analysis shows that C1QL proteins are produced in neurons that are well-described afferents of neurons expressing BAI3, such as inferior olivary neurons that connect Purkinje cells (PCs). It also indicates that different C1QL/BAI3 complexes could control synaptogenesis in various regions of the brain. The C1QL3/BAI3 complex is prominent in the cortex and hippocampus, whereas the C1QL1/BAI3 complex might be particularly important for excitatory synaptogenesis on cerebellar PCs. Indeed, the expression pattern of the C1QL1/BAI3 couple correlates with the developmental time course of excitatory synaptogenesis in PCs: these neurons receive their first functional synapses from the climbing fibers, the axons of the inferior olivary neurons, on their somata around P3, at a time when *C1ql1* mRNA expression starts to increase sharply (Figures 1A and 1B), and when *Bai3* mRNA is already found in PCs (Figures 1 and S2). PCs are subject to an intense period of synaptogenesis with their second excitatory inputs, the parallel fibers, starting at P14, when *Bai3* expression in the cerebellum reaches its maximum (Figure 1B). Given the well-described timing and specificity of PC excitatory connectivity, we focused our studies on the olivocerebellar network to identify the function of the C1QL/BAI3 complexes during the formation of neuronal circuits.

### The Adhesion-GPCR BAI3 Promotes the Development of Excitatory Synaptic Connectivity on Cerebellar PCs

Inferior olivary neurons send their axons to the cerebellum, where they start forming functional synapses on somata of PCs at around P3. These projections mature into climbing fibers (CFs) while PCs develop their dendritic arbor during the second postnatal week. Starting at P9, a single CF translocates and forms a few hundred synapses on thorny spines of PC proximal dendrites (Hashimoto et al., 2009). Each PC also receives information from up to 175,000 parallel fibers (PFs) through synapses formed on distal dendritic spines, in particular during the second and third postnatal weeks (Sotelo, 1990). To test the role of the BAI3 receptor during the development of the olivocerebellar network, we developed an RNAi approach: two different short hairpin RNAs targeting different regions of the *Bai3* mRNA

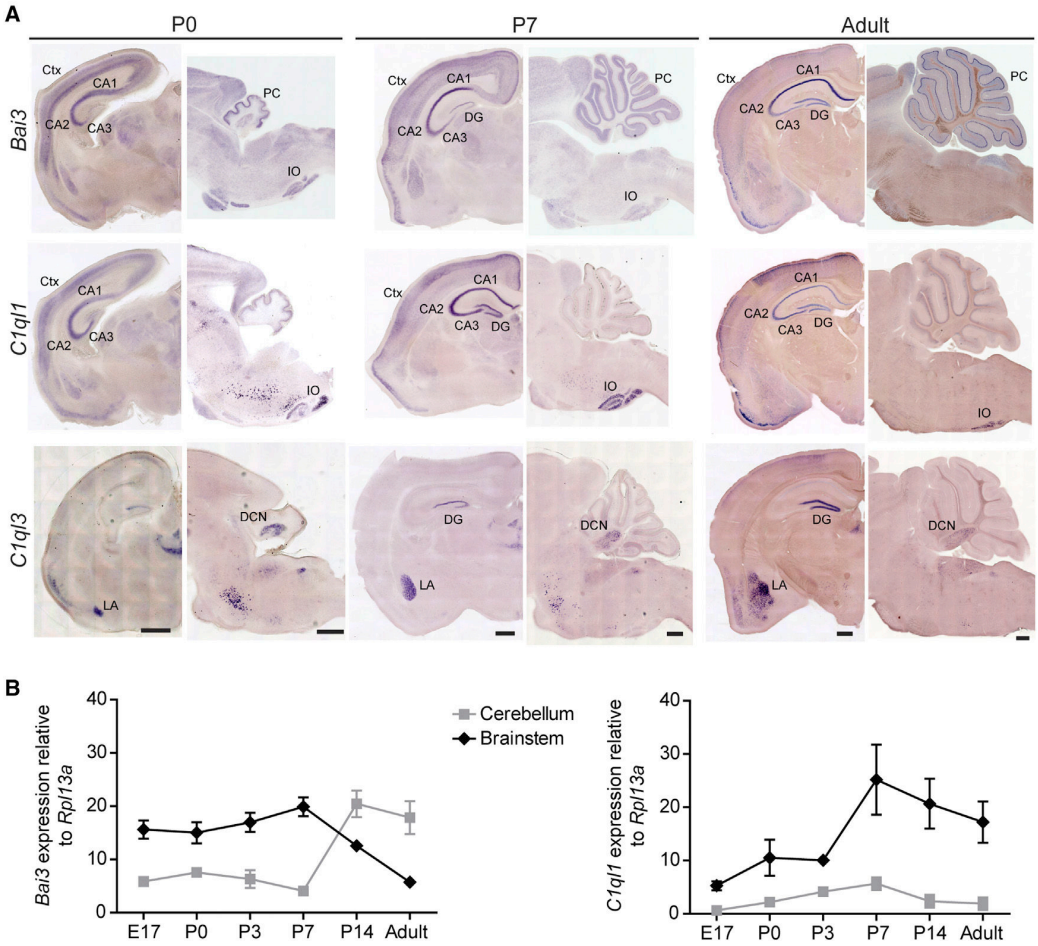


**Figure 1. Developmentally Regulated Expression of the *Bai3* and *C1ql* Genes in the Mouse Brain**

(A) In situ hybridization experiments were performed using probes specific for *Bai3*, *C1ql1*, and *C1ql3* on coronal (left) and sagittal (right) sections of mouse brain taken at postnatal day 0 (P0), P7, and adult. Ctx, cortex; DCN, deep cerebellar nuclei; DG, dentate gyrus; Hp, hippocampus; IO, inferior olive; LA, lateral amygdala; PC, Purkinje cell. The scale bars represent 500 μm; each scale bar applies to the whole column.

(B) Expression of *Bai3* and *C1ql1* was assessed at different stages of mouse brain development with qRT-PCR on mRNA extracts from brainstem and cerebellum (E17, embryonic day 17; P0–P14, postnatal day 0 to 14). Expression levels are normalized to the *Rpl13a* gene. n = 3 samples per stage. Data are presented as mean ± SEM.

See also Figure S2.

(shBAI3) were designed and selected after testing their efficiency in transfected HEK293 cells (data not shown). A lentiviral vector was then used to drive their expression in neurons both in vivo and in vitro, together with the expression of enhanced GFP (eGFP; under the control of the ubiquitous PGK1 promoter). In mixed cerebellar cultures transduced at 4 days in vitro (DIV4), both shRNAs led to about 50% knockdown of *Bai3* by DIV7 and did not affect the expression level of another PC-expressed gene, *Pcp2*, confirming their specificity (Figure S3A). Knockdown of *Bai3* was still present after 10 days in culture (Figure S3A). Morphological analysis in mixed cerebellar cultures confirmed that both shRNAs against *Bai3* induced the same phenotype (cf. below). Because one of the shRNA constructs was more efficient (similar levels of knockdown with half the amount of lentiviral particles), it was chosen for in vivo experiments.

Recombinant lentiviral particles driving either shBAI3 or a control non-targeting shRNA (shCTL) were injected in the molecular layer of the cerebellum of mouse pups at P7, when the most intense period of PF synaptogenesis starts and just before the translocation of the strongest CF (Hashimoto et al., 2009). *Bai3* knockdown induced visible deficits in the connectivity between CFs and their target PCs visualized at P21 using an antibody against VGLUT2, a specific marker of CF presynaptic boutons in the molecular layer (Figure 2). The extension of the CF synaptic territory on arbors of PCs expressing shBAI3 was reduced by about 35% when compared to shCTL-expressing PCs (Figures 2A and 2C). This effect is

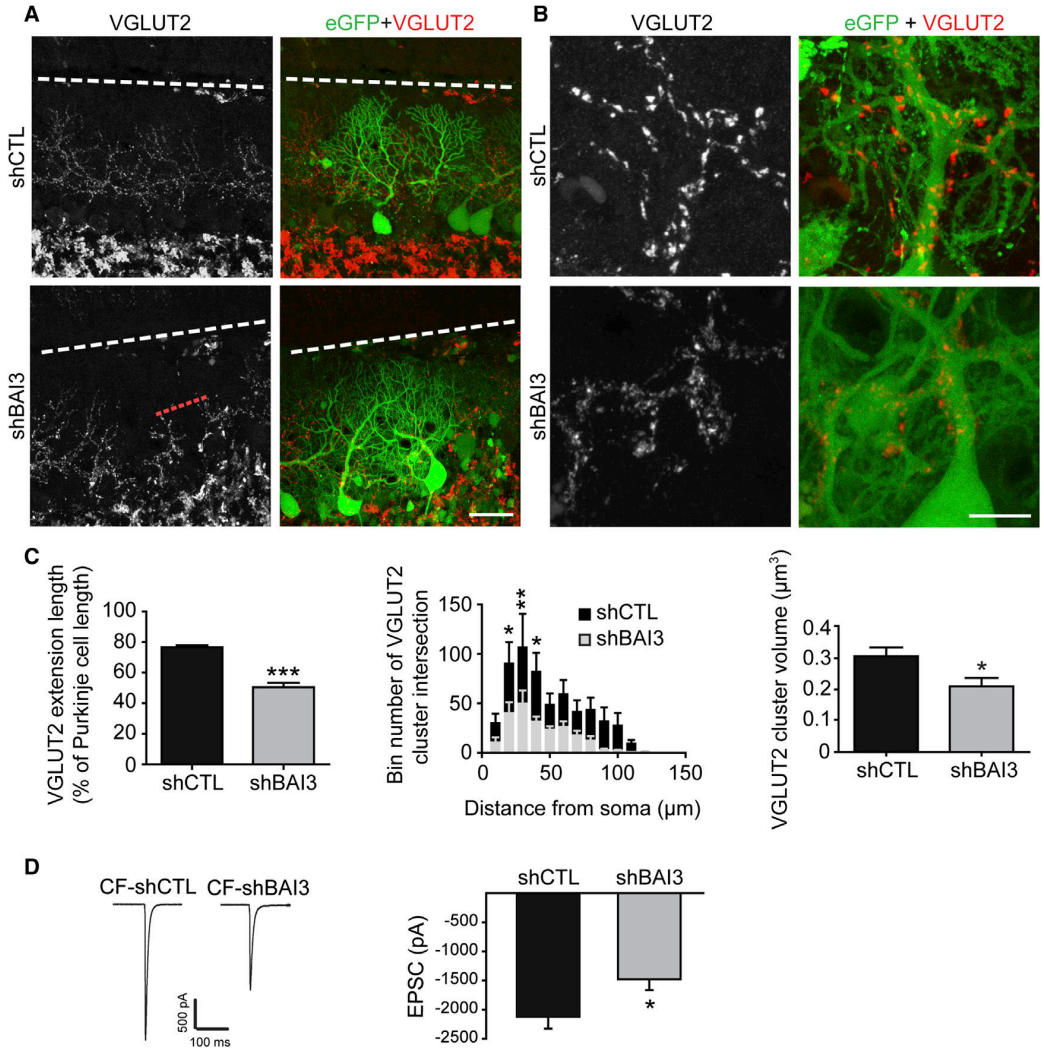


**Figure 2. The Adhesion-GPCR BAI3 Promotes Synaptogenesis and the Innervation Territory of CFs on PCs**

(A and B) Defects in CF synapses were assessed at P21 after stereotaxic injections at P7 of recombinant lentiviral particles driving expression of shRNA against *Bai3* (shBAI3) or control shRNA (shCTL). Immunostaining for vesicular glutamate transporter 2 (VGLUT2) was used to label specifically CF synapses on transduced PCs (eGFP positives). (A) Representative images of VGLUT2 extension. Pial surface: white dashed line. The scale bar represents 40 µm. (B) Representative images of VGLUT2 cluster morphology. The scale bar represents 10 µm.

(C) The extension of VGLUT2 clusters relative to PC height, their mean number, and volume were quantified using Image J. n ≥ 22 cells, n = 3 animals per condition. Data are presented as mean ± SEM; unpaired Student's t test or two-way ANOVA followed by Bonferroni post hoc test; *p < 0.05; **p < 0.01; ***p < 0.001.

(D) Electrophysiological recordings of P18–P23 PCs transduced with recombinant lentiviral particles driving expression of either shBAI3 or shCTL. CF-mediated whole-cell currents are shown in the left panel. Averages of five stimuli for two representative cells are shown. Traces were recorded at −10 mV following CF stimulation. Total CF-mediated EPSCs were quantified and plotted in the bar graph shown in the right panel. Bars represent mean ± SEM. Unpaired Student's t test; *p < 0.05.

See also Figures S3A and S4A.

cell-autonomous because it is not observed in non-eGFP PCs in the transduced region (Figure S4A). Quantification of synaptic puncta revealed a reduction in number (507.75 ± 109.94 versus 217.10 ± 37.21; *p ≤ 0.05, Student's unpaired t test) and volume (about 30%) of VGLUT2 clusters on shBAI3-PCs when compared to shCTL-PCs (Figure 2). These morphological changes were accompanied by a deficiency in CF transmission, as shown by the reduced whole-cell currents elicited by CF stimulation in PCs recorded in acute cerebellar slices from P18 to P23 mice (Figure 2D; shCTL = −2,122.54 ± 204.77 pA, n = 5 cells; shBAI3 = −1,478.6 ± 186.24 pA, n = 8 cells; Student's t test; *p < 0.05).

A reduced spine density was also evident at P21 in distal dendrites of shBAI3-PCs (Figure 3A), suggesting a potential defect in PF connectivity. To confirm this, we recorded PF-EPSCs of PCs and input-output relationships were examined. Their amplitudes gradually increased with PF stimulus intensity but reached a plateau for much smaller values of stimulation in BAI3-deficient PCs than in control PCs (Figure 3B). The high density of PF synapses in the cerebellar molecular layer impedes precise morphological quantifications of synaptic defects in transduced PCs in vivo. We thus turned to mixed cerebellar cultures that recapitulate PF synaptogenesis with similar characteristics as in vivo because, in this system, PCs develop highly branched dendrites studded with numerous spines on which granule cells form synapses. The effect of *Bai3* knockdown on PF/PC spinogenesis and synaptogenesis was assessed at DIV14, 10 days post-transduction, by co-immunolabeling followed by high-resolution confocal imaging and quantitative analysis. An antibody against the soluble calcium-binding protein CaBP allowed us to label PC dendrites and spines, and an antibody against the vesicular transporter VGLUT1 was used to label specifically the PF presynaptic boutons (Figure 3C). A reduced spine density and a decreased mean spine head diameter was measured on 3D-reconstructed dendrites after transduction of PCs with either of the two shRNAs targeting *Bai3* (32% and 22% for shRNA no. 1 and shRNA no. 2, respectively, when compared to shCTL; cf. Figures 3D and S5). A significant reduction in the density of PF contacts was also revealed in shBAI3-PCs compared to controls, at a level similar to the one observed for spine density (24% and 22% for shRNA no. 1 and shRNA no. 2, respectively; cf. Figures 3E and S5C). Both shRNAs against *Bai3* induced similar defects. These reductions in spine and synapse density were not observed in non-transduced (non-eGFP) PCs in transduced mixed cultures, showing that the effect of *Bai3* knockdown was cell-autonomous (Figures S4B and S4C). These results show that the adhesion-GPCR BAI3 regulates PF connectivity on PCs by controlling spinogenesis and synaptogenesis.

Thus, the adhesion-GPCR BAI3 is a general promoter of excitatory synaptogenesis during development of the olivocerebellar circuit, given that it controls the connectivity of both PF and CF excitatory inputs on cerebellar PCs.

## The Ligand C1QL1 Is Indispensable for CF/PC Synaptogenesis

In the developing olivocerebellar circuit, *C1ql1* is expressed at high levels by inferior olivary neurons. The deficits in CF/PC synaptogenesis induced by knockdown of the adhesion-GPCR BAI3 suggested that the secretion of its ligand C1QL1 by CFs could also regulate this process. An RNAi approach was developed to target *C1ql1* by designing and selecting a shRNA efficient for *C1ql1* knockdown (shC1QL1) in transfected HEK293 cells (data not shown). To enable transduction of neurons in vitro and in vivo, this shRNA was then integrated in a lentiviral vector co-expressing eGFP under the ubiquitous PGK1 promoter. qRT-PCR analysis showed that a 90% reduction in *C1ql1* mRNA expression was induced by DIV7, 3 days post-transduction, an effect that was maintained at DIV14 (Figure S3B). *C1ql1* expression levels could be entirely restored by co-transduction with lentiviral particles driving the expression of a resistant *C1ql1* cDNA construct under the PGK1 promoter, but not by a wild-type *C1ql1* construct (Figure S3B).

The morphology and function of CF/PC synapses were assessed after injection of lentiviral particles driving shC1QL1 in the inferior olive of P4 neonates (Figure S6). This stage corresponds to the beginning of CF synaptogenesis on PC somata and precedes their translocation on PC dendrites (Figure S6). Compared to control shCTL-CFs that extended to 61% of the PC dendritic height by P14, there was a small but significant reduction in the extension of shC1QL1-CFs to about 56% (Figures 4A and 4B). There was little difference in the proportion of translocating CFs at P9 (11/35 for shCTL, 8/31 for shC1QL1, and 14/46 for shC1QL1+C1QL1 Rescue; Figure S6C). These results suggest that *C1ql1* knockdown in inferior olivary neurons has only a small effect on the ability of CFs to translocate. In contrast, the extension of the synaptic territory of shC1QL1-CFs, as assessed by anti-VGLUT2 immunolabeling, was decreased by half compared to control shCTL-CFs (30% and 60% of PC dendritic height, respectively; Figure 4). The mean number of VGLUT2-positive clusters per transduced CF was also reduced by 50% by *C1ql1* knockdown (Figure 4). Co-transduction with lentiviral particles driving the expression of the resistant *C1ql1* construct could partially rescue these phenotypes, showing that they were dependent on *C1ql1* expression (Figure 4). To confirm these synaptic phenotypes at the electrophysiology level, CF-EPSCs were recorded in PCs in acute slices from animals injected with shC1QL1 and shCTL lentiviral particles. Recordings were performed in lobule II, a region targeted by transduced CFs. A 49% decrease in CF transmission was observed in PCs from animals injected with shC1QL1 particles when compared to PCs from animals injected with shCTL particles (Figure 4C; shCTL = −1,771.27 ± 220.87 pA, n = 8 cells; shC1QL1 = −907.59 ± 131.67 pA, n = 8 cells; Mann Whitney *U* test; $^*p < 0.05$). All together, these results show that *C1ql1* expression by CFs is indispensable for their normal connectivity on PCs.

## Restriction of *C1ql1* Expression to CFs in the Cerebellum Is Necessary for Their Proper Innervation of the Target PC

The translocation of the "winner" CF on PC proximal dendrites starts at around P9 and continues until about P21, when the CF acquires its final synaptic territory (Figure 2; Hashimoto et al., 2009). At P7, just before CF translocation, the expression of *C1ql1* decreases in the cerebellum whereas it starts to increase in the brainstem to reach a plateau by P14 (Figure 1). To assess whether the specific expression pattern of *C1ql1* contributes to the acquisition of the final innervation territory of CFs on PCs, we misexpressed *C1ql1* in the cerebellum, by injecting lentiviral particles driving expression of a *C1ql1* cDNA (under the control of the PGK1 promoter) in the molecular layer at P7 (Figure 5). The synaptic territory of CFs on PC dendrites was significantly reduced at P14 by *C1ql1* misexpression when compared to eGFP controls (VGLUT2 puncta extending to 45% and 60% of PC height, respectively). Thus, the restricted and specific expression of *C1ql1* by inferior olivary neurons that is progressively established during development is

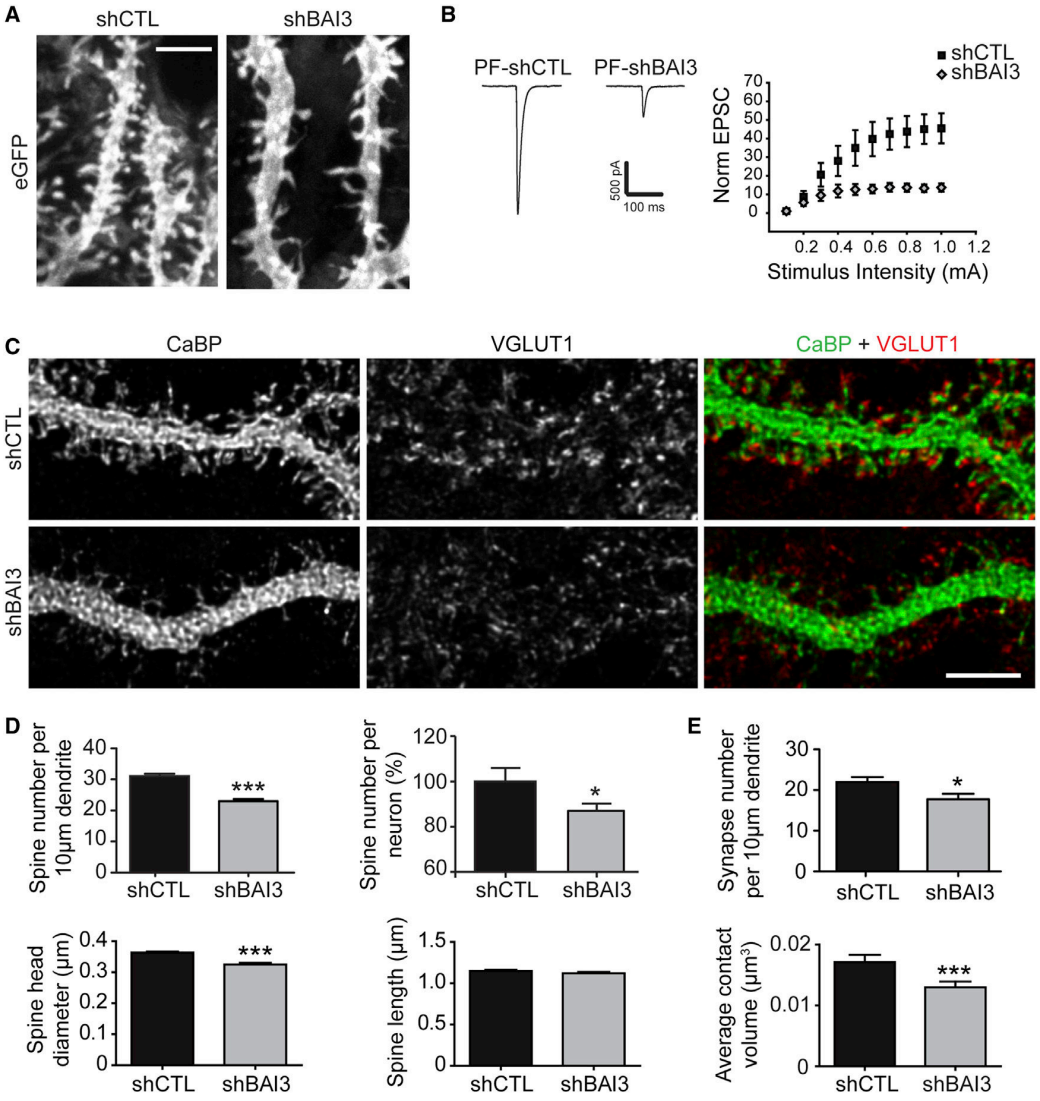


**Figure 3. The Adhesion-GPCR BAI3 Promotes Spinogenesis and PF Synaptogenesis in PCs**

(A) Reduced spine density in distal dendrites of PCs after in vivo knockdown of *Bai3* using stereotaxic injections of lentiviral particles in the vermis of P7 mice. Effects of shBAI3 or shCTL expression were visualized at P21 on transduced PCs (eGFP positives). The scale bar represents 5 μm.

(B) PF-ESPCs recorded in PCs (P18–P23) after stereotaxic injections of lentiviral particles at P7. Averaged traces recorded at maximum stimulus intensity are shown for one representative cell per condition (control: PF-shCTL, left; BAI3 knockdown: PF-shBAI3, right). Input/output curves obtained for both conditions are significantly different (right panel: Kolmogorov-Smirnov test; $p < 0.001$). Data are normalized to the mean value of responses elicited by the minimum stimulus intensity ($-29.63 \pm 9.92$ pA for shCTL and $-32.54 \pm 10.57$ pA for shBAI3) and are plotted as mean ± SEM against stimulus intensity (shCTL black square, n = 9, and shBAI3 gray diamond, n = 10).

(C) Cerebellar mixed cultures were transduced at DIV4 with recombinant lentiviral particles driving expression of eGFP together with shBAI3 or control shCTL. Dendritic spines and PF synapses in transduced PCs (eGFP positives) were imaged at DIV14 after immunostaining for calbindin (CaBP) and VGLUT1. The scale bar represents 5 μm.

(D) Quantitative assessment of the number and morphology of PC spines was performed using the NeuronStudio software. $n \geq 31$ cells per condition, three independent experiments (data are presented as mean ± SEM; unpaired Student's t test; *$p < 0.05$; ***$p < 0.001$).

(E) Quantitative assessment of the number and size of VGLUT1 synaptic contacts in DIV14 PCs was performed using ImageJ. $n \geq 30$ cells per condition, three independent experiments (data are presented as mean ± SEM; unpaired Student's t test and Mann-Whitney *U* test, respectively; *$p < 0.05$; ***$p < 0.001$).

See also Figures S3A, S4, and S5.

OPEN ACCESS
CellPress

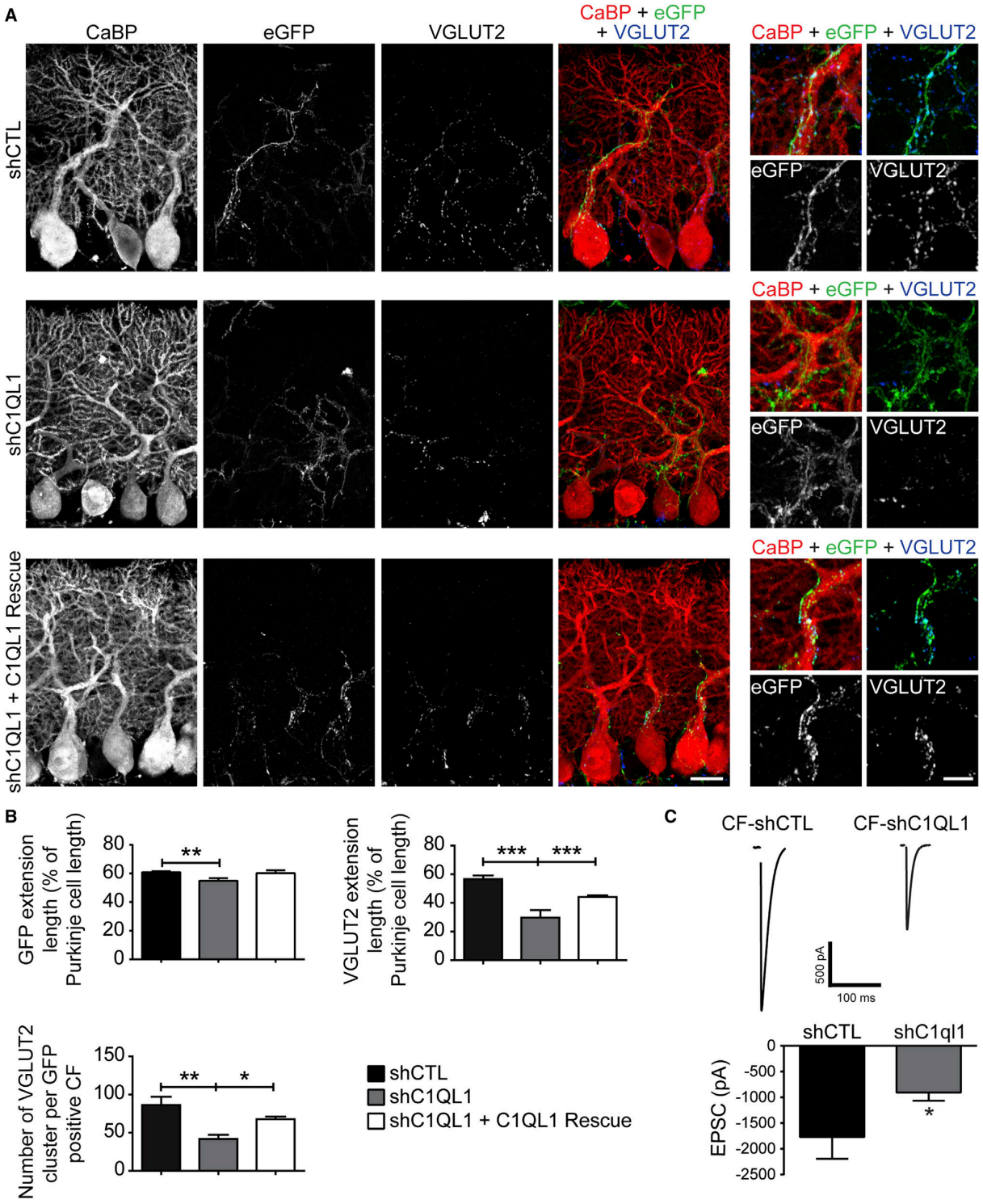


*(legend on next page)*

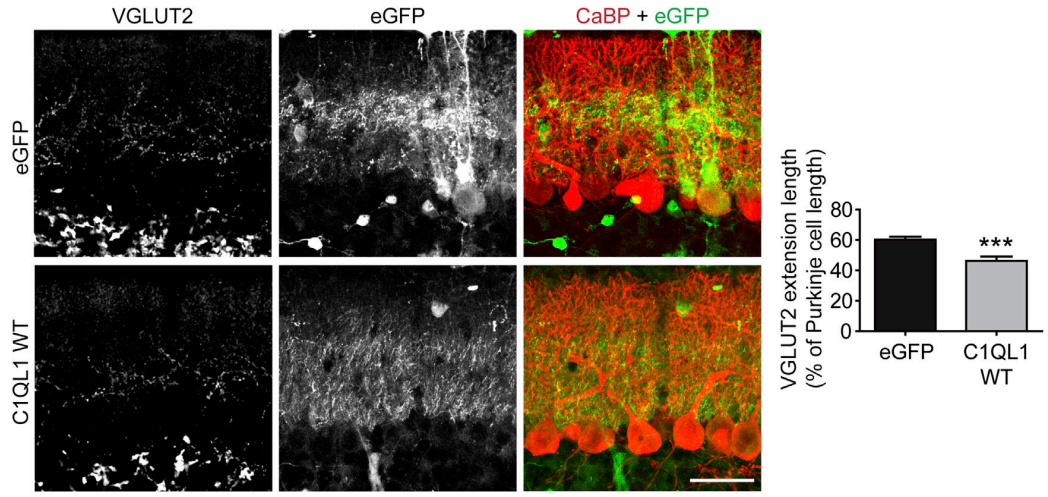


**Figure 5. Misexpression of *C1ql1* Reduces the Synaptic Territory of CFs on PCs**

*C1ql1* misexpression in the cerebellum was performed using stereotaxic injections in the vermis of P7 mice of lentiviral particles, driving the expression of GFP (eGFP) alone or together with C1QL1 (C1QL1 WT). CF extension was imaged at P14 after immunostaining for VGLUT2 (CF synapses) and CaBP (entire PC). n = 6 animals per condition. Data are presented as mean ± SEM; unpaired Student's t test with Welch's correction; ***p < 0.001. The scale bar represents 40 μm.

necessary for the development of the proper synaptic territory of the "winner" CF on the PC dendritic arbor.

## The Ligand C1QL1 Promotes PC Spinogenesis in a BAI3-Dependent Manner

The deficits in PF spinogenesis and synaptogenesis induced by knockdown of the adhesion-GPCR BAI3 cannot be explained by its role in controlling CF/PC synaptogenesis. Because BAI3 has been identified at the PF/PC synapses (Selimi et al., 2009) and *C1ql1* is transiently expressed in the cerebellum (Figure 1B; Iijima et al., 2010), the C1QL1/BAI3 signaling pathway could directly regulate PC spinogenesis and PF synaptogenesis. We tested this hypothesis in cerebellar mixed cultures because the expression pattern of *C1ql1* in this system is similar to the pattern observed in vivo, with a peak at DIV7 (Figure S7). As for its receptor BAI3, the effects of *C1ql1* knockdown were assessed at DIV14, 10 days post-transduction, using CaBP and VGLUT1 immunostaining, high-resolution confocal imaging, and quantitative analysis. Our results show a 47% reduction in PC spine density, a small but significant increase in spine head diameter, but no effect on the mean spine length in shC1QL1-treated cultures compared to shCTL-treated ones (Figure 6). No change in the density of VGLUT1 contacts on PC spines was detected, suggesting that the proportion of PFs able to synapse on the available spines remains stable and that the reduction in spine density is overcome by an increase in the contact ratio between PFs and PCs in our culture system. All these effects were rescued by the concomitant expression of the resistant *C1ql1* cDNA construct, but not by a wild-type *C1ql1* cDNA driven by the same PGK1 promoter (Figure 6). Thus, C1QL1 secretion in the cerebellum modulates spine production in PCs, thereby regulating the amount of postsynaptic sites available for innervation by PFs.

C1QL proteins bind the BAI3 receptor with high affinity (Bolliger et al., 2011), suggesting that C1QL1 could regulate spinogenesis in PCs through the adhesion-GPCR BAI3. In this case, the simultaneous knockdown of both proteins should not induce an additive phenotype. Knockdown of both *Bai3* and *C1ql1*, by co-transduction of cerebellar cultures with a mixture of lentiviral particles, led to a 30% reduction in spine density, similar to the one observed for knockdown of *Bai3* only (Figure 7). Co-transduction of the control shCTL together with either shBAI3 or shC1QL1 induced the same level of spine reduction compared to shBAI3 or shC1QL1 alone (about 30% and 50%, respectively;

**Figure 4. The C1QL1 Protein from Inferior Olivary Neurons Promotes CF/PC Synaptogenesis**

(A) Defects in CF/PC synapses were assessed at P14 after *C1ql1* knockdown. Stereotaxic injections of recombinant lentiviral particles driving expression of a shRNA against *C1ql1* (shC1QL1), a control shRNA (shCTL), or shC1QL1 together with a *C1ql1* rescue cDNA were performed in the inferior olive of P4 mice. Immunostaining for VGLUT2 antibody was used to visualize CF synapses. eGFP-positive CFs correspond to transduced inferior olivary neurons. The scale bar in the left panel represents 20 μm and in the right panel represents 10 μm.

(B) Extension of CFs (eGFP) or of CF synapses (VGLUT2) relative to PC height, as well as the number of CF synapses, were quantified using Image J. n = 4–8 animals and n ≥ 95 CFs per condition. Data are presented as mean ± SEM; one-way ANOVA followed by Kruskal-Wallis post hoc test or Dunn's test; *p < 0.05; **p < 0.01; ***p < 0.001.

(C) Top CF-induced EPSCs recorded in PCs located in the target zone of virally transduced CFs (cf. text). Bottom panel: summary bar graphs showing the averaged peak amplitude of CF-EPSCs for each condition. Bars represent mean ± SEM values. Mann Whitney *U* test; *p < 0.05.

See also Figure S6.

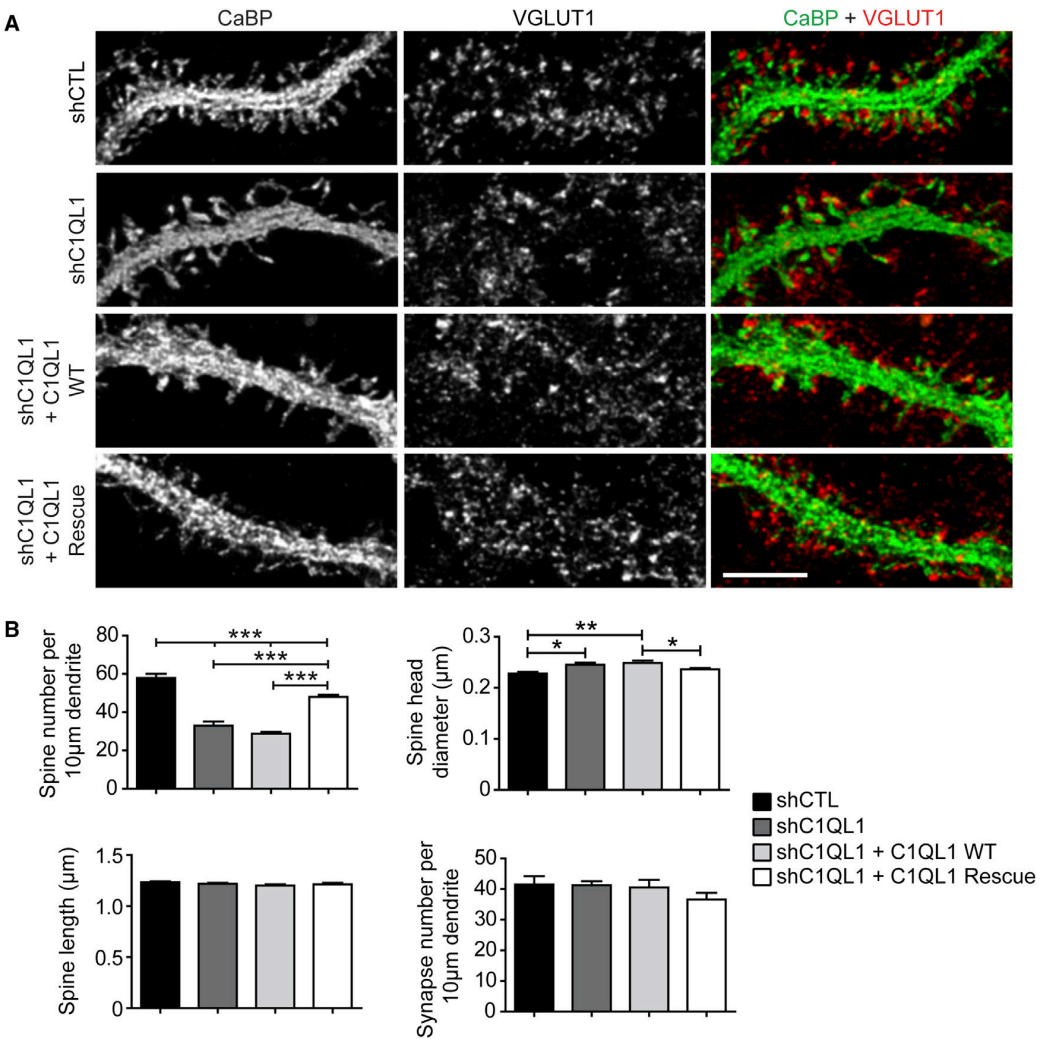


**Figure 6. Transient C1QL1 Secretion in the Cerebellum Promotes PC Spinogenesis**

(A) The role of cerebellar C1QL1 was assessed in mixed cultures using an RNAi approach. Neurons were transduced at DIV4 with recombinant lentiviral particles driving expression of control shRNA (shCTL) or shC1QL1, a mixture of recombinant lentiviral particles driving either shC1QL1 space and wild-type *C1ql1* (knockdown condition), or shC1QL1 and *C1ql1 Rescue* cDNA (control condition). High-resolution confocal imaging was performed at DIV14 after immunostaining for calbindin (CaBP) and VGLUT1 (specific for PF synapses). The scale bar represents 5 µm.

(B) Effects of *C1ql1* knockdown on spine density, head diameter, and length, as well as on the number of VGLUT1 synaptic contacts were quantified. n ≥ 30 cells, three to four independent experiments. Data are presented as mean ± SEM; one-way ANOVA followed by Newman-Keuls or Kruskal-Wallis post hoc test; *p < 0.05; **p < 0.01; ***p < 0.001. Spine density was significantly reduced in all conditions when compared to the shCTL condition.

See also Figure S3B.

Figures 3, 6, and 7), showing that there was no non-specific effect of co-transduction itself on spine density. A non-specific effect of shC1QL1 and shCTL co-expression prevented the interpretation of the data on spine morphology (Figure 7B). The level of reduction in spine density after double knockdown corresponds to the one detected for *Bai3* knockdown alone and is smaller than for *C1ql1* knockdown alone. Thus, whereas C1QL1 and BAI3 do not control spine density independently, their regulation of this process is complex.

## DISCUSSION

Each neuron receives synapses from multiple types of afferents with specific morphological, quantitative, and physiological characteristics. These patterns are stereotyped for each type of neuronal population and are key to the proper integration of signals during brain function. Here, we show that the signaling pathway formed by the secreted protein C1QL1 and the adhesion-GPCR BAI3 regulates the development of proper excitatory

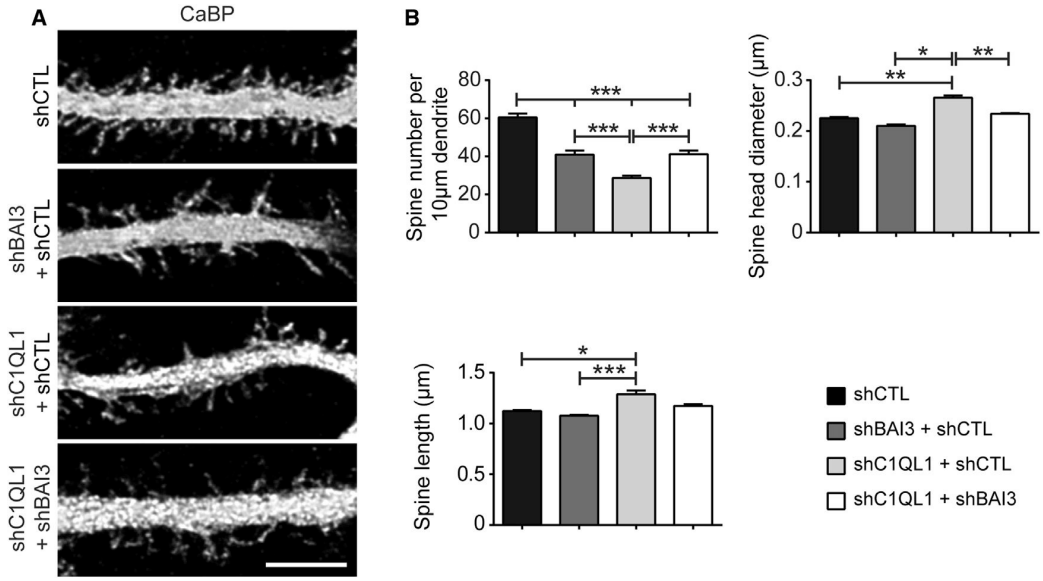


**Figure 7. The Modulation by C1QL1 of PC Spinogenesis Depends on Normal Levels of the BAI3 Receptor**

(A) The functional interaction between C1QL1 and BAI3 was assessed by simultaneous reduction of their expression in cerebellar cultures using an RNAi approach. Neurons were transduced at DIV4 with a mixture of recombinant lentiviral particles driving either shC1QL1 and shBAI3 (double knockdown), shBAI3 and shCTL (*Bai3* knockdown alone), shC1QL1 and shCTL (*C1ql1* knockdown alone), or double amounts of shCTL. Analysis was performed using high-resolution confocal imaging at DIV14 after immunostaining for calbindin (CaBP). The scale bar represents 5 µm.

(B) Quantitative analysis of spine density performed using Neuron Studio. n ≥ 30 cells, three to four independent experiments (data are presented as mean ± SEM; one-way ANOVA followed by Newman-Keuls post hoc test; *p < 0.05; **p < 0.01; ***p < 0.001). Spine density was significantly reduced in all conditions when compared to the shCTL condition.

connectivity on cerebellar PCs. First, the BAI3 receptor promotes both PF and CF connectivity on PCs and is thus a general regulator of excitatory synaptogenesis. Second, the C1QL1 protein is indispensable for proper CF/PC synaptogenesis and the development of the proper synaptic territory, but not for CF translocation. C1QL1 also modulates the production of the final number of distal dendritic spines by PCs, thereby regulating the number of available contact sites for PFs. Given the broad expression of the C1QL/BAI3 pathway in the developing brain, our study informs about a general mechanism used for the control of brain connectivity.

Most excitatory synapses are made on dendritic spines. In the cerebellum, studies of mouse mutants such as *weaver* and *reeler* indicate that PCs can generate spines through an intrinsic program (Sotelo, 1990). Whereas models involving the incoming axons in the process of spine induction have been put forward in other neuronal types such as cortical or hippocampal pyramidal cells, current data do not exclude an intrinsic program for spinogenesis in these neurons (Salinas, 2012; Yuste and Bonhoeffer, 2004). In all cases, the regulation of the actin cytoskeleton, in particular through modulation of RhoGTPases such as RAC1, is essential for the proper morphology and maturation of dendritic spines and associated synapses (Luo, 2002). The BAI receptors can regulate RAC1 activity both in neurons (Duman et al., 2013; Lanoue et al., 2013) and other cell types (Park et al., 2007). Our results show that, as BAI1 in cultured hippocampal neurons (Duman et al., 2013), the adhesion-GPCR BAI3 regulates spinogenesis in distal dendrites of PCs in vivo. PCs produce two types of spines: a small number of thorny spines on the proximal dendrites that are contacted by CFs and very dense spines on the distal dendrites that are contacted by PFs. In the adult cerebellum, PCs generate spines of the distal type in their proximal dendrites if the CF is removed through lesions or activity blockade (Rossi and Strata, 1995), showing an intrinsic ability to produce spines of this type. The adhesion-GPCR BAI3 could be part of this intrinsic program because its expression is maintained at high levels in adult PCs, contrary to many other neurons. Transient expression of *C1ql1* in the external granular layer (Figure 1; Iijima et al., 2010), by a yet-to-be defined cell type, during PC growth can modulate to a certain extent the number of spines produced in PCs, suggesting a local extrinsic regulation of the number of available contact sites for PFs.

Various classes of membrane adhesion proteins regulate the proper formation of mature excitatory synapses, including cadherins, neuroligins, and SynCAM (Shen and Scheiffele, 2010). Besides the well-described role of neurotrophins, increasing evidence also shows a role for other classes of secreted proteins, such as WNTs (Salinas, 2012) or complement C1Q-related proteins (Yuzaki, 2011). The complement C1Q-related family is composed of three different subfamilies: the classical C1Q-related; the cerebellins (CBLN); and the little-studied C1QL proteins. The classic C1Q complement protein promotes synapse elimination in the visual system (Stevens et al., 2007). Secretion

of CBLN1 by granule cells is essential for the formation and stability of their synapses with PCs by bridging beta-neurexin and the glutamate receptor delta 2 (GluRδ2) (Hirai et al., 2005; Matsuda et al., 2010; Uemura et al., 2010). CBLN1 can also stimulate the maturation of presynaptic boutons to match the size of the postsynaptic density (Ito-Ishida et al., 2012). Our results now show that expression of C1QL1 by inferior olivary neurons and of its receptor BAI3 by the target PCs is necessary for the development of CF/PC synapses. Thus, the C1QL and CBLN subfamilies play similar and essential roles during brain development by promoting synaptogenesis between neurons that secrete them and target neurons that express their receptors. Their distinct and non-overlapping expression patterns ensure proper connectivity between different neuronal populations, suggesting that C1QL and CBLN subfamilies are part of the potential "chemoaffinity code" contributing to synapse specificity during circuit formation (Sanes and Yamagata, 2009; Sperry, 1963).

Interestingly, these two subfamilies of complement C1Q-related proteins have distinct types of receptors, both at the structural and functional level: the BAI3 receptor is an adhesion-GPCR that binds C1QL proteins and controls RAC1 activation, whereas GluRδ2, the receptor for CBLN1, has a structure homologous to the glutamate ionotropic receptors and is coupled intracellularly to various signaling molecules such as PDZ proteins or the protein phosphatase PTPMEG (Yuzaki, 2012). GluRδ2 becomes restricted to the PF/PC synapses after P14 and is necessary for synapse formation and maintenance between PFs and PCs. Its removal in genetically modified mice decreases the number of PF/PC synapses and consequently increases the synaptic territory of CFs (Uemura et al., 2007). Thus, each excitatory input of PCs is characterized by a member of a specific C1Q-related subfamily that controls synaptogenesis on PCs through a different signaling pathway. Both GluRδ2 and BAI3 receptors are expressed early in PCs and remain highly expressed in the adult: whether and how these two signaling pathways functionally interact to regulate synaptogenesis remains to be determined.

The subcellular localization of synapses between different types of inputs on a given target neuron is precisely controlled. For example, PFs contact PCs on spines of distal dendrites, whereas CFs make their synapses on proximal dendrites. What regulates this level of specificity, essential for proper integration of signals in the brain, is poorly understood. Adhesion proteins have been involved, such as cadherin-9 for excitatory synapses in the hippocampus (Williams et al., 2011) or L1 family proteins for inhibitory synapses in cerebellar PCs (Ango et al., 2004). Studies of mutant mouse models, together with experiments involving lesions or modulation of activity, have demonstrated that PFs and CFs compete to establish their non-overlapping innervation pattern on cerebellar PCs (Cesa and Strata, 2009; Rossi and Strata, 1995). Whereas PF/PC synaptogenesis has already begun on the developing dendrites, a single CF starts translocating at P9 on the PC primary dendrite (Hashimoto et al., 2009). These data suggest an active mechanism for the control of CF translocation and synaptic territory. *C1ql1* expression highly increases in inferior olivary neurons and becomes restricted to CFs in the olivocerebellar network starting at P7. Removing either C1QL1 from inferior olivary neurons or BAI3 from PCs or misexpressing *C1ql1* in the cerebellum during postnatal development reduces the extent of the synaptic territory of CFs on their target PCs, showing that the secreted protein C1QL1 and its receptor the adhesion-GPCR BAI3 promote CF synaptic territory. The adhesion-GPCR BAI3 is also located at PF/PC synapses and modulates the number of distal dendritic spines where those synapses are formed. Thus, the proper territory of innervation on PCs could be controlled by the competition of excitatory afferents for a limited amount of BAI3 receptor sites. A deficient C1QL1/BAI3 pathway is not enough to prevent CF translocation (Figures 2 and 4) and does not induce PF invasion of the CF territory (data not shown). Eph receptor signaling has been shown to prevent invasion of the CF territory by PFs given that its deficit induces spinogenesis and PF synaptogenesis in the proximal dendrites (Cesa et al., 2011). Thus, CF synaptogenesis and translocation on PCs are controlled by different signaling pathways during development.

The C1QL/BAI3 signaling pathway might regulate synapse specificity in multiple neuronal populations that display segregation of synaptic inputs. In the hippocampus, mossy fibers from the dentate gyrus connect pyramidal cells on thorny excrescences close to the soma, whereas entorhinal afferents form their contacts on distal portions of the dendrites. *C1ql3* is expressed by granule cells in the dentate gyrus and could thus control the segregation pattern of inputs on the dendritic tree of hippocampal pyramidal cells through interaction with the BAI3 receptor. Recently, the importance of secreted proteins in defining synapse specificity has also been highlighted in the invertebrate nervous system by the study of Ce-Punctin (Pinan-Lucarré et al., 2014). Thus, the timely and restricted expression of secreted ligands and their interaction with receptors that regulate spinogenesis, synaptogenesis, and synaptic territory constitute a general mechanism that coordinates the development of a specific and functional neuronal connectivity.

## EXPERIMENTAL PROCEDURES

All animal protocols and animal facilities were approved by the Comité Régional d'Ethique en Expérimentation Animale (no. 00057.01) and the veterinary services (C75 05 12).

### cDNA and RNAi Constructs

The shRNA sequences were 5′tcgtcatagcgtgcatagg3′ for CTL, 5′ggtgaag ggagtcatttat3′ for *Bai3*, and 5′ggcaagtttacatgcaaca3′ for *C1ql1*. They were subcloned under the control of the H1 promoter in a lentiviral vector that also drives *eGFP* expression under the control of PGK1 promoter (Avci et al., 2012). The *C1ql1 WT* cDNA construct (mouse clone no. BC118980) was cloned into the lentiviral vector pSico (Addgene) under the control of the PGK1 promoter. The *eGFP* sequence of the original pSico was replaced by the cerulean sequence. The *C1ql1 Rescue* is a mutated form of *C1ql1 WT* with three nucleotide changes (T498C, A501C, and C504T) that do not modify the amino acid sequence.

### In Vivo Injections

Injections of lentiviral particles in the cerebellum were performed in the vermis of anesthetized P7 Swiss mice at a 1.25-mm depth from the skull to target the molecular and PC layers and at 1.120 mm for Figure 5. Injections of lentiviral particles in the inferior olive were performed in anesthetized P4 Swiss mice, on the left side of the basilar artery in the brainstem. Calibration of the injections showed that this procedure led to transduction of parts of the principal

and dorsal accessory olive. 0.5–1 μl of lentivirus was injected per animal using pulled calibrated pipets.

### Dendritic Spine and Synapse Analysis

For each PC, a dendritic segment of about 100 μm in length and in the distal part of the arborization or after the second branching point was considered. Dendritic spines were analyzed with the NeuronStudio software (version 9.92; Rodriguez et al., 2008). The spine head diameter corresponds to the minimal diameter of the ellipse describing the spine head, calculated in the xy axis. The spine length is the distance from the "tip" of the spine to the surface of the model. Minimum height was set to 0.5 μm and maximum to 8 μm. Synaptic contacts were analyzed using ImageJ-customized macro. The CaBP and the VGLUT1 objects found above a user-defined threshold were selected. Image calculator was used to extract the signal common to CaBP and VGLUT1 images: the number and volume of these puncta were quantified with the 3D Object counter plugin from ImageJ. The size of presynaptic VGLUT2 clusters was analyzed using the ImageJ plugin 3D object counter. Bin number of VGLUT2 cluster intersection was assessed using the Advanced Scholl analysis plugin from ImageJ.

### Statistical Analysis

Data generated with NeuronStudio or ImageJ were imported in GraphPad Prism for statistical analysis. Data were analyzed by averaging the values for each neuron in each condition. Values are given as mean ± SEM. Student's t test or one-way ANOVA followed by Newman-Keuls post hoc test were performed for comparison of two or more samples, respectively. When distribution did not fit the Normal law (assessed using Graphpad Prism), Mann-Whitney *U* test or one-way ANOVA followed by Kruskal-Wallis post hoc test were used. Two-way ANOVA followed by Bonferroni post hoc test was performed for the analysis of bin number of VGLUT2. *$p < 0.05$; **$p < 0.01$; ***$p < 0.001$.

Supplemental Experimental Procedures (cerebellar mixed cultures, qRT-PCR, in situ hybridization, immunohistochemistry, image acquisition, and electrophysiology) are available online.

## SUPPLEMENTAL INFORMATION

Supplemental Information includes Supplemental Experimental Procedures and seven figures and can be found with this article online at http://dx.doi.org/10.1016/j.celrep.2015.01.034.

## AUTHOR CONTRIBUTIONS

F.S., S.M.S., and P.I. designed the experiments. S.M.S., K.I., F.B., I.G.-C., and M.T. performed experiments. G.V. provided critical reagents. All authors discussed the data. F.S., S.M.S., and P.I. wrote the manuscript.

## ACKNOWLEDGMENTS

We would like to thank Pr. A. Prochiantz for critical reading of the manuscript; Dr. M. Wassef for help with in situ hybridization and inferior olive injections; J. Teillon, N. Quenech'du, and P. Mailly from the CIRB Imaging Facility; and J.-C. Graziano from the CIRB Animal Facility. This work has received support under the Investissements d'Avenir program launched by the French government and implemented by the ANR with the references ANR-10-LABX-54 MEMO LIFE (to S.M.S. and F.S.) and ANR-11-IDEX-0001-02 PSL* Research University (to I.G.-C. and F.S.) and under the TIGER project funded by INTERREG IV Rhin Supérieur program and European Funds for Regional Development (FEDER; nos. A31, FB, and PI). Funding was also provided by Fondation Bettencourt Schuller, CNRS, NeRF Ile de France (to S.M.S.), Ecole des Neurosciences de Paris (to K.I.), Fondation pour la Recherche Médicale (to M.T.), ATIP AVENIR (to F.S.), Fondation Jérôme Lejeune (to F.S.), Association Française pour le Syndrôme de Rett (to F.S.), ANR-2010-JCJC-1403-1 (to P.I.), and ANR-13-SAMA-0010-01 (to F.S.).

Received: July 29, 2014
Revised: January 8, 2015
Accepted: January 15, 2015
Published: February 5, 2015

## REFERENCES

Ango, F., di Cristo, G., Higashiyama, H., Bennett, V., Wu, P., and Huang, Z.J. (2004). Ankyrin-based subcellular gradient of neurofascin, an immunoglobulin family protein, directs GABAergic innervation at purkinje axon initial segment. Cell *119*, 257–272.

Ango, F., Wu, C., Van der Want, J.J., Wu, P., Schachner, M., and Huang, Z.J. (2008). Bergmann glia and the recognition molecule CHL1 organize GABAergic axons and direct innervation of Purkinje cell dendrites. PLoS Biol. *6*, e103.

Avci, H.X., Lebrun, C., Wehrlé, R., Doulazmi, M., Chatonnet, F., Morel, M.-P., Ema, M., Vodjdani, G., Sotelo, C., Flamant, F., and Dusart, I. (2012). Thyroid hormone triggers the developmental loss of axonal regenerative capacity via thyroid hormone receptor α1 and krüppel-like factor 9 in Purkinje cells. Proc. Natl. Acad. Sci. USA *109*, 14206–14211.

Bolliger, M.F., Martinelli, D.C., and Südhof, T.C. (2011). The cell-adhesion G protein-coupled receptor BAI3 is a high-affinity receptor for C1q-like proteins. Proc. Natl. Acad. Sci. USA *108*, 2534–2539.

Cesa, R., and Strata, P. (2009). Axonal competition in the synaptic wiring of the cerebellar cortex during development and in the mature cerebellum. Neuroscience *162*, 624–632.

Cesa, R., Premoselli, F., Renna, A., Ethell, I.M., Pasquale, E.B., and Strata, P. (2011). Eph receptors are involved in the activity-dependent synaptic wiring in the mouse cerebellar cortex. PLoS ONE *6*, e19160.

Collins, M.O., Husi, H., Yu, L., Brandon, J.M., Anderson, C.N.G., Blackstock, W.P., Choudhary, J.S., and Grant, S.G.N. (2006). Molecular characterization and comparison of the components and multiprotein complexes in the postsynaptic proteome. J. Neurochem. *97* (1), 16–23.

DeRosse, P., Lencz, T., Burdick, K.E., Siris, S.G., Kane, J.M., and Malhotra, A.K. (2008). The genetics of symptom-based phenotypes: toward a molecular classification of schizophrenia. Schizophr. Bull. *34*, 1047–1053.

Duman, J.G., Tzeng, C.P., Tu, Y.-K., Munjal, T., Schwechter, B., Ho, T.S.-Y., and Tolias, K.F. (2013). The adhesion-GPCR BAI1 regulates synaptogenesis by controlling the recruitment of the Par3/Tiam1 polarity complex to synaptic sites. J. Neurosci. *33*, 6964–6978.

Hashimoto, K., Ichikawa, R., Kitamura, K., Watanabe, M., and Kano, M. (2009). Translocation of a "winner" climbing fiber to the Purkinje cell dendrite and subsequent elimination of "losers" from the soma in developing cerebellum. Neuron *63*, 106–118.

Hirai, H., Pang, Z., Bao, D., Miyazaki, T., Li, L., Miura, E., Parris, J., Rong, Y., Watanabe, M., Yuzaki, M., and Morgan, J.I. (2005). Cbln1 is essential for synaptic integrity and plasticity in the cerebellum. Nat. Neurosci. *8*, 1534–1541.

Iijima, T., Miura, E., Watanabe, M., and Yuzaki, M. (2010). Distinct expression of C1q-like family mRNAs in mouse brain and biochemical characterization of their encoded proteins. Eur. J. Neurosci. *31*, 1606–1615.

Ito-Ishida, A., Miyazaki, T., Miura, E., Matsuda, K., Watanabe, M., Yuzaki, M., and Okabe, S. (2012). Presynaptically released Cbln1 induces dynamic axonal structural changes by interacting with GluD2 during cerebellar synapse formation. Neuron *76*, 549–564.

Lanoue, V., Usardi, A., Sigoillot, S.M., Talleur, M., Iyer, K., Mariani, J., Isope, P., Vodjdani, G., Heintz, N., and Selimi, F. (2013). The adhesion-GPCR BAI3, a gene linked to psychiatric disorders, regulates dendrite morphogenesis in neurons. Mol. Psychiatry *18*, 943–950.

Liao, H.-M., Chao, Y.-L., Huang, A.-L., Cheng, M.-C., Chen, Y.-J., Lee, K.-F., Fang, J.-S., Hsu, C.-H., and Chen, C.-H. (2012). Identification and characterization of three inherited genomic copy number variations associated with familial schizophrenia. Schizophr. Res. *139*, 229–236.

Luo, L. (2002). Actin cytoskeleton regulation in neuronal morphogenesis and structural plasticity. Annu. Rev. Cell Dev. Biol. *18*, 601–635.

Matsuda, K., Miura, E., Miyazaki, T., Kakegawa, W., Emi, K., Narumi, S., Fukazawa, Y., Ito-Ishida, A., Kondo, T., Shigemoto, R., et al. (2010). Cbln1 is a ligand for an orphan glutamate receptor delta2, a bidirectional synapse organizer. Science *328*, 363–368.

O'Rourke, N.A., Weiler, N.C., Micheva, K.D., and Smith, S.J. (2012). Deep molecular diversity of mammalian synapses: why it matters and how to measure it. Nat. Rev. Neurosci. *13*, 365–379.

Okajima, D., Kudo, G., and Yokota, H. (2011). Antidepressant-like behavior in brain-specific angiogenesis inhibitor 2-deficient mice. J. Physiol. Sci. *61*, 47–54.

Park, D., Tosello-Trampont, A.-C., Elliott, M.R., Lu, M., Haney, L.B., Ma, Z., Klibanov, A.L., Mandell, J.W., and Ravichandran, K.S. (2007). BAI1 is an engulfment receptor for apoptotic cells upstream of the ELMO/Dock180/Rac module. Nature *450*, 430–434.

Pinan-Lucarré, B., Tu, H., Pierron, M., Cruceyra, P.I., Zhan, H., Stigloher, C., Richmond, J.E., and Bessereau, J.-L. (2014). C. elegans Punctin specifies cholinergic versus GABAergic identity of postsynaptic domains. Nature *511*, 466–470.

Rodriguez, A., Ehlenberger, D.B., Dickstein, D.L., Hof, P.R., and Wearne, S.L. (2008). Automated three-dimensional detection and shape classification of dendritic spines from fluorescence microscopy images. PLoS ONE *3*, e1997.

Rossi, F., and Strata, P. (1995). Reciprocal trophic interactions in the adult climbing fibre-Purkinje cell system. Prog. Neurobiol. *47*, 341–369.

Salinas, P.C. (2012). Wnt signaling in the vertebrate central nervous system: from axon guidance to synaptic function. Cold Spring Harb. Perspect. Biol. *4*, a008003.

Sanes, J.R., and Yamagata, M. (2009). Many paths to synaptic specificity. Annu. Rev. Cell Dev. Biol. *25*, 161–195.

Selimi, F., Cristea, I.M., Heller, E., Chait, B.T., and Heintz, N. (2009). Proteomic studies of a single CNS synapse type: the parallel fiber/purkinje cell synapse. PLoS Biol. *7*, e83.

Shen, K., and Scheiffele, P. (2010). Genetics and cell biology of building specific synaptic connectivity. Annu. Rev. Neurosci. *33*, 473–507.

Sia, G.-M., Béïque, J.-C., Rumbaugh, G., Cho, R., Worley, P.F., and Huganir, R.L. (2007). Interaction of the N-terminal domain of the AMPA receptor GluR4 subunit with the neuronal pentraxin NP1 mediates GluR4 synaptic recruitment. Neuron *55*, 87–102.

Sotelo, C. (1990). Cerebellar synaptogenesis: what we can learn from mutant mice. J. Exp. Biol. *153*, 225–249.

Sperry, R.W. (1963). Chemoaffinity in the orderly growth of nerve fiber patterns and connections. Proc. Natl. Acad. Sci. USA *50*, 703–710.

Stevens, B., Allen, N.J., Vazquez, L.E., Howell, G.R., Christopherson, K.S., Nouri, N., Micheva, K.D., Mehalow, A.K., Huberman, A.D., Stafford, B., et al. (2007). The classical complement cascade mediates CNS synapse elimination. Cell *131*, 1164–1178.

Südhof, T.C. (2008). Neuroligins and neurexins link synaptic function to cognitive disease. Nature *455*, 903–911.

Uemura, T., Kakizawa, S., Yamasaki, M., Sakimura, K., Watanabe, M., Iino, M., and Mishina, M. (2007). Regulation of long-term depression and climbing fiber territory by glutamate receptor delta2 at parallel fiber synapses through its C-terminal domain in cerebellar Purkinje cells. J. Neurosci. *27*, 12096–12108.

Uemura, T., Lee, S.-J., Yasumura, M., Takeuchi, T., Yoshida, T., Ra, M., Taguchi, R., Sakimura, K., and Mishina, M. (2010). Trans-synaptic interaction of GluRdelta2 and Neurexin through Cbln1 mediates synapse formation in the cerebellum. Cell *141*, 1068–1079.

Williams, M.E., Wilke, S.A., Daggett, A., Davis, E., Otto, S., Ravi, D., Ripley, B., Bushong, E.A., Ellisman, M.H., Klein, G., and Ghosh, A. (2011). Cadherin-9 regulates synapse-specific differentiation in the developing hippocampus. Neuron *71*, 640–655.

Yamagata, M., and Sanes, J.R. (2008). Dscam and Sidekick proteins direct lamina-specific synaptic connections in vertebrate retina. Nature *451*, 465–469.

Yuste, R., and Bonhoeffer, T. (2004). Genesis of dendritic spines: insights from ultrastructural and imaging studies. Nat. Rev. Neurosci. *5*, 24–34.

Yuzaki, M. (2011). Cbln1 and its family proteins in synapse formation and maintenance. Curr. Opin. Neurobiol. *21*, 215–220.

Yuzaki, M. (2012). The ins and outs of GluD2—why and how Purkinje cells use the special glutamate receptor. Cerebellum *11*, 438–439.

**Cell Reports**

**Supplemental Information**

# The Secreted Protein C1QL1 and Its Receptor BAI3 Control the Synaptic Connectivity of Excitatory Inputs Converging on Cerebellar Purkinje Cells

**Séverine M. Sigoillot, Keerthana Iyer, Francesca Binda, Inés Gonzalez-Calvo, Maëva Talleur, Guilan Vodjdani, Philippe Isope, and Fekrije Selimi**

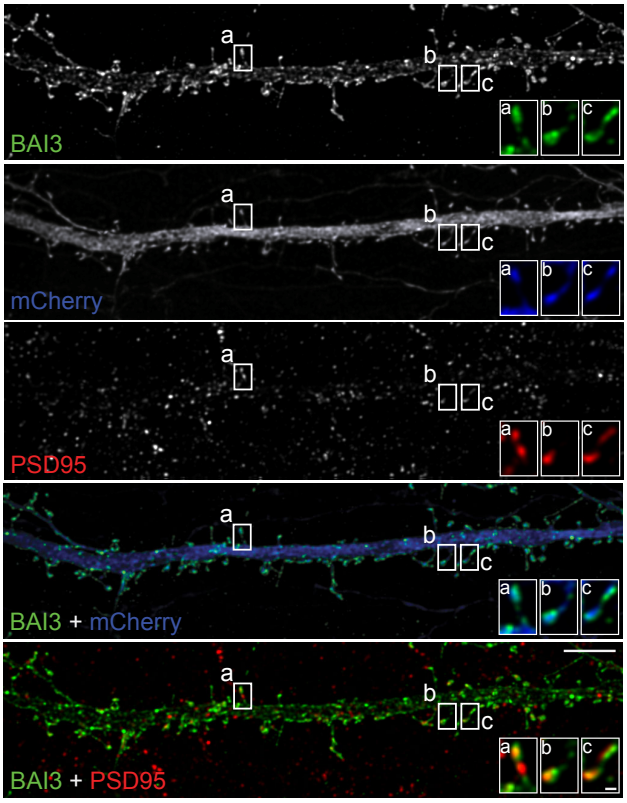


**Figure S1, related to Figure 2 and 3. BAI3 is localized in spines and partially colocalized with the postsynaptic density in cultured hippocampal neurons.**
DIV20 hippocampal neurons co-transfected at DIV18 with BAI3 and mCherry constructs were immunostained for BAI3 and the postsynaptic density marker PSD95. Higher magnifications of regions (a-c) are shown in the insets on the bottom right. Scale bars, 5µm and 0.5µm for insets.

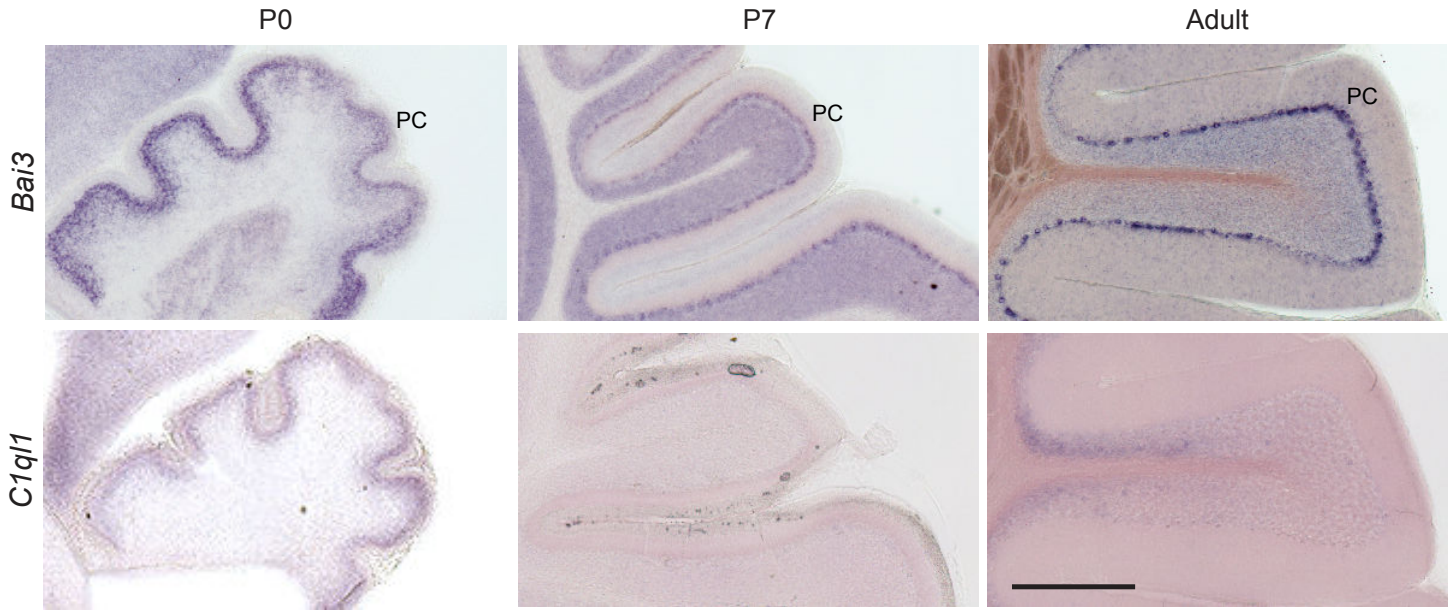


**Figure S2, related to Figure 1. *In situ* hybridization analysis of *Bai3* and *C1ql1* mRNA expression in the cerebellar cortex during postnatal development.**
*In situ* hybridization experiments performed using a probe specific for *Bai3* or *C1ql1* on sagittal sections of mouse brain taken at postnatal day 0, 7 and adult. PC, Purkinje cell. Scale bar, 500μm.

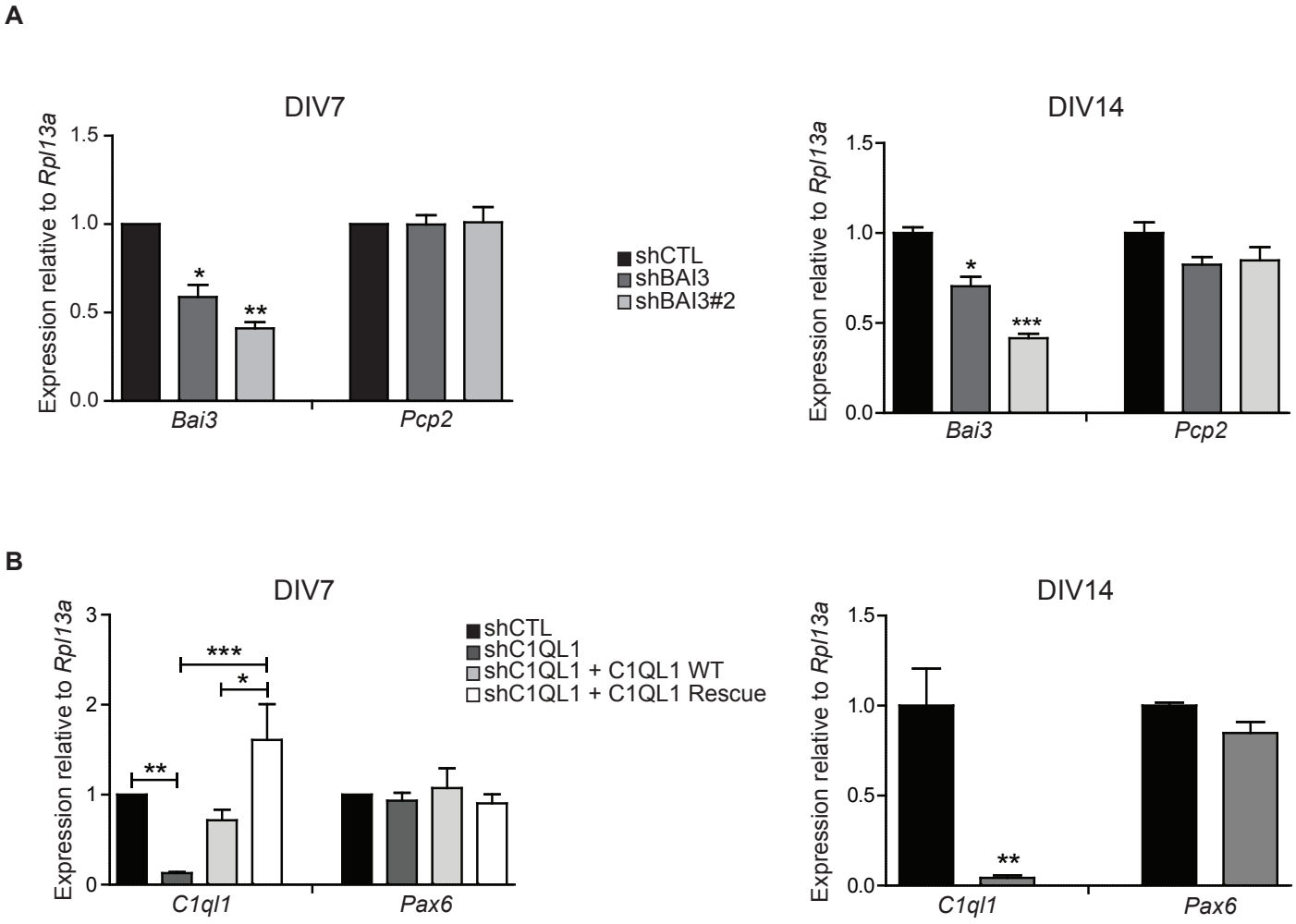


**Figure S3, related to Figures 2, 3 and 6. Characterization of knockdown and rescue efficiency for our RNAi approach in cerebellar mixed cultures.**

**(A)** Expression of *Bai3* and *Pcp2* mRNAs was assessed using quantitative RT-PCR on extracts from cerebellar mixed cultures. Transduction was performed at days in vitro 4 (DIV4) with lentiviruses driving the expression of two different shRNAs directed against *Bai3*, or the control shCTL and analysis at DIV7 (left) or DIV14 (right). Expression levels are normalized to the *Rpl13a* gene. Note that twice as many lentiviral particles are used for shBAI3#2. **(B)** Expression of *C1ql1* and *Pax6* mRNAs was assessed using quantitative RT-PCR on cerebellar mixed cultures at DIV7 or DIV14, respectively after 3 days or 10 days of transduction by lentiviruses driving the expression of a shRNA directed against *C1ql1* alone or in combination with lentiviruses expressing *C1ql1 WT* or *C1ql1 Rescue*, or the shCTL as control. Expression levels are normalized to the *Rpl13a* gene. N=3-7 independent experiments (Data are presented as mean ± SEM; One-way ANOVA followed by Newman-Keuls posthoc test, *$p < 0.05$, **$p < 0.01$, ***$p < 0.001$).

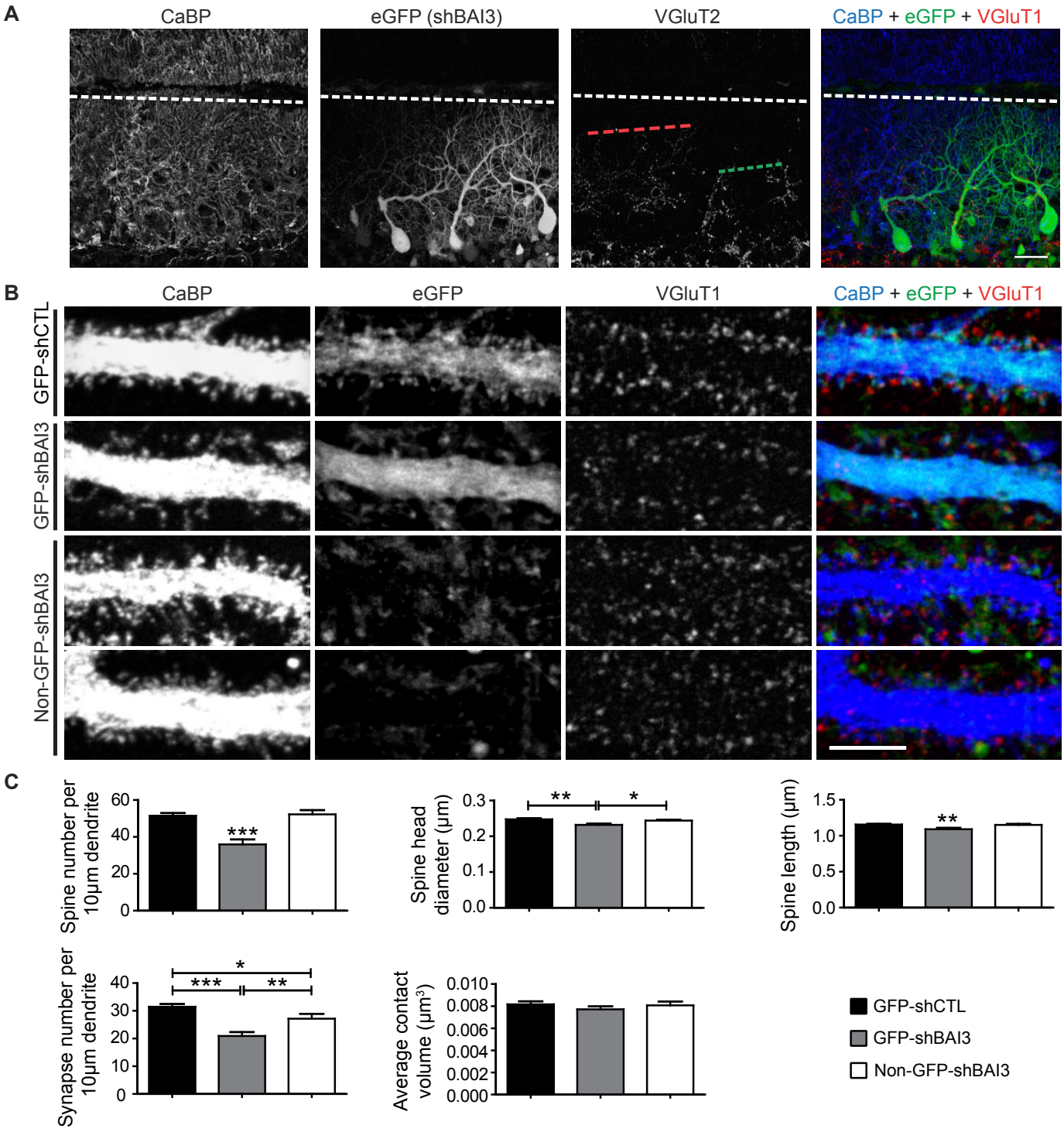


**Figure S4, related to Figure 2 and 3. Cell autonomous role of BAI3 in Purkinje cells. (A)** P21 immunostaining for vesicular glutamate transporter 2 antibody (VGluT2), a marker specific for climbing fiber synapses, on non-transduced PCs (GFP negative) or transduced PCs (GFP positive). Stereotaxic injections of recombinant lentiviral particles driving expression of a small hairpin RNA against *Bai3* (shBAI3) or control shRNA (shCTL) were performed at P7. Normal VGluT2 extension was observed in GFP-negative cells in contrast to the decreased extension visible on GFP-positive PCs. Granule cells are GFP-positives in the region of both GFP positive and negative cells. Pial surface: white dashed lines. Scale bar, 30µm. **(B)** Cerebellar mixed cultures were transduced at DIV4 with recombinant lentiviral particles driving expression of GFP together with a shRNA targeting *Bai3* (shBAI3) or a control shRNA (shCTL). Dendritic spines and parallel fiber synapses in transduced Purkinje cells (GFP) or non-transduced PCs (Non-GFP) were imaged at DIV14 after immunostaining for calbindin (CaBP) and vesicular glutamate transporter 1 antibody (VGluT1). Scale bar: 5µm. **(C)** Quantitative assessment of the number and morphology of spines was performed in cultured Purkinje cells using the NeuronStudio software. Quantitative assessment of the number and size of vGluT1 synaptic contacts was performed using ImageJ. N≥18 cells per condition, 3 independent experiments (Data are presented as mean ± SEM; One-way ANOVA followed by Newman-Keuls posthoc test, *p < 0.05; **p < 0.01; ***p < 0.001).

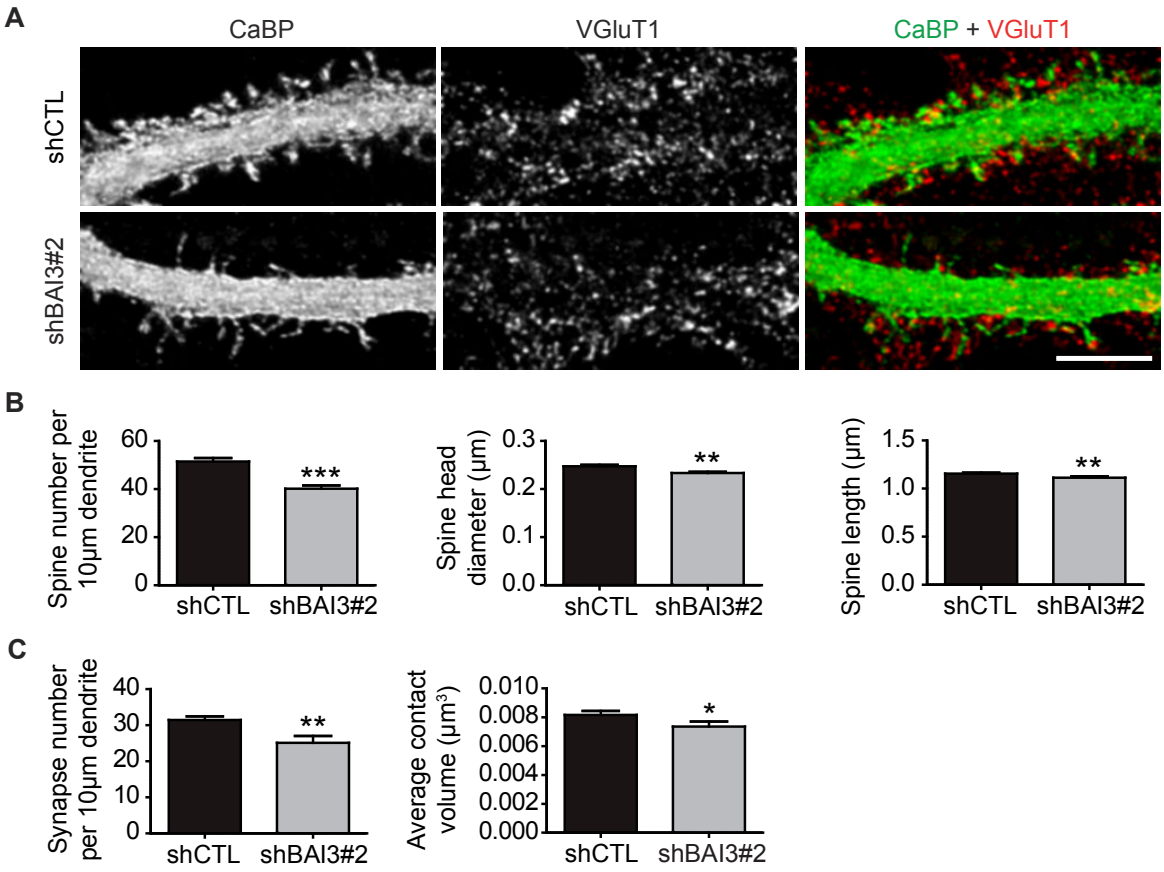


**Figure S5, related to Figure 3. Data obtained with a second shRNA targeting BAI3 show similar effects on Parallel fiber/Purkinje cell spinogenesis and synaptogenesis in vitro.** **(A)** Cerebellar mixed cultures were transduced at DIV4 with lentiviral particles driving expression of GFP together with a small hairpin RNA targeting *Bai3* (shBAI3#2) or a control shRNA (shCTL). Dendritic spines and parallel fiber synapses in transduced Purkinje cells (GFP positive) were imaged at DIV14 after immunostaining for calbindin (CaBP) and vesicular glutamate transporter 1 antibody (VGluT1), respectively. Scale bar: 5µm **(B)** Quantitative assessment of the number and morphology of Purkinje cell spines was performed using the NeuronStudio software. N≥40 cells per condition, 4 independent experiments (Data are presented as mean ± SEM; unpaired Student t test and Mann-Whitney *U* test for spine length, $^{**}p < 0.01$; $^{***}p < 0.001$). **(C)** Quantitative assessment of the number and size of vGluT1 synaptic contacts in DIV14 transduced Purkinje cells was performed using ImageJ. N≥40 cells per condition, 4 independent experiments (Data are presented as mean ± SEM; unpaired Student *t* test, $^{*}p < 0.05$; $^{**}p < 0.01$).

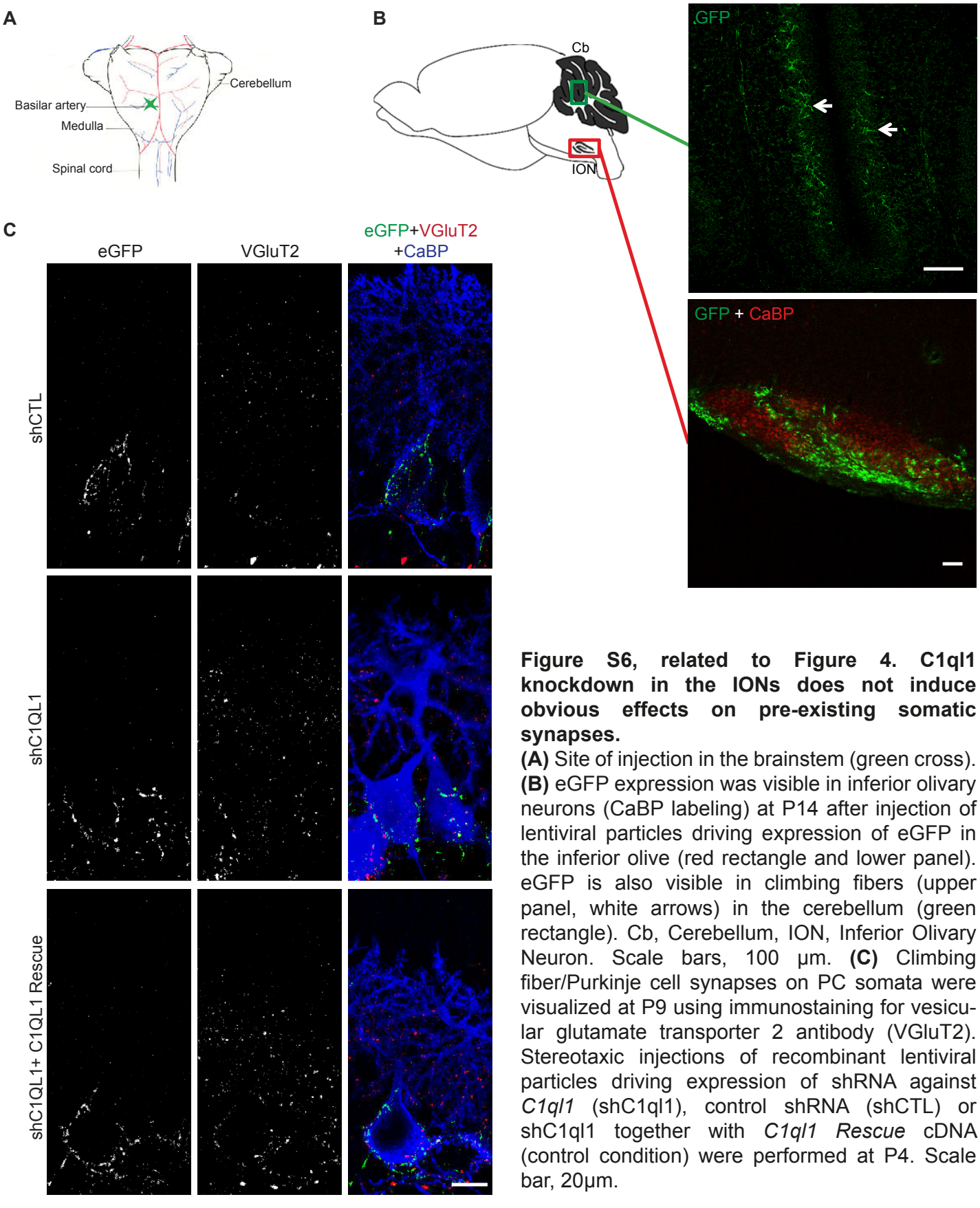


**Figure S6, related to Figure 4. C1ql1 knockdown in the IONs does not induce obvious effects on pre-existing somatic synapses.**
**(A)** Site of injection in the brainstem (green cross). **(B)** eGFP expression was visible in inferior olivary neurons (CaBP labeling) at P14 after injection of lentiviral particles driving expression of eGFP in the inferior olive (red rectangle and lower panel). eGFP is also visible in climbing fibers (upper panel, white arrows) in the cerebellum (green rectangle). Cb, Cerebellum, ION, Inferior Olivary Neuron. Scale bars, 100 µm. **(C)** Climbing fiber/Purkinje cell synapses on PC somata were visualized at P9 using immunostaining for vesicular glutamate transporter 2 antibody (VGluT2). Stereotaxic injections of recombinant lentiviral particles driving expression of shRNA against *C1ql1* (shC1ql1), control shRNA (shCTL) or shC1ql1 together with *C1ql1 Rescue* cDNA (control condition) were performed at P4. Scale bar, 20µm.

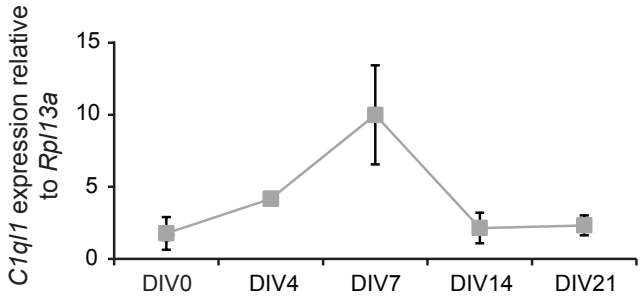


**Figure S7, related to Figure 1. *C1ql1* expression in cerebellar cultures.**
Expression of *C1ql1* was assessed at different stages of cerebellar culture development using quantitative RT-PCR on cell extracts (days in vitro, DIV0 to 21). Expression levels are normalized to the *Rpl13a* gene. N=2 samples per stage. Data are presented as mean ± SEM.

## -Supplemental Experimental Procedures

*cDNA and RNAi constructs*

The *BAI3-WT* construct was cloned into the pEGFP-C2 vector from mouse cDNA clone #BC099951. The shRNA #2 sequence for BAI3 was: 5'tgcagaatttacccttga3', and was subcloned under the H1 promoter in a lentiviral vector that also drives eGFP expression (Avci et al., 2012).

*RTqPCR*

RNA samples were obtained from mixed cerebellar cultures using the RNeasy Mini kit (QIAGEN, Hilden, Germany), cDNA were amplified using the SuperScript® VILO™ cDNA Synthesis kit (Life technologies, Paisley, UK) according to manufacturer's instructions. Quantitative PCR was performed using the TaqMan Universal Master Mix II with UNG (Applied Biosystems, Courtaboeuf, France) and the following TaqMan probes: *Bai3* (#4331182_Mm00657451_m1), *C1ql1* (#4331182_Mm00657289_m1), *Rpl13a* (#4331182_Mm01612986_gH), *Pcp2* (#4331182_Mm00435514_m1), *Pax6* (#4331182_Mm00443081_m1).

*In situ Hybridization*

*In situ* hybridization was performed using a previously described protocol with minor modifications (Bally-Cuif et al., 1992). Briefly, paraformaldehyde-fixed freely floating vibratome sections were obtained (100 µm thickness) from mouse brains at postnatal day 0 (P0), P7 and adult (more than 6 weeks). The probe sequences corresponded to the following nucleotide residues for the indicated mouse cDNA: 3955-4708 bp for *Bai3* (NM_175642.4), 641-1200 bp for *C1ql1* (NM_011795.2) and 501-1017 bp for *C1ql3* (NM_153155.2). The riboprobes were used at a final concentration of 2 µg/µL. The proteinase K (10µg/mL)

treatment was given for 30 seconds for P0 and P7 brain sections, and 10 minutes for adult brain sections. The anti-digoxigenin-AP antibody was used at a dilution of 1/2000.

*Primary neuronal cultures*

Cerebellar mixed cultures were prepared from P0 Swiss mouse cerebella and were dissected and dissociated according to previously published protocol (Tabata et al., 2000). Neurons were seeded at a density of $5x10^6$ cells/ml. Hippocampal cultures were prepared from E18 Swiss mouse embryos as previously published with minor modifications (Fath et al., 2008). Hippocampal neurons were transfected at DIV18 using Lipofectamine-2000 (Life technologies, Carlsbad, USA) according to the manufacturer's protocol.

*Immunocytochemistry, immunohistochemistry and antibodies*

Immunostaining was performed on cells fixed with 2% paraformaldehyde in PBS or on 30 micrometer thick sagittal cerebellar sections obtained using a freezing microtome from brains of mice perfused with 4% paraformaldehyde in PBS. The following antibodies were used: anti-CaBP mouse antibody (Swant, Marly, Switzerland, #300), anti-VGluT1 guinea pig antibody (Millipore, Molsheim, France, #AB5905), anti-VGluT2 guinea pig antibody (Millipore, Molsheim, France, #AB2251), anti-BAI3 rabbit antibody (Sigma, St Louis, USA, #HPA015963) and anti-PSD95 rabbit antibody (Cell signaling, Leiden, The Netherlands, #3450).

*Image acquisition and analysis*

Image stacks were acquired using a Confocal Microscope (SP5, Leica), using either 40x (1.25 NA, oil immersion, pixel size: 211 nm and 144 nm for vGluT2 extension in shBAI3 and C1QL1 misexpression experiments, respectively) or 63x (1.4 NA, oil immersion, pixel size: 57 nm for *in vitro* imaging, pixel size: 38 nm for *in vivo* imaging of vGluT2 staining) or 20X (0.7 NA, pixel size 60 nm for hippocampal neurons) objectives. The pinhole aperture was set

to 1 Airy Unit and a z-step of 200 nm was used. Laser intensity and photomultiplier tube (PMT) gain was set so as to occupy the full dynamic range of the detector. Images were acquired in 16-bit range. For spine and synapse analysis, deconvolution was performed with Huygens 4.1 software (Scientific Volume Imaging) using Maximum Likelihood Estimation algorithm. 40 iterations were applied in classical mode, background intensity was averaged from the voxels with lowest intensity, and signal to noise ratio values were set to a value of 25.

*Electrophysiology*

Responses to parallel (PF) and climbing fibers (CF) stimulation were recorded in Purkinje cells in acute cerebellar slices from Swiss mice (P18 to P23) after lentivirus injection at P7 in the cerebellum and from Swiss mice (P14 to P19) after lentivirus injection at P4 in the inferior olive. Briefly: mice were anesthetized by exposure to isoflurane 4% and sacrificed by decapitation. Cerebellum was dissected in ice cold oxygenated Bicarbonate Buffered Solution (BBS) containing (in mM): NaCl 120, KCl 3, $NaHCO_3$ 26, $NaH_2PO_4$ 1.25, $CaCl_2$ 2 mM, $MgCl_2$ 1 and glucose 35. 280 µm sagittal slices were cut with a vibratome in the NMDG-based cutting buffer (in mM): NMDG 93, KCl 2.5, $NaH_2PO_4$ 1.2, $NaHCO_3$ 30, HEPES 20, glucose 25, sodium ascorbate 5, thiourea 2, sodium pyruvate 3, $MgSO_4$ 10 and $CaCl_2$ 0.5 (pH 7.3). Immediately after cutting, slices were allowed to briefly recovery at 34°C in the oxygenated sucrose-based buffer (in mM): sucrose 230, KCl 2.5, $NaHCO_3$ 26, $NaH_2PO_4$ 1.25, glucose 25, $CaCl_2$ 0.8 and $MgCl_2$ 8. D-APV and minocycline at a final concentration of 50 µM and 500 nM respectively were added to the sucrose-based and cutting buffers. Slices were allowed to fully recover in 95% $O_2$/5% $CO_2$ bubbled BBS at 34°C for at least 30 minutes before starting experiments.

Patch clamp borosilicate pipettes with 3-5 MΩ resistance were filled with the internal solution containing (in mM): $CsMeSO_3$ 135, NaCl 6, $MgCl_2$ 1, HEPES 10, MgATP 4, $Na_2GTP$ 0.4,

EGTA 1.5 and QX314Cl 5 (pH 7.3). Stimulation electrodes with 5 MΩ resistance were pulled from borosilicate pipettes and filled with HEPES Buffered Solution (HBS) containing (in mM): NaCl 120, KCl 3, HEPES 10, $NaH_2PO_4$ 1.25, $CaCl_2$ 2, $MgCl_2$ 1 and glucose 10 (pH7.3). The IsoStim A320 (WPI Inc, USA) stimulator was used to elicit CF and PF mediated responses in PC. Patch clamp experiments were conducted in voltage clamp mode using a MultiClamp 700B amplifier (Molecular Devices Inc, USA). Currents were low-pass filtered at 2 kHz and digitized at 20 kHz. Recordings were performed at room temperature on slices continuously perfused with 95% $O_2$/5% $CO_2$ bubbled BBS and in presence of picrotoxin 100 µM. CF and PF currents were monitored at a holding potential of respectively -10 mV and -60 mV.

During CF recordings the stimulation electrode was placed in the granule cells layer below the clamped cell; CF-mediated responses were identified by the typical all or nothing response and strong depression displayed by the second response elicited during paired pulse stimulations (20 Hz).

PF stimulation was achieved by placing the stimulation electrode in the molecular layer at the minimum distance required to avoid direct stimulation of the dendritic tree of the recorded PC. The input/output curve was obtained by incrementally increasing the stimulation strength. Peak EPSC values for PF were obtained following averaging of five consecutive traces and were normalized to the EPSC recorded at the lowest stimulus intensity in order to determine the fold increase in PF responses. Data analyses were performed with the scientific data analysis software Igor Pro (WaveMetrics, USA).

## -Supplemental References

Avci, H.X., Lebrun, C., Wehrle, R., Doulazmi, M., Chatonnet, F., Morel, M.-P., Ema, M., Vodjdani, G., Sotelo, C., Flamant, F., et al. (2012). Thyroid hormone triggers the developmental loss of axonal regenerative capacity via thyroid hormone receptor alpha1 and kruppel-like factor 9 in Purkinje cells. Proc. Natl. Acad. Sci. U.S.A. *109*, 14206–14211.

Bally-Cuif, L., Alvarado-Mallart, R.M., Darnell, D.K., and Wassef, M. (1992). Relationship between Wnt-1 and En-2 expression domains during early development of normal and ectopic met-mesencephalon. Development *115*, 999–1009.

Fath T1, Ke YD, Gunning P, Götz J, Ittner LM. (2009). Primary support cultures of hippocampal and substantia nigra neurons. Nat Protoc. *4*, 78-85.

Tabata, T., Sawada, S., Araki, K., Bono, Y., Furuya, S., and Kano, M. (2000). A reliable method for culture of dissociated mouse cerebellar cells enriched for Purkinje neurons. J. Neurosci. Methods *104*, 45–53.

## 3. Complement control-related protein SUSD4 promotes the stabilization and functional maturation of Climbing Fiber/Purkinje Cell synapses in the cerebellar cortex

### - Preface -

Our comparative analysis of gene expression profiles in adult mice reveals a combinatorial expression of complement-related genes in the two input cell populations sending excitatory afferents to the Purkinje cells (Results I, Figure 5). Among these complement-related genes, the Sushi Domain containing protein 4 (SUSD4) is specifically enriched in the adult Inferior Olivary Neurons (ION). This was confirmed by in situ hybridization, which also revealed a Purkinje cell-specific expression of *Susd4* in the cerebellum throughout development. Quantitative analysis showed that the expression of *Susd4* was high in the brainstem during the developmental stages of Climbing Fiber/Purkinje cell (CF/PC) synaptogenesis and increased in the cerebellum towards adulthood. Moreover, SUSD4 has been shown to interact with the gC1Q domain *in vitro* (Holmquist et al., 2013), the signature domain of the C1q family, whose members have established roles in the development and refinement of neural circuits (Yuzaki, 2010). In the olivo-cerebellar network, C1Q-related protein C1QL1 promotes the formation of CF/PC synapses and plays an instructive role in the establishment of CF innervation territory (Kakegawa et al., 2015; Sigoillot et al., 2015). Taken together, this suggests a role for SUSD4 in CF/PC synaptogenesis.

SUSD4 belongs to the SUSD family of proteins that contains the Sushi or Complement Control Protein (CCP) domain. Originally identified in proteins that regulate the complement cascade, CCP domains are highly evolutionarily conserved and found in complement-related and non-complement proteins with roles in neural development (Reid & Day, 1989). In our study, we analysed the *in vivo* functional role of SUSD4 using a constitutive knockout mouse model. We show that Susd4 knockout (KO) mice develop motor coordination defects at a juvenile age. This ataxic phenotype is not characterized by gross morphological cerebellar abnormalities, but is associated with defects in cerebellar synaptic function and long-term stability. The motor defects in juvenile Susd4 KO mice are accompanied by defects in CF/PC transmission and impaired short term plasticity. This is followed by defects in the functional and morphological stabilization of these synapses well into adulthood. The synaptic morphology and function of Parallel Fiber/Purkinje cell

(PF/PC) synapses are unaffected. Unlike its human homolog, murine SUSD4 exists only as a transmembrane protein. We also show that SUSD4 interacts in transfected cells with Purkinje cell-receptor Brain Angiogenesis Inhibitor 3 (BAI3) which is known to promote excitatory synaptogenesis (Kakegawa et al., 2015; Sigoillot et al., 2015). Given the role of CCP-containing LEV-9 in postsynaptic receptor clustering in *C.elegans*, the CF synaptic functional defects seen in the *Susd4*-null mice could be due to a defective postsynaptic receptor clustering mechanism mediated by the interaction of SUSD4 with BAI3. Interestingly, the BAI3 receptor is characterized by TSR1 domains that are also found in Ce-punctin, an ADAMTS-like secreted protein whose isoforms control the proper localization of cholinergic and GABAergic synapses at the *C.elegans* neuromuscular junction (NMJ) (Gendrel et al., 2009; Pinan-Lucarré et al., 2014). Given that BAI3 specifies CF innervation territory on Purkinje cells through its interaction with C1QL1 (Kakegawa et al., 2015; Sigoillot et al., 2015), it is possible that the protein domains of SUSD4 and BAI3 constitute an evolutionarily conserved synaptic scaffold that stabilizes the CF synaptic contacts by clustering postsynaptic receptors.

Thus, our study is suggestive of a potential evolutionarily conserved role for CCP-containing proteins in promoting the stability and functional maturation of synapses. Moreover, LEV-9 in invertebrates is the only CCP-containing protein to be reported with this postsynaptic receptor clustering role (Gendrel et al., 2009). This study would therefore implicate SUSD4 as the first complement control protein in vertebrates to have a postsynaptic receptor clustering function in excitatory synapses.

**- Article in preparation -**

**Complement control-related protein SUSD4 promotes the stabilization and functional maturation of Climbing Fiber/Purkinje cell synapses in the cerebellar cortex**

Keerthana Iyer[1,2,3], Ines Gonzalez-Calvo[1,2,3], Severine M Sigoillot[1,2,3], Melanie Albert[1,2,3], Yann Nadjar[4], Andrea Dumoulin[4], Antoine Triller[4], Philippe Isope[5], Fekrije Selimi[1,2,3]

[1]Equipe Mice, Molecules and Synapse Formation, CIRB-Collège de France, 75231 Paris Cedex 05, France

[2]CNRS, UMR 7241, 75005 Paris, France

[3]INSERM, U1050, 75005 Paris, France

[4]Equipe Biologie de la synapse et régulation de la survie neuronale, Ecole Normale Supérieure, 75005 Paris, France

[5]Equipe Physiology of Neural Networks, Institute of Cellular and Integrative Neurosciences, Strasbourg 67084 Cedex, France

**Abstract**

Complement Control Protein (CCP) or Sushi domains are emerging as important evolutionarily conserved protein domains with roles in neurodevelopment and synaptogenesis. Sushi domain containing protein 4 (SUSD4) is a complement control-related protein that binds the gC1Q domain *in vitro*, a domain found in several proteins with established roles in synaptogenesis. Despite its expression in the brain, no known role for this protein has been described in CNS development and function. Using a constitutive knockout mouse model, we show that loss of SUSD4 is associated with motor coordination defects that appear from a juvenile age. Morphological and electrophysiological analyses reveal that this behavioural phenotype is accompanied by a significant reduction in the kinetic of Climbing fiber transmission followed by a reduction in the size and number of Climbing fiber synapses that appears with age. These defects in stabilization and functional maturation are not observed in Parallel fiber/Purkinje cell synapses. We also find that SUSD4 interacts *in vitro* with Brain Angiogenesis Inhibitor 3 (BAI3), an adhesion GPCR expressed by Purkinje cells. BAI3 contains thrombospondin repeat (TSR) domains and promotes excitatory synaptogenesis on Purkinje cells, and in particular controls Climbing fiber innervation territory. Thus a complex formed by BAI3 and SUSD4 could control several aspects of excitatory synapse formation in Purkinje cells. This is reminiscent of the extracellular scaffold machinery at the *C.elegans* neuromuscular junction (NMJ). TSR domain-containing Ce-punctin isoforms control the proper localization of cholinergic and GABAergic synapses at the NMJ whereas CCP-containing LEV-9 ensures proper neurotransmission by clustering postsynaptic acetylcholine receptors. Thus, it is possible that the protein domains of SUSD4 and BAI3 constitute an evolutionarily conserved synaptic scaffold that stabilizes the Climbing Fiber synaptic contacts by clustering post-synaptic receptors. Given the broad expression of SUSD4 in the mouse brain, this study highlights a potential role of SUSD4 in promoting synapse maturation and efficient neurotransmission in different neural circuits.

**Keywords**: CCP domain, SUSD4, Climbing fiber synaptogenesis, motor coordination, neurotransmission

## Introduction

Synaptic function largely depends on both the local density and the activity of neurotransmitter receptors in postsynaptic membranes. Proteins that are secreted or inserted in the plasma membrane have been found to regulate neurotransmitter receptor clustering or functioning. For example, the TARPs family of transmembrane proteins recruits AMPA receptors at excitatory synapses and modulates receptor trafficking and gating (Jackson & Nicoll, 2011). Secreted neuronal activity regulated pentraxin (Narp) is selectively enriched in hippocampal excitatory synapses and aggregates AMPA receptors (O'Brien et al., 1999). Recent studies have implicated complement control-related proteins in synapse development and neurotransmission in vertebrates and invertebrates (Nakayama & Hama, 2011). These proteins contain the Complement Control Protein (CCP) or sushi domains, which were originally identified in proteins that regulate complement activation such as complement receptors CR1 and CR2, and Decay Accelerating Factor (DAF) to name a few (Kirkitadze & Barlow, 2001). In *C.elegans*, complement control-related protein LEV-9 is secreted by muscle cells and localized at cholinergic neuromuscular junctions where it specifically aggregates L-Acetylcholine Receptors (L-AChRs) (Gendrel et al., 2009). Defects in complement control-related proteins cause a number of psychiatric phenotypes, notably seizures, epilepsy and schizophrenia (Waruiru, 2004; Royer-Zemmour et al., 2008), suggesting that proteins with CCP domains play key roles in the development and function of neural circuits.

The Sushi Domain containing protein family (SUSD) comprises four members, SUSD1-4. Among these, SUSD2 and SUSD3 have been implicated in cell adhesion, cell migration and tumorigenesis (Watson et al., 2013; Moy et al., 2014). So far, SUSD2 is the only member of this family shown to have a role in synapse formation in hippocampal cultures (Nadjar et al., 2015). The Sushi domain-containing protein 4 (SUSD4) is a complement control-related protein whose gene is part of the chromosome deletion linked with Fryns syndrome (Shaffer et al., 2007), an autosomal recessive multiple congenital neurodevelopmental disorder in humans. Its deletion also leads to locomotion defects in zebrafish (Tu et al., 2010). Phylogenetic analysis using ClustalW shows that murine SUSD4 has homologs only in vertebrates, with a high level of amino acid sequence conservation (Figure 1A). Murine SUSD4 encodes a 490 amino acid protein that contains four CCP domains, a transmembrane region, an intracellular lymphocyte signaling adaptor protein domain (SLY) and a cytoplasmic tail (Figure 1B). Each CCP domain contains a receptor/ligand interaction site and the SLY domain has roles in actin cytoskeleton

reorganization and adaptive immune signalling responses (Beer et al., 2000; Holleben et al., 2011). The role of SUSD4 in complement cascade inhibition has been demonstrated using *in vitro* immunological assays on human SUSD4 extracts (Tu et al., 2010; Holmquist et al., 2013). A soluble isoform of human SUSD4 inhibits the classical complement pathway by interacting with the complement components C1 complex and globular C1q (gC1q) domain (Holmquist et al., 2013). Interestingly, the gC1q domain is also identified in the C1q family whose roles in synaptogenesis and refinement of functional neural circuits are well described (Stevens et al., 2007; Matsuda et al., 2010; Kakegawa et al., 2015; Sigoillot et al., 2015). All these data strongly suggest a role for SUSD4 in synaptogenesis.

In our study, we show that Susd4 KO mice develop motor coordination defects at a juvenile age, accompanied by defects in Climbing fiber/Purkinje cell (CF/PC) transmission. This is followed by a decline in the morphological stabilization of these synapses well into adulthood. We also show that *susd4* mRNA is strongly expressed in the olivo-cerebellar network throughout development and in adulthood, and that SUSD4 interacts *in vitro* with Purkinje cell-receptor BAI3 which is known to promote CF/PC synaptogenesis (Sigoillot et al., 2015). Given the role of CCP-containing LEV-9 in postsynaptic receptor clustering in *C.elegans*, the CF synaptic functional defects seen in the Susd4 KO mice could be explained by a defective postsynaptic receptor clustering mechanism mediated by the interaction of SUSD4 with BAI3. Thus, our study provides insights into a potential evolutionarily conserved role for CCP-containing proteins in promoting the stability and functional maturation of synapses.

## Experimental procedures

### *Generation of susd4 null mice and constructs*

*Susd4*-null mice were generated and maintained on C57BL/6J background by Lexicon Genetics, Incorporated. Out of the 8 *Susd4* exons, coding exon 1 (NCBI accession NM_144796.2) and the preceeding non-coding exon (NCBI accession BM944003) were targeted by homologous recombination. This resulted in the deletion of a 1.3 kb sequence spanning the transcription initiation site and exon 1. Subsequent genotyping of mice was performed using PCR to detect the wild-type allele (primer 62 : CTGTGGTTTCAACTGGCGCTGTG and primer 63 : GCTGCCGGTGGGTGTGCGAACCTA) or the targeted allele (primer 83 : TTGGCGGTTTCGCTAAATAC and primer 84 : GGAGCTCGTTATCGCTTGAC). Full-length Susd4 was cloned into the mammalian expression

vector pEGFP-N1 to obtain a Susd4-GFP fusion construct. Full-length Susd4, with an insertion of an N-terminal HA tag just after the signal peptide, was similarly cloned to obtain the pHA-Susd4-GFP construct. The BAI3-wild type (BAI3-WT) construct was cloned into the pEGFP-C2 vector from mouse cDNA clone #BC099951 (Lanoue et al., 2013) (See annexe).

***HEK cell culture and transfection***

HEK293 cells were cultured in a 12-well plate (4 $cm^2$ surface area per well) at 37 °C in humidified 5% $CO_2$ incubators in Dulbecco's Modified Eagle Medium (DMEM) containing penicillin, streptomycin, L-glutamine and 10% fetal bovine serum (Gibco). Cells were then transfected with 1.6 µg of total plasmid DNA and 4 µL of Lipofectamine-2000 (Invitrogen) per well.

***Immunofluorescence***

The following antibodies were used: anti-CaBP mouse antibody (Swant, Marly, Switzerland, #300), anti-VGluT1 guinea pig antibody (Millipore, Molsheim, France, #AB5905), anti-VGluT2 guinea pig antibody (Millipore, Molsheim, France, #AB2251), anti-HA rat antibody (Roche Life Science, #11867423001), anti GluR2/3 rabbit antibody (Millipore, Molsheim, France, #AB1506), anti GluRδ2 rabbit antibody (Millipore, Molsheim, France, #AB2285). Secondary antibodies were: AlexaFluor568-conjugated donkey anti-mouse (Invitrogen #A10037), AlexaFluor647-conjugated goat anti-guinea pig (Invitrogen #A21450), AlexaFluor488-conjugated donkey anti-rabbit (Invitrogen #A21206), AlexaFluor594-conjugated donkey anti-rat (Invitrogen #A21209). Immunostainings were performed on transfected HEK cells fixed with 4% paraformaldehyde or on 30 µm thick sagittal cerebellar sections obtained using a freezing microtome from brains of mice perfused with 4% paraformaldehyde in PBS. Fixed HEK cells or floating sections were blocked with PBS1X / 4% Donkey Serum, primary and secondary antibodies were incubated in PBS1X / 1% Triton-X / 1% Donkey Serum, sections were incubated in primary antibody overnight at 4°C. For the GluR2/3 labeling, floating sections were blocked with PBS1X / 1% Triton-X / 5% Normal Goat Serum, primary and secondary antibodies were incubated in PBS1X / 1% Triton-X, sections were incubated in primary antibody over two nights at 4°C.

***Western Blot analysis***

Proteins were extracted from transfected HEK cells using RIPA buffer (TrisHCl 50mM, NaCl 150mM, SDS 0.1%, Sodium azide 0.02%, Sodium deoxycholate 0.5%, NP-40 1%) with protease inhibitors. Proteins were first separated by a 4-12% NuPAGE Bis-Tris-Acetate Gel according to Invitrogen protocols, then electrotransferred (using TransBlot® Transfer Medium, Bio-Rad) to PVDF membrane (Immobilon-P transfer membrane, Millipore). Membranes were blocked in PBS supplemented with Tween 0.2% (PBST) and non-fat milk 5% and incubated with various antibodies in PBST- milk 5%. After washing in PBST, membranes were incubated with Horseradish Peroxidase-conjugated secondary antibodies in PBST-milk 5%. Bound antibodies were revealed using ECL plus detection reagents (GE Healthcare-Amersham) and visualized with hyperfilm ECL.

***In situ hybridization***

The probe sequence corresponded to the nucleotide residues 287-1064 bp for mouse Susd4 (NM_144796.4) cDNA. For the adult stage (postnatal day 21), fresh frozen brain sections of 20µm thickness were prepared from Susd4 WT and KO mice using a cryostat. The riboprobes were used at a final concentration of 0.05 µg/µL, and hybridization was done overnight at a temperature of 72°C. The anti-digoxigenin-AP antibody was used at a dilution of 1/5000. Alkaline phosphatase detection was done using BCIP/NBT colorimetric revelation. For postnatal age P0, in situ hybridization was performed using a previously described protocol with a few modifications (Bally-Cuif et al., 1992). PFA-fixed freely floating vibratome sections of 100µm thickness were prepared from wild type mice. The riboprobes were used at a final concentration of 2 µg/µL. Proteinase K (10µg/mL) treatment was given for 30 seconds. The anti-digoxigenin-AP antibody was used at a dilution of 1/2000.

***Footprint analysis***

The fore and hind paws of mice were dipped in blue and pink non-toxic paint respectively. Mice were allowed to walk through a rectangular plastic tunnel (9cm W x 57cm L x 16cm H), whose floor is covered with a sheet of white paper. Habituation was done the day before the test. 5 footsteps were considered for the analysis and length measurements were made using ImageJ.

***RT-PCR and RTqPCR***

For standard RT-PCR, total RNA was isolated from the cortex, cerebellum and brainstem of 2 month old susd4-null mice and littermate controls using the Qiagen RNAeasy mini kit. Equivalent amounts of total RNA (100 ng) were reverse-transcribed according to the protocol of SuperScript® VILO™ cDNA Synthesis kit (Life technologies, Paisley, UK). Primers used for Susd4 (5'-3') were: forward TGTTACTGCTCGTCATCCTGG, reverse GAGAGTCCCCTCTGCACTTGG. PCR was performed with an annealing temperature of 61°C, for 39 cycles, using the manufacturer's instructions (Taq polymerase, New England Biolabs).

For RTqPCR, RNA samples were obtained from mixed cerebellar cultures using the RNeasy Mini kit (QIAGEN, Hilden, Germany), cDNA were amplified using the SuperScript® VILO™ cDNA Synthesis kit (Life technologies, Paisley, UK) according to manufacturer's instructions. Quantitative PCRs were done using the TaqMan Universal Master Mix II with UNG (Applied Biosystems, Courtaboeuf, France) and the following TaqMan probes: SUSD4 (#4331182_Mm01312134_m1), RPL13a (#4331182_Mm01612986_gH).

***Co-immunoprecipitation***

Transfected cells were lysed in 1% (v/v) Triton-X100, 150 mM NaCl, 50 mM Tris-HCl and 2 mM EDTA supplemented with protease inhibitors (SIGMA #P8340) and phosphatase inhibitors (SIGMA #P2850) 30 min at 4°C. After a 15 min centrifugation (10000 g, 4°C), the supernatant was incubated for 1h at 4°C with a GFP antibody (Abcam, #6556) cross-linked to Dynabeads-Protein G (Invitrogen #100.03D). Affinity-purified samples were run on a NuPAGE 4-12% Bis-Tris Gel (Invitrogen) in NuPAGE MOPS SDS running buffer (Invitrogen) for immunoblot analysis. Anti-BAI3 antibody (Sigma, #HPA015963) was used to test biochemical interactions.

***Electrophysiology***

Responses to PF and CF stimulation were recorded in Purkinje Cells of the lobule VI in acute cerebellar slices from Susd4$^{-/-}$ mutant mice (P25 to P29). Susd4$^{+/+}$ littermates were used as controls. Mice were anesthetized by exposure to isoflurane 4% and sacrificed by decapitation. The cerebellum was dissected in ice cold oxygenated Bicarbonate Buffered Solution (BBS) containing (in mM): NaCl 120, KCl 3, $NaHCO_3$ 26, $NaH_2PO_4$ 1.25, $CaCl_2$ 2, $MgCl_2$ 1 and glucose 35. Para-sagittal cerebellar slices slices (300µm) were cut with a vibratome in the Gluconate cutting buffer (in mM): K-Gluconate 130, KCl 14, EGTA 2,

HEPES 20 and Glucose 25 (pH7.3). Immediately after cutting, slices were allowed to briefly recover at 34°C in the oxygenated sucrose-based buffer (in mM): sucrose 230, KCl 2.5, $NaHCO_3$ 26, $NaH_2PO_4$ 1.25, glucose 25, $CaCl_2$ 0.8 and $MgCl_2$ 8. D-APV and minocycline at a final concentration of 50µM and 50nM respectively were added to the sucrose-based and cutting buffers. Slices were allowed to fully recover in 95% $O_2$/5% $CO_2$ bubbled BBS at 34°C for at least 30 minutes before starting experiments. All experiments were carried out at room temperature. Patch clamp borosilicate pipettes with 5-7 MΩ resistance were filled with the internal solution containing: $CsMeSO_3$ 135 mM, NaCl 6 mM, $MgCl_2$ 1 mM, HEPES 10 mM, MgATP 4 mM, $Na_2GTP$ 0.4 mM, EGTA 1.5 mM, QX314Cl 5 mM, TAE 5 mM and Biocytin 2.6 mM (pH 7.3). The pipette access resistance was not compensated. Stimulation electrodes with 5 MΩ resistances were pulled from borosilicate pipettes and filled with BBS. The IsoStim A320 (WPI Inc, USA) stimulator was used to elicit CF and PF and neuronal connectivity responses in PC. Patch clamp experiments were conducted in voltage clamp mode using a MultiClamp 700B amplifier (Molecular Devices Inc, USA). Currents were low-pass filtered at 2 kHz and digitized at 20 kHz. Recordings were performed at room temperature on slices continuously perfused with 95% $O_2$/5% $CO_2$ bubbled BBS and in presence of picrotoxin 0.1 mM, TEA 10 mM, D-AP5 10 mM, CGP52432 0.001 mM, JNJ16259685 0.002 mM, DPCPX 0.0005 mM and AM251 0.001 mM. CF and PF currents were monitored at a holding potential of -10 mV. During CF recordings, the stimulation electrode was placed in the granule cell layer below the clamped cell; CF-mediated responses were identified by the typical all or none response and strong depression displayed by the second response elicited during paired pulse stimulations (20 Hz). The number of CFs innervating the recorded PC was estimated from the number of discrete CF-EPSC steps. PF stimulation was achieved by placing the stimulation electrode in the molecular layer at the minimum distance required to avoid direct stimulation of the dendritic tree of the recorded PC. The input-output curve was obtained by incrementally increasing the stimulation strength. Peak EPSC values for PF were obtained following averaging of three consecutive recordings. Data analyses were performed with the scientific data analysis software WinWCP and GraphPad.

***Image acquisition and quantification***

In situ hybridization images were acquired using a brightfield microscope (Leica DMRB) using 10x (pixel size 670 nm) objective. The immunofluorescence image stacks were acquired using a confocal microscope (SP5, Leica), using 63x (1.4 NA, oil immersion,

pixel size: 57 nm for *in vitro* imaging, pixel size: 228 nm for 63x; 76 nm, 57 nm, 45 nm for higher magnifications for *in vivo* imaging) objectives. The pinhole aperture was set to 1 Airy Unit and a z-step of 200 nm was used. Laser intensity and photomultiplier tube (PMT) gain was set so as to occupy the full dynamic range of the detector. Images were acquired in 16-bit range. Deconvolution was performed for the VGluT1 images with Huygens 4.1 software (Scientific Volume Imaging) using Maximum Likelihood Estimation algorithm. 40 iterations were applied in classical mode, background intensity was averaged from the voxels with lowest intensity, and signal to noise ratio values were set to a value of 25. VGluT1 and VGluT2 synaptic puncta were analyzed using a Matlab program. The number, area and intensity of puncta were quantified by this program using the mask of each puncta generated by the Multidimensional Image analysis software (MIA) from Metamorph. For each animal, puncta parameters were measured from four equidistant images within a 35-image stack at 160nm interval, acquired from three different lobules (n=12).

### *Statistical analysis*

Data generated with ImageJ or Matlab were imported in GraphPad Prism for statistical analysis. All normally distributed data are expressed as mean ± SEM, and the Student's unpaired *t* test was used for testing the significance of *p* values. When distribution did not fit the Normal law (assessed using Graphpad Prism), Mann-Whitney *U* test used. Two-way ANOVA followed by Bonferroni post hoc test was performed for the effect of genotype and lobule on VGluT1 and VGluT2 puncta. *$p < 0.05$; **$p < 0.01$; ***$p < 0.001$.

## Results

### *Global expression of Susd4 mRNA in the developing and adult mouse brain*

To play a role in synaptogenesis, the expression of Susd4 should be developmentally regulated. In situ hybridization data from the Allen Brain Atlas (http://www.brain-map.org) shows a widespread expression of *Susd4* in the adult mouse brain. We confirmed this expression pattern in the adult mouse brain, observing especially strong labeling in certain regions such as the olfactory bulb, hippocampus, cortex, striatum, hypothalamus, Purkinje cells and brainstem (Figure 2). In the developing postnatal mouse brain at P0, a more widespread expression pattern was obtained. In the forebrain, it is expressed by the olfactory tubercle, olfactory bulb, cortex, various nuclei of the septum, thalamus, the ventromedial nucleus of hypothalamus, and the hippocampus. In the midbrain and

hindbrain, it is expressed by various neurons in the brainstem and cerebellum. In the cerebellum, its expression is specific to the Purkinje cells. In the brainstem, the inferior olivary neurons, the trapezoid body of the superior olivary complex, pontine nuclei, red nucleus, vestibular and reticular nuclei are all regions that express *Susd4*. All these areas are integral components of the sensorimotor, auditory, olfactory and vestibular systems. This expression map is suggestive of a general role of SUSD4 in multiple sensory-processing regions with stereotyped patterns of synaptic connectivity.

***Susd4 knockout mice are associated with gait alterations***

To determine the function of SUSD4 in the CNS, we used a constitutive SUSD4 knockout (KO) mouse model with a deletion of a 1.3 kb sequence spanning the transcription initiation site and first exon (Figure 3A). The functional inactivation of the *Susd4* gene in the KO mouse brain was confirmed by in situ hybridization and RT-PCR (Figure 3B, 3C). The Susd4 KO mice had a normal appearance with no prominent growth defects.

However, on closer observation, they appeared to have an abnormal gait compared to their littermate controls. To quantify this altered motor phenotype, we assessed gait parameters by performing the footprint test, a commonly used paradigm to evaluate motor tasks. Since age can be an influential factor in motor performance, we assessed the gait in juvenile (1 month old) and adult (6 months old) KO mice and littermate controls. Wild type mice have a characteristic coordinated movement, wherein the hindpaw is placed where the forepaw of the same side is previously placed, resulting in a near overlap of footprints or a small distance of "print separation". The Susd4 KO mice demonstrated a significantly increased "print separation" between the fore- and hindpaws compared to littermate control mice in both juvenile and adult mice (Figure 3D). This phenotype indicated abnormal paw placement and gait compared to wild type. The overall marginally increased effect in juvenile mice was due to a higher level of variance in the KO mice, indicating that the phenotype was more consistent in older KO mice and strongly consolidated with increase in age. No significant differences were observed in other parameters measured, such as the stride and stance length between fore- and hind limbs in consecutive steps. This indicated that the loss of SUSD4 leads to an ataxic phenotype with defects in motor coordination and not in balance or muscle strength. Unlike other classic ataxic mouse models like the Lurcher and Staggerer mice (Lalonde & Strazielle, 2007), the Susd4 KO mice had no prominent tremors, infertility or early mortality.

The cerebellum has a conserved foliation pattern with ten lobules, and a well-organized trilaminar structure consisting of the molecular layer, Purkinje cell layer and granular layer. Since cerebellar abnormalities are hallmarks of ataxic mice models (Dumesnil-Bousez & Sotelo, 1992), we checked for morphology defects in the cerebellum and Purkinje cells by DAPI and PC-specific CaBP immunostaining respectively. Quantification showed no differences in the cerebellar area and foliation between the WT and KO mice (Figure 3E). The trilaminar structure was maintained and Purkinje cells in the KO mice also appeared to have no defects in dendrite morphology or thickness of the molecular layer (Figure 3E). This suggested that the Susd4 KO ataxic phenotype was due to a subtler defect in the cerebellar microcircuitry rather than gross neuroanatomical aberrations.

***Susd4 deletion leads to defects in CF/PC synapses in the adult cerebellum***

In the cerebellum of ataxic models like the Lurcher mutant mice, the rate of Parallel fiber (PF) synaptogenesis is decreased and very few Climbing fibers (CF) undergo dendritic translocation (Dumesnil-Bousez & Sotelo, 1992). As the Susd4 KO mice are ataxic but show no gross cerebellar abnormalities, the motor deficits in the Susd4 KO model could be due to underlying defects in synaptogenesis in the olivo-cerebellar network. For this, the timing and pattern of expression of Susd4 in the olivo-cerebellar network should coincide with the timing of synaptogenesis. CF/PC synaptogenesis begins at P0, while PF/PC synaptogenesis and the establishment of specific synaptic connectivity of both inputs occur during the second and third postnatal weeks (Sotelo, 1990; Hashimoto & Kano, 2005; Hashimoto et al., 2009). Susd4 expression in the olivo-cerebellar network was determined by RTqPCR analysis on cerebellar and brainstem extracts. In the brainstem, *Susd4* mRNA is detected as early as E17; its expression increases and plateaus at P7. In the cerebellum, *Susd4* expression is low during the first postnatal week, after which it sharply increases at a rate such that in adulthood, its expression reaches comparable levels as in the brainstem (Figure 3F). In situ hybridization data show that *Susd4* expression is restricted to the Purkinje cells in the cerebellum, and found in the inferior olivary neurons among others in the brainstem. This dynamic regulation of *Susd4* expression in the developing olivo-cerebellar network suggested its role in synaptogenesis.

Since CFs and PFs are important afferents controlling Purkinje cell output, we proceeded to analyze the morphology of CF/PC and PF/PC synapses on cerebellar sections from adult (2-7 months old) wild type and SUSD4 KO mice. Given the constitutive deletion

of *Susd4* in the KO model and regional differences within the cerebellum, quantitative measurements were taken from different cerebellar lobules.

CFs undergo a process of pruning and remodelling during postnatal development and by postnatal day 21 (P21), its final innervation territory is established, extending to about 80% of the Purkinje cell (PC) dendritic arbor (Crepel et al., 1976; Sotelo, 2007). In the adult KO mice, the absence of Susd4 did not affect the extent of CF innervation territory on Purkinje cells (Figure 4A). This was quantified by measuring the extent of the CF-synapse specific VGluT2 puncta relative to PC dendritic length. However, there were defects in the morphology of the VGluT2 puncta formed in KO mice compared to controls. The average number of VGluT2 puncta in the KO was reduced by about 25%, accompanied by a decrease in the size and intensity of VGluT2 contacts made in the KO by 20% and 35% respectively (**$P<0.05$ for all parameters, Student's unpaired t-test) (Figure 4B). These defects in VGluT2 morphology were observed in all the lobules. These results indicate that in the absence of Susd4 in adult mice, the CFs underwent proper dendritic translocation and established synaptic contacts within the expected territory, but failed to either mature or stabilize their contacts on PC dendrites.

Parallel fiber synaptogenesis occurs during the second and third postnatal weeks and by P21, PF synapses innervate distal Purkinje cell dendrites throughout the cerebellar molecular layer (Sotelo, 1990). Morphological analysis of the PF-synapse specific VGluT1 puncta did not reveal any obvious defects. While difficult to measure because of the high density and small size of these puncta, quantifications using MIA-Metamorph and Matlab revealed a marginal but insignificant tendency for the size and number of VGluT1 puncta to decrease (Figure 5).

These results indicate that the abnormal motor phenotype observed in SUSD4 KO mice is accompanied by underlying CF synaptic deficits, as shown by their abnormal morphology.

***Impaired Climbing fiber synapse transmission in juvenile Susd4-null mice***

Since the locomotion defect was observed as early as in 1 month old mice, we wanted to determine whether synaptic defects were already observed at this stage. Morphological analysis of CF/PC and PF/PC synapses was done by immunostaining for VGluT2 and VGluT1 respectively, using brain sections from 1-month-old KO and littermate control mice. Unlike the adult KO mice, global analysis of the morphological defects in juveniles showed no significant differences in any of the assessed parameters such as

extent of CF innervation territory, the size, number or intensity of VGluT2 puncta compared to controls (Figure 6A,B). However, a small but significant decrease in area and intensity of synaptic puncta in lobule VI was detected in Susd4 KO, when lobules were analysed separately. This result indicates that in the absence of SUSD4, morphological defects in CF/PC synapse do not appear synchronously in all regions of the cerebellum, and have only started to appear in lobule VI at one month. The magnitude of the phenotype increases with age, as is shown by larger and significant differences in all lobules in the adult KO mice. No differences were observed in the size, number and intensity of VGluT1 puncta between the juvenile WT and KO mice (Figure 7A,B).

A functional defect in excitatory transmission in PCs could precede visible morphological deficits at early stages and be associated with the observed behavioral deficits. We thus analysed CF and PF transmission from cerebellar PCs in acute slices from WT and KO mice around P25-P29. During development, each PC receives multiple CFs that innervate the PC soma (Crepel et al., 1976). After a period of postnatal synapse elimination between P7 and P21, each PC is innervated by 1 CF that makes several hundred synapses and generates a complex spike with an all or none response (Isope & Barbour, 2002). We found no difference in the number of CFs innervating the recorded PCs between the WT and KO mice. Indeed, in the WT mice, 95% and in the KO mice, 93.75% of PCs attained a one-to-one relationship with CFs. Only 5% of PCs in the WT mice and 6.25% of PCs in the KO mice remained innervated by two CFs, indicating that SUSD4 did not affect CF synapse elimination (Figure 6C). When examining input-output relationships for CF-EPSCs, there were no differences in the peak amplitude between WT and KO slices. However, there was a significant increase in the charge of the EPSC (Figure 6C). This increased charge was associated with an increased decay time constant with no significant difference in the rise time between WT and KO (Figure 6C). Each PC receives inputs from around 170,000 PFs. Each PF makes only 1 synapse with a given PC and 85% of these PF synapses are silent (Isope & Barbour, 2002). Electrophysiological recordings of PF-EPSCs from PCs confirmed that there are no differences in whole cell currents elicited by increasing PF stimulation, indicating normal PF transmission in the KO (Figure 7C). Next, we analysed the short-term plasticity of both CF and PF synapses. The PF is known to present a paired pulse enhancement or facilitation (PPF) and the CF presents a paired pulse depression (PPD)(Konnerth & Llano, 1990). In case of the PF-EPSC, there was no difference in the PPF between the WT and KO (Figure 7C). When CFs were successively stimulated after a 50ms or 150ms interval, as expected, the WT EPSC was reduced with the time interval, but the

KO EPSC continued to stay at the same level (Figure 6C), suggesting a deficient short term plasticity at the CF/PC synapse. Thus SUSD4 deletion leads to functional deficits in CF/PC synapses that appear as early as one month, while it does not affect PF/PC synapse formation and function. Our analysis of adult KO mice shows that these functionally defective CF synapses are then unable to stabilize their contact on Purkinje cells.

***No obvious morphological abnormalities in localization of post-synaptic receptors at Climbing fiber and Parallel fiber synapses in the absence of SUSD4***

The postsynaptic membrane contains a high concentration of glutamate receptors, associated signaling proteins, and cytoskeletal proteins, all assembled by a variety of scaffold proteins into an organized structure called the postsynaptic density (PSD) (Sheng & Hoogenraad, 2007). AMPA receptors and their associated scaffolding proteins are recruited to nascent synapses to stabilize them (Song & Huganir, 2002; Malenka, 2003). Moreover, the regulated insertion and removal of AMPA receptors at the PSD are major mechanisms underlying the strengthening and weakening of synaptic transmission (Shepherd & Huganir, 2007). Given that the loss of SUSD4 led to defects in CF function, in particular slower AMPA current kinetics and increased charge, we wanted to determine whether there were any morphological defects in postsynaptic receptors at the CF/PC synapse. The neonatal PSD of CF synapses contains the AMPAR subunits GluR1 and GluR2/3 but the adult PSD contains only GluR2/3 (Petralia et al., 1998). GluR2/3 immunostaining of cerebellar sections from 1-month-old WT mice revealed that GluR2/3 was present in the PC soma and dendrites. A double labeling with VGluT2 revealed a close association of two to four GluR2/3 clusters around the VGLuT2 puncta. This pattern was observed even in the Susd4 KO cerebellar sections, indicating that GluR2/3 receptors are recruited to CF/PC synapses in the absence of SUSD4 (Figure 8A). To check for abnormalities at the post-synaptic level of the PF/PC synapse, the morphology of PF postsynaptic marker GluRδ2 was also analyzed. In both the WT and KO sections, GluRδ2 was found in the molecular layer with no obvious differences in the density of GluRδ2 puncta (Figure 8B). This indicated that, as for CF synapses, PF synaptic contacts did not display any major deficits at the postsynaptic level.

***Membrane-bound SUSD4 biochemically interacts with Purkinje cell receptor BAI3 in vitro***

In human, SUSD4 is predicted to be alternatively spliced to express either a membrane-bound or a soluble protein (Holmquist et al., 2013). Membrane-bound SUSD4a contains four CCP domains, a transmembrane region, and a cytoplasmic tail. The soluble isoform, SUSD4b, contains three CCP domains (identical to CCP1-3 in the membrane isoform) and a region of unknown homology. A bioinformatics aided comparison using Ensembl Genome Browser (http://www.ensembl.org/index.html) and NCBI HomoloGene (http://www.ncbi.nlm.nih.gov/homologene) revealed that unlike its human homolog, murine SUSD4 exists only as a membrane-bound isoform. To confirm the topology of this membrane protein, a cDNA coding for extracellularly HA-tagged SUSD4-GFP fusion protein was expressed in HEK cells, and HA-immunofluorescence staining was performed with and without triton permeabilization. SUSD4 accumulation, as visualized by GFP expression, was strong at the cell surface and in the Golgi complex (Figure 9B). In cells transfected with the HA-tagged construct, in the absence of triton, cell surface labeling was obtained using an anti-HA antibody. Upon triton permeabilization, this labeling encompassed all the GFP fluorescence corresponding to total HA-SUSD4-GFP. No staining was observed using the HA antibody in control conditions (either with a SUSD4-GFP construct or GFP construct) with or without triton permeabilization (Figure 9B). These results confirmed that SUSD4 is expressed as a membrane-bound protein with extracellular CCP domains. To determine whether murine SUSD4 undergoes proteolysis, we expressed recombinant HA-SUSD4-GFP protein in HEK cells and probed for the extracellular HA tag and intracellular GFP by western blot. The predicted size of the HA-SUSD4-GFP protein is 82 kDa, and a major band was detected at this size with no smaller products, suggesting that SUSD4 does not undergo cleavage in HEK cells (Figure 9A).

SUSD4 has been shown to bind to the gC1q domain *in vitro* (Holmquist et al., 2013). Interestingly, the gC1q domain is present in C1QL1, a secreted C1Q-related protein shown to regulate CF/PC synaptogenesis through its interaction with Brain Angiogenesis Inhibitor 3 (BAI3) (Kakegawa et al., 2015; Sigoillot et al., 2015), a seven transmembrane adhesion GPCR highly expressed in PCs throughout development (Sigoillot et al., 2015). Our in situ hybridization data revealed a strong expression of *Susd4* mRNA in the olivo-cerebellar network during development and in adulthood (Figure 2). It is possible that SUSD4 interacts with the C1QL1/BAI3 complex to regulate CF/PC functional maturation and stability. To ask whether BAI3 could directly interact with SUSD4, we performed

coimmunoprecipitation experiments using extracts of HEK-293H cells co-transfected with BAI3 (BAI3-WT) and SUSD4-GFP. Extracts obtained by anti-GFP affinity-purification were analyzed by immunoblot. Using an anti-BAI3 antibody, we were able to show that BAI3-WT was affinity purified from cells expressing SUSD4-GFP, but not from control cells expressing mbGFP (Figure 9C). Anti-GFP immunoblot confirmed the pull down of SUSD4-GFP or of membrane GFP in the control condition.

**Discussion**

The formation, stability and function of a synapse depend on several processes like cytoskeletal reorganization, accumulation of pre-synaptic vesicles and post-synaptic neurotransmitter receptors. CCP domains are emerging as important evolutionarily conserved protein domains with roles in synaptogenesis and neurotransmission. Genes encoding CCP-containing proteins in humans, for example, have been reported to have psychiatric implications: *Srpx2* has been associated with epilepsy (Roll, 2006), *Csmd1/2* is associated with schizophrenia (Håvik et al., 2011), and *Sez6* has been linked to epilepsy, memory retention and motor coordination (Yu et al., 2006; Gunnersen et al., 2007). In the present study, we demonstrate a role for CCP-containing SUSD4 in the stabilization and function of Climbing fiber synaptic contacts on cerebellar Purkinje cells, possibly through its interaction with the BAI3 receptor expressed in Purkinje cells. The loss of SUSD4 in the knockout mouse model results in slower Climbing fiber synapse transmission, manifesting in long lasting motor coordination defects. These early functional deficits are followed by a reduction in the Climbing fiber synaptic puncta size and number, suggesting a gradual decline in the ability of synaptic contacts to stabilize.

We find that, in cerebellar Purkinje cells, SUSD4 influences synaptogenesis primarily in Climbing fibers. However, similar to previous studies of cerebellar ataxic animal models, it is possible that this protein controls synaptogenesis in other synapses of the olivo-cerebellar network. For example, the Cbln1-null mice display an ataxic phenotype, accompanied by deficits in the synaptogenesis of both PF and CF synapses such as reduced number of PF terminals, diminished LTD, free spines in the distal dendrites, mismatched spines in the proximal dendrites and ectopic CF synapses in PF territory (Hirai et al., 2005). The normal morphology and transmission of PF synapses in our study indicate that PF synaptogenesis is not directly affected by the deletion of SUSD4 in the knockout model. However, immunofluorescence labeling and quantifications are needed to test the potential effects of SUSD4 on Purkinje cell-innervating inhibitory synapses. It would also be

interesting to determine if SUSD4 has a general role in other regions, for example the hippocampus, where *Susd4* mRNA is strongly expressed. Another remaining question is SUSD4 subcellular localization in neurons since *Susd4* mRNA is expressed by both the presynaptic ION and postsynaptic Purkinje cells of the CF/PC synapse. An antibody against SUSD4 suitable for immunolocalization remains to be generated.

In the current study, electrophysiological data provide clear evidence that SUSD4 influences the emergence of normal synaptic neurotransmission. Recordings of CF-EPSCs demonstrate a slower transmission of CF synaptic current in the SUSD4 KO mice. This could be explained by possible defects in presynaptic glutamate release or a slower rate of glutamate clearance from the synaptic cleft (Takahashi et al., 1995). Analysis of the CF paired pulse depression showed a tendency for deficient short-term plasticity in SUSD4 KO mice. However, additional time points are needed to test whether a longer time interval of CF stimulation results in the CF-EPSC to return to baseline or continue to stay stimulated. A slower glutamate removal might result from a defect in the number, localization, clustering or saturation of postsynaptic receptors (Bergles et al., 1999; Foster et al., 2002). To test for a rate-limiting role of glutamate removal in determining the EPSC duration, it would be useful to block glutamate uptake and see if it slows the decay of the EPSCs. It is known that the amplitude of the synaptic current depends on the number of accessible postsynaptic receptors in the vicinity of the release sites (Redman, 1990). Since we found no difference in CF-EPSC amplitude between the WT and KO, and we could detect GluR2/3 in the synapse by immunofluorescence, a defect in the number of postsynaptic receptors in the absence of SUSD4 is unlikely. Thus, the slower CF transmission in the current study could be due to a defect in the postsynaptic glutamate receptor clustering, resulting in scattered receptors along the PSD that do not efficiently receive glutamate from the presynaptic site. This needs to be assessed using high resolution imaging such as EM or super-resolution. Alternatively, the aggregates of neurotransmitter receptors could be present but not localized and immobilized appropriately. This effect of SUSD4 on AMPA receptor dynamics could be assayed using super resolution imaging as previously shown (Triller & Choquet, 2008). Another possibility is that SUSD4 influences the synaptic scaffold and ensures the proper apposition of the PSD to the presynaptic active zone which in turn ensures that receptors are in close proximity to presynaptic neurotransmitter release sites. Even though we find no obvious differences in the morphology and localization of GluR2/3 through immunofluorescence labelling, additional antibodies and quantification methods are needed to confirm this.

Although the localization of SUSD4 protein was not assayed in the current project, the role of this protein in the developing synapse can be hypothesized from the data presented and from previous studies in invertebrates. In the current study, in situ hybridization data show that *Susd4* mRNA is expressed at both the pre and postsynaptic sites of the CF/PC synapse. SUSD4 KO mice showed a disruption in the ability of established Climbing Fiber synaptic contacts to stabilize and function properly, suggesting a role for SUSD4 in the aggregation and/or localization of postsynaptic receptors to the Climbing fiber PSD. This function is similar to what has been described in the *C.elegans* NMJ, for the secreted CCP-containing protein LEV-9, which is critical for clustering L-AChRs at cholinergic synapses. We additionally showed that SUSD4 can interact with the postsynaptic receptor BAI3. BAI3 specifies Climbing fiber innervation territory on Purkinje cells through its interaction with C1QL1 (Kakegawa et al., 2015; Sigoillot et al., 2015) and is characterized by TSR1 domains. Interestingly, TSR1 domains are also found in *C.elegans* Ce-punctin, an ADAMTS-like secreted protein that exists in two isoforms and controls the proper localization of cholinergic and GABAergic synapses at the NMJ (Gendrel et al., 2009; Pinan-Lucarré et al., 2014). It is thus possible that the protein domains of SUSD4 and BAI3 constitute an evolutionarily conserved synaptic scaffold that stabilizes the Climbing Fiber synaptic contacts by determining the proper localization and clustering of postsynaptic receptors.

In summary, our study indicates a role for SUSD4 in CF/PC synapse stabilization and function that potentially involves an interaction with PC-specific BAI3 receptor. This role could be played through a regulation of post-synaptic AMPA receptor clustering. Members of the TARP family of proteins have four transmembrane domains and specifically interact with AMPA receptors through PDZ binding domains (Tomita et al., 2003). In contrast, CCP domain-containing proteins have a long extra-cellular region with only one transmembrane domain. Thus, TARPs and CCP domain-containing proteins likely bind to neurotransmitter receptors via distinct modes and may interact with different auxiliary proteins in the receptor protein complexes. So far, LEV-9 in invertebrates is the only CCP-containing protein to be reported with this postsynaptic receptor clustering role (Gendrel et al., 2009). In vertebrates, CCP-containing SRPX2 has been identified to interact with extracellular matrix proteins like ADAMTS4, however, no functional role or mechanism has been determined (Royer-Zemmour et al., 2008). Our study would implicate SUSD4 as the first complement control protein in vertebrates to have a postsynaptic receptor clustering function in excitatory synapses.

**Acknowledgments**

The authors wish to thank Caroline Moreau-Fauvarque from the laboratory of Alain Chédotal and Dr. Marion Wassef for help with *in situ* hybridization, Jérémie Teillon and Nicole Quenech'du from the CIRB Imaging facility, Yasmine Belarif and Amulya Nidhi Shrivastava from the laboratory of Antoine Triller for help with the MIA-Metamorph and Matlab analysis, and animal facility personnel from the CIRB and ENS. This work was supported by funding from Nerf (SS), Labex Memolife (SS) and Collège de France (SS), Ecole des Neurosciences de Paris (KI), Fondation pour la Recherche Médicale (MA), ATIP AVENIR (FS), PSL (IGC), Fondation Jérôme Lejeune (FS), ANR-13-SAMA-0010-01(FS). K.I is the recipient of a PhD grant from the Ecole des Neurosciences de Paris (ENP) and the ENS Labex MemoLife. The authors declare no conflict of interest.

**References**

Bally-Cuif, L., Alvarado-Mallart, R. M., Darnell, D. K., & Wassef, M. (1992). Relationship between Wnt-1 and En-2 expression domains during early development of normal and ectopic met-mesencephalon. *Development*, *115*(4), 999–1009.

Beer, S., Simins, A. B., Schuster, A., & Holzmann, B. (2000). Molecular cloning and characterization of a novel SH3 protein (SLY) preferentially expressed in lymphoid cells. *Biochimica Et Biophysica Acta (BBA) - Gene Structure and Expression*, *1520*(1), 89–93.

Bergles, D. E., Diamond, J. S., & Jahr, C. E. (1999). Clearance of glutamate inside the synapse and beyond. *Current Opinion in Neurobiology*, *9*(3), 293–298.

Crepel, F., Mariani, J., & Delhaye-Bouchaud, N. (1976). Evidence for a multiple innervation of purkinje cells by climbing fibers in the immature rat cerebellum. *Journal of Neurobiology*, *7*(6), 567–578.

Dumesnil-Bousez, N., & Sotelo, C. (1992). Early development of the Lurcher cerebellum: Purkinje cell alterations and impairment of synaptogenesis. *Journal of Neurocytology*, *21*(7), 506–529.

Foster, K. A., Kreitzer, A. C., & Regehr, W. G. (2002). Interaction of postsynaptic receptor saturation with presynaptic mechanisms produces a reliable synapse. *Neuron*, *36*(6), 1115–1126.

Gendrel, M., Rapti, G., Richmond, J. E., & Bessereau, J.-L. (2009). A secreted complement-control-related protein ensures acetylcholine receptor clustering. *Nature*, *461*(7266), 992–996.

Gunnersen, J. M., Kim, M. H., Fuller, S. J., De Silva, M., Britto, J. M., Hammond, V. E., Davies, P. J., Petrou, S., et al. (2007). Sez-6 Proteins Affect Dendritic Arborization Patterns and Excitability of Cortical Pyramidal Neurons. *Neuron*, *56*(4), 621–639.

Hashimoto, K., & Kano, M. (2005). Postnatal development and synapse elimination of climbing fiber to Purkinje cell projection in the cerebellum. *Neuroscience Research*, *53*(3), 221–228.

Hashimoto, K., Yoshida, T., Sakimura, K., Mishina, M., Watanabe, M., & Kano, M. (2009). Influence of parallel fiber–Purkinje cell synapse formation on postnatal development of climbing fiber–Purkinje cell synapses in the cerebellum. *Neuroscience*, *162*(3), 601–611.

Håvik, B., Le Hellard, S., Rietschel, M., Lybæk, H., Djurovic, S., Mattheisen, M., Mühleisen, T. W., Degenhardt, F., et al. (2011). The Complement Control-Related Genes CSMD1 and CSMD2 Associate to Schizophrenia. *Biological Psychiatry*, *70*(1), 35–42.

Hirai, H., Pang, Z., Bao, D., Miyazaki, T., Li, L., Miura, E., Parris, J., Rong, Y., et al. (2005). Cbln1 is essential for synaptic integrity and plasticity in the cerebellum. *Nature Neuroscience*, *8*(11), 1534–1541.

Holleben, M., Gohla, A., Janssen, K.-P., Iritani, B. M., & Beer-Hammer, S. (2011). Immunoinhibitory Adapter Protein Src Homology Domain 3 Lymphocyte Protein 2 (SLy2) Regulates Actin Dynamics and BCell Spreading. *The Journal of Biological Chemistry*, *286*(15), 13489–13501.

Holmquist, E., Okroj, M., Nodin, B., Jirstrom, K., & Blom, A. M. (2013). Sushi domain-containing protein 4 (SUSD4) inhibits complement by disrupting the formation of the classical C3 convertase. *The FASEB Journal*, *27*(6), 2355–2366.

Isope, P., & Barbour, B. (2002). Properties of unitary granule cell - Purkinje cell synapses in adult rat cerebellar slices. *Journal of Neuroscience*, *22*(22), 9668–9678.

Jackson, A. C., & Nicoll, R. A. (2011). The expanding social network of ionotropic glutamate receptors: TARPs and other transmembrane auxiliary subunits. *Neuron*, *70*(2), 178–199.

Kakegawa, W., Mitakidis, N., Miura, E., Abe, M., Matsuda, K., Takeo, Y. H., Kohda, K., Motohashi, J., et al. (2015). Anterograde C1ql1 Signaling Is Required in Order to Determine and Maintain a Single-Winner Climbing Fiber in the Mouse Cerebellum. *Neuron*, *85*(2), 316–329.

Kirkitadze, M. D., & Barlow, P. N. (2001). Structure and flexibility of the multiple domain proteins that regulate complement activation. *Immunological Reviews*, *180*, 146–161.

Konnerth, A., & Llano, I. (1990). Synaptic currents in cerebellar Purkinje cells. *Proceedings of the National Academy of Sciences U S A*, *87*(7), 2662–2665.

Lalonde, R., & Strazielle, C. (2007). Spontaneous and induced mouse mutations with cerebellar dysfunctions: behavior and neurochemistry. *Brain Research*, *1140*, 51–74.

Lanoue, V., Usardi, A., Sigoillot, S. M., Talleur, M., Iyer, K., Mariani, J., Isope, P., Vodjdani, G., et al. (2013). The adhesion-GPCR BAI3, a gene linked to psychiatric disorders, regulates dendrite morphogenesis in neurons. *Molecular Psychiatry*, *18*(8), 943–950.

Malenka, R. C. (2003). Synaptic plasticity and AMPA receptor trafficking. *Annals of the New York Academy of Sciences*, *1003*, 1–11.

Matsuda, K., Miura, E., Miyazaki, T., Kakegawa, W., Emi, K., Narumi, S., Fukazawa, Y., Ito-Ishida, A., et al. (2010). Cbln1 Is a Ligand for an Orphan Glutamate Receptor 2, a Bidirectional Synapse Organizer. *Science*, *328*(5976), 363–368.

Moy, I., Todorović, V., Dubash, A. D., Coon, J. S., Parker, J. B., Buranapramest, M., Huang, C. C., Zhao, H., et al. (2014). Estrogen-dependent sushi domain containing 3 regulates cytoskeleton organization and migration in breast cancer cells. *Oncogene*, *34*(3), 323–333.

Nadjar, Y., Triller, A., Bessereau, J.-L., & Dumoulin, A. (2015). The Susd2 protein regulates neurite growth and excitatory synaptic density in hippocampal cultures. *Molecular and Cellular Neuroscience*, *65*, 82–91.

Nakayama, M., & Hama, C. (2011). Modulation of neurotransmitter receptors and synaptic differentiation by proteins containing complement-related domains. *Neuroscience Research*, *69*(2), 87–92.

O'Brien, R. J., Xu, D., Petralia, R. S., Steward, O., Huganir, R. L., & Worley, P. F. (1999). Synaptic clustering of AMPA receptors by the extracellular immediate-early gene product Narp. *Neuron*, *23*(2), 309–323.

Petralia, R. S., Zhao, H. M., Wang, Y. X., & Wenthold, R. J. (1998). Variations in the tangential distribution of postsynaptic glutamate receptors in Purkinje cell parallel and climbing fiber synapses during development. *Neuropharmacology*, *37*(10-11), 1321–1334.

Pinan-Lucarré, B., Tu, H., Pierron, M., Cruceyra, P. I., Zhan, H., Stigloher, C., Richmond, J. E., & Bessereau, J.-L. (2014). *C. elegans* Punctin specifies cholinergic versus GABAergic identity of postsynaptic domains. *Nature*, *511*(7510), 466–470.

Redman, S. (1990). Quantal analysis of synaptic potentials in neurons of the central nervous system. *Physiological Reviews*, *70*(1), 165–198.

Reid, K. B. M., & Day, A. J. (1989). Structure-function relationships of the complement components. *Immunology Today*, *10*(6), 177–180.

Roll, P., Rudolf, G., Pereira, S., Royer, B., Scheffer, I E., Massacrier, A., Valenti, M-P., Roeckel-Trevisiol, N., Jamali, S., Beclin, C., Seegmuller, C., Metz-Lutz, M-N., Lemainque, A., Delepine, M., Caloustian, C., Martin, A., Bruneau, N., Depetris, D., Mattei, M-G., Flori, E., Robaglia-Schlupp, A., Levy, N., Neubauer, B A., Ravid, R., Marescaux, C., Berkovic, S F., Hirsch, E., Lathrop, M., Cau, P., & Szepetowski, P. (2006). SRPX2 mutations in disorders of language cortex and cognition. *Human Molecular Genetics*, *15*(7), 1195–1207.

Royer-Zemmour, B., Ponsole-Lenfant, M., Gara, H., Roll, P., Leveque, C., Massacrier, A., Ferracci, G., Cillario, J., et al. (2008). Epileptic and developmental disorders of the speech cortex: ligand/receptor interaction of wild-type and mutant SRPX2 with the plasminogen activator receptor uPAR. *Human Molecular Genetics*, *17*(23), 3617–3630.

Shaffer, L. G., Theisen, A., Bejjani, B. A., Ballif, B. C., Aylsworth, A. S., Lim, C., McDonald, M., Ellison, J. W., et al. (2007). The discovery of microdeletion syndromes in the post-genomic era: review of the methodology and characterization of a new 1q41q42 microdeletion syndrome. *Genetics in Medicine*, *9*(9), 607–616.

Sheng, M., & Hoogenraad, C. C. (2007). The Postsynaptic Architecture of Excitatory Synapses: A More Quantitative View. *Annual Review of Biochemistry*, *76*(1), 823–847.

Shepherd, J. D., & Huganir, R. L. (2007). The Cell Biology of Synaptic Plasticity: AMPA Receptor Trafficking. *Annual Review of Cell and Developmental Biology*, *23*(1), 613–643.

Sigoillot, S. M., Iyer, K., Binda, F., González-Calvo, I., Talleur, M., Vodjdani, G., Isope, P., & Selimi, F. (2015). The Secreted Protein C1QL1 and Its Receptor BAI3 Control the Synaptic Connectivity of Excitatory Inputs Converging on Cerebellar Purkinje Cells. *Cell Reports*, *10*(5), 820–832.

Song, I., & Huganir, R. L. (2002). Regulation of AMPA receptors during synaptic plasticity. *Trends in Neurosciences*, *25*(11), 578–588.

Sotelo, C. (1990). Cerebellar synaptogenesis: what we can learn from mutant mice. *The*

*Journal of Experimental Biology*, *153*, 225–249.

Sotelo, C. (2007). Development of "Pinceaux" formations and dendritic translocation of climbing fibers during the acquisition of the balance between glutamatergic and γ-aminobutyric acidergic inputs in developing Purkinje cells. *Journal of Comparative Neurology*, *506*(2), 240–262.

Stevens, B., Allen, N. J., Vazquez, L. E., Howell, G. R., Christopherson, K. S., Nouri, N., Micheva, K. D., Mehalow, A. K., et al. (2007). The Classical Complement Cascade Mediates CNS Synapse Elimination. *Cell*, *131*(6), 1164–1178.

Takahashi, M., Kovalchuk, Y., & Attwell, D. (1995). Pre- and postsynaptic determinants of EPSC waveform at cerebellar climbing fiber and parallel fiber to Purkinje cell synapses. *Journal of Neuroscience*, *15*(8), 5693–5702.

Tomita, S., Chen, L., Kawasaki, Y., Petralia, R. S., Wenthold, R. J., Nicoll, R. A., & Bredt, D. S. (2003). Functional studies and distribution define a family of transmembrane AMPA receptor regulatory proteins. *The Journal of Cell Biology*, *161*(4), 805–816.

Triller, A., & Choquet, D. (2008). New Concepts in Synaptic Biology Derived from Single-Molecule Imaging. *Neuron*, *59*(3), 359–374.

Tu, Z., Cohen, M., Bu, H., & Lin, F. (2010). Tissue Distribution and Functional Analysis of Sushi Domain-Containing Protein 4. *The American Journal of Pathology*, *176*(5), 2378–2384.

Waruiru, C. (2004). Febrile seizures: an update. *Archives of Disease in Childhood*, *89*(8), 751–756.

Watson, A. P., Evans, R. L., & Egland, K. A. (2013). Multiple Functions of Sushi Domain Containing 2 (SUSD2) in Breast Tumorigenesis. *Molecular Cancer Research*, *11*(1), 74–85.

Yu, Z.-L., Jiang, J.-M., Wu, D.-H., Xie, H.-J., Jiang, J.-J., Zhou, L., Peng, L., & Bao, G.-S. (2006). Febrile seizures are associated with mutation of seizure-related (SEZ) 6, a brain-specific gene. *Journal of Neuroscience Research*, *85*(1), 166–172.

Yuzaki, M. (2010). Synapse formation and maintenance by C1q family proteins: a new class of secreted synapse organizers. *European Journal of Neuroscience*, *32*(2), 191–197.

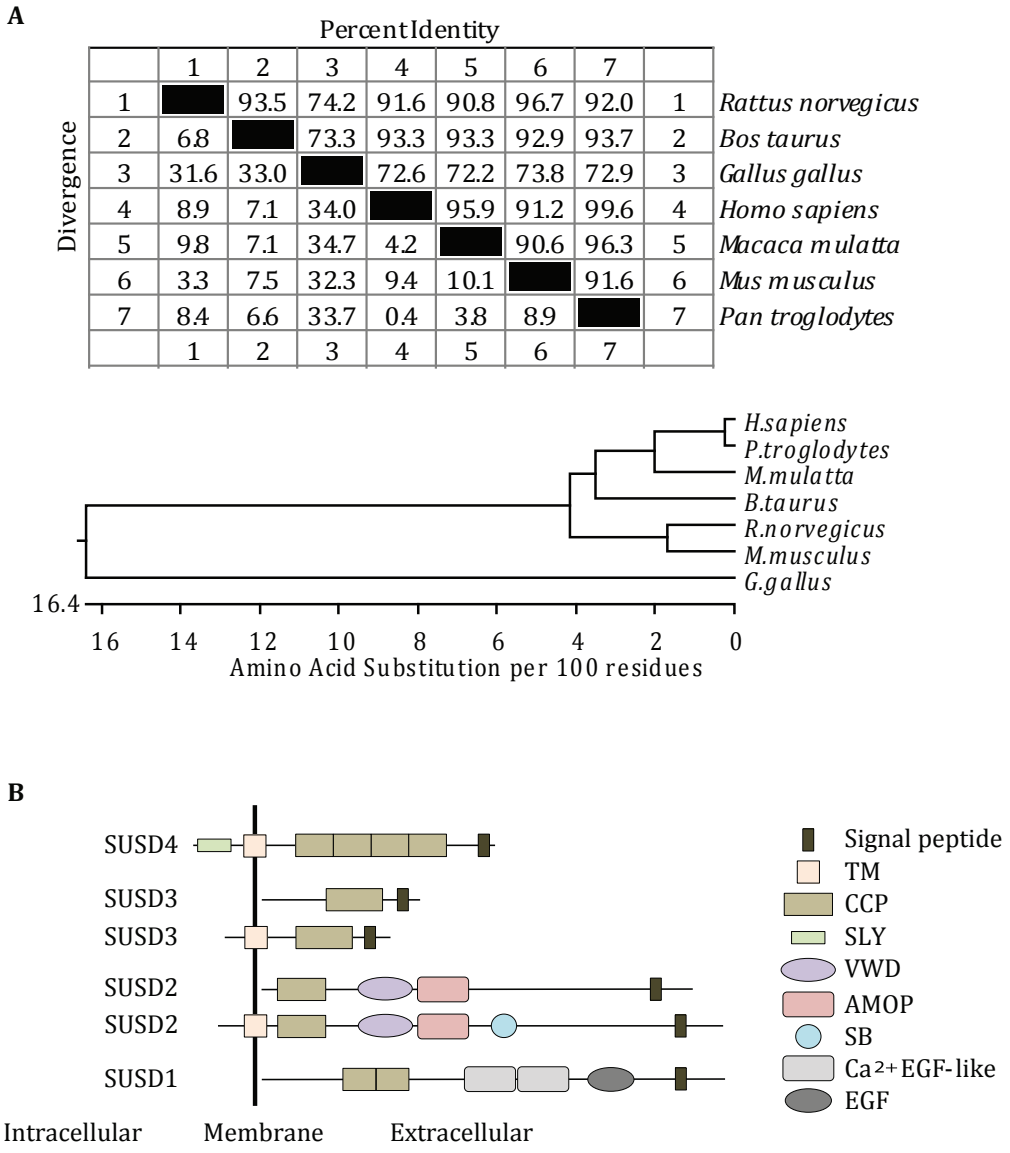


**Figure 1. SUSD4 phylogenetic description and structural comparison with SUSD proteins**
**(A)** Phylogenetic analysis of the SUSD4 protein in vertebrates using ClustalW alignment **(B)** Members of SUSD family, SUSD1-4. TM, transmembrane; CCP, complement control protein; SLY, lymphocyte signaling adaptor; VWD, von Willebrand factor type D domain mutant; AMOP, Adhesion-associated domain in MUC4 and Other Proteins; SB, somatomedin-B; EGF, epidermal growth factor

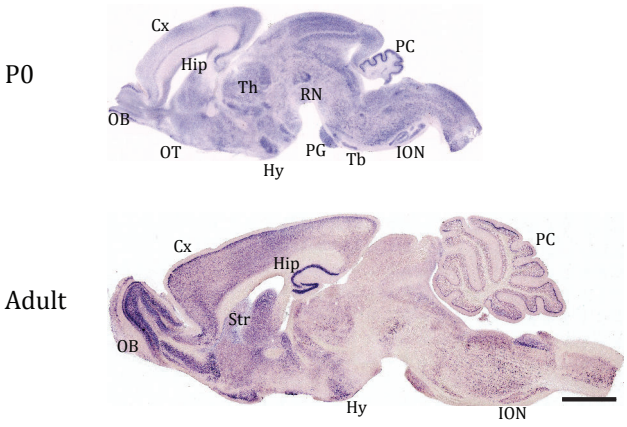


**Figure 2. Developmentally regulated expression of Susd4 gene in the mouse brain**
In situ hybridization experiments were performed using probes specific for *Susd4* on sagittal sections of mouse brain taken at postnatal day 0 (P0) and adult. OB, olfactory bulb; OT, olfactory tubercle; Cx, cortex; Hip, hippocampus; Str, striatum; Th, thalamus; Hy, hypothalamus; RN, red nuclei; PG, pontine gray; Tb, trapezoid body of superior olive; IO, inferior olive; PC, Purkinje cell. Scale bars, 500μm; each scale bar applies to the whole column.

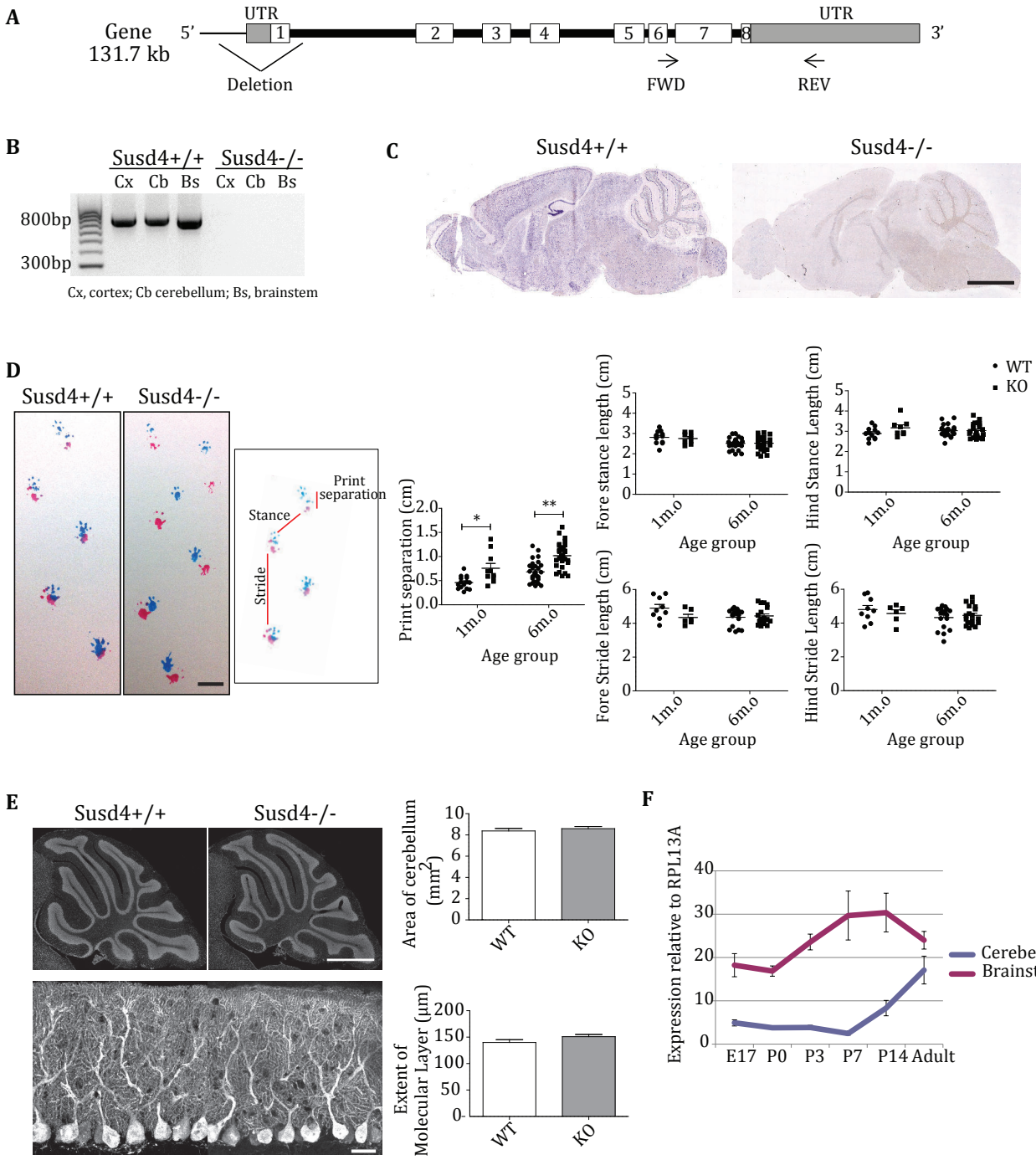
A
Gene
131.7 kb
5'
UTR
1
2
3
4
5
6
7
8
UTR
3'
Deletion
FWD
REV
B
Susd4+/+
Susd4-/-
Cx Cb Bs Cx Cb Bs
800bp
300bp
Cx, cortex; Cb cerebellum; Bs, brainstem
C
Susd4+/+
Susd4-/-
D
Susd4+/+
Susd4-/-
Print separation
Stance
Stride
Print separation (cm)
Age group
1m.o
6m.o
Fore stance length (cm)
Hind Stance Length (cm)
Fore Stride length (cm)
Hind Stride Length (cm)
WT
KO
E
Susd4+/+
Susd4-/-
Area of cerebellum (mm2)
Extent of Molecular Layer (µm)
WT
KO
F
Expression relative to RPL13A
E17
P0
P3
P7
P14
Adult
Cerebellum
Brainstem

**Figure 3**

**Figure 3. Characterization of Susd4 knockout mice**

**(A)** Structure of the gene coding for Susd4 mRNA; Localization of the deletion in the Susd4 KO mouse as well as primers used for RT-PCR **(B,C)** Absence of Susd4 gene transcript in KO confirmed by RT-PCR on cortex, cerebellum, brainstem cDNA extracts (B) and by in situ hybridization (C) Scale bar, 500µm. **(D)** Representative footprint patterns of wild type and KO mice (left) and quantitative analysis of footprint based on measurements of print separation, stride length and stance length (right). Symbols indicate mean ± SEM by genotype of each age group, *p<0.05; **<0.01. N=3 animals aged 1 month, N=6 animals aged 6 months. Scale bar, 1cm. **(E)** DAPI stained sagittal sections of adult wild type and KO cerebellum and quantitative analysis of cerebellar area. Scale bar, 500µm. Calbindin (CaBP) immunostaining of adult wild type and KO Purkinje cells, and quantitative analysis of extent of molecular layer. Scale bar, 30 µm. **(F)** Expression of *Susd4* at different stages of mouse brain development using quantitative RT-PCR on extracts from brainstem and cerebellum (E17: embryonic day 17; P0 to P14: postnatal day 0 to 14). Expression levels are normalized to the RPL13A gene. N=3 samples per stage.

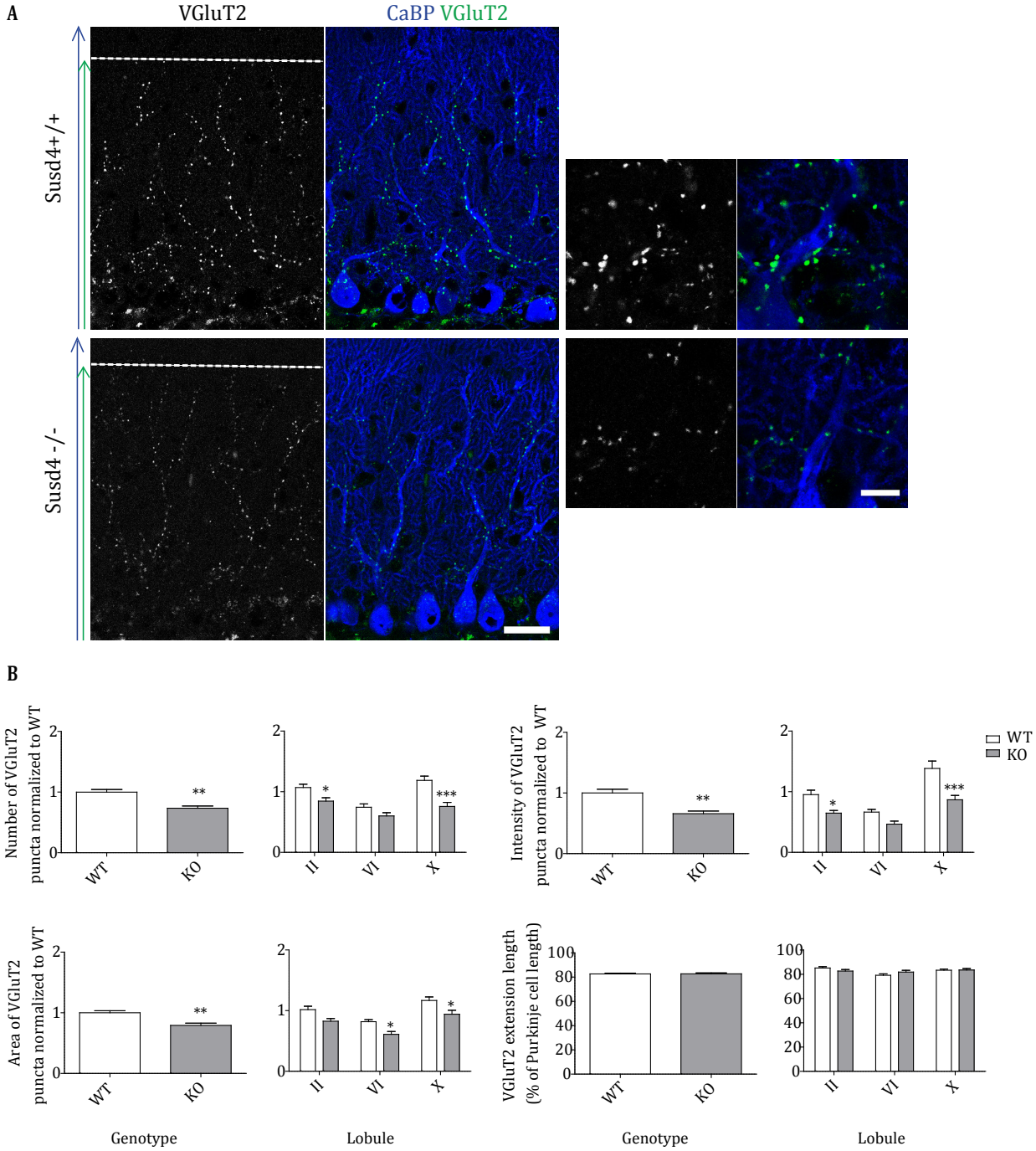


**Figure 4. Defects in the morphology of Climbing fiber synapses in adult Susd4 KO mice**
**(A)** Defects in Climbing fiber synapses were assessed in Susd4 KO and WT mice aged 2-7 months by co-immunostaining for CF synapse specific marker vesicular glutamate transporter 2 antibody (VGluT2) and PC-specific marker Calbindin (CaBP). Representative images of VGuT2 extension marked with white dashed line (left), scale bar, 30µm; representative images of VGluT2 cluster morphology (right), scale bar, 10µm. **(B)** Quantitative analyses of VGluT2 cluster extension, number and morphological defects were performed using Matlab from masks created on MIA-Metamorph. N=3-5 animals per condition. (Data are presented as mean ± SEM; unpaired Student t test, *p<0.05; **p<0.01; ***p<0.001).

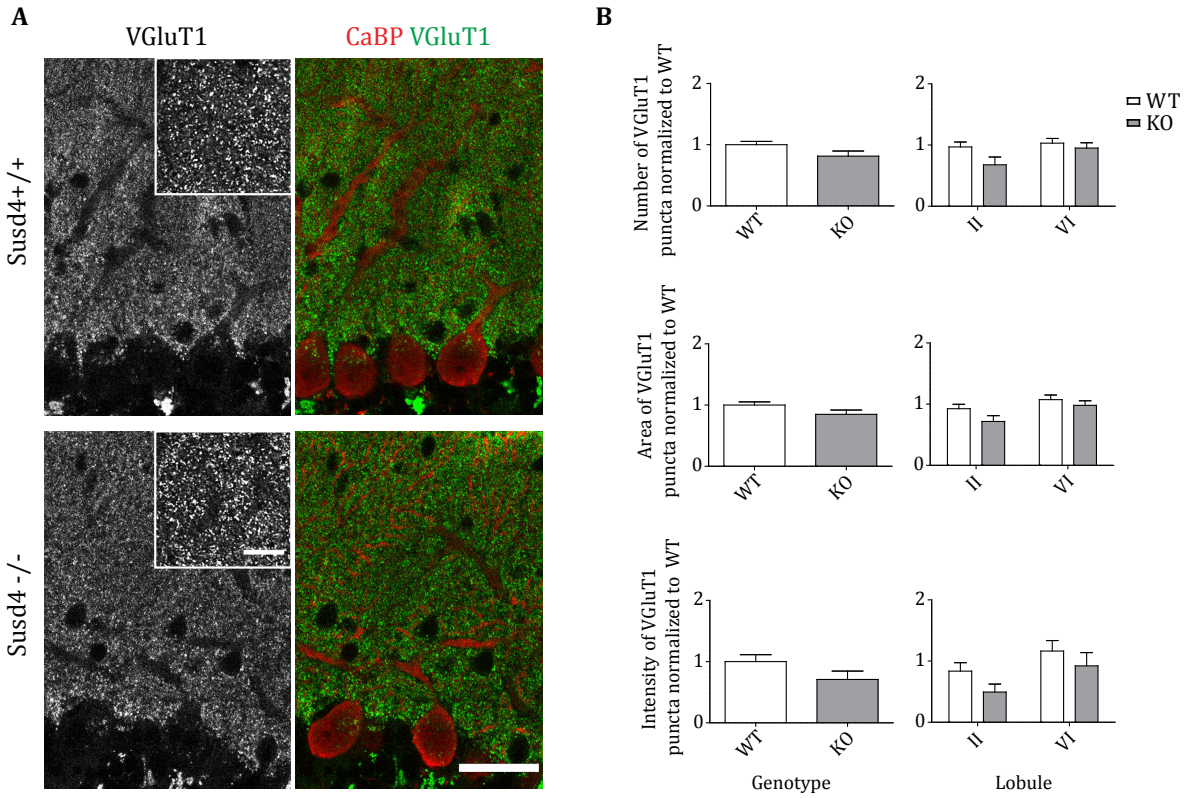


**Figure 5. Normal Parallel fiber synapse morphology in adult Susd4 KO mice**
**(A)** Defects in Parallel fiber synapses were assessed in Susd4 KO and WT mice aged 2-7 months by co-immunostaining for PF synapse specific marker vesicular glutamate transporter 1 antibody (VGluT1) and PC-specific marker Calbindin (CaBP). Scale bar, 30µm. Magnified images of VGluT1 puncta in inset. Scale bar, 10µm **(B)** Quantitative analyses of VGluT1 cluster number and morphological defects were performed using Matlab from masks created on MIA-Metamorph. N=3-5 animals aged 2-7mo. Data are presented as mean ± SEM; unpaired Student t test, *p<0.05; **p<0.01; ***p<0.001.

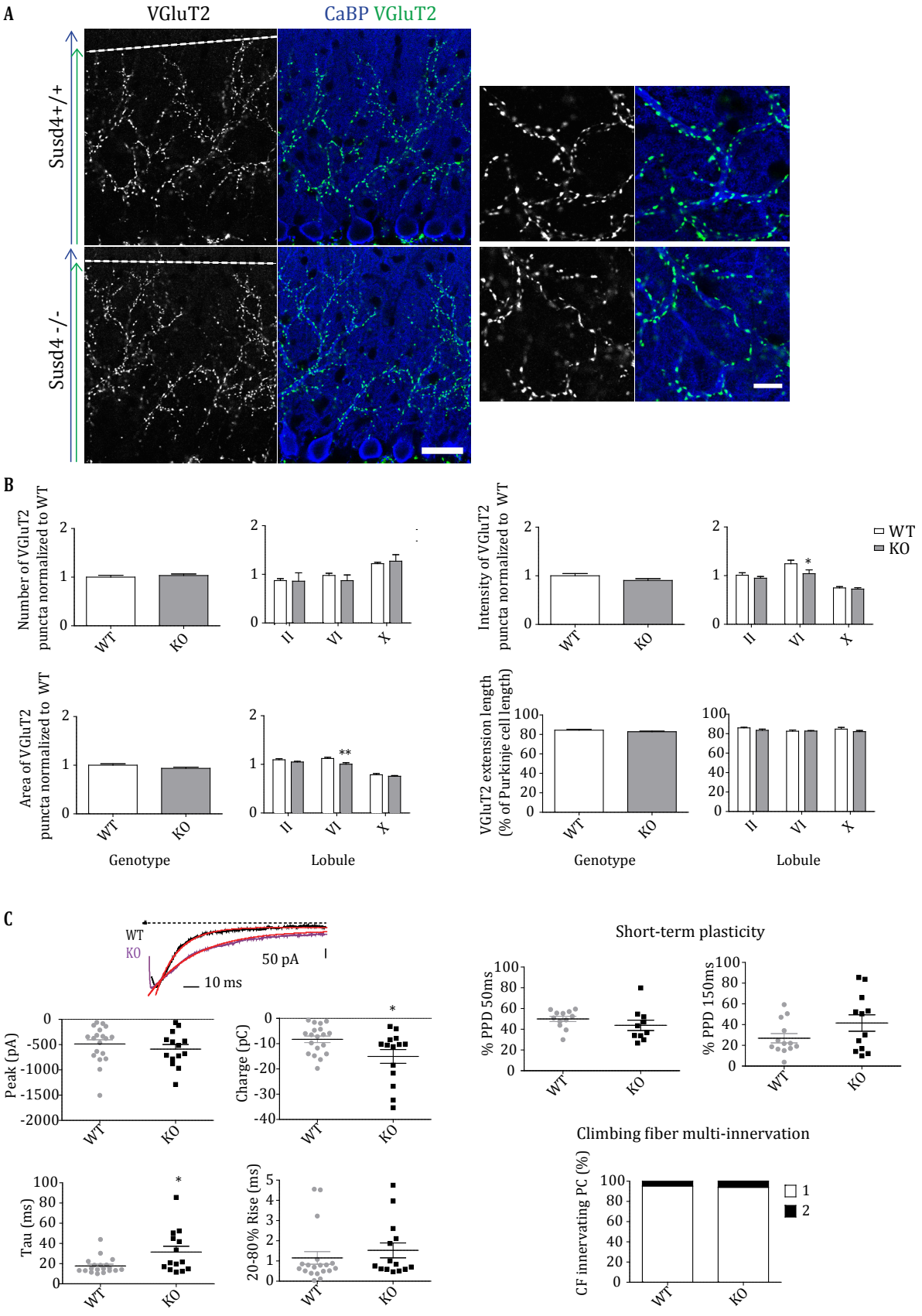
A
VGluT2
CaBP VGluT2
Susd4+/+
Susd4 -/-
B
Number of VGluT2 puncta normalized to WT
Intensity of VGluT2 puncta normalized to WT
Area of VGluT2 puncta normalized to WT
VGluT2 extension length (% of Purkinje cell length)
WT
KO
II
VI
X
Genotype
Lobule
C
WT
KO
50 pA
10 ms
Peak (pA)
Charge (pC)
Tau (ms)
20-80% Rise (ms)
Short-term plasticity
% PPD 50ms
% PPD 150ms
Climbing fiber multi-innervation
CF innervating PC (%)
1
2

**Figure 6**

**Figure 6. Functional deficits in Climbing fiber synapses with normal morphology in juvenile Susd4 KO mice**

**(A)** Defects in Climbing fiber synapses were assessed in Susd4 KO and WT mice aged 1 month by co-immunostaining for CF synapse specific marker vesicular glutamate transporter 2 antibody (VGluT2) and PC-specific marker Calbindin (CaBP). Representative images of VGuT2 extension marked with white dashed line (left), scale bar, 30µm; representative images of VGluT2 cluster morphology (right), scale bar, 10µm. **(B)** Quantitative analyses of VGluT2 cluster extension, number and morphological defects were performed using Matlab from masks created on MIA-Metamorph. N=3 animals per condition. (Data are presented as mean ± SEM; unpaired Student *t* test, *p<0.05; **p<0.01; ***p<0.001). **(C)** Electrophysiological recordings of P25 to P29 Purkinje cells from Susd4 KO and WT mice. Climbing fiber-mediated whole cell currents are shown in the left panel. Traces were recorded at –10 mV following CF stimulation. Peak amplitude, charge, decay time constant (tau), rise time and paired pulse depression (PPD) of the CF-EPSCs are represented as scatterplots. Multiple innervation is represented as a histogram depicting percentage of control and mutant PCs innervated by CFs. (WT n=19, KO n=14). For the PPD experiment at 50ms, WT n=11, KO n=10). For the PPD experiment at 150ms, WT n=13, KO n=12. Mann Whitney test for all parameters; Student *t* test for tau and PPD assessment, *p<0.05; **p<0.01; ***p<0.001.

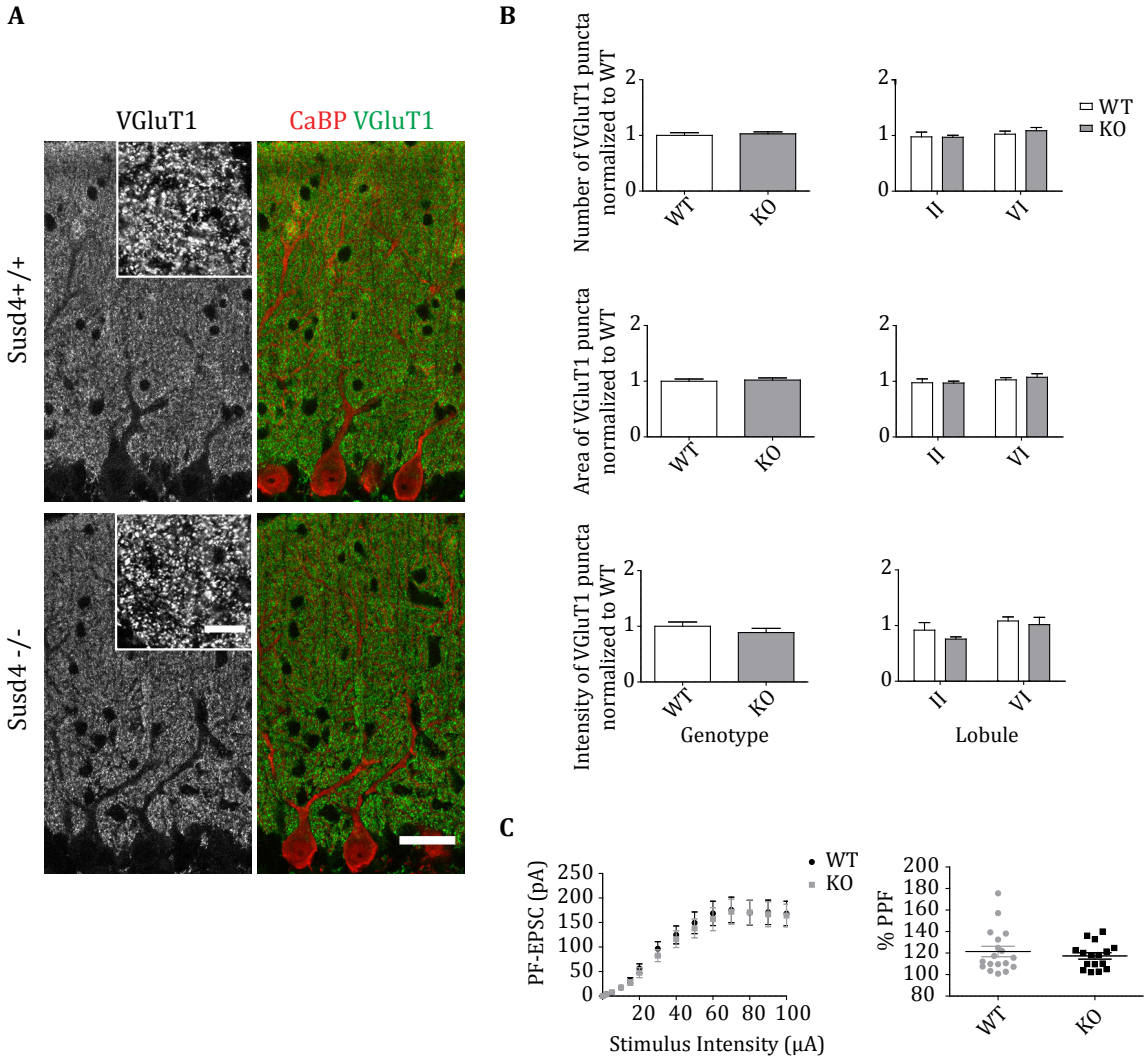


**Figure 7. No morphological and functional defects in Parallel fiber synapses in juvenile Susd4 KO mice**

**(A)** Defects in Parallel fiber synapses were assessed in Susd4 KO and WT mice aged 1 month by co-immunostaining for PF synapse specific marker vesicular glutamate transporter 1 antibody (VGluT1) and PC-specific marker Calbindin (CaBP). Scale bar, 30µm. Magnified images of VGluT1 puncta in inset. Scale bar, 10µm **(B)** Quantitative analyses of VGluT1 cluster number and morphological defects were performed using Matlab from masks created on MIA-Metamorph. N=3 animals aged 1mo. (Data are presented as mean ± SEM; unpaired Student t test, *p<0.05; **p<0.01; ***p<0.001). **(C)** PF-ESPCs recorded in PCs of P25–P29 WT and Susd4 KO. Purkinje cells were clamped at -10mV and PF response was elicited by stimulation in the molecular layer. Input/output curves are plotted as mean±SEM (WT n=20, KO n=14). The classical 20Hz PF/PC paired pulse facilitation (PPF) is represented as a scatterplot (WT n=19, KO n=16).

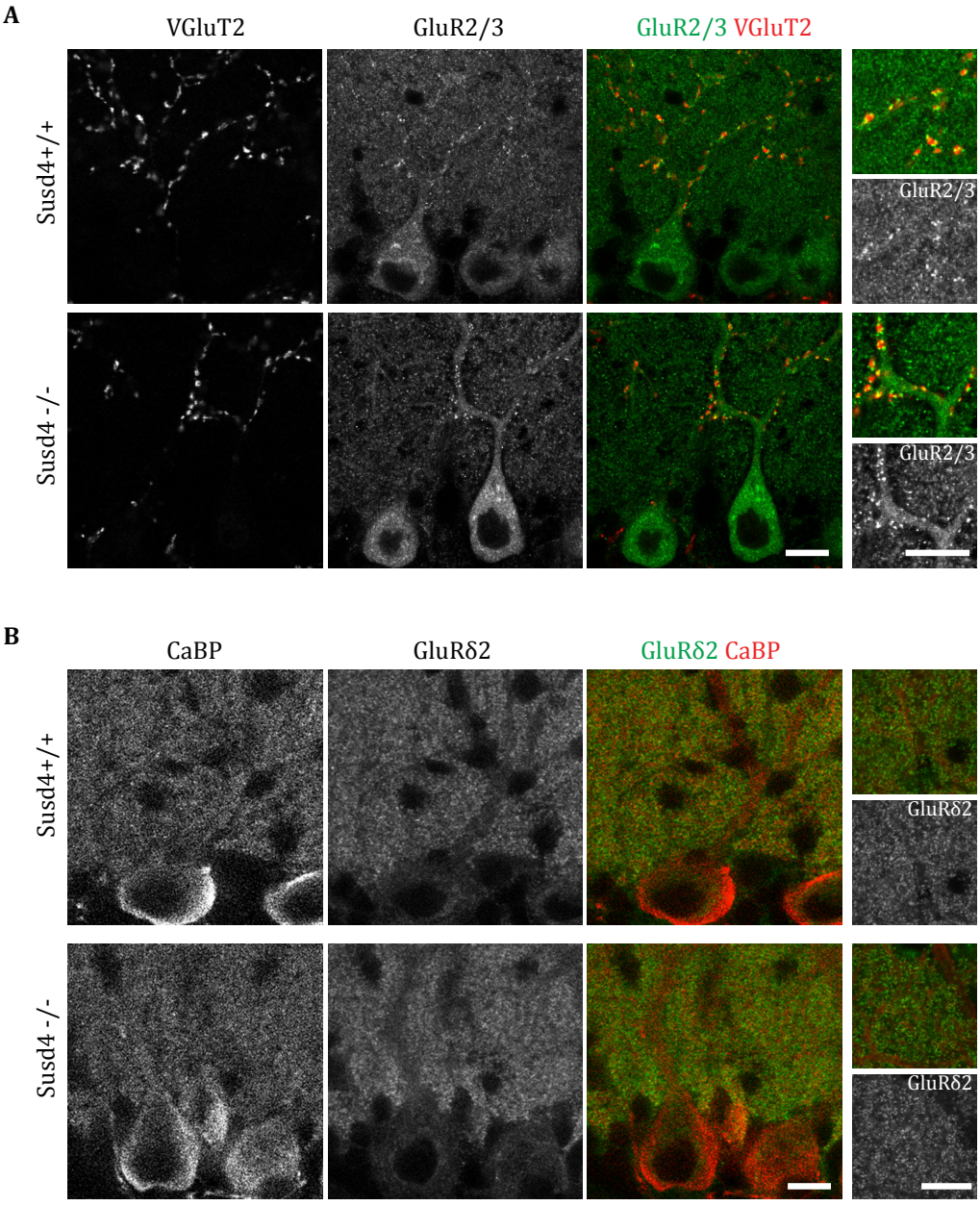


**Figure 8. No obvious morphological defects in postsynaptic receptor localization at Climbing fiber and Parallel fiber synapses**

**(A)** Defects in Climbing fiber postsynaptic AMPA receptor GluR2/3 were assessed in Susd4 KO and WT mice aged 1 month by co-immunostaining for CF presynaptic marker vesicular glutamate transporter 2 antibody (VGluT2) and postsynaptic GluR2/3. Scale bar, 10μm. Magnified images of GluR2/3 puncta surrounding VGluT2 in inset. Scale bar, 10μm **(B)** Defects in Parallel fiber postsynaptic receptor GluRδ 2 were assessed in Susd4 KO and WT mice aged 1 month by co-immunostaining for PF presynaptic marker vesicular glutamate transporter 1 antibody (VGluT1) and postsynaptic GluRδ2. Scale bar, 10μm. Magnified images of GluRδ2 puncta. Scale bar, 10μm. N=3 animals.

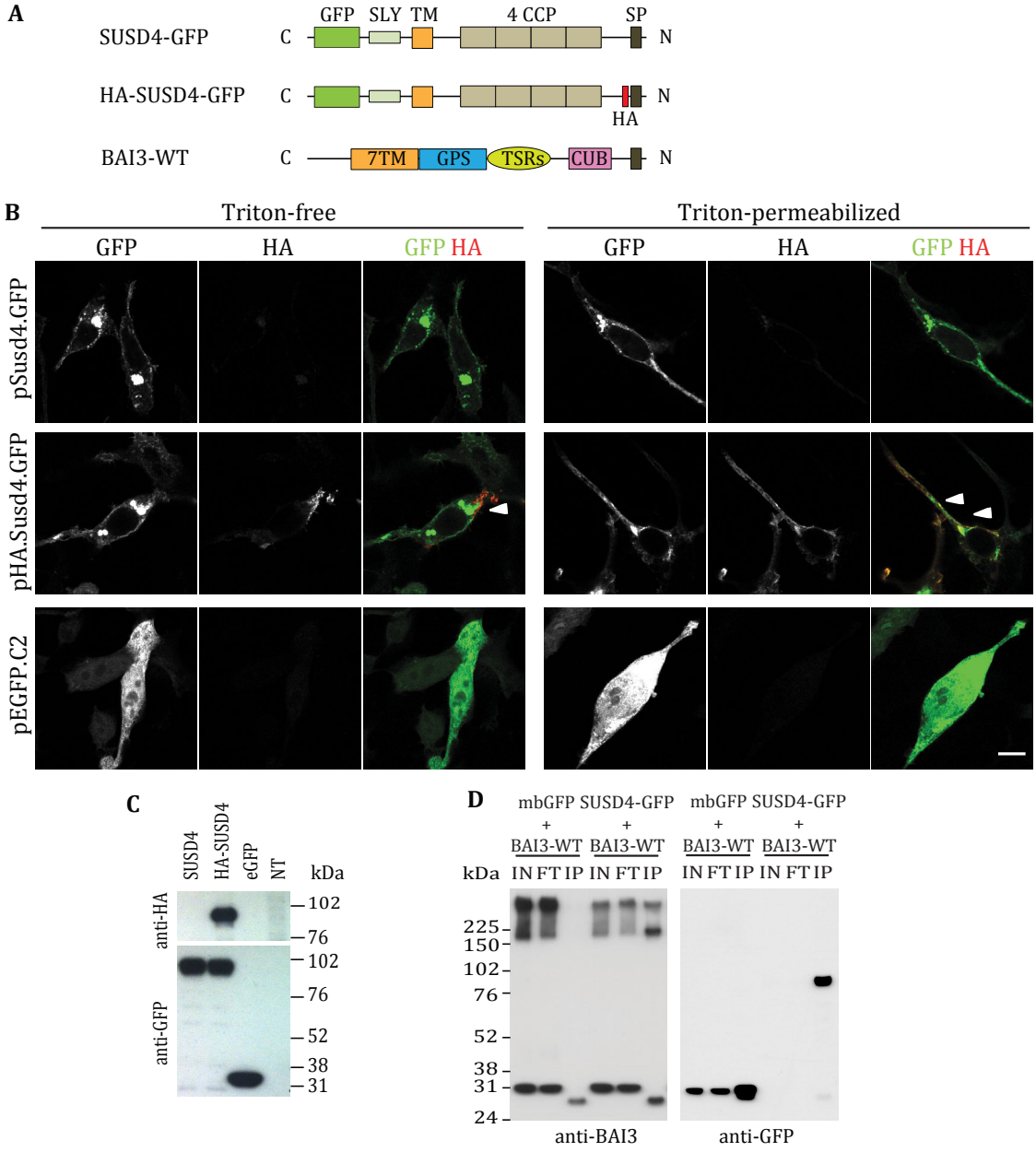


**Figure 9. Membrane-bound SUSD4 interacts with Purkinje cell receptor adhesion-GPCR BAI3 in vitro**

**(A)** Different expression constructs used for SUSD4 and BAI3. SUSD4 is a 490 aa, membrane-bound protein with a short intracellular sequence and a large extracellular region. For expression in HEK cells, an HA tag was added at the N-ter position, and a GFP tag at the C-ter (HA-SUSD4-GFP). SLY, lymphocyte signaling adaptor; TM, transmembrane; CCP, complement control protein; SP, Signal Peptide; GPS, GPCR proteolysis site; TSR, thrombospondin repeat; CUB, C1r/C1s, Uegf, BMP1 **(B)** Immunostaining of HEK-293H cells transfected with SUSD4-GFP, HA-SUSD4-GFP. HA-tagged construct detected with an antibody against HA, without (left) and with (right) triton permeabilization. Arrows denote surface staining of SUSD4, as detected by anti-HA antibody. Scale bar, 10µm **(C)** Western blot of HA-SUSD4-GFP-transfected HEK cells lysate, using antibodies against HA (left) or GFP (right). **(D)** Affinity-purification of SUSD4 from transfected HEK293 cell extracts using an anti-GFP antibody followed by immunoblot analysis with anti-GFP, anti-BAI3 antibodies. IN: input. FT: flow through. IP: immunoprecipitate.

# DISCUSSION

## Summary of main results

Synapse formation occurs in a very precise and coordinated manner between neurons whose cell bodies are either in close proximity or far apart. The proper formation of a synapse involves large arrays of receptors, soluble factors and signaling molecules that trigger the assembly of pre- and postsynaptic specializations. The fate of an assembled synapse is determined by synaptic activity that either stabilizes or eliminates the synapse, during development as well as in the adult brain (Lichtman & Colman, 2000; Stevens et al., 2007; Shatz, 2009). Therefore, structural and functional development of a synapse are intricately coupled processes and equally important for the proper formation of neural circuits.

Each neuron receives synapses from multiple types of afferents with specific morphological and physiological properties. The subcellular connectivity of the presynaptic afferent on the postsynaptic partner occurs in a very specific manner such that no two incoming afferents select the same subcellular domain for innervation. These patterns of connectivity are stereotyped for each type of neuronal population and the mechanisms that ensure the specificity of these connections are still poorly understood. Using the olivo-cerebellar network as a model system, we provide novel insights into the molecular mechanisms that regulate the formation and specific connectivity of two excitatory synapses formed on the same target neuron.

1. In the olivo-cerebellar network, two excitatory synapses are made by Parallel fibers and Climbing fibers that converge on their target, the Purkinje cells. Within this work, I characterized the differences in the gene expression profiles of the presynaptic input cell populations, the Granule cells and Inferior Olivary Neurons, highlighting those that could contribute to determine synapse specificity. A high diversity is observed in the differentially expressed genes coding for membrane and secreted proteins, in particular those that belong to immune system-related pathways. This diversity is apparent at both input cell populations, but Inferior Olivary Neurons are characterized by a greater complexity since they express many more specific genes belonging to this category. Moreover, a specific combination of complement-related genes is expressed by each input cell population in a pattern that coincides with the timing of synaptogenesis in the olivo-cerebellar network. This suggests that the complement-related genes contribute to a potential “chemoaffinity code” that defines the identity of each excitatory synapse in the olivo-cerebellar network.

2. Two complement-related proteins, namely C1QL1 and SUSD4, specifically expressed by the Inferior Olivary Neurons mediate different aspects of Climbing Fiber/Purkinje cell synaptogenesis. Secreted C1Q-related protein C1QL1 promotes Climbing fiber synaptogenesis and plays an instructive role in specifying Climbing fiber innervation territory on Purkinje cells. Input specificity of C1QL1 in the form of its restricted expression in the Inferior Olivary Neurons is necessary but not sufficient to maintain the Climbing fiber innervation territory. The second complement-related protein, membrane-bound sushi domain containing protein 4 (SUSD4) promotes the stabilization and functional maturation of CF/PC synapses, potentially through its interaction with Purkinje cell receptor Brain Angiogenesis Inhibitor 3 (BAI3), an adhesion-GPCR. The loss of SUSD4 in a knockout mouse model results in slower Climbing fiber synapse transmission, and long lasting motor coordination defects. C1QL1 is a high affinity ligand for BAI3 (Bolliger et al., 2011; Kakegawa et al., 2015) and SUSD4 interacts with gC1Q domain *in vitro* (Holmquist et al., 2013). Taken together, it is likely that SUSD4, C1QL1 and BAI3 constitute a complement-related synaptic scaffold machinery that promotes the formation, stabilization and specificity of the Climbing fiber/Purkinje cell synapse.

## Perspectives

### Understanding the molecular diversity of excitatory synapses in the olivo-cerebellar network

The transcriptome reflects the genes that are being actively expressed in a cell and provides an overview of the key molecular pathways and biological properties of the cell. Using the bacTRAP strategy and microarray data, I showed that a high diversity of genes coding for membrane and nuclear proteins are found in both the ION and GC. However, the IONs are more complex in the diversity of genes coding for membrane and secreted proteins while the GCs are more complex in the diversity of genes coding for nuclear proteins and transcription factors. These overall differences between the molecular composition of the ION and GC are likely to be reflective of differences in the developmental profiles and range of connectivity of the CF and PF afferents.

CF synaptogenesis is a more complex and dynamic process compared to PF synaptogenesis. Clusters of inferior olivary neurons project to narrow parasagittally-oriented strips of cerebellar cortex (Groenewegen & Voogd, 1977) and these strips represent functional compartments (Oscarsson, 1979). This topographic organization of

connectivity is dependent on molecular cues and starts to be established as early as embryonic stage E15/16 (Wassef et al., 1992; Paradies & Eisenman, 1993). A second step in CF synaptogenesis leads to refinement of connectivity through synapse elimination. During development, each PC receives multiple CFs that innervate the PC soma (Crepel et al., 1976; Hashimoto & Kano, 2003). During a period of postnatal synapse elimination between P7 and P21, each PC becomes innervated by 1 CF that undergoes dendritic translocation, a process that is unique to the CFs in the cerebellar cortex (Crepel et al., 1976; Chédotal & Sotelo, 1992). Each CF varicosity establishes synaptic contacts with clusters of 4-6 thorny spines protruding from the smooth surface of the proximal Purkinje cell dendrites (Palay & Chan-Palay, 1974) and each CF makes a total of several 100 synaptic contacts generating a complex spike with an all or none response (Isope & Barbour, 2002). In contrast, PF/PC synaptogenesis occurs only during the second and third postnatal weeks (Sotelo, 1990). The spiny branchlets on the Purkinje cell distal dendrites are contacted by almost 150,000 synapses, each synapse being made by a single PF emerging from a single granule cell (Harvey & Napper, 1991). Granule cells are generated in the cerebellum, migrate in bulk through the PC layer and start making contacts with PCs through PFs which grow orthogonally across Purkinje cells (Komuro et al., 2001; Kumada et al., 2009). Each PF makes only 1 “en passant” synapse with a given PC, contributing to simple spike generation. Moreover, 85% of these PF synapses are silent (Isope & Barbour, 2002). The remodeling events such as surplus CF elimination and strengthening of the winning CF begin before the onset of PF/PC synaptogenesis (Crepel, 1982). In our bacTRAP data, the ION was enriched with a number of axon-target recognition molecules including members of classic guidance molecule families such as semaphorins (Eg. SEMA4F) and ephrinA (Eg. EPHA4), and other CAMs like cadherins (Eg. CDH9) and protocadherins (Eg. PCDH20). Some of these proteins like the Eph-Ephrin system have already been established as molecules essential for ION axon guidance (Chedotal et al., 1997). In this regard, adhesive functions mediated by membrane and secreted proteins could be more important at the ION to aid in the axon-target recognition and ascendance of CFs up the cerebellum from the brainstem to establish their synaptic territory on PCs.

Both the ION and GC express genes coding for homeobox proteins and proteins involved in transcription regulation, DNA binding and metal ion binding. However, the GCs are unique in expressing genes involved in chromatin modification processes such as acetylation and methylation. Nuclear migration and organization are processes crucial for the proliferation and differentiation of cells. This could explain the importance of enriched

nuclear genes in the GCs since the normal generation and migration of cerebellar GC precursors are necessary for normal PF/PC synaptogenesis (Komuro et al., 2001; Kumada et al., 2009). Moreover, chromatin-modifying genes are known to mediate long-term plasticity and memory storage at synapses by histone acetylation processes and gene silencing (Kandel, 2000; Barrett & Wood, 2008). Since up to 85% of GC-originating PF/PC synapses are "silent" without generating detectable electrical responses (Isope & Barbour, 2002), epigenetic mechanisms mediated by chromatin modification could play an important role in this cell population. Transcription regulation factors such as Wnts are another class of secreted molecules that promote synaptogenesis. As expected, Wnt7a was found in our GC transcriptome, as it is involved transiently in cerebellar glomerular development *in vivo* (Hall et al., 2000). In hippocampal cultures, Wnt7a increases synaptic vesicle clustering and mEPSC frequency without altering postsynaptic properties (Cerpa et al., 2008). Wnts are also known to contribute to synapse specificity. In C. elegans, Wnts act as anti-synaptogenic factors, and spatially regulate the patterning of synaptic connections by subdividing an axon into discrete domains, creating regions that inhibit synaptogenesis (Klassen & Shen, 2007). Thus, the high percentage of transcription factors enriched in the GC transcriptome could contribute to mechanisms promoting synapse specificity, possibly through the regulation of transcription.

An unexpected result of our study is that genes belonging to immune system pathways are significantly enriched in the ION compared to GCs. However, both cell populations express a variety of genes belonging to cytokine signaling pathways. All the cytokines expressed by IONs are pro-inflammatory, a majority of which are regulated by IFN-γ and TNF. In contrast, all the cytokines expressed by GCs are anti-inflammatory, and regulated by TGFβ. A highly dynamic balance exists between pro- and anti-inflammatory cytokines and this signaling can result in diverse outcomes, such as an increased, cascaded or decreased, truncated expression of membrane proteins, proliferation, and/or secretion of effector molecules. To add to this complexity, the result of cytokine signaling depends on a complex network of feedback loops. This type of signalling could provide key control of the molecular signature of each PC excitatory input and contribute to synapse specificity. For example, pro-inflammatory cytokines IFN-γ and TNF-α regulate MHC-I expression, and are already known to mediate different aspects of synaptogenesis. In the adult mammalian visual cortex, TNF-α mediates synapse plasticity by promoting synapse elimination (Kaneko et al., 2008) and MHC-I also has effects on synaptic plasticity and activity-dependent remodeling of the retinogeniculate system (Huh et al., 2000). IFN-γ is found at

neuronal synapses (Vikman et al., 1998), and in an IFN-γ knockout mouse model, the resulting decrease in MHC-I and β2m expression affects synapse elimination in the spinal cord (Victório et al., 2012). In this manner, cytokine signaling could control the expression of a specific combination of proteins that are related to synapse formation or maturation.

Further, it is often difficult to make generalizations about the roles of individual cytokines due to their frequently redundant and functional pleiotropic effects. For example, mice deficient in the chemokine receptor CXCR4 display abnormalities in the architecture of the cerebellum, characterized by premature migration of granule cell precursors from the external to the internal granular layer, a process that normally does not occur until after birth, and abnormal clustering of neurons despite the presence of intact radial glia (Zou et al., 1998). Given that chemokines often act as chemotactic molecules for immune cells (Ransohoff et al., 2007), their effect on neuronal migration in the nervous system may not be all that surprising. Thus, cytokines may also play a role in generating specificity by mediating the target recognition of migrating neurons.

Our study has identified an input-specific molecular code corresponding to the set of specific genes expressed by each input. Analysing the functional roles of select candidate genes has shown that at least part of this input-specific code plays a role in controlling the specific connectivity of the corresponding synapse on the target neuron, here Purkinje cells. As a next step, it would be interesting to compare the input cell transcriptome with that of the target cell. The PC transcriptome obtained from the Pcp2 bacTRAP adult transgenic mouse line, has already been characterized by the Heintz laboratory at Rockefeller University (Doyle et al., 2008). A comparison between the PC transcriptome and the input ION and GC transcriptomes would help in the identification of homophilic and heterophilic interactions between the input and target cell types that could contribute to synapse specificity. For example, GCs express NRXN3 and their interacting partner NLGN3 is found in the PC transcriptome. Nectin-2 is found in both the ION and PC transcriptomes. Moreover, the target PC population could express regulators that could modulate molecules expressed in the input cell populations. Indeed the bacTRAP data show that PCs express TGF-β1, a molecule which we identified as a key regulator of a majority of the GC-specific immune system-related genes, and IFNGR2 and IL-18 that induce IFN-γ signaling, a pathway that is over-represented in the ION. Finally, comparing the input and target gene expression profiles could identify ligand/receptor couples that are specific to each synapse. Using mice that are genetically engineered to facilitate the purification of the PF/PC synapse, a detailed proteomic analysis has identified about 60

proteins specific to the PF/PC postsynaptic density (Selimi et al., 2009). This study exploited the specific localization of GluRδ2 at the PF/PC postsynaptic density to develop transgenic mice that express an affinity tag only at the PF/PC synapse. Similarly, the identification of a postsynaptic receptor specific to the CF synapse will enable the application of the synaptic protein profiling strategy and characterization of the CF/PC synapse at the proteomic level. Together, these data would allow us to extend our vision from an input-specific molecular code to a synapse-specific code, and provide a comprehensive description of the molecular composition and key signaling mechanisms that are orchestrated at the CF/PC synapse.

## C1QL/BAI3, a general mechanism for the development of functional neural circuits

In comparison to the Cbln subfamily, the *in vivo* functional roles of the C1ql subfamily are only beginning to be understood. C1QL1 was initially demonstrated to be an inhibitor of synaptogenesis since incubating primary hippocampal neurons with low concentrations of C1QL1 led to a decrease in the density of excitatory synapses (Bolliger et al., 2011). Further, C1QL proteins are high affinity ligands for BAI3, and their *in vitro* inhibitory effect on synaptogenesis was blocked by the addition of a TSR-containing fragment of BAI3 (Bolliger et al., 2011). In contrast with this result, we have shown that C1QL1 and BAI3 are promoting CF/PC synaptogenesis. In particular, the more pronounced effect of C1QL1 knockdown during development is an impairment in the ability of translocated CFs to form synaptic contacts, as is evidenced by a reduction in the extent of CF innervation territory at P14. Since the *in vivo* injection site was located outside of the cerebellum, these results demonstrate a cell autonomous effect of C1QL1. Moreover, our study identified a role for C1QL1 in being necessary but not sufficient to control the identity and specificity of the CF synapse. The group of Yuzaki et al. studied the same process using knockout and over-expression approaches for each of these proteins (Kakegawa et al., 2015). Their results show that C1QL1 regulates the specification of the "winning" Climbing fiber through an interaction with the CUB domain of BAI3. *Bai3*-null mice phenocopy *C1ql1*-null mice, in that, less dominant and weak CFs around the PC soma do not undergo synapse elimination and instead translocate to PC dendrites because the dominant CF is not specified and strengthened enough to prevent this process. This phenotype is rescued by expression of C1ql1 in the ION of adult *C1ql1*-null mice, and Bai3 in the PCs of adult *Bai3*-null mice, wherein the single-winner CF emerges by promoting the

maturation of the dominant CF and eliminating less dominant weak CFs (Kakegawa et al., 2015). This appears divergent from our study, where the *in vivo* knockdown of C1QL1 during development at postnatal day 4 does not affect the specification of the "winning" CF and only has a small but significant decrease in the CFs ability to undergo dendritic translocation as is observed at P9, the stage when translocation of the winning CF begins (Crepel, 1982; Chédotal & Sotelo, 1992; Hashimoto et al., 2009a). This discrepancy could be due to the difference in the types of approaches: our approach uses knockdown starting at P4, while Kakegawa et al. analyse full knockout mice for C1QL1. C1QL1 could possibly have an age-specific dual role, in the specification of the "winning" CF before P4, and in synapse formation and specificity after P4. It also remains to be tested whether the effect on synapse elimination is direct or not: if C1QL1 is essential for synapse formation and stability, then the "winning" climbing fiber might remain as weak as the others and never initiate synapse elimination. Taken together, these data confirm that C1QL1 is critical for normal CF synaptogenesis.

Given the broad expression of C1QL and BAI proteins in the developing mouse brain, this suggests a general role for their signaling pathway in regulating synapse specificity in other neural circuits with subcellular segregation of synaptic input. For example, in the hippocampus, mossy fiber afferents from the dentate gyrus contact pyramidal cells on thorny excrescences close to the soma, whereas entorhinal afferents connect to distal portions of the dendrites (Bayer, 1985). Other C1QL family members, C1ql2 and C1ql3 are strongly expressed by the dentate gyrus of the hippocampus, while Bai3 is strongly expressed by the cerebellar Purkinje cells, hippocampus and cortex (Sigoillot et al., 2015). These molecular complexes could thus be involved in controlling the specificity of inputs on the hippocampal pyramidal cells through interaction with the BAI3 receptor.

### CCP domain of SUSD4, a potential synaptic scaffold at excitatory synapses

In the present study, we demonstrate a role for CCP-containing SUSD4 in the stabilization and function of Climbing fiber synaptic contacts on cerebellar Purkinje cells, possibly through its interaction with the BAI3 receptor expressed by Purkinje cells. In the olivo-cerebellar network, *Susd4* mRNA expression is detected in the ION and in PCs. The loss of SUSD4 in the knockout mouse model results in slower Climbing fiber synapse transmission. Given previous data on the functional roles of complement control-related proteins (Gendrel et al., 2009), it is likely that SUSD4 mediates CF synapse transmission

through a postsynaptic role. For example, in the *C. elegans* NMJ, secreted CCP-containing LEV-9 is crucial for clustering L-AChRs at cholinergic synapses. We showed that SUSD4 can interact with the postsynaptic receptor BAI3. Interestingly, the TSR1 domains found in BAI3 are also found in Ce-punctin, an ADAMTS-like secreted protein that exists in two isoforms that control the proper localization of cholinergic and GABAergic synapses at the NMJ (Gendrel et al., 2009; Pinan-Lucarré et al., 2014). Given that BAI3 specifies Climbing fiber innervation territory on Purkinje cells through its interaction with C1QL1 (Kakegawa et al., 2015; Sigoillot et al., 2015), it is possible that the protein domains of SUSD4 and BAI3 constitute a synaptic scaffold that stabilizes the Climbing Fiber synaptic contacts by clustering postsynaptic receptors.

It is important to emphasize that our functional analyses were carried out in the constitutive SUSD4 mutant, characterized by the deletion of SUSD4 from both the ION and PCs. Thus, one cannot exclude the possibility of a presynaptic role for SUSD4 in CF/PC synapse maturation and maintenance. This can be assessed by deleting the expression of SUSD4 from the ION of adult mice by knockdown experiments. Alternatively, to confirm a postsynaptic role for SUSD4, we can check whether the morphological and functional deficits in CF/PC synapses are rescued by expressing SUSD4 in the Purkinje cells of SUSD4-null mice.

Scaffold-mediated receptor clustering at postsynaptic sites is a key element of synaptic transmission and the activity of scaffold proteins can be regulated by several post-translational mechanisms including phosphorylation and degradation (Kim & Sheng, 2004). Generally, functional AMPARs are tightly associated with and regulated by accessory proteins including the Stargazin family of transmembrane AMPA regulatory proteins (TARPs) (Chen et al., 2000). The TARPs family of transmembrane proteins recruits AMPA receptors at excitatory synapses via vesicle trafficking and also modulates the gating of the receptors (Milstein & Nicoll, 2008). The work herein indicates a potential role for SUSD4 in mediating postsynaptic AMPA receptor clustering through an interaction with the BAI3 receptor on PCs. Scaffold molecules that form glutamatergic PSDs, such as the TARP family of proteins, are characterized by the canonical PDZ protein-protein interaction domains. SUSD4 has a long extracellular region with only one transmembrane domain, compared to TARPs that have four transmembrane domains and specifically interact with AMPA receptors through PDZ binding domains (Tomita et al., 2003). Contrary to TARPs, SUSD4 appears to play its role indirectly through the binding of BAI3 via CCP domains. Given the structural similarity between CCP and CUB domains, it is perhaps not

surprising that SUSD4 biochemically interacts with BAI3 that contains CUB and TSR domains. Further, BAI3 also regulates Purkinje cell dendritic arborisation via reorganization of the actin cytoskeleton through activation of the RhoGTPase Rac1 and ELMO1, a key Rac1 regulator (Lanoue et al., 2013), suggesting that SUSD4 could contribute to the modifications of the postsynaptic actin cytoskeleton.

## Significance of results in the current model of synapse formation and specificity

### Complement family of proteins part of a molecular synaptic code?

A large number of studies in both vertebrate and invertebrate nervous systems have shown that the specificity of synapses depends on multiple mechanisms, including homophilic and heterophilic interactions between adhesion molecules, secreted synaptic organizers, interactions with guidepost/scaffold cells, temporally restricted expression of transcription factors, and neuronal activity (Sanes & Yamagata, 2009). In this regard, the olivo-cerebellar network is an ideal model system to understand subcellular synapse organization on a common target neuron. The axon targeting and subcellular localization of each inhibitory afferent formed on cerebellar Purkinje cells is controlled by different adhesion proteins from the L1CAM Ig subfamily, namely CHL1 and Neurofascin (Ango et al., 2004; 2008). The specific innervation of basket cell axons occurs by the recruitment of L1CAM member Neurofascin by ankyrinG, a membrane adaptor protein that is restricted to the AIS of Purkinje cells. On the other hand, the formation of stellate cell synapses depends on CHL1, another member of the same family of adhesion molecules, localized along Bergmann glia fibers. In both cases, the control of specific targeting occurs either by an external guidepost or by domains on the postsynaptic site. This is similar to the neuromuscular junction, where recognition molecules such as laminins, collagens and proteoglycans associated with the basal lamina of the muscle fiber act as recognition domains for the incoming motor axons and guide their specific subcellular innervation (Fox et al., 2007). Likewise, the lamina specific innervation of hippocampal CA3 pyramidal neurons is maintained by inhibitory Semaphorin-6A and restrictive Plexin-A2 signals on the target pyramidal neuron (Suto et al., 2007). All these evidences do not exclude the fact that different presynaptic binding partners could also contribute to the specificity of synaptic connectivity and differential synaptic functional properties. For example, the binding of postsynaptic LRRTMs or neuroligins to presynaptic neurexin is mutually

exclusive and suggests that these ligands compete for neurexin binding (Siddiqui et al., 2010). β-NRXN-induced clustering of neuroligins results in co-clustering of NMDARs but not AMPARs (Graf et al., 2004), and NLGN-1 knockout mice have decreased NMDAR but not AMPAR-dependent synaptic transmission (Chubykin et al., 2007). Whereas, lentiviral-mediated knockdown of LRRTM2 in hippocampal granule cells *in vivo* strongly reduces evoked NMDAR as well as AMPAR-mediated transmission compared to neighboring uninfected cells (De Wit et al., 2009). These data show that presynaptic NRXN isoforms could influence sub-type specific synaptic properties by preferential interaction with specific postsynaptic NLGN and LRRTM proteins. Our results suggest that the segregation of synaptic inputs on the same target neuron is defined by an underlying difference in the molecular profiles at the presynaptic level. Originally identified at the PF/PC PSD, BAI3 is now seen to promote synaptogenesis of both the CF and PF excitatory synapses on PCs (Selimi et al., 2009; Sigoillot et al., 2015). However, the molecular composition of presynaptic inputs lends a synapse-specific identity. Secretion of different members of the complement C1q family by the incoming excitatory afferents controls the specific innervation of the corresponding synapses on Purkinje cells. This strengthens the idea that each type of connection possesses a specific synaptic identity, a concept that albeit suggested by Sperry in 1963 and others, has never been formally proven until now. Thus, it is interesting to extrapolate this feature to other neural circuits with segregation of synaptic inputs on a common target, such as the dorsal cochlear nucleus that is innervated by Parallel fibers and auditory nerve fibers (Hirsch & Oertel, 1988) as well as the whisker-to-barrel cortex system, where a single barreloid in the ventroposterior medial nucleus (VPM) of the thalamus receives connections from lemniscal fibers and corticothalamic inputs on distinct target sites on the head and core of the VPM barreloid (Hoogland et al., 1987).

Membrane-bound and secreted adhesion proteins are known to play a role in the formation, maturation and function of synapses. These synaptic organizers exist in great diversity and their functions are complex depending on their localization at the synapse and interacting partners. Large-scale proteomic analyses of the postsynaptic density of the mouse brain suggest that anything from 200 to over a 1000 different proteins reside at the excitatory PSD (Collins et al., 2006). This supports the proposed idea that different combinations of molecules encode the specificity of neuronal connections, implying the existence of a ‘‘molecular synaptic code.’’ This is best illustrated by the complex organization of neuroligins at inhibitory synapses (Sassoè-Pognetto et al., 2011). NLGN2 is

present in nearly all inhibitory synapses throughout the brain, whereas other NLGN isoforms have a more restricted distribution. NLGN3 is expressed with NLGN2 in subsets of GABAergic synapses (Patrizi et al., 2008) and NLGN4 is mainly associated with glycinergic synapses (Hoon et al., 2011). Thus the differential localization of neuroligins may be responsible for the variability in synaptic properties of individual synapses. Moreover, the differential interactions of neurexin variants with NLGNs, CBLN1 and LRRTMs may be involved in specifying distinct types of excitatory and inhibitory synapses. CBLN subtypes exert synaptogenic activities in cortical neurons by differentially interacting with NRXN variants containing a variant at splice site S4. In contrast to NLGN1, CBLN1 and CBLN2 preferentially induce inhibitory presynaptic differentiation in cortical cultures (Joo et al., 2011). Thus, synapse specificity is likely to be encoded by multiple interactions between distinct combinations of synaptogenic molecules rather than a single unique ligand-receptor couple. Given that we find a distinct combination of complement proteins at each excitatory input innervating the cerebellar Purkinje cell, it is interesting to speculate whether a similar combinatorial expression of complement proteins occurs at inhibitory synapses.

## Potential evolutionarily conserved synaptic scaffold domain and function

An evolutionary study of synapse proteomes suggests that there has been a great expansion in the number of proteins present at the mammalian postsynaptic density compared to those of *Drosophila* and other invertebrates (Emes et al., 2008). This, combined with the enormous molecular diversity at synapses, highlights the potential for tremendous complexity in the vertebrate CNS. For example, complement control related proteins have roles in the regulation of the complement cascade as well as in neural development in both vertebrates and invertebrates. In vertebrates, CCP-containing proteins SUSD2 and SRPX2 regulate excitatory synapse numbers in the hippocampus and cortex respectively (Sia et al., 2013; Nadjar et al., 2015). Similar to scaffold proteins like MAGUK, Shank and Homer, CCP domains are found starting in unicellular protozoan choanoflagellates (King et al., 2003; Emes et al., 2008). Interestingly, even though the complement system is absent in protostomes, a role for complement control-related proteins in synapse formation and function have been described in *C.elegans* (Gendrel et al., 2009). This suggests a primary and evolutionarily conserved role for CCP-containing proteins in synapse development, followed by the expansion of its roles in immune functions in higher vertebrates (Nadjar et al., 2015).

In our study, the Climbing fiber synaptic machinery comprising BAI3, SUSD4 and C1QL1 reveals striking parallels with the *C.elegans* NMJ synaptic scaffold proteins. At the *c. elegans* neuromuscular cholinergic synapses, Ce-Punctin, an ADAMTS-like secreted protein, controls the proper localization of L-Ach-R clusters, while LEV-9, a complement control related protein, requires proteolytic cleavage at an evolutionarily conserved site to promote aggregation of L-AchR receptors (Gendrel et al., 2009; Briseno-Roa & Bessereau, 2014; Pinan-Lucarré et al., 2014). In the mouse, C1QL1/BAI3 signaling controls the localization of CF/PC synapses while SUSD4 controls the functional maturation and stabilization of synapses possibly through an effect on postsynaptic receptors. Ce-Punctin and BAI3 share common thrombospondin (TSR) repeats, while LEV-9 and SUSD4 share common CCP domains. The addition of the C1q domain containing family of proteins in mammals would help increase the diversity of potential synaptic complexes in correlation with the increased synapse diversity found in mammals.

# ANNEXE

## 1. The adhesion-GPCR BAI3, a gene linked to psychiatric disorders, regulates dendrite morphogenesis in neurons.

Vanessa Lanoue[1,2,3,4 *], Alessia Usardi[1,2,3 *], Séverine M. Sigoillot[1,2,3*], Maëva Talleur [1,2,3], Keerthana Iyer[1,2,3], Jean Mariani[4,5], Philippe Isope[6], Guilan Vodjdani[7], Nathaniel Heintz[8], Fekrije Selimi[1,2,3 ‡]

[1]Center for Interdisciplinary Research in Biology, Collège de France, Paris, F-75005, France;

[2]CNRS, UMR 7241, Paris, F-75005, France; INSERM, U1050, Paris, F-75005, France;

[3]PSL Research University, Paris, 75005, France ;

[4]UMR7102, UPMC, CNRS, 75005 Paris, France ;

[5]Institut de la Longevité, Hôpital Charles Foix, Ivry sur Seine 94200, France;

[6]INCI, CNRS UPR3212, Strasbourg, France;

[7]CRICM, UPMC/Inserm UMR_S975/CNRS UMR7225, 75013 Paris, France;

[8]Laboratory For Molecular Biology, The Rockefeller University, NY, USA;

[‡] Correspondence to Dr. Fekrije Selimi, Collège de France, CIRB, 11 Place Marcelin Berthelot, 75005 Paris, France, tel: +33 144271654, fax: +33 144271691, fekrije.selimi@college-de-france.fr

[*]These authors contributed equally to this work.

OPEN

Molecular Psychiatry (2013) 18, 943–950

www.nature.com/mp

ORIGINAL ARTICLE

# The adhesion-GPCR *BAI3*, a gene linked to psychiatric disorders, regulates dendrite morphogenesis in neurons

V Lanoue[1,2,3,4,5,10], A Usardi[1,2,3,4,10], SM Sigoillot[1,2,3,4,10], M Talleur[1,2,3,4], K Iyer[1,2,3,4], J Mariani[5,6], P Isope[7], G Vodjdani[8], N Heintz[9] and F Selimi[1,2,3,4]

Adhesion-G protein-coupled receptors (GPCRs) are a poorly studied subgroup of the GPCRs, which have diverse biological roles and are major targets for therapeutic intervention. Among them, the Brain Angiogenesis Inhibitor (BAI) family has been linked to several psychiatric disorders, but despite their very high neuronal expression, the function of these receptors in the central nervous system has barely been analyzed. Our results, obtained using expression knockdown and overexpression experiments, reveal that the BAI3 receptor controls dendritic arborization growth and branching in cultured neurons. This role is confirmed in Purkinje cells *in vivo* using specific expression of a deficient BAI3 protein in transgenic mice, as well as lentivirus driven knockdown of BAI3 expression. Regulation of dendrite morphogenesis by BAI3 involves activation of the RhoGTPase Rac1 and the binding to a functional ELMO1, a critical Rac1 regulator. Thus, activation of the BAI3 signaling pathway could lead to direct reorganization of the actin cytoskeleton through RhoGTPase signaling in neurons. Given the direct link between RhoGTPase/actin signaling pathways, neuronal morphogenesis and psychiatric disorders, our mechanistic data show the importance of further studying the role of the BAI adhesion-GPCRs to understand the pathophysiology of such brain diseases.

*Molecular Psychiatry* (2013) **18,** 943–950; doi:10.1038/mp.2013.46; published online 30 April 2013

**Keywords:** adhesion-GPCR; dendrite; morphogenesis; ELMO1; BAI3; Purkinje cell

## INTRODUCTION

The increased complexity of behaviors that appeared during evolution has been correlated with an increased molecular complexity of upstream signaling membrane proteins.[1] Genetic studies have linked mutations and copy number variations in genes coding for these upstream signaling pathways with many psychiatric and neurodevelopmental diseases, such as autism and schizophrenia. Deciphering these signaling pathways and how they regulate the formation of a functional neuronal network in mammals will thus help understand their contribution to brain diseases.

The Brain Angiogenesis Inhibitor (BAI) family is part of the poorly understood family of adhesion-G protein-coupled receptors (GPCRs).[2] Adhesion-GPCRs are unique in that they contain a very long extracellular domain with multiple modules potentially conferring adhesive and recognition properties. The few studies of those receptors have shown their roles in physiology, including in the central nervous system, and pathology. For example, CELSR3 deficiency leads to abnormal neuronal migration, defects in tract development and reduced dendritic development.[1,3–5] Mutations in the adhesion-GPCR GPR56 lead to deficits in neuronal migration in patients with bilateral frontoparietal polymicrogyria.[6] The BAI proteins are highly expressed in the brain and have been identified at post-synaptic densities in the forebrain[7] and in the cerebellum.[8] These proteins have several structural features that suggest their potential involvement in the development of functional neuronal networks: their extracellular domain contains several thrombospondin type 1 repeats domains that could provide adhesive and recognition properties. A PDZ-binding domain in their C-terminus could enable their association with synaptic scaffolding proteins such as PSD95. Sequence analysis shows that this subfamily of adhesion-GPCRs has homologs only in vertebrates, and that these homologs are extremely well conserved (Supplementary Figure 1). The BAI proteins may thus have important functions in controlling the development of complex cognitive abilities that are specific to vertebrates. This is highlighted by the fact that BAI proteins could contribute to behaviors defective in psychiatric disorders: single nucleotide polymorphisms and copy number variations in the *BAI3* gene have been associated with schizophrenia,[9–11] bipolar disorder[12] and addiction,[13] and the *Bai2* knockout mouse has an anti-depressant phenotype.[14]

The regulation of dendrite morphogenesis in neurons is key to the formation of functional neuronal networks and is deficient in several neurodevelopmental disorders, such as autism, Fragile X syndrome or schizophrenia.[15–18] This process involves stabilization of dynamic filopodia through regulation of the actin cytoskeleton,[19] in particular by the modulation of RhoGTPases.[20,21] Direct interference with the activity of RhoGTPases, such as RAC1, or their guanylate exchange factor activators, such as Tiam1, betaPIX, kalirin and the ELMO1/DOCK180 complex, leads to defects in dendrite morphogenesis.[22–24] However, which upstream pathways coordinate RhoGTPases activation by integrating extracellular cues during dendrite morphogenesis is

[1]Center for Interdisciplinary Research in Biology (CIRB) , Collège de France, Paris, France; [2]CNRS, UMR 7241, Paris, France; [3]INSERM, U1050, Paris, France; [4]PSL Research University, Paris, France; [5]UMR7102, UPMC, CNRS, Paris, France; [6]Institut de la Longevité, Hôpital Charles Foix, Ivry sur Seine, France; [7]INCI, CNRS UPR3212, Strasbourg, France; [8]CRICM, UPMC/Inserm UMR_S975/CNRS UMR7225, Paris, France and [9]Laboratory For Molecular Biology, The Rockefeller University, New York, NY, USA. Correspondence: Dr F Selimi, Center for Interdisciplinary Research in Biology (CIRB), Collège de France, 11 Place Marcelin Berthelot, 75005 Paris, France.
E-mail: fekrije.selimi@college-de-france.fr
[10]These authors contributed equally to this work.
Received 16 May 2012; revised 21 February 2013; accepted 18 March 2013; published online 30 April 2013

not well understood. The BAI1 receptor regulates phagocytosis through the modulation of the ELMO1/DOCK180/RAC1 signaling pathway.[25] BAI1 interacts with ELMO1 through a motif conserved in BAI2 and BAI3, suggesting that the control of the small GTPase RAC1 through the ELMO1/DOCK180 module is a general feature of the BAI receptors and might be important for their role in the central nervous system. Here we show that the BAI3 protein controls dendritic arborization growth and complexity in neurons, partially through its interaction with ELMO1.

## MATERIALS AND METHODS

### BAI3 constructs, knockdown and transgenic mice

The BAI3-wild-type (WT) construct was cloned into the pEGFP-C2 vector from mouse cDNA clone no. BC099951. The Quikchange Site-Directed Mutagenesis kit (Agilent technologies, Santa Clara, CA, USA) was used to change the RKR sequence to AAA (residues 1431–1433) for the BAI3-WT-A construct. The BAI3-FLT construct codes for the entire BAI3 protein with an insertion of green fluorescent protein (GFP) after amino acid 1349. In BAI3-EMT, the cytoplasmic tail is replaced by GFP after amino acid 1174. The BAI3-SCT construct is a fusion between GFP and the cytoplasmic tail of BAI3 starting at amino acid 1166. The cDNA coding for BAI3-EMT was subcloned in the BamHI site of the L7/pcp2 promoter.[26] A HindIII fragment was then purified for microinjection in the male pronucleus of C57BL/6N oocytes (Institut Clinique de la Souris, Strasbourg, France). The small hairpin RNA (shRNA) sequence for BAI3 was: 5′-ggtgaagggagtcatttat-3′, and was subcloned under the H1 promoter in either pSUPER vector for transfection in cultured hippocampal neurons or in a lentiviral vector that also drives GFP expression.[27]

## RESULTS

### The adhesion-GPCR BAI3 modulates dendrite morphogenesis in neurons

The BAI3 receptor was found to localize to actin-rich cell protrusions, such as filopodia and lamelipodia in HEK-293H cells, and dendrites and filopodia in cultured DIV5 hippocampal neurons (Supplementary Figure 2). Moreover, quantitative reverse transcription PCR (qRT-PCR) analysis shows expression of the endogenous BAI3 in developing hippocampal neurons in culture (Supplementary Figure 3). Given these data and the fact that BAI1 regulates RAC1, a major modulator of actin function, and dendrite and spine morphogenesis, we hypothesized that the BAI3 receptor has a role in the regulation of the actin cytoskeleton and dendrite morphogenesis in neurons. We first used a RNA interference strategy to knockdown the expression of the BAI3 protein in cultured hippocampal neurons, a classical model for the study of signaling pathways controlling dendrite morphogenesis (Supplementary Figure 3). Our quantitative analysis showed a significant increase in total dendrite length per neuron after BAI3 knockdown compared with control conditions (Figure 1a). We also observed a tendency for an increased total number of dendrites per neuron following BAI3 knockdown due to a significant increase in the number of dendrites of order 2 and more. As BAI3 is highly expressed in cerebellar Purkinje cells *in vivo*, a neuronal type of exquisite complexity in terms of dendritic arborization, we tested BAI3′s role in this neuronal type by transducing cerebellar mixed cultures with a lentivirus driving the expression of a shRNA directed against BAI3 or the corresponding controls. Knockdown of BAI3 also increased dendrite length in Purkinje cells significantly (Figure 1b). Hence, the role of the BAI3 protein in dendrite morphogenesis is a general feature of this adhesion-GPCR that can be found in multiple neuronal types.

### BAI3 interacts with ELMO1, a regulator of RAC1 activity

Next we were interested in determining the signaling pathway used by the BAI3 receptor to control dendrite morphogenesis. The BAI1 receptor interacts with the N-terminal part of ELMO1, through an RKR motif present in its cytoplasmic tail[25] and conserved throughout the BAI family. To test whether BAI3 also binds ELMO1 through the same motif, we performed coimmunoprecipitation experiments using extracts of HEK-293H cells cotransfected with several tagged mutants of BAI3 and ELMO1 (Figure 2a). Using an anti-GFP antibody, we were able to affinity purify the wild-type form of BAI3 (BAI3-WT) from cells expressing ELMO1-GFP, but not from cells expressing soluble GFP, showing the specific interaction of BAI3 with ELMO1 (Figure 2a). This result was further confirmed by performing the reverse experiment in which we affinity purified different GFP-tagged forms of the BAI3 receptor and checked for the copurification of myc-tagged ELMO1. ELMO1-myc was coimmunopurified with the cytoplasmic tail of BAI3 (BAI3-SCT, soluble cytoplasmic tagged), but not with the mutant BAI3 receptor lacking the whole cytoplasmic domain (BAI3-EMT, extracellular membrane tagged). The interaction was reduced when using the full-length BAI3 with a GFP inserted in its cytoplasmic tail close to the RKR motif (BAI3-FLT, full length tagged), and totally abolished by mutagenesis of the RKR motif in the BAI3 protein (BAI3-WT-A). These results were further confirmed by immunofluorescence analysis and quantification, which showed that the colocalization of BAI3 with ELMO1 in actin-rich filopodia of transfected HEK-293H cells was dependent on the presence of the cytoplasmic tail of BAI3, and more particularly of the RKR motif (Figure 2b). Overall, these results show that ELMO1 interacts with the RKR motif located in the cytoplasmic tail of the BAI3 receptor.

### The BAI3 protein regulates cell morphogenesis, partly through binding of ELMO1

ELMO1 is part of the RAC1 guanylate exchange factor ELMO1/DOCK180[28] and BAI1 has been shown to regulate RAC1 activity through its binding to the ELMO1/DOCK180 module.[25] The modulation of dendrite morphogenesis mediated by BAI3 could thus be a result of the regulation of Rac1 activity. We tested this hypothesis using a classical *in vitro* assay, the cell-spreading assay,[28] which consists in measuring the spreading of transfected HEK-293H cells at different time points after plating on fibronectin (Figure 2c). BAI3-expressing cells showed a significant reduction in their spreading both at 30 min (BAI3-WT: $140 \pm 3\,\mu m^2$; GFP: $192 \pm 5\,\mu m^2$, respectively) and at 5 min (BAI3-WT: $118 \pm 3\,\mu m^2$; GFP: $139 \pm 6\,\mu m^2$) when compared with control GFP-expressing cells. This effect on cell spreading was totally absent when the cytoplasmic tail of BAI3 was deleted (BAI3-EMT), and partially abolished when the RKR motif was mutated (BAI3-WT-A). Thus overexpression of the BAI3 receptor inhibits cell spreading through its cytoplasmic tail, partially through ELMO1 binding, suggesting that BAI3 signaling could indeed regulate dendrite morphogenesis through RAC1 modulation.

### The BAI3/ELMO1 interaction is involved in the regulation of dendrite morphogenesis

Our data suggested the implication of a new BAI3/ELMO1 signaling pathway controlling neuronal morphogenesis. We first confirmed that the BAI3 receptor could colocalize with ELMO1-myc in DIV5 hippocampal neurons, in particular in developing dendrites (Supplementary Figure 2). We then transfected hippocampal neurons with either a construct coding for BAI3 WT or BAI3 mutant constructs deficient for ELMO1 interaction (BAI3-WT-A, BAI3-EMT, see Figure 2). As shown in Figure 3, overexpression of the BAI3 protein results in a 55% increase in the total dendritic length per neuron when compared with GFP-expressing neurons, as well as in an increase in the number of branches of order 2 and more per neuron (Figure 3a). These effects were partially abolished when mutant BAI3 constructs unable to bind ELMO1 were used (see Figure 3a) or when BAI3-WT was cotransfected with a truncated ELMO1 unable to bind DOCK180 (see Figure 3b). Finally cotransfecting a dominant-negative RAC1 with BAI3-WT

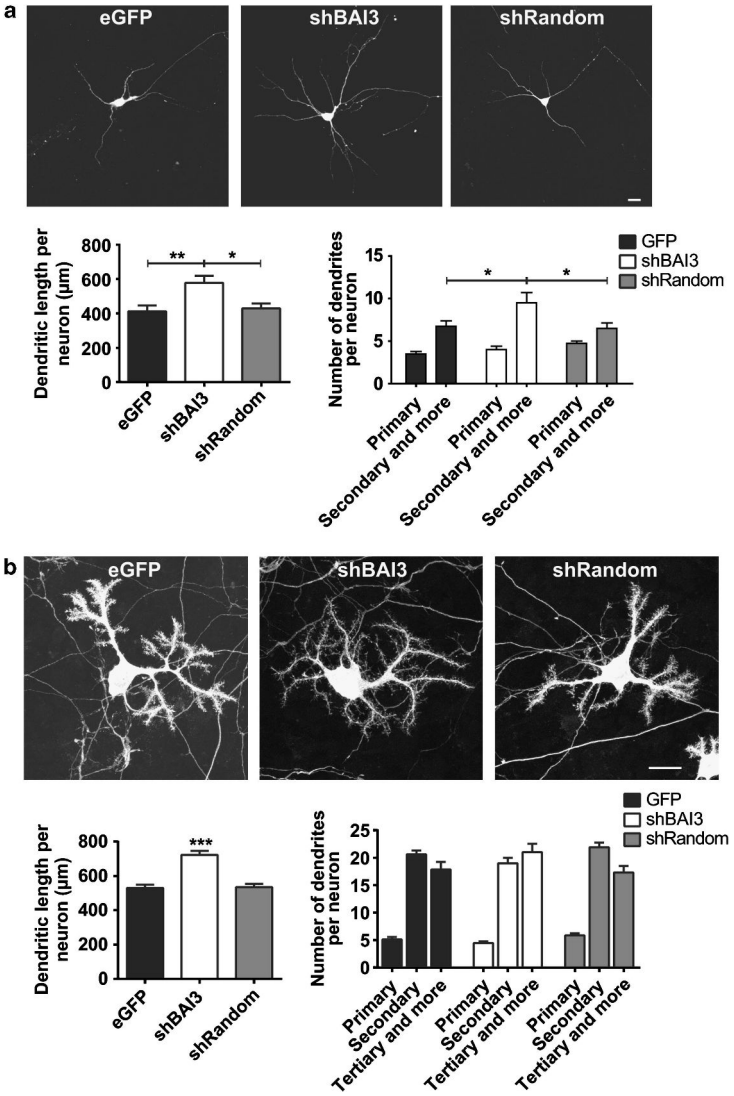


**Figure 1.** Knockdown of BAI3 promotes growth and branching of dendrites in several neuronal populations. (**a**) DIV5 hippocampal neurons were fixed two days after transfection with mCherry, and either a vector driving the expression of eGFP or a small hairpin RNA against BAI3 (shBAI3) or a control small hairpin RNA (shRandom). $N = 35–40$ neurons per condition, four independent experiments. (**b**) DIV7 cerebellar cultures infected at DIV4 with a lentivirus driving either GFP alone, shBAI3 or shRandom were immunostained for calbindin, a Purkinje cell-specific marker. $N = 40–50$ neurons per condition, three independent experiments. Scale bars: 20 µm. '*' denotes $P < 0.05$, '**' denotes $P < 0.01$, '***' denotes $P < 0.001$.

totally prevented BAI3's induced promotion of dendritogenesis (see Figure 3c). Taken together, our data show that the BAI3 protein regulates dendrite morphogenesis by regulating RAC1 activity, partially through binding to the ELMO1/DOCK180 complex. They also suggest another, yet to be found, BAI3 signaling pathway associated with domains other than its C-terminus.

The BAI3 protein regulates dendrite morphogenesis *in vivo*

Katoh *et al.*[29] have shown by *in situ* hybridization that ELMO1 is expressed in multiple neuronal populations in the mouse brain, including Purkinje cells. Double immunolabeling of mouse cerebellar sections using an antibody against the ELMO1 protein and an antibody against calbindin, a Purkinje cell marker (Figure 4a), showed the presence of ELMO1 in the growing tips of Purkinje cell dendrites at postnatal day 3. By P10, it was filling the whole Purkinje cell dendritic arborization. This pattern, together with the expression of BAI3 in Purkinje cells[8,30] and in the cerebellum during development (Figure 4b), is in agreement with a potential role of the BAI3/ELMO1 signaling pathway in the morphogenesis of Purkinje cells, whose elaborate dendritic arborization is the result of extensive reorganization between P0

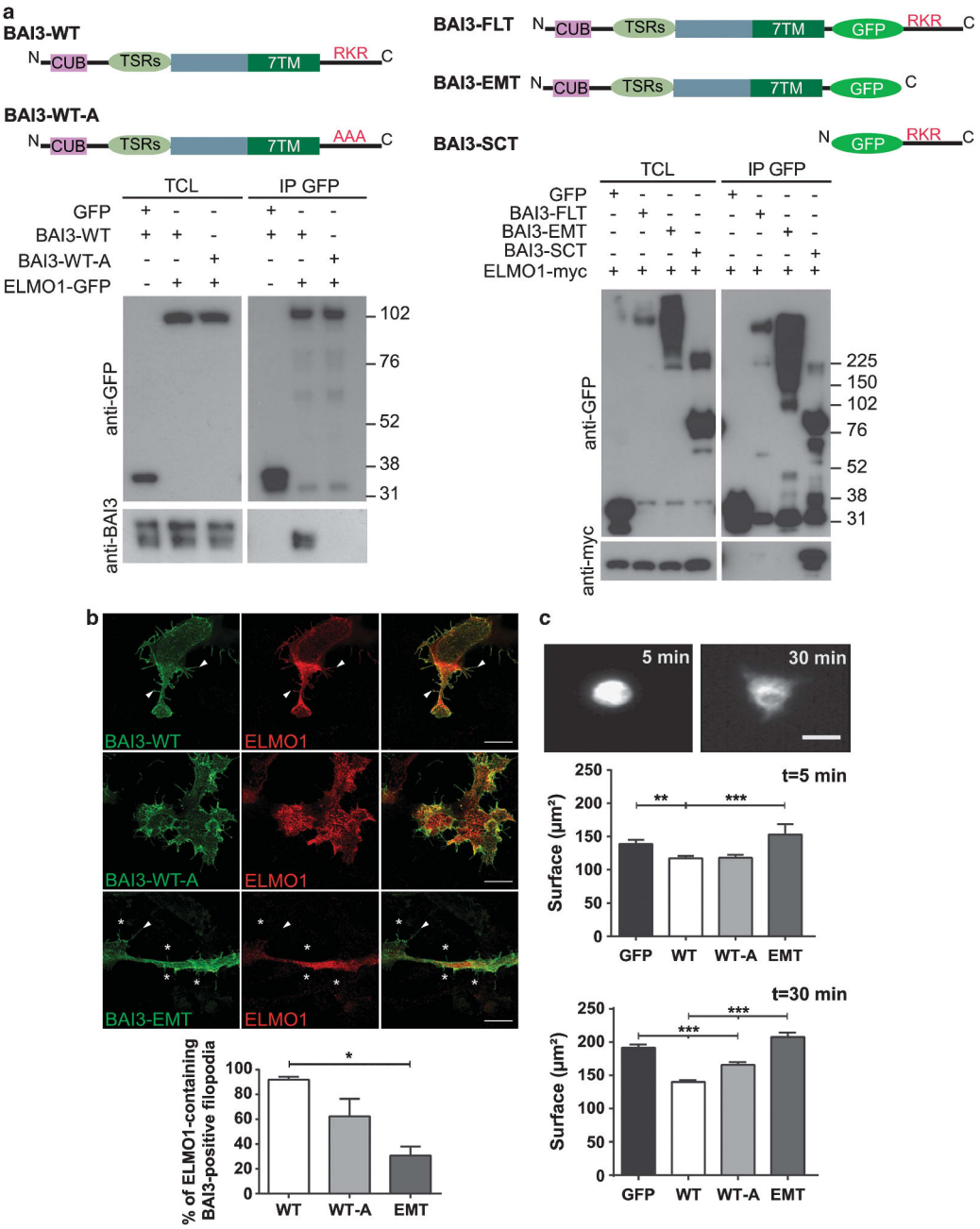


**Figure 2.** BAI3 regulates cell morphogenesis, partially through its interaction with ELMO1, a critical regulator of Rac1 signaling. (**a**) Top: schematic representations of the BAI3 constructs. Bottom affinity-purified proteins from transfected HEK-293H cells were detected by immunoblot analysis with anti-GFP, anti-BAI3 antibodies and anti-myc antibodies. ELMO1 was either tagged with GFP (expected molecular weight 112 kDa, left) or with myc (expected molecular weight 85 kDa, right). Control experiments were performed in parallel on HEK-293H cells expressing a soluble GFP instead of the GFP-tagged constructs. TCL: total cell lysate. IP GFP: samples affinity purified using an anti-GFP antibody. (**b**) Top: immunostaining of HEK-293H cells cotransfected with ELMO1-myc (detected with an anti-myc antibody) and either BAI3-WT, BAI3-WT-A (detected with an antibody against the N-terminus of the receptor) or BAI3-EMT (detected with an antibody against GFP). Arrows denote filopodia colabelled for BAI3 and ELMO1; asterisks denote filopodia missing ELMO1. Scale bar: 10 µm. Bottom: quantification of BAI3/ELMO1 colocalization in filopodia. Mean ± s.e.m., $n = 40$ cells per condition, 4 independent experiments. (**c**) Top: example of HEK293 cell shapes after 5 or 30 min of spreading on fibronectin. Scale bar: 20 µm. Middle and bottom: quantification of the cell surface area at 5 or 30 min of spreading. Mean ± s.e.m., $n = 600–900$ cells per condition, six independent experiments. '*' denotes $P < 0.05$, '**' denotes $P < 0.01$, '***' denotes $P < 0.001$.

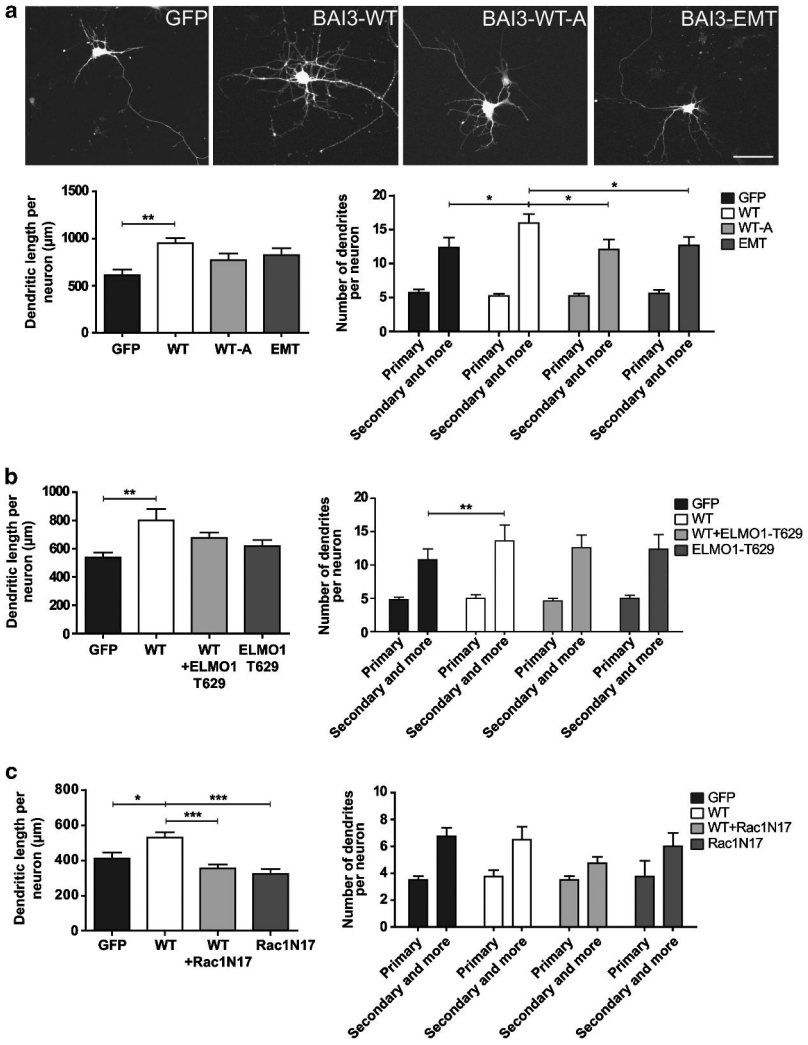


**Figure 3.** Overexpression of BAI3 promotes dendritic arborization growth and complexity through interaction with ELMO1 and Rac1 activity. (**a**) Top: confocal images of representative neurons transfected with the indicated constructs at DIV3 and fixed at DIV5. Scale bar: 50 µm. Bottom: the total dendrite length and the number of dendrites per neuron were quantified on DIV5 hippocampal neurons transfected with mCherry and either a GFP control construct, wild-type BAI3 (WT) or BAI3 mutants (WT-A, EMT). Mean ± s.e.m., $n = 30$ neurons per construct, four independent experiments. (**b**) Cotransfection of BAI3-WT and a mutant ELMO1 protein unable to bind DOCK180 (ELMO1T629) partially abolishes BAI3's promotion of dendrite morphogenesis in DIV5 hippocampal neurons. Mean ± s.e.m., $n = 55$ neurons per construct, five independent experiments. (**c**) Cotransfection of BAI3-WT and a dominant-negative Rac1 (Rac1N17) totally prevents BAI3's effect on dendrite morphogenesis in DIV5 hippocampal neurons. Mean ± s.e.m., $n = 40$ neurons per construct, four independent experiments. '*' denotes $P < 0.05$, '**' denotes $P < 0.01$, '***' denotes $P < 0.001$.

and P15 in the mouse cerebellum. To test this role *in vivo*, we generated transgenic mice expressing the BAI3-EMT mutant protein, which lacks the entire cytoplasmic domain and the ability to regulate neuronal morphogenesis (see Figures 2 and 3). In addition, the BAI3-EMT construct reduces by 44% the effect of the BAI3-WT receptor on dendritogenesis in hippocampal neurons (Supplementary Figure 4), and can thus act partially as a dominant-negative form. We used the *Pcp2* promoter to specifically drive the expression of BAI3-EMT in Purkinje cells in the cerebellum.[26] This specific expression was confirmed by immunoblot and was detected as early as P3 by GFP immunohistochemistry (Supplementary Figure 5). It was estimated by qRT-PCR to be equivalent to 60% of the endogenous *Bai3* gene. Calbindin immunostaining of cerebellar sections and morphometric measurements did not reveal any gross reorganization as a consequence of the expression of the mutant construct (Supplementary Figure 5). However, quantitative analysis of single-labeled Purkinje cells from Pcp2/BAI3-EMT mice revealed important changes in their dendritic morphology: increased dendritic length, number of junctions and terminal dendrites when compared with wild-type Purkinje cells (Figure 5a). Scholl analysis shows that the complexity of Purkinje cell dendritic arborization is

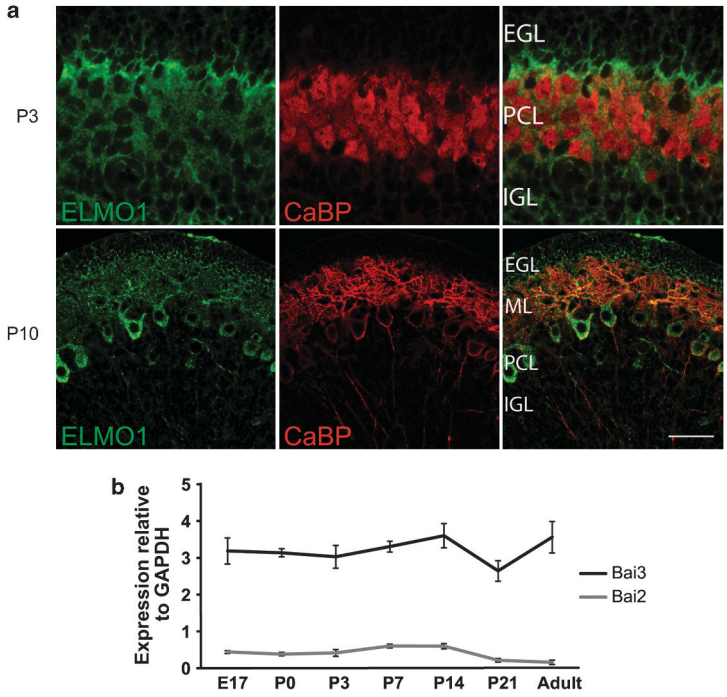


**Figure 4.** The BAI3 receptor and ELMO1 are expressed in the developing cerebellum. (**a**) Cerebellar sections from wild-type mice were immunolabelled for the endogenous ELMO1 protein and for calbindin (CaBP), a marker of Purkinje cells, at P3 and P10. EGL: external granular layer, ML: molecular layer, PCL: Purkinje cell layer, IGL: internal granular layer. Scale bar: 50 μm. (**b**) qRT-PCR shows a high expression of the *Bai3* gene during postnatal development in the mouse cerebellum relative to the *Gapdh* gene.

particularly increased in distal parts of the cells relative to the soma. Finally, we analyzed the effects of BAI3 knockdown *in vivo* by injecting the lentiviral vectors in the cerebellar cortex of P6 pups (Figure 5b), and imaging after 4 days of infection. Defects in dendritic arborization were clearly visible as dendrites were longer, thinner and misoriented in Purkinje cells transduced with the shRNA against BAI3 compared with the control shRNA. Alltogether, these results show a major role for BAI3 in regulating Purkinje cell dendritic arbor formation *in vivo*.

## DISCUSSION

The brain is composed of thousands of different types of neurons that differ drastically in their morphology, in particular in the shape and complexity of their dendritic arborization. This morphology underlies functional differences between neurons, in particular how they integrate signals coming from different inputs. Its proper development is thus essential for the normal function of the central nervous system, and deficits in neuronal morphogenesis have been correlated to psychiatric disorders such as schizophrenia. We have now provided evidence, both *in vitro* and *in vivo*, for a new signaling pathway regulating dendrite morphogenesis involving the BAI receptor BAI3, a member of the poorly studied family of adhesion-GPCRs, and the protein ELMO1, an important regulator of the RAC1 RhoGTPase.

The regulation of dendrite morphogenesis involves integration of extracellular signals and intrinsic molecular programs in order to control the growth and branching of the actin cytoskeleton. The BAI receptors constitute a new regulator of this process that can sense extracellular signals and signal in the cell through their interaction with effectors such as ELMO1. Another family of adhesion-GPCRs, the CELSR proteins, has been shown to have a role in dendrite morphogenesis through regulation of intracellular calcium signaling. Knockdown of CELSR2 in organotypic cultures in pyramidal neurons and Purkinje cells induces a simplification of their dendritic arborization,[31] whereas CESLR3 has an opposite role.[3] This function is conserved as the *Drosophila* homolog, Flamingo, is also involved in neuronal morphogenesis and more particularly in regulating dendritic field through repulsion.[32] Our results show that control of neuronal morphogenesis could be a property of many adhesion-GPCRs *in vivo*. Given the diversity of domains found in the extracellular part of adhesion-GPCRs, an attractive hypothesis is that each type of adhesion-GPCR might regulate the morphology of particular neuronal populations and thus contributes to the diversity of shape, and of function, in the vertebrate central nervous system.

What is the signaling pathway of BAI3 during neuronal morphogenesis? Our results show that its interaction with the protein ELMO1 is partially involved in this process. Previous results have shown that BAI1 can regulate RAC1 and phagocytosis through an interaction with ELMO1.[25] Regulation of RhoGTPases is essential for driving changes in the actin cytoskeleton and cell morphogenesis during development. Moreover modifying RAC1 activity in neurons is known to induce changes in dendrite morphogenesis[22] and interferes with BAI3's function as shown by our results. Hence BAI3's interaction with ELMO1 constitutes a direct pathway linking extracellular cues and intracellular modification of the actin cytoskeleton during neuronal development. It will be of interest to analyze the role of other potential intracellular partners of BAI3. In particular, IRSp53/BAIAP2 was originally identified as a partner for BAI1,[33] and has since been shown to regulate actin morphogenesis through

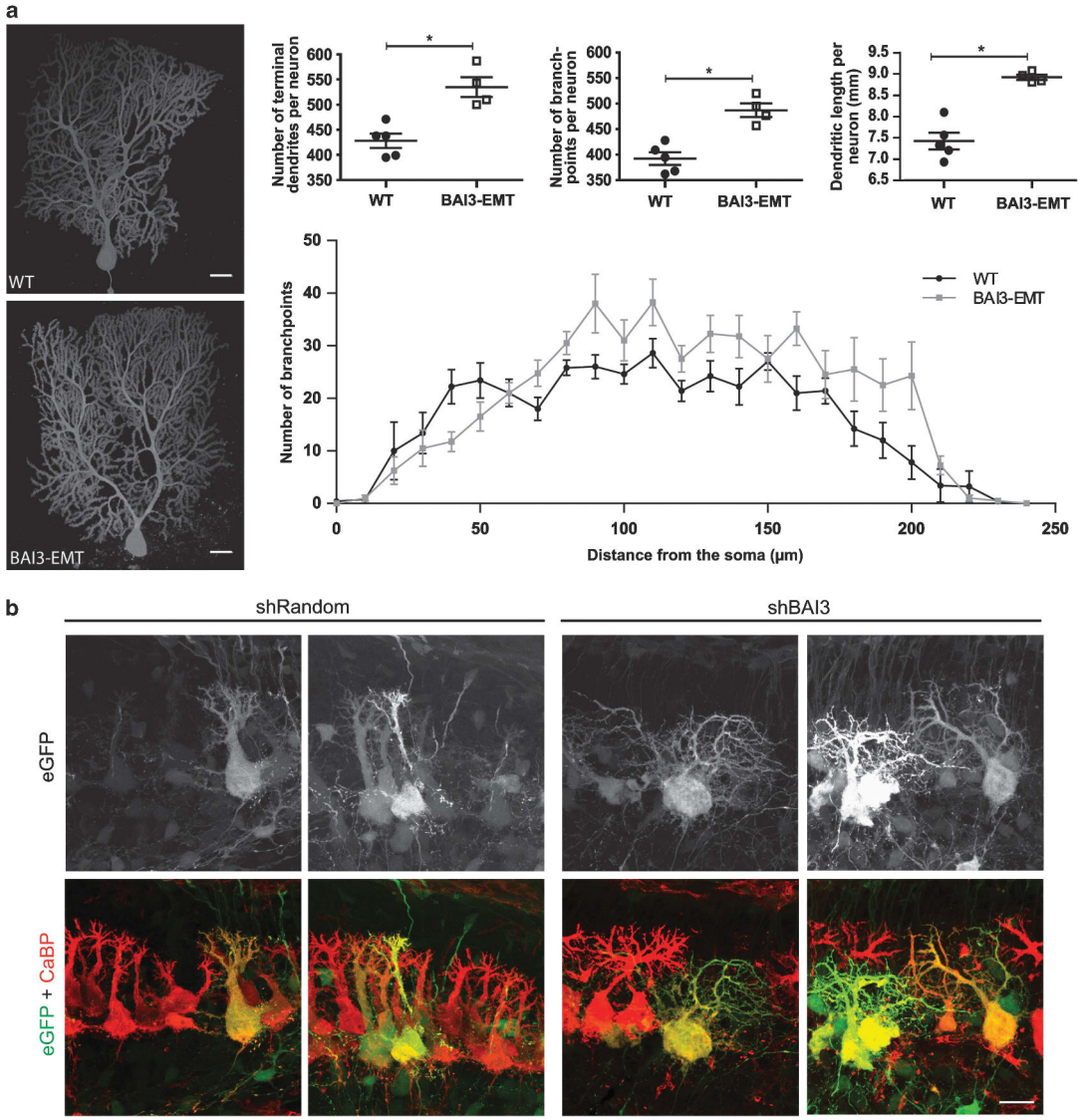


**Figure 5.** The BAI3 protein controls neuronal development and dendrite morphogenesis *in vivo*. (**a**) Left: images of representative reconstructed Purkinje cells in 1–month-old Pcp2/BAI3-EMT transgenic mice and age-matched wild-type (WT) mice. Right: quantification of total dendritic length, number of junctions and terminal branches per Purkinje cell as well as Scholl analysis. Mean ± s.e.m., $n = 4–5$ Purkinje cells per genotype. Student's *t*-test followed by Mann–Whitney, '*' denotes $P < 0.05$. (**b**) Purkinje cells transduced at P6 with lentivirus particles driving either shBAI3 or control shRandom (eGFP positive) were analyzed at P10 using calbindin immunostaining (CaBP). Massive defects in dendritic arborization were observed after BAI3 knockdown when compared with non transduced adjacent cells or cells transduced with the control virus. Scale bars: 20 µm.

binding of small RhoGTPAses and the WAVE complex.[34] Small G protein binding, although yet to be demonstrated for BAI proteins, could also have an important role through binding of the third intracytoplasmic loop. Extracellularly, binding of the secreted protein C1QL1 has recently been shown to promote synapse elimination *in vitro*, but no effect was demonstrated on dendrite morphogenesis.[35] These results were obtained in mature hippocampal neurons and, taken together with our data, suggest that the function of BAI proteins in the regulation of dendrite morphogenesis is critical at early stages of neuronal development. Alternatively, other unknown ligands of BAI3 might be critical for this function.

Several candidate genes linked with neurodevelopmental disorders are proteins regulating neuronal morphogenesis.[36] For example, mutations in SHANK3 associated with autism induce defects in spine morphogenesis and in actin polymerization.[37] Neuregulin1's mutation at valine 321, previously linked to schizophrenia, has been shown to prevent neuregulin's

control of dendritic arborization growth and complexity.[36] Given the evidence associating *BAI* genes with psychiatric disorders,[9,13,14,10,12] our data reveals a new pathway involved in the etiology of these brain diseases through regulation of dendrite morphogenesis, and highlights the potential of the BAI signaling pathway for therapeutic intervention.

## CONFLICT OF INTEREST

The authors declare no conflict of interest.

## ACKNOWLEDGEMENTS

We would like to thank Dr Sophie Vriz and Dr Jean-Louis Bessereau for critical reading of the manuscript. The ELMO1-GFP and ELMO1T629-GFP constructs were a kind gift of Dr Lorraine Santy (PennState, USA). We would like to thank R Schwartzman and S Bolte at the IFR83 imaging facility (UPMC, Paris, France), and J Teillon at the CIRB imaging facility (Collège de France, Paris, France). We would like to thank J Bakouche and V Gautheron for helping us with cloning and mouse colonies. This work was supported by the CNRS (PEPS, PICS), ATIP-AVENIR, Association Française du Syndrome de Rett, UPMC (Emergence), Ecole des Neurosciences de Paris. VL was supported by the ED3C (UPMC) and the Ministère de la Recherche et de l'Enseignement Supérieur, AU by UPMC and AVENIR, SMS by NERF and LABEX MEMOLIFE, and MT by FRM, PI by ANR-09-MNPS-038 and ANR-2010-JCJC-1403-1.

## REFERENCES

1 Emes RD, Pocklington AJ, Anderson CNG, Bayes A, Collins MO, Vickers CA *et al.* Evolutionary expansion and anatomical specialization of synapse proteome complexity. *Nat Neurosci* 2008; **11**: 799–806.
2 Bjarnadóttir TK, Fredriksson R, Schiöth HB. The adhesion GPCRs: a unique family of G protein-coupled receptors with important roles in both central and peripheral tissues. *Cell Mol Life Sci* 2007; **64**: 2104–2119.
3 Shima Y, Kawaguchi S-Y, Kosaka K, Nakayama M, Hoshino M, Nabeshima Y *et al.* Opposing roles in neurite growth control by two seven-pass transmembrane cadherins. *Nat Neurosci* 2007; **10**: 963–969.
4 Lagerström MC, Schiöth HB. Structural diversity of G protein-coupled receptors and significance for drug discovery. *Nat Rev Drug Discov* 2008; **7**: 339–357.
5 Zhou L, Bar I, Achouri Y, Campbell K, De Backer O, Hebert JM *et al.* Early forebrain wiring: genetic dissection using conditional Celsr3 mutant mice. *Science* 2008; **320**: 946–949.
6 Luo R, Jeong S-J, Jin Z, Strokes N, Li S, Piao X. G protein-coupled receptor 56 and collagen III, a receptor-ligand pair, regulates cortical development and lamination. *Proc Natl Acad Sci USA* 2011; **108**: 12925–12930.
7 Collins MO, Husi H, Yu L, Brandon JM, Anderson CNG, Blackstock WP *et al.* Molecular characterization and comparison of the components and multiprotein complexes in the postsynaptic proteome. *J Neurochem* 2006; **97**(Suppl 1): 16–23.
8 Selimi F, Cristea IM, Heller E, Chait BT, Heintz N. Proteomic studies of a single CNS synapse type: the parallel fiber/purkinje cell synapse. *PLoS Biol* 2009; **7**: e83.
9 DeRosse P, Lencz T, Burdick KE, Siris SG, Kane JM, Malhotra AK. The genetics of symptom-based phenotypes: toward a molecular classification of schizophrenia. *Schizophr Bull* 2008; **34**: 1047–1053.
10 Liao H-M, Chao Y-L, Huang A-L, Cheng M-C, Chen Y-J, Lee K-F *et al.* Identification and characterization of three inherited genomic copy number variations associated with familial schizophrenia. *Schizophr Res* 2012; **139**: 229–236.
11 Lips ES, Cornelisse LN, Toonen RF, Min JL, Hultman CM, Holmans PA *et al.* Functional gene group analysis identifies synaptic gene groups as risk factor for schizophrenia. *Mol Psychiatry* 2011; **17**: 996–1006.
12 McCarthy MJ, Nievergelt CM, Kelsoe JR, Welsh DK. A survey of genomic studies supports association of circadian clock genes with bipolar disorder spectrum illnesses and lithium response. *PLoS ONE* 2012; **7**: e32091.
13 Liu Q-R, Drgon T, Johnson C, Walther D, Hess J, Uhl GR. Addiction molecular genetics: 639,401 SNP whole genome association identifies many 'cell adhesion' genes. *Am J Med Genet* 2006; **141B**: 918–925.
14 Okajima D, Kudo G, Yokota H. Antidepressant-like behavior in brain-specific angiogenesis inhibitor 2-deficient mice. *J Physiol Sci* 2010; **61**: 47–54.
15 Cahill ME, Jones KA, Rafalovich I, Xie Z, Barros CS, Müller U *et al.* Control of interneuron dendritic growth through NRG1/erbB4-mediated kalirin-7 disinhibition. *Mol Psychiatry* 2011; **17**: 99–107.
16 Scotto-Lomassese S, Nissant A, Mota T, Néant-Féry M, Oostra BA, Greer CA *et al.* Fragile X mental retardation protein regulates new neuron differentiation in the adult olfactory bulb. *J Neurosci* 2011; **31**: 2205–2215.
17 Kalus P, Müller TJ, Zuschratter W, Senitz D. The dendritic architecture of prefrontal pyramidal neurons in schizophrenic patients. *Neuroreport* 2000; **11**: 3621–3625.
18 Raymond GV, Bauman ML, Kemper TL. Hippocampus in autism: a Golgi analysis. *Acta Neuropathol* 1996; **91**: 117–119.
19 Luo L. Actin cytoskeleton regulation in neuronal morphogenesis and structural plasticity. *Annu Rev Cell Dev Biol* 2002; **18**: 601–635.
20 Cerri C, Fabbri A, Vannini E, Spolidoro M, Costa M, Maffei L *et al.* Activation of Rho GTPases triggers structural remodeling and functional plasticity in the adult rat visual cortex. *J Neurosci* 2011; **31**: 15163–15172.
21 Van Aelst L, Cline HT. Rho GTPases and activity-dependent dendrite development. *Curr Opin Neurobiol* 2004; **14**: 297–304.
22 Luo L, Hensch TK, Ackerman L, Barbel S, Jan LY, Jan YN. Differential effects of the Rac GTPase on Purkinje cell axons and dendritic trunks and spines. *Nature* 1996; **379**: 837–840.
23 Hayashi-Takagi A, Takaki M, Graziane N, Seshadri S, Murdoch H, Dunlop AJ *et al.* Disrupted-in-Schizophrenia 1 (DISC1) regulates spines of the glutamate synapse via Rac1. *Nat Neurosci* 2010; **13**: 327–332.
24 Kim J-Y, Oh MH, Bernard LP, Macara IG, Zhang H. The RhoG/ELMO1/Dock180 signaling module is required for spine morphogenesis in hippocampal neurons. *J Biol Chem* 2011; **286**: 37615–37624.
25 Park D, Tosello-Trampont A-C, Elliott MR, Lu M, Haney LB, Ma Z *et al.* BAI1 is an engulfment receptor for apoptotic cells upstream of the ELMO/Dock180/Rac module. *Nature* 2007; **450**: 430–434.
26 Smeyne RJ, Chu T, Lewin A, Bian F, S Crisman S, Kunsch C *et al.* Local control of granule cell generation by cerebellar Purkinje cells. *Mol Cell Neurosci* 1995; **6**: 230–251.
27 Avci HX, Lebrun C, Wehrlé R, Doulazmi M, Chatonnet F, Morel M-P *et al.* Thyroid hormone triggers the developmental loss of axonal regenerative capacity via thyroid hormone receptor $\alpha$1 and kruppel-like factor 9 in Purkinje cells. *Proc Natl Acad Sci USA* 2012; **109**: 14206–14211.
28 Katoh H, Negishi M. RhoG activates Rac1 by direct interaction with the Dock180-binding protein Elmo. *Nature* 2003; **424**: 461–464.
29 Katoh H, Fujimoto S, Ishida C, Ishikawa Y, Negishi M. Differential distribution of ELMO1 and ELMO2 mRNAs in the developing mouse brain. *Brain Res* 2006; **1073-1074**: 103–108.
30 Kee HJ, Ahn KY, Choi KC, Won Song J, Heo T, Jung S *et al.* Expression of brain-specific angiogenesis inhibitor 3 (BAI3) in normal brain and implications for BAI3 in ischemia-induced brain angiogenesis and malignant glioma. *FEBS Lett* 2004; **569**: 307–316.
31 Shima Y, Kengaku M, Hirano T, Takeichi M, Uemura T. Regulation of dendritic maintenance and growth by a mammalian 7-pass transmembrane cadherin. *Dev Cell* 2004; **7**: 205–216.
32 Gao F-B, Kohwi M, Brenman JE, Jan LY, Jan YN. Control of dendritic field formation in Drosophila. *Neuron* 2000; **28**: 91–101.
33 Oda K, Shiratsuchi T, Nishimori H, Inazawa J, Yoshikawa H, Taketani Y *et al.* Identification of BAIAP2 (BAI-associated protein 2), a novel human homologue of hamster IRSp53, whose SH3 domain interacts with the cytoplasmic domain of BAI1. *Cytogenet Cell Genet* 1999; **84**: 75–82.
34 Abou-Kheir W, Isaac B, Yamaguchi H, Cox D. Membrane targeting of WAVE2 is not sufficient for WAVE2-dependent actin polymerization: a role for IRSp53 in mediating the interaction between Rac and WAVE2. *J Cell Sci* 2008; **121**: 379–390.
35 Bolliger MF, Martinelli DC, Sudhof TC. The cell-adhesion G protein-coupled receptor BAI3 is a high-affinity receptor for C1q-like proteins. *Proc Natl Acad Sci USA* 2011; **108**: 2534–2539.
36 Chen Y, Hancock ML, Role LW, Talmage DA. Intramembranous valine linked to schizophrenia is required for neuregulin 1 regulation of the morphological development of cortical neurons. *J Neurosci* 2010; **30**: 9199–9208.
37 Durand CM, Perroy J, Loll F, Perrais D, Fagni L, Bourgeron T *et al.* SHANK3 mutations identified in autism lead to modification of dendritic spine morphology via an actin-dependent mechanism. *Mol Psychiatry* 2012; **17**: 71–84.



Supplementary Information accompanies the paper on the Molecular Psychiatry website (http://www.nature.com/mp)

## Supplemental figure legends

**Supplemental figure 1: Phylogenetic analysis of the BAI3 protein in vertebrates using ClustalW**

**Supplemental figure 2: The BAI3 receptor is localized in actin-rich structures, in particular in dendrites of neurons, and colocalizes with ELMO1.**

A. In HEK-293H cells, transfected wild-type BAI3 (BAI3) colocalizes with F-actin (labeled with phalloidin-TRITC) in cell protrusions such as lamellipodia (arrows) and filopodia (arrowheads). Scale bar: 10 $\mu$m.

B. The BAI3 protein (BAI3) is detected in dendrites and protrusions of DIV5 hippocampal neurons transfected with mCherry and wild-type BAI3. Scale bar: 10 $\mu$m

C. In dendrites of DIV5 hippocampal neurons, clear colocalization is detected between transfected BAI3 (BAI3) and F-actin (stained with phalloidin-TRITC), in particular in protrusions (arrows). Scale bar: 10 $\mu$m.

D. Immunostaining for transfected BAI3 and ELMO1-myc (ELMO1) in DIV5 hippocampal neurons shows partial colocalization with the BAI3 protein (arrows). Scale bar: 10 µm

**Supplemental figure 3: Characterization of the specificity of BAI3 knockdown**

Left: Immunoblot analysis of total protein extracts from HEK-293H cells co-transfected with a vector coding for GFP-tagged full length BAI3 (FLT, cf. figure 2) and with a vector coding for either eGFP, a small hairpin RNA against BAI3 (shBAI3), or a non targeting control small hairpin RNA (shRandom). Actin immunoblotting was used to confirm analysis of equal amounts of proteins between samples.

Right: *Bai3* and *Bai2* mRNA expression quantified by RTqPCR on cDNA extracts from hippocampal neurons transduced with the corresponding lentivirus particles. Data are presented normalized to expression of the housekeeping gene GAPDH and relative to control

shRandom values. Note that only the expression of Bai3 is significantly reduced by shBAI3. Mean±SEM of 3 independent experiments.

**Supplemental figure 4: The BAI3-EMT construct has a partial dominant-negative effect on wild-type BAI3 function**

Top: Confocal images of representative neurons transfected with the indicated constructs at DIV3 and fixed at DIV5. Scale bar: 50 μm. Bottom: The total dendrite length per neuron was quantified on DIV5 hippocampal neurons transfected with mCherry and either a GFP control construct, wild-type BAI3 (WT) or wild-type BAI3 and BAI3-EMT mutant (WT+EMT) at equimolar ratio. Mean ±SEM, n= 60 neurons per condition, 3 independent experiments. * $p<0.05$.

**Supplemental figure 5: Characterization of the pcp2/BAI3-EMT transgenic mice**

Copy number was estimated at about 21 using quantitative PCR on genomic DNA extracts (6 samples per genotype). Relative expression levels were quantified using quantitative RT-PCR performed on cDNA from cerebella of transgenic and wild-type mice: the transgene was expressed at about 60% of the BAI3 wild-type level (mean from 3 different animals per genotype).

A. Left: Affinity-purification using an anti-GFP antibody (anti-GFP IP) on total cerebellar protein extracts (Input) and immunoblot analysis showed the expression of the BAI3-EMT transgene in cerebella from adult transgenic mice at the expected size (detected either using the GFP antibody or the BAI3 antibody).

Right: Anti-GFP immunohistochemistry on parasagittal cerebellar sections from P3 and 4 weeks-old Pcp2/BAI3-EMT mice. Scale bar= 50 μm.

B. Cerebellar sagittal sections from 4 weeks-old transgenic mice expressing the mutant BAI3-EMT protein specifically in Purkinje cells (Pcp2/BAI3-EMT) and from wild-type mice (WT) immunostained for calbindin. Scale bar= 500 μm. Morphometric measurements using ImageJ

showed no significant changes in total cerebellar area and mean molecular height. N=3 animals per genotype.

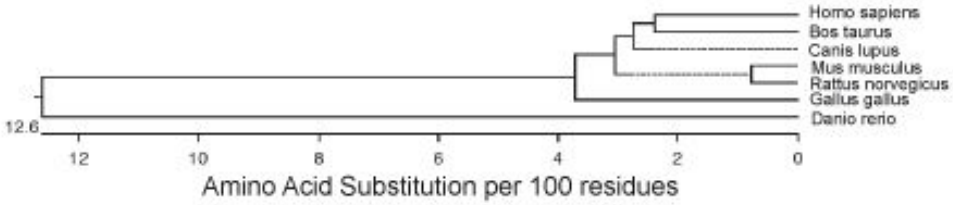


Percent Identity

Divergence

| | 1 | 2 | 3 | 4 | 5 | 6 | 7 | | |
|---|---|---|---|---|---|---|---|---|---|
| 1 | | 98.3 | 98.0 | 94.9 | 98.6 | 95.4 | 79.0 | 1 | Homo sapiens |
| 2 | 1.7 | | 98.5 | 94.7 | 98.1 | 94.8 | 79.4 | 2 | Mus musculus |
| 3 | 2.0 | 1.5 | | 94.3 | 97.6 | 94.3 | 79.0 | 3 | Rattus norvegicus |
| 4 | 5.3 | 5.5 | 6.0 | | 95.1 | 91.9 | 79.4 | 4 | Gallus gallus |
| 5 | 1.5 | 1.9 | 2.5 | 5.1 | | 95.4 | 79.5 | 5 | Canis lupus |
| 6 | 4.8 | 5.4 | 5.9 | 8.6 | 4.8 | | 76.8 | 6 | Bos taurus |
| 7 | 24.7 | 24.1 | 24.7 | 24.1 | 24.0 | 27.8 | | 7 | Danio rerio |
| | 1 | 2 | 3 | 4 | 5 | 6 | 7 | | |

Supplemental figure 1
Lanoue et al.

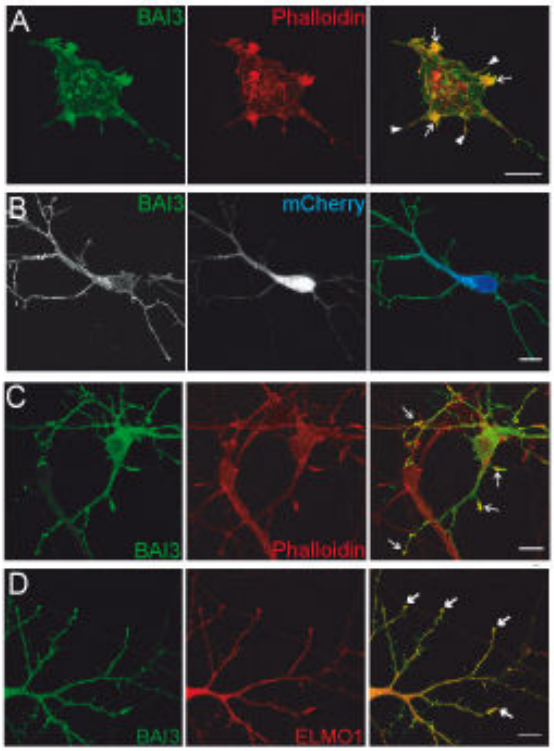


Supplemental figure 2
Lanoue et al.

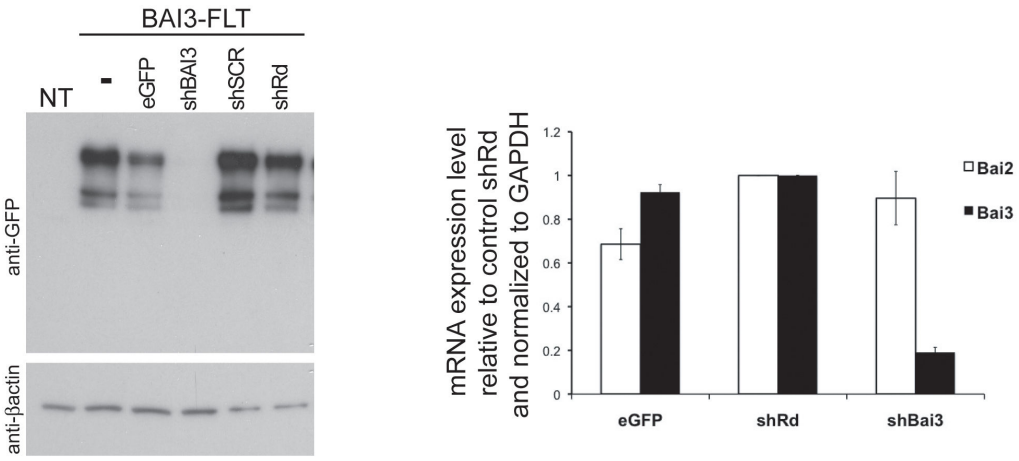


Supplemental figure 3
Lanoue et al.

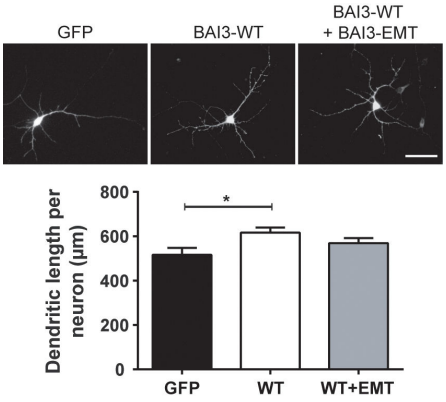


Supplemental figure 4
Lanoue et al.

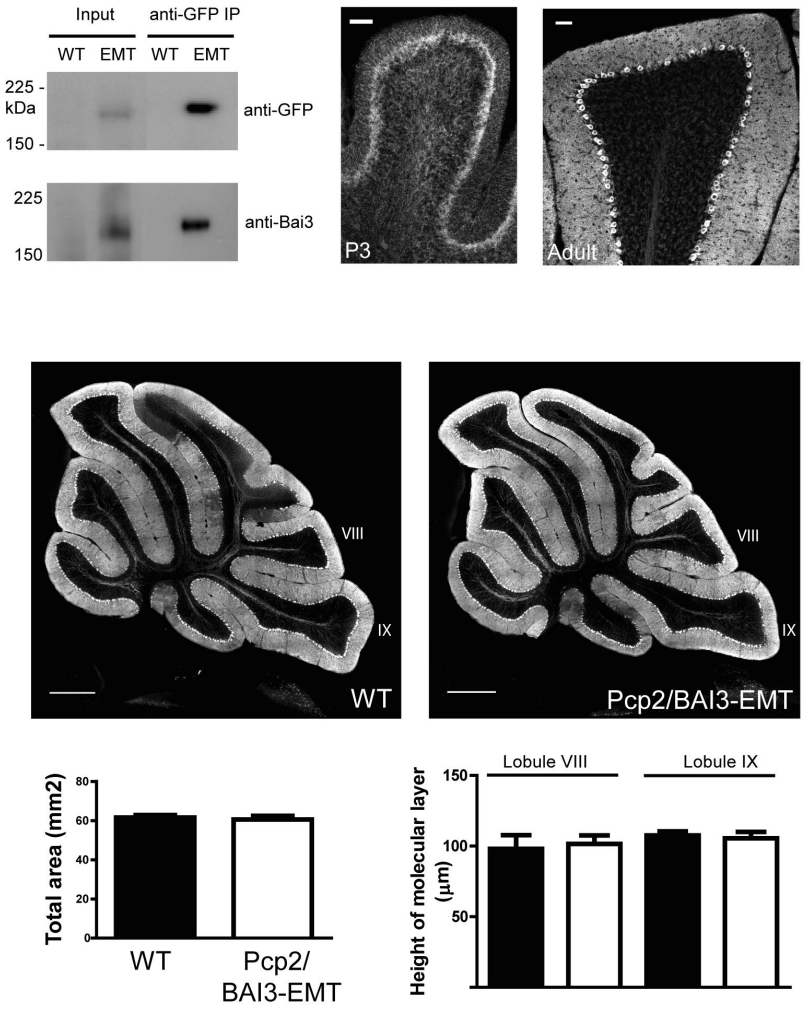


Supplemental figure 5
Lanoue et al.

## Supplemental material and methods

All animal protocols were approved by the Comité Régional d'Ethique en Expérimentation Animale.

**Additional constructs**

A myc tag (ELMO-myc) or a GFP tag (ELMO1-GFP) was fused to the C-terminus of the ELMO1 cDNA in the pEBB vector. ELMO1GFP and ELMO1T629GFP were a kind gift of Dr. LC Santy. The dominant-negative Rac1 construct was pcDNA3-EGFP-Rac1(T17N) (Invitrogen, [1]).

**Neuronal cultures and image analysis**

Hippocampal cultures were prepared from E18 Swiss mouse embryos as previously published with minor modifications [2]. Neurons were transfected at DIV3 using Lipofectamine-2000 (Life technologies, Carlsbad, USA) according to the manufacturer's protocol and fixed after 48 hours. Cerebellar mixed cultures were prepared from P0 mouse cerebella were dissected and dissociated according to previously published protocol [3]. Neurons were seeded at a density $5x10^6$ cells/ml.

Neurons were imaged using a Leica SP5 confocal microscope at 20X (for hippocampal neurons) or at 63X (for Purkinje cells). Dendrites were analyzed using the NeuronJ pluggin of ImageJ. Statistical analysis was performed using for dendrite length: One-way ANOVA followed by Tukey's or Dunn's *posthoc* test; for dendrite number: Two-way ANOVA followed by Bonferroni *posthoc* test.

**Immunocytochemistry, immunohistochemistry and antibodies**

Actin staining was performed on fixed cells using 100 nM phalloidin-TRITC (Sigma-Aldrich, St-Louis, USA). For immunohistochemistry, thirty micrometers sagittal cerebellar sections were obtained from 4% paraformaldehyde perfused mice using a freezing microtome. Immunohistochemistry for ELMO1 was performed using the TSA amplification kit (Perkin Elmer, Waltham, USA). Antibodies used were: anti-ELMO1, 1/1000 (Abcam, Cambridge, UK, #ab2239); anti-BAI3, 1/500 (Sigma, #HPA015963); anti-GFP, 1/100 (Abcam, #6556); anti-CaBP, 1/5000 (Swant, Marly, Switzerland, #300); anti-myc, 1/500 (Sigma, #M4439).

**Cell spreading assay**

Transfected HEK-293H cells were incubated for 30 min in 2.5 $\mu$M Cell Tracker (Invitrogen) diluted in DMEM, washed for 30 min in DMEM/10% FBS, and mechanically detached in DMEM/10% FBS. After 30 min of recovery, cells were plated at a concentration of $5x10^4$ cells/ml on coverslips coated with 10 $\mu g.mL^{-1}$ fibronectin. Cells were fixed after 5 or 30 min of spreading and imaged under epifluorescence at 20X magnification with a Qicam camera. Quantification of the cell surface area was performed using the ImageJ software by an investigator without knowledge of the condition.

**qPCR and RT-qPCR**

Copy number was estimated using genomic DNA purified from mouse tails followed by quantitative PCR using the LightCycler 480 SYBR Green I Master kit (Roche Diagnostics, Meylan, France) and the following primers for the Bai3 gene : forward : 5'ctggccatgacagataaacg3' and reverse 5'ctctccgaagaatgcagtgg3'.

Relative expression levels were quantified for the BAI3EMT transgene using RT-qPCR. RNA samples were obtained from cerebella using the RNeasy Mini kit (QIAGEN, Hilden, Germany), cDNA were amplified using the SuperScript® VILO™ cDNA Synthesis kit (Life technologies, Paisley, UK) according to manufacturer's instructions. Quantitative PCRs were performed as for the copy number assessment.

**Single Purkinje cell reconstruction**

Single Purkinje cells were filled with biocytin in cerebellar slices obtained from 4 weeks old-animals as described in [4], slices were fixed with 4% paraformaldehyde and biocytin labelling was revealed using the Vectastain ABC kit coupled with the TSA-FITC substrate (tyramide signal amplification kit, Perkin Elmer). Purkinje cells were imaged using a SP5 Leica confocal microscope, a 300 nm z-step and a x63 objective with a zoom of 1.7. Images were deconvolved using the Huygens Essential software (Scientific Volume Imaging B.V., Hilversum, Netherlands) and dendritic arbors were reconstructed using the Neuron Studio software (CNIC, Mount Sinai School of Medicine, New York, USA).

## Supplemental references


1. Kraynov VS, Chamberlain C, Bokoch GM, Schwartz MA, Slabaugh S, Hahn KM. Localized Rac activation dynamics visualized in living cells. *Science* 2000 Oct. 13; **290**: 333–7.

2. Fath T, Ke YD, Gunning P, Götz J, Ittner LM. Primary support cultures of hippocampal and substantia nigra neurons. *Nat Protoc* 2008 Dec.; **4**: 78–85.

3. Tabata T, Sawada S, Araki K, Bono Y, Furuya S, Kano M. A reliable method for culture of dissociated mouse cerebellar cells enriched for Purkinje neurons. *J Neurosci Methods* 2000 Dec. 15; **104**: 45–53.

4. Valera AM, Doussau F, Poulain B, Barbour B, Isope P. Adaptation of granule cell to Purkinje cell synapses to high-frequency transmission. *J Neurosci* 2012 Feb. 29; **32**: 3267–80.

## 2. IgSF3, a novel member of the immunoglobulin-like superfamily, as a new regulator of cerebellar development (Article in preparation)

Alessia Usardi[1], Keerthana Iyer[1], Antoine Dusonchet[1], Fekrije Selimi[1]

[1]Equipe Mice, Molecules and Synapse Formation, CIRB-Collège de France, 11, Place Marcelin Berthelot, 75231 Paris Cedex 05, France
Corresponding author : Fekrije Selimi, fekrije.selimi@college-de-france.fr, tel.: +33 1 44 27 16 54, fax: +33 1 44 27 16 91

**Abstract**

The establishment of a functional brain depends on the fine regulation of the succession of many steps, including neurogenesis, differentiation, dendritogenesis, axonogenesis, and synaptogenesis. Proteins of the immunoglobulin-like superfamily (IgSF) control many of these processes at specific developmental stages, as shown in particular by studies of cerebellar development. We have identified IgSF3, a member of the little studied EWI subfamily of IgSF, as a new regulator of neuronal morphogenesis and axonal growth. IgSF3 is expressed in a neuron- and time- dependent manner during brain development. In the cerebellum, it is transiently expressed in membranes of granule cells. In particular, it is concentrated at axon terminals where it co-localizes with other IgSF members such as TAG-1 and L1. Our results show that IgSF3 controls the differentiation of cultured granule cells, in particular by inhibiting axonal growth and branching. In the developing brain, IgSF3 forms a complex with tetraspanin 7, a protein implicated in several forms of X-linked intellectual disabilities. IgSF3 might be a key player during brain development.

**Introduction**

Many steps of brain development involve cell-cell interactions, including neuronal migration, elongation of dendritic and axonal protrusions as well as formation and maintenance of synapses. For example, in the developing cerebellar cortex, granule cell precursors (GCPs) migrate tangentially from the rhombic lip to the surface of the cerebellar primordium where they form the external granular layer (EGL) (Sotelo, 2004; Alder et al., 1996). GCPs go through a second period of proliferation in the outer EGL, before starting their differentiation in the inner EGL where they extend their axons, the parallel fibers, and their radial migration along the Bergman glia that serves as a scaffold. When they reach the internal granular layer, below the Purkinje cells (Hatten and Heintz, 1995; Sotelo, 2004)

they terminate their differentiation and are contacted by their inputs, the mossy fibers. Their axons, the parallel fibers, form synapses with their targets in the molecular layer, the Purkinje cells and the interneurons.

All these steps need to be finely orchestrated during development. The cell adhesion molecules (CAMs) family, which includes cadherins, Ig superfamily (IgSF) proteins, and integrins, plays a crucial role (Shapiro et al., 2007; Maness and Schachner, 2007). IgSFs are characterized by at least one immunoglobulin (Ig) domain, and generally contain a transmembrane and a short intracellular domain. Many also contain Fibronectin type III domains like NCAM, L1 or DSCAM proteins (Bian, 2013). Perturbations of the function of the IgSF proteins have been shown to lead to defects in neuronal migration and axonal growth, including in the cerebellum (for review Maness and Schachner, 2007; Stoeckli, 2010). The EWI subfamily of IgSF proteins comprises four members (EWI-2/IgSF8/PGRL, EWI-F/Ptgfrn/CD9P-1 and EWI-101/IgSF2 and EWI-3/IgSF3) that all share a Glu-Trp-Ile (EWI) motif in their extracellular region (Stipp et al., 2001). They are strongly similar to each other (23-35% similarity), and differ by the number of C2-type IgG domains that they contain (Charrin et al., 2001; Clark et al., 2001; Ruegg et al., 1995; Stipp et al., 2001) IgSF8, Ptgfrn and IgSF2 have been involved in diverse cellular processes requiring cell-cell interaction such as oocyte fertilization (Ellerman et al., 2003), viral infection (Bhella, 2015; Gordón-Alonso et al., 2012; Montpellier et al., 2011), T cell proliferation and formation and maintenance of the immune synapse (Rivas et al., 1995). In the brain, IgSF8 is expressed in the growing axons of olfactory sensory neurons where it colocalizes with NCAM (Ray and Treloar, 2012). IgSF3 is structurally closely related to IgSF2 (Stipp et al., 2001), and is expressed in placenta, kidney, lung and brain (Saupe et al., 1998). No reports, until now, have described its function.

Here we show that IgSF3 is expressed in various brain regions in a developmentally regulated manner. In the cerebellum, IgSF3 is highly expressed at early stages of development and controls granule cell differentiation. We also present evidence that IgSF3 binds to the tetraspanin Tspan7 in the developing brain. Our findings indicate that IgSF3 participates in the control of cerebellar development and might have similar roles in other brain regions.

## Experimental methods

### *Quantitative RT-PCR*

RNA samples were obtained from mouse cerebella at different ages or mixed cerebellar cultures using the RNeasy Mini kit (#74104 Qiagen). cDNA were amplified using the SuperScript® VILO™ cDNA Synthesis kit (#11754050, Life technologies) according to manufacturer's instructions. Quantitative PCR was performed using the Light Cycler 480 SYBR Green I Master Mix (#04 887 352 001, Roche Applied Science) and the following primers: *Igsf3* Fwd 5'-aagtacagatcgttagcacggt-3' and Rev 5'-ggtgtgacattcatactcgcc-3', *Igsf8* Fwd 5'-ggactctggcttttatgagtgc-3' and Rev 5'-ggaggggcagcagatacc-3', *Igsf2* Fwd 5'-agcccttggaactcacctgt-3' and Rev 5'-catcaccggccacaaacct-3', *Ptgfrn* Fwd 5'-gaccaaggccactacaagtgt-3' and Rev 5'-gacgtggtagacgcgatacat-3', *Tspan7* Fwd 5'-atggcatcgaggagaatggag-3' and Rev 5'-tgagcacatagggagcatttg-3', *Gapdh* Fwd 5'-cctgcgacttcaacagcaact-3' and Rev 5'-ggtccagggtttcttactccttg-3', *Rpl13* Fwd 5'-cactctggaggagaaacggaagg-3' and Rev 5'-gcaggcatgaggcaaacagtc-3'.

### *Neuronal cultures and gene expression modification*

We prepared dissociated cultures of mouse cerebellar neurons by using a modified version of a protocol described elsewhere (Tabata et al., 2000). Briefly, neurons were dissociated from P0 cerebella obtained from Swiss mice, in the case of mixed cerebellar cultures, or P6 cerebella for granule cell cultures. Ninety microliters of the cell suspension (5x10^6 cells/mL) was plated onto the centre of poly L-ornithine (0.5 mg/mL) coated glass coverslips. Cells were maintained in medium supplemented with bovine serum albumin (100 µg/ml) and a glial proliferation inhibitor, cytosine arabinoside (4 µM).

For loss of function experiments, granule cells were treated at DIV0 with either 0.5 µM Accell Non-Targeting siRNA as control (#D-001910-10-20, Thermo Fisher Scientific Biosciences GmbH) or 0.5 µM Mouse siIgSF3 siRNA following manufacturer's instructions (#E-048685-00-0010, Thermo Fisher Scientific Biosciences GmbH). For gain of function experiments, granule cells were transfected at DIV1 using Lipofectamine 2000 (#11668, Life Technologies) according to the manufacturer's protocol. Plasmids used were: pCAG (Matsuda and Cepko, 2004) plus pCAG-mbGFP vectors as control or pCAG-IgSF3 plus pCAG-mbGFP. After 96 hours granule cells were fixed for immunocytochemistry or lysed for mRNA extraction.

***Transfection of HEK293 cells***

HEK293 cells were maintained in DMEM-glutamax 4.5 g/L glucose plus pyruvate (#31966, Life Technologies) supplemented with 10% fetal bovine serum and 100 $U/mL^{-1}$ penicillin/ 100 $\mu g/mL^{-1}$ streptomycin, at 37 C in a 5% CO2 atmosphere. Cells were transfected 24 hours after plating with pBImbGFP or pBImbGFP-IgSF3 or pCAG-IgSF3 or pIRES2eGFP-Tspan7 (Bassani et al., 2012) by using Lipofectamine 2000 (#11668, Life Technologies). After 48 hours cells were fixed for immunocytochemistry or lysed for western blots.

***In situ hybridization***

In situ hybridization was performed using a previously described protocol with few modifications (Bally-Cuif et al., 1992). Briefly, 100 µm thick-floating vibratome sections were obtained from paraformaldehyde fixed mouse brains at postnatal day 0 (P0), P7 and P21. The probe sequence for IgSF3 corresponded to 1608-2479 bp for mouse cDNA NM_207205.1. The riboprobe was used at a final concentration of 2 µg/µL. Duration of the proteinase K (10µg/mL) treatment was 30 seconds for P0 and P7 brain sections, and 10 minutes for P21 brain sections. The anti-digoxigenin conjugated to alkaline phosphatase antibody was used at a dilution of 1/2000.

***Immunohistochemistry***

Swiss mice (Janvier, France) were perfused with 4% paraformaldehyde in PBS, pH 7.4. Brains were post-fixed for 1hr (for adult mice) or overnight (for P0 and P7) with 4% PFA in PBS at 4°C, then cryoprotected in 30% sucrose/PBS for two nights. 30µM-thick sections were obtained using a freezing microtome.

Blocking of non specific binding sites was performed using 4% Donkey serum/PBS. Primary antibodies were diluted in 1% Donkey serum/1% Triton X-100/PBS and incubated at 4°C overnight. Donkey Alexa Fluor® 488, 594 and 647 conjugated secondary antibodies (Invitrogen) were diluted in 1% Donkey serum/1% Triton X-100/PBS. Washes were performed with 1% Triton X-100/PBS.

***Immunocytochemistry***

Cells were fixed with cold 4% PFA in PBS for 15 min at room temperature, rinsed with PBS and incubated with 4% Donkey serum/0.2% Triton X-100/PBS. Primary and secondary antibodies were diluted in 0.2% Triton X-100/PBS. Nuclear counterstaining was performed with Hoechst for 15 min at room temperature.

***Primary antibodies***

Sheep anti-IgSF3 (1:750 for brain sections, 1:400 for fixed cells, R&D Systems), rabbit anti-IgSF3 (for Western blotting, 1:1000, Sigma), mouse anti-Calbindin (1:5000, Swant), guinea pig anti-GLAST (1:7000, Chemicon), anti-Pax6 (Covance, 1:300), anti-NCAM L1 (1:500, Millipore), guinea pig anti-VGluT1 (1:5000, Millipore), anti-TSPAN7 (1:500, donated by Dr Passafaro, anti-TAG1 (1:2, donated by Dr Hatten) mouse anti-β actin (1:50000, Abcam).

***Immunoprecipitation***

P8 cerebella were homogenized in cold lysis buffer (50 mM Tris-HCl pH 7.5, 2 mM EDTA, 150 mM NaCl, 1% Triton X-100, protease inhibitor cocktail (Sigma). Protein crosslinking was performed using 2 mM dithiobis succinimidylpropionate (DSP) (ThermoFisher) for 30 min at room temperature, and stopped by adding 20 mM Tris-HCl pH 7.5. Immunoprecipitation was performed by incubating with Dynabeads (Invitrogen) pre-coated with either 10 µg of goat/sheep IgG (Sigma) or 10 µg of anti-IgSF3 (R&D system) for 60 min at 4°C with constant rocking. After several washes with lysis buffer, immune complexes were eluted by resuspending the beads in sample buffer (6 M Urea, 2% (v/v) SDS, 200 µL of 20 mg/mL Bromophenol blue, 62.5 mM Tris-HCl, 10% (v/v) β-mercaptoethanol, 20% (v/v) glycerol) and heating the samples at 65°C for 15 min. Samples were run on a NuPAGE Novex 4-12% Bis-Tris gel (Invitrogen).

***Protein extraction and immunoblotting***

HEK-293H cells (Gibco) were plated at a density of $5x10^5$/well on coverslips previously coated with 10 ug/ml poly-D-lysine (Sigma). The day after plating cells were transfected with constructs of interest using Lipofectamine 2000 (Invitrogen). Cells were harvested in lysis buffer (50 mM Tris-HCl pH 7.5, 150 mM NaCl, 1% (v/v) SDS, 0.2% (v/v) sodium azide, 5% (w/v) sodium deoxycholate, 0.1% (v/v) NP-40), sonicated for 5 seconds three times and incubated at 4°C for 30 min. Lysates were then centrifuged at 20,000 *g* for 30 min and supernatants were collected for protein estimation using the Pierce BCA Protein Assay kit (Thermo Fisher Scientific). 10 µg of proteins were resolved on a NuPAGE Novex 4-12% Bis-Tris gel (Invitrogen). Immunoblotting was performed in 0.2% Tween/PBS, and signals were revealed in Amersham ECL Prime Western Blotting Detection Reagent (GE Healthcare) or SuperSignal West Femto Chemiluminescent Substrate (Thermo Fisher).

### *Microscopy and data analysis*

Imaging was performed using either a Nikon Digital Camera (DXM 1200) mounted on a Leica epifluorescence microscope (DMRB) or a confocal laser-scanning microscope (TCS SP5, Leica, Germany). Images for quantification of granule cell/Purkinje cell synapses (VGluT1/CaBP positive puncta) in mixed cultures were acquired on the confocal microscope at 63X magnification using a 0.2µM z-step. Synaptic contacts were analyzed using ImageJ-customized macro as follow. The CaBP and the VGluT1 objects found above a user-defined threshold were selected. Image calculator was used to extract the signal common to CaBP and VGluT1 images: the number and volume of these puncta were quantified with the 3D Object counter plugin from ImageJ. Images for measurements of dendritic length of granule cells were acquired on the confocal microscope at 40X magnification using 0.5µM z-step. A maximal stack projection was performed for each image using ImageJ and dendrites and axons were traced using the NeuronJ plugin of ImageJ.

### *Statistical analysis*

Statistical analysis was conducted using the unpaired T-test and the GraphPad Prism software (GraphPad software).

## Results

### *IgSF3, a new IgSF-CAM developmentally regulated in the brain*

Expression of IgSF8 and IgSF3 proteins in the human brain and their role of EWI proteins in regulating cell-cell interactions in diverse systems suggest a role during normal brain development. In accordance with this hypothesis, both *Igsf3* and *Igsf8* mRNAs are expressed at high levels and dynamically in the mouse cerebellum during the first three postnatal weeks, a critical period for the development of this structure. *Ptgfrn* and *Igsf2* are expressed at low levels or absent, respectively (Figure 1A). In situ hybridization (ISH) experiments for *Igsf3*, the most abundant member of the family in the developing cerebellum, confirmed a strikingly dynamic expression: *Igsf3* mRNA was detected at high levels at P0 and P7 but totally disappeared in the adult, in accordance with our qRT-PCR results. These ISH analyses also showed high and dynamically regulated levels of *Igsf3* mRNA in various other brain regions during the first postnatal weeks, such as the olfactory bulb, cortex, hippocampus, superior colliculus, inferior olive and spinal cord (Figure 1B).

To determine the expression pattern of the IgSF3 protein, we used a polyclonal antibody recognizing IgSF3 whose specificity was confirmed using immunocytochemistry and immunoblot in transfected HEK293 cells (Figure sup. 1) as well as RNA interference in cerebellar granule cells (Figure sup. 2C). The expression pattern of the IgSF3 protein, detected by immunolabeling experiments on mouse brain sections, correlated with the in situ hybridization data. In the cerebral cortex, the IgSF3 protein is found in the most superficial layer at P0 and becomes restricted to layer 2/3 with maturation. In the hippocampus, IgSF3, initially seen in all subfields, becomes restricted to the dentate gyrus. In the olfactory bulb, IgSF3 localizes to both mitral cells and granule cell layers.

This developmentally regulated expression pattern of IgSF3 in various brain regions is reminiscent of the one observed for other molecules belonging to the IgSF-CAMs family such as F3, TAG-1 and L1-CAM (Bizzoca et al., 2009; (Kuhar et al., 1993; Stottmann and Rivas, 1998; Powell et al., 1997; Sakurai et al., 2001)

***IgSF3 is a marker of differentiating cerebellar granule cells and parallel fibers***

The various functions played by IgSF-CAMs depend on the tight spatio-temporal control of their cellular and subcellular localization during development, as has been shown in particular for F3/contactin (Bizzoca et al., 2003, 2009; Liljelund et al., 1994). To gain further insight into the role of IgSF3 during brain development, we performed a detailed analysis of its cellular and subcellular localization in the mouse cerebellum at P0 and P7. ISH experiments showed that IgSF3 mRNA strongly localizes to the developing internal granular layer (IGL) (Figure 2A), whereas the IgSF3 protein is found both in the IGL and the nascent molecular layer (Figure 2B). This pattern is consistent with an expression of IGSF3 by post-mitotic granule cells, which extend their axons in the molecular layer and are the major cell type in the IGL. Pax6 is a transcription factor expressed in both mature granule cells and their precursors in the external granular layer (EGL) (Engelkamp et al., 1999; Yamasaki et al., 2001). Co-immunostaining experiments showed that nuclei from IgSF3 expressing cells were positive for Pax6 both in mouse brain sections (Figure 3A), and in dissociated cerebellar cultures at DIV0, a timepoint when cells can be clearly isolated (Figure 3B). Taken together, these results demonstrate that granule cells are the major source of IgSF3 expression during cerebellar development. IgSF3 immunostaining in the developing molecular layer could arise from its localization in parallel fibers, axons of granule cells, or in Purkinje cell dendritic spines. Co-immunolabeling with an antibody against Calbindin (CaBP), a cytoplasmic marker

specifically labeling PCs (Takahashi-Iwanaga et al., 1986), revealed IgSF3 around Purkinje cell dendrites (Figure 2C), but ISH experiments did not show any evident expression of IgSF3 mRNA in Purkinje cells (Figure 2A). Thus the abundant labeling for IgSF3 in the developing molecular layer is due to its localization in parallel fibers. The intense staining for IgSF3 detected at P0, a time when only few granule cells and parallel fibers are present, suggested that glia might be another source of IgSF3 expression in the developing brain. Indeed, the developing molecular layer also contains fibers from Bergmann glia that provide a scaffold for granule cell radial migration towards the IGL. Immunolabeling for IGSF3 using sections from a reporter mouse line that fluorescently label astrocytes and radial glial cells (Nolte et al., 2001) revealed some colocalization of IgSF3 immunostaining in fibers corresponding to Bergman glia in the P7 molecular layer (Figure 3C and D). Moreover, some isolated glial cells, identified in cerebellar cultures at DIV0 using immunolabeling for the glutamate aspartate transporter (GLAST) (Schmitt et al., 1997), clearly expressed also IgSF3 (arrows in Figure 3E). Taken together, these results show that differentiating granule cells are the major source of IgSF3 in the developing cerebellum, while glia also express this marker at early stages of development.

The successive stages of granule cell differentiation are characterized by the expression of different combinations of cell adhesion molecules, in particular of the IgSF-CAM family. TAG-1 is transiently expressed in pre-migratory granule cells in the inner part of the external granular layer (iEGL) starting from the time of parallel fiber extension (Yamamoto et al., 1986; Baeriswyl and Stoeckli, 2008; Kuhar et al., 1993), and disappears from granule cell axons when they connect Purkinje cell dendrites (Stottmann and Rivas, 1998). L1-CAM, another IGF-CAM, is expressed by more differentiated granule cells, and localizes in fasciculating parallel fibers (Persohn and Schachner, 1987). IgSF3 could likewise characterize a specific stage of granule cell differentiation. Extensive colocalization between IgSF3 and both TAG1 in the iEGL (Figure 4A and B), and L1 in the molecular layer (Fig. 4C and D) was shown by co-immunolabeling experiments in P7 cerebellar sections. IgSF3 was also detected, albeit at lower levels, all around granule cell somata and ascending axons in the internal granular layer. These results show that IgSF3 is a marker of developing parallel fibers.

The high levels of IgSF3 found in granule cell axonal terminals around Purkinje cell dendrites suggested it might be present at the parallel fiber/Purkinje cell (PF/PC) synapses. Colocalization experiments did not show extensive colocalization of IgSF3 with

VGluT1, a marker of mature PF/PC synapses (Miyazaki et al., 2003)(Figure 4E and F), suggesting that IgSF3 disappears when PF/PC synapses starts to mature.

Taken together, these results show that IgSF3 in the cerebellum is a marker of developing, but not mature, granule cells, both at the pre- and post-migratory stages. These findings raise several possibilities as to the developmental processes in which IgSF3 could be implicated during cerebellar development.

***IgSF3 regulates cerebellar granule cell differentiation***

IgSF CAMs have been implicated in several processes controlling cerebellar development, including proliferation, differentiation, migration and synaptogenesis (Buttiglione et al., 1996, 1998; Xenaki et al., 2011; Baeriswyl and Stoeckli, 2008; Burden-Gulley and Lemmon, 1995; Hortsch and Umemori, 2009; Maness and Schachner, 2007b; Schäfer and Frotscher, 2012; Stoeckli, 2004; Walsh and Doherty, 1997; Washbourne et al., 2004; Wiencken-Barger et al., 2004; Yoshihara et al., 1991). To gain further insights as to which one of these processes involves IgSF3, functional experiment using knockdown or overexpression approaches were performed in cerebellar cultures. First, we developed an RNA interference approach to suppress IgSF3 expression using small interfering RNAs (siRNA). In mixed cerebellar cultures, the expression pattern of IgSF3 mirrors the one found *in vivo*, since its mRNA levels are highest during the first few days with a peak at DIV4, and then decrease greatly (Figure 5A and sup. 2A). As *in vivo*, IgSF8 expression was much lower than the one for IgSF3 during the first week of culture. A mixture of four different siRNAs targeting IgSF3 (siIgSF3) applied at DIV0 induced more than 80% down-regulation of IgSF3 mRNA by DIV4 when compared to control non-targeting siRNAs (siCTR) as assessed by qRT-PCR (Figure sup. 2B), and greatly reduced the signal obtained by IgSF3 immunolabeling (Figure sup. 2C). No significant effect on the mRNA levels of IgSF8 and BAI3, two other genes expressed in cerebellar mixed cultures, could be detected in these conditions, further showing the specificity of our approach. This knockdown strategy was then used on cerebellar granule cell cultures (PAX6 positive cells are about 87% of total cells) to test whether IgSF3 is important for their survival and proliferation. In both IgSF3 and CTR siRNAs treated cultures, the total cell density remained relatively stable between DIV1 and DIV4, with only a small, but not significant, decrease in siIgSF3 cultures between DIV2 and DIV4 (Figure 5B, left graph). The proportion of proliferating (Ki67 positive) cells in granule cell cultures at the different stages examined was not changed by siIgSF3 compared to siCTR (Figure 5B, right graph).

Because of its high concentration in growing and maturing axons, IgSF3 could control GC differentiation. To test this hypothesis, we quantified dendritic and axonal morphology in isolated GFP labeled granule cells following knockdown of IgSF3. A 65% increase in total axonal length was shown in granule cells treated with siIgSF3 when compared to control cells (siCTR: 393.3±29.77 mm and siIgSF3: 651.8±80.09 mm. Figure 5C). No significant effect was detected on the number and length of dendritic processes or the number of axonal branches (Figure 5C). Conversely, IgSF3 overexpression in granule cells resulted in significantly shorter axons (siCTR: 1096±110.4 mm and IgSF3: 769±61.54 mm. Figure 5D) and less axonal branches. In this case, dendritic morphology was also affected with an increased number and length of dendrites (number of dendritic processes – CTR: 23.88±1.792 mm and IgSF3: 15.71±1.627 mm; length of dendritic processes – CTR: 20.27±1.867 mm and IgSF3: 40.98±5.250 mm. Figure 5D). Altogether, these results show that IgSF3 controls granule cell differentiation by inhibiting the growth of their axons and altering their dendritic morphology. Because IgSF3 inhibits axonal growth, it could control the timing of synapse formation. Quantification of the number and size of VGLUT1 puncta in cerebellar mixed cultures at DIV4 after IgSF3 knockdown did not reveal any changes compared to control conditions (Figure sup. 2D).

Overall, our results show that a major role for IgSF3 is to control the morphological differentiation of cerebellar granule cells, before they make synaptic contacts with their targets. Moreover, IgSF3 does not play a major role in regulating the proliferation and survival of cerebellar granule cells.

***IgSF3 forms a complex with Tetraspanin7 in the developing brain***

L1-CAM has been shown to promote neurite outgrowth by either homophilic binding or heterophilic binding to other Ig-CAMs, such as NCAM (Grumet and Edelman, 1988; Lemmon et al., 1989). To test whether IgSF3 could interact with L1-CAM, we affinity-purified IgSF3 from P8 cerebellar (Figure 6B, top panel) or forebrain homogenates (data not shown). In both cases, the presence of L1-CAM in the IgSF3 molecular complexes could not be detected.

EWI proteins have been shown to bind directly to tetraspanins (Sala-Valdés et al., 2006; Stipp et al., 2001), which are transmembrane proteins with diverse functions such as regulation of cell migration, fusion and signaling (Hemler, 2005). Using database mining (Doyle et al., 2008; http://mouse.brain-map.org/) and analysis of mRNA expression levels by qRT-PCR (Figure 6A), we identified tetraspanin 7 (TSPAN7) as a gene highly expressed

during cerebellar development starting at E17. A sharp increase in its expression was shown after P7, at the same time as granule cell differentiation. In situ hybridization data from the BGEM database showed that TSPAN7 was highly expressed by cerebellar granule cells during development (http://www.stjudebgem.org/, Figure 6A). Unlike L1-CAM, TSPAN7 was readily detected in IgSF3 affinity-purified samples from P8 cerebellar extracts showing that IgSF3 and TSPAN7 form a complex in the developing mouse cerebellum (Figure 6B, bottom panel). Furthermore, immunolabeling of HEK293H cells co-transfected with cDNAs coding for both IgSF3 and TSPAN7 showed the presence of IgSF3 in TSPAN7 domains at the plasma membrane (Figure 6C).

Overall, our results show that IgSF3 forms a complex with TSPAN7 both in transfected cells and in the developing mouse brain, while it does not stably interact with L1-CAM.

**Discussion**

The role of the EWI subfamily of IgSF-CAMs during brain development is still unknown. Our study shows that IgSF3, one of its four members, is expressed in various neuronal populations during the formation of neuronal circuits. In the cerebellum, it is transiently expressed in granule cells before their final maturation. It is highly concentrated in their axon terminals where it colocalizes with TAG-1 and L1, two other IgCAMs. Functional analysis shows that IgSF3 controls the differentiation of cultured cerebellar granule cells, in particular axonal growth. Moreover, IgSF3 and the tetraspanin TSPAN7 are part of the same molecular complex in the developing brain, suggesting a new signaling pathway for the regulation of neuronal differentiation.

In the cerebellum, different IgSF-CAMs mark different stages of granule cell maturation (Stoeckli, 2010; Kuhar et al., 1993). In the early postnatal period, the external granular layer (EGL) contains granule cell precursors (GCPs), whose proliferation is sustained by homotypic interneuronal contacts and whose differentiation is induced by interactions with astrocytes (Gao et al., 1991). Postmitotic/premigratory granule cells express TAG-1, and sit in the inner part of the external granular layer(Pickford et al., 1989; Furley et al., 1990; Yamamoto et al., 1990; Kuhar et al., 1993; Stottmann and Rivas, 1998). After a period of tangential migration, their soma migrates radially along glial fibers towards the internal granular layer, while the axon grows to form the parallel fibers. At this stage they express L1, another IgSF-CAM that is highly concentrated in granule cells axonal terminals (Lindner et al., 1983; Xenaki et al., 2011). IgSF3 is found in both TAG-1 positive

and L1 positive granule cells. It is particularly concentrated in the developing molecular layer where it completely overlaps with L1, but is also found in the cell bodies of granule cells in the IGL. Therefore, IgSF3 is a new marker that defines postmitotic differentiating granule cells, and whose expression is downregulated once differentiation is completed.

IgSF-CAMs regulate cell migration, axon growth, fasciculation and guidance, and synaptic plasticity (Kamiguchi and Lemmon, 2000; Schachner, 1997; Walsh and Doherty, 1997). In particular, they play important roles in granule cell differentiation. They control the differentiation of granule cell precursors cells, with TAG-1 and F3 acting antagonistically to regulate the proliferation of GCPs (Xenaki et al. 2011). TAG-1 is required for granule cell axon pathfinding (Baeriswyl and Stoeckli, 2008; Buttiglione et al., 1998) and the use of TAG-1 interfering antibodies in cerebellar cultures and slices is enough to impair axon emergence (Wang et al., 2011). L1 promotes axon growth, GC migration and synapse plasticity (Lemmon et al., 1989; Lindner et al., 1983; Schäfer and Frotscher, 2012). Our results, obtained using both loss-of-function and gain-of-function experiments, show that, while the protein IgSF3 does not regulate neuronal survival, it is an additional player in the regulation of granule cell differentiation, in particular axon elongation. It remains to be determined whether IgSF3 shares other functions with L1 and TAG-1 in the development of the cerebellum. IgSF3 is found in glial cells in dissociated cerebellar cultures at early stages and some IgSF3 can be localized in Bergmann glia fibers. Moreover the time course of IgSF3 expression in the developing cerebellum is similar to the one of astrotactin-1, a transmembrane protein that regulates granule cell migration along radial glia (Wilson et al., 2010). Therefore, It would be interesting to test whether IgSF3 can also regulate radial migration of granule cells.

Competition between IgCAMs regulates neuronal differentiation. For example TAG-1 is able to antagonize inhibitory effects on granule cell proliferation and axonal growth induced by F3, another IgCAM (Buttiglione et al., 1998; Xenaki et al., 2011). Similarly to F3, IgSF3 inhibits axonal elongation suggesting a possible interplay between IgSF3 and TAG-1/L1 for the control of axonal elongation during development. L1 has been shown to bind to Ig-class recognition molecules including TAG-1, F3 and NCAM (Thelen et al., 2002) Our results show no interaction of IgSF3 with L1 during brain development, suggesting that IgSF3 signaling involves other molecular partners. IgSF8 can directly bind several tetraspanins (Charrin et al., 2003; Clark et al., 2001; Sala-Valdés et al., 2006; Stipp et al., 2001), while both IgSF8 and Ptgfrn interact indirectly with the tetraspanin CD151 (Clark et al., 2001; Sala-Valdés et al., 2006). Tetraspanins are a large family of membrane proteins

expressed in a broad range of cell types and tissues and whose main function is to spatially organize transmembrane protein partners into functional microdomains called tetraspanin-enriched microdomains (TEMs) (Hemler, 2005). IgSF8 links TEMs and the actin cytoskeleton by forming a bridge between tetraspanins and ezrin-radixin-moesin proteins (Sala-Valdés et al., 2006). Regulation of the cytoskeleton dynamics, through the control of both actin and microtubule filaments, is necessary for axon growth and guidance (Schaefer et al., 2008; Dent and Gertler, 2003). Our results show that, in the developing brain and cerebellum, IgSF3 forms a molecular complex with the tetraspanin TSPAN7, which is highly expressed by cerebellar granule cells during development and in the adult cerebellum. TSPAN7 has been recently shown to be a key molecule for synapse maturation and function in hippocampal neurons (Bassani et al., 2012). While down-regulation of IgSF3 expression at early stages of neuronal differentiation does not modify the ability of granule cells to form synaptic contacts with Purkinje cells, it remains to be determined whether IgSF3 regulates the final number of synapses or synapse plasticity in mature neurons. Moreover, it will be interesting to study how the TSPAN7/IgSF3 interaction could regulate other processes during neuronal differentiation, such as axonal growth, and cell migration. Recently, it was shown that the level of the IgSF8 protein in the axon terminals of olfactory sensory neurons is downregulated by sensory input during development and is upregulated by lesion-induced reinnervation of the olfactory bulb (Ray and Treloar, 2012). Similarly F3 and TAG-1 are also regulated upon lesion (Haenisch et al., 2005; Soares et al., 2005). IgSF3 expression is downregulated at the time of mossy fiber synaptogenesis on granule cells and in many other neuronal populations after circuit maturation, suggesting a regulation of IgSF3 expression by neuronal activity in the circuit.

Proteins belonging to the IgSF-CAMs family play different functions depending on the neuronal population expressing them and their subcellular localization. The developmentally regulated expression of IgSF3 in various regions of the brain is reminiscent of the one found for other IgSF-CAMs. IgSF3 could play diverse and specific roles in the different cell types and regions where it is expressed during brain development, and in the adult brain. In particular, IgSF3 expression is very high in regions of adult neurogenesis, including the olfactory bulb and the hippocampus, suggesting a potential role in the integration of adult born neurons into neuronal circuits.

**Bibliography**


Baeriswyl, T., and Stoeckli, E.T. (2008). Axonin-1/TAG-1 is required for pathfinding of granule cell axons in the developing cerebellum. Neural Develop. *3*, 7.

Bassani, S., Cingolani, L.A., Valnegri, P., Folci, A., Zapata, J., Gianfelice, A., Sala, C., Goda, Y., and Passafaro, M. (2012). The X-linked intellectual disability protein TSPAN7 regulates excitatory synapse development and AMPAR trafficking. Neuron *73*, 1143–1158.

Bhella, D. (2015). The role of cellular adhesion molecules in virus attachment and entry. Philos. Trans. R. Soc. Lond. B. Biol. Sci. *370*, 20140035.

Bian, S. (2013). Cell Adhesion Molecules in Neural Stem Cell and Stem Cell- Based Therapy for Neural Disorders. In Neural Stem Cells - New Perspectives, L. Bonfanti, ed. (InTech),.

Bizzoca, A., Virgintino, D., Lorusso, L., Buttiglione, M., Yoshida, L., Polizzi, A., Tattoli, M., Cagiano, R., Rossi, F., Kozlov, S., et al. (2003). Transgenic mice expressing F3/contactin from the TAG-1 promoter exhibit developmentally regulated changes in the differentiation of cerebellar neurons. Dev. Camb. Engl. *130*, 29–43.

Bizzoca, A., Corsi, P., and Gennarini, G. (2009). The mouse F3/contactin glycoprotein. Cell Adhes. Migr. *3*, 53–63.

Burden-Gulley, S.M., and Lemmon, V. (1995). Ig superfamily adhesion molecules in the vertebrate nervous system: binding partners and signal transduction during axon growth. Semin. Dev. Biol. *6*, 79–87.

Buttiglione, M., Revest, J.-M., Rougon, G., and Faivre-Sarrailh, C. (1996). F3 Neuronal Adhesion Molecule Controls Outgrowth and Fasciculation of Cerebellar Granule Cell Neurites: A Cell-Type-Specific Effect Mediated by the Ig-like Domains. Mol. Cell. Neurosci. *8*, 53–69.

Buttiglione, M., Revest, J.M., Pavlou, O., Karagogeos, D., Furley, A., Rougon, G., and Faivre-Sarrailh, C. (1998). A functional interaction between the neuronal adhesion molecules TAG-1 and F3 modulates neurite outgrowth and fasciculation of cerebellar granule cells. J. Neurosci. Off. J. Soc. Neurosci. *18*, 6853–6870.

Charrin, S., Le Naour, F., Oualid, M., Billard, M., Faure, G., Hanash, S.M., Boucheix, C., and Rubinstein, E. (2001). The major CD9 and CD81 molecular partner. Identification and characterization of the complexes. J. Biol. Chem. *276*, 14329–14337.

Charrin, S., Le Naour, F., Labas, V., Billard, M., Le Caer, J.-P., Emile, J.-F., Petit, M.-A., Boucheix, C., and Rubinstein, E. (2003). EWI-2 is a new component of the tetraspanin web in hepatocytes and lymphoid cells. Biochem. J. *373*, 409–421.

Clark, K.L., Zeng, Z., Langford, A.L., Bowen, S.M., and Todd, S.C. (2001). PGRL is a major CD81-associated protein on lymphocytes and distinguishes a new family of cell surface proteins. J. Immunol. Baltim. Md 1950 *167*, 5115–5121.

Dent, E.W., and Gertler, F.B. (2003). Cytoskeletal Dynamics and Transport in Growth Cone Motility and Axon Guidance. Neuron *40*, 209–227.

Doyle, J.P., Dougherty, J.D., Heiman, M., Schmidt, E.F., Stevens, T.R., Ma, G., Bupp, S., Shrestha, P., Shah, R.D., Doughty, M.L., et al. (2008). Application of a translational profiling approach for the comparative analysis of CNS cell types. Cell *135*, 749–762.

Ellerman, D.A., Ha, C., Primakoff, P., Myles, D.G., and Dveksler, G.S. (2003). Direct binding of the ligand PSG17 to CD9 requires a CD9 site essential for sperm-egg fusion. Mol. Biol. Cell *14*, 5098–5103.

Engelkamp, D., Rashbass, P., Seawright, A., and van Heyningen, V. (1999). Role of Pax6 in development of the cerebellar system. Dev. Camb. Engl. *126*, 3585–3596.

Furley, A.J., Morton, S.B., Manalo, D., Karagogeos, D., Dodd, J., and Jessell, T.M. (1990). The axonal glycoprotein TAG-1 is an immunoglobulin superfamily member with neurite outgrowth-promoting activity. Cell *61*, 157–170.

Gao, W.O., Heintz, N., and Hatten, M.E. (1991). Cerebellar granule cell neurogenesis is regulated by cell-cell interactions in vitro. Neuron *6*, 705–715.

Gordón-Alonso, M., Sala-Valdés, M., Rocha-Perugini, V., Pérez-Hernández, D., López-Martín, S., Ursa, A., Álvarez, S., Kolesnikova, T.V., Vázquez, J., Sánchez-Madrid, F., et al. (2012). EWI-2 Association with α-Actinin Regulates T Cell Immune Synapses and HIV Viral Infection. J. Immunol. *189*, 689–700.

Grumet, M., and Edelman, G.M. (1988). Neuron-glia cell adhesion molecule interacts with neurons and astroglia via different binding mechanisms. J. Cell Biol. *106*, 487–503.

Haenisch, C., Diekmann, H., Klinger, M., Gennarini, G., Kuwada, J.Y., and Stuermer, C.A.O. (2005). The neuronal growth and regeneration associated Cntn1 (F3/F11/Contactin) gene is duplicated in fish: expression during development and retinal axon regeneration. Mol. Cell. Neurosci. *28*, 361–374.

Hemler, M.E. (2005). Tetraspanin functions and associated microdomains. Nat. Rev. Mol. Cell Biol. *6*, 801–811.

Hortsch, M., and Umemori, H. (2009). The Sticky Synapse: Cell Adhesion Molecules and Their Role in Synapse Formation and Maintenance (Springer Science & Business Media).

Kamiguchi, H., and Lemmon, V. (2000). IgCAMs: bidirectional signals underlying neurite growth. Curr. Opin. Cell Biol. *12*, 598–605.

Kondo, H., Yamamoto, M., Yamakuni, T., and Takahashi, Y. (1988). An immunohistochemical study of the ontogeny of the horizontal cell in the rat retina using an antiserum against spot 35 protein, a novel Purkinje cell-specific protein, as a marker. Anat. Rec. *222*, 103–109.

Kuhar, S.G., Feng, L., Vidan, S., Ross, M.E., Hatten, M.E., and Heintz, N. (1993). Changing patterns of gene expression define four stages of cerebellar granule neuron differentiation. Dev. Camb. Engl. *117*, 97–104.

Lemmon, V., Farr, K.L., and Lagenaur, C. (1989). L1-mediated axon outgrowth occurs via a homophilic binding mechanism. Neuron *2*, 1597–1603.

Liljelund, P., Ghosh, P., and van den Pol, A.N. (1994). Expression of the neural axon adhesion molecule L1 in the developing and adult rat brain. J. Biol. Chem. *269*, 32886–32895.

Lindner, J., Rathjen, F.G., and Schachner, M. (1983). L1 mono- and polyclonal antibodies modify cell migration in early postnatal mouse cerebellum. Nature *305*, 427–430.

Maness, P.F., and Schachner, M. (2007). Neural recognition molecules of the immunoglobulin superfamily: signaling transducers of axon guidance and neuronal migration. Nat. Neurosci. *10*, 19–26.

Matsuda, T., and Cepko, C.L. (2004). Electroporation and RNA interference in the rodent retina in vivo and in vitro. Proc. Natl. Acad. Sci. U. S. A. *101*, 16–22.

Miyazaki, T., Fukaya, M., Shimizu, H., and Watanabe, M. (2003). Subtype switching of vesicular glutamate transporters at parallel fibre-Purkinje cell synapses in developing mouse cerebellum. Eur. J. Neurosci. *17*, 2563–2572.

Montpellier, C., Tews, B.A., Poitrimole, J., Rocha-Perugini, V., D'Arienzo, V., Potel, J., Zhang, X.A., Rubinstein, E., Dubuisson, J., and Cocquerel, L. (2011). Interacting regions of CD81 and two of its partners, EWI-2 and EWI-2wint, and their effect on hepatitis C virus infection. J. Biol. Chem. *286*, 13954–13965.

Nolte, C., Matyash, M., Pivneva, T., Schipke, C.G., Ohlemeyer, C., Hanisch, U.K., Kirchhoff, F., and Kettenmann, H. (2001). GFAP promoter-controlled EGFP-expressing transgenic mice: a tool to visualize astrocytes and astrogliosis in living brain tissue. Glia *33*, 72–86.

Persohn, E., and Schachner, M. (1987). Immunoelectron microscopic localization of the neural cell adhesion molecules L1 and N-CAM during postnatal development of the mouse cerebellum. J. Cell Biol. *105*, 569–576.

Pickford, L.B., Mayer, D.N., Bolin, L.M., and Rouse, R.V. (1989). Transiently expressed, neural-specific molecule associated with premigratory granule cells in postnatal mouse cerebellum. J. Neurocytol. *18*, 465–478.

Powell, S.K., Rivas, R.J., Rodriguez-Boulan, E., and Hatten, M.E. (1997). Development of polarity in cerebellar granule neurons. J. Neurobiol. *32*, 223–236.

Ray, A., and Treloar, H.B. (2012). IgSF8: a developmentally and functionally regulated cell adhesion molecule in olfactory sensory neuron axons and synapses. Mol. Cell. Neurosci. *50*, 238–249.

Rivas, A., Ruegg, C.L., Zeitung, J., Laus, R., Warnke, R., Benike, C., and Engleman, E.G. (1995). V7, a novel leukocyte surface protein that participates in T cell activation. I. Tissue distribution and functional studies. J. Immunol. Baltim. Md 1950 *154*, 4423–4433.

Ruegg, C.L., Rivas, A., Madani, N.D., Zeitung, J., Laus, R., and Engleman, E.G. (1995). V7, a novel leukocyte surface protein that participates in T cell activation. II. Molecular cloning and characterization of the V7 gene. J. Immunol. Baltim. Md 1950 *154*, 4434–4443.

Sakurai, T., Lustig, M., Babiarz, J., Furley, A.J., Tait, S., Brophy, P.J., Brown, S.A., Brown, L.Y., Mason, C.A., and Grumet, M. (2001). Overlapping functions of the cell adhesion molecules Nr-CAM and L1 in cerebellar granule cell development. J. Cell Biol. *154*, 1259–1273.

Sala-Valdés, M., Ursa, A., Charrin, S., Rubinstein, E., Hemler, M.E., Sánchez-Madrid, F., and Yáñez-Mó, M. (2006). EWI-2 and EWI-F link the tetraspanin web to the actin cytoskeleton through their direct association with ezrin-radixin-moesin proteins. J. Biol. Chem. *281*, 19665–19675.

Saupe, S., Roizès, G., Peter, M., Boyle, S., Gardiner, K., and De Sario, A. (1998). Molecular cloning of a human cDNA IGSF3 encoding an immunoglobulin-like membrane protein: expression and mapping to chromosome band 1p13. Genomics *52*, 305–311.

Schachner, M. (1997). Neural recognition molecules and synaptic plasticity. Curr. Opin. Cell Biol. *9*, 627–634.

Schaefer, A.W., Schoonderwoert, V.T.G., Ji, L., Mederios, N., Danuser, G., and Forscher, P. (2008). Cytoskeletal Dynamics Underlying Neurite Outgrowth. Dev. Cell *15*, 146–162.

Schäfer, M.K.E., and Frotscher, M. (2012). Role of L1CAM for axon sprouting and branching. Cell Tissue Res. *349*, 39–48.

Schmitt, A., Asan, E., Püschel, B., and Kugler, P. (1997). Cellular and regional distribution of the glutamate transporter GLAST in the CNS of rats: nonradioactive in situ hybridization and comparative immunocytochemistry. J. Neurosci. Off. J. Soc. Neurosci. *17*, 1–10.

Shapiro, L., Love, J., and Colman, D.R. (2007). Adhesion molecules in the nervous system: structural insights into function and diversity. Annu. Rev. Neurosci. *30*, 451–474.

Soares, S., Traka, M., von Boxberg, Y., Bouquet, C., Karagogeos, D., and Nothias, F. (2005). Neuronal and glial expression of the adhesion molecule TAG-1 is regulated after peripheral nerve lesion or central neurodegeneration of adult nervous system. Eur. J. Neurosci. *21*, 1169–1180.

Sotelo, C. (2004). Cellular and genetic regulation of the development of the cerebellar system. Prog. Neurobiol. *72*, 295–339.

Stipp, C.S., Kolesnikova, T.V., and Hemler, M.E. (2001). EWI-2 is a major CD9 and CD81 partner and member of a novel Ig protein subfamily. J. Biol. Chem. *276*, 40545–40554.

Stoeckli, E.T. (2004). Ig superfamily cell adhesion molecules in the brain. Handb. Exp. Pharmacol. 373–401.

Stoeckli, E.T. (2010). Neural circuit formation in the cerebellum is controlled by cell adhesion molecules of the Contactin family. Cell Adhes. Migr. *4*, 523–526.

Stottmann, R.W., and Rivas, R.J. (1998). Distribution of TAG-1 and synaptophysin in the developing cerebellar cortex: relationship to Purkinje cell dendritic development. J. Comp. Neurol. *395*, 121–135.

Tabata, T., Sawada, S., Araki, K., Bono, Y., Furuya, S., and Kano, M. (2000). A reliable method for culture of dissociated mouse cerebellar cells enriched for Purkinje neurons. J. Neurosci. Methods *104*, 45–53.

Takahashi-Iwanaga, H., Kondo, H., Yamakuni, T., and Takahashi, Y. (1986). An immunohistochemical study on the ontogeny of cells immunoreactive for spot 35 protein, a novel Purkinje cell-specific protein, in the rat cerebellum. Brain Res. *394*, 225–231.

Thelen, K., Kedar, V., Panicker, A.K., Schmid, R.-S., Midkiff, B.R., and Maness, P.F. (2002). The neural cell adhesion molecule L1 potentiates integrin-dependent cell migration to extracellular matrix proteins. J. Neurosci. Off. J. Soc. Neurosci. *22*, 4918–4931.

Walsh, F.S., and Doherty, P. (1997). Neural cell adhesion molecules of the immunoglobulin superfamily: role in axon growth and guidance. Annu. Rev. Cell Dev. Biol. *13*, 425–456.

Wang, W., Karagogeos, D., and Kilpatrick, D.L. (2011). The Effects of Tag-1 on the Maturation of Mouse Cerebellar Granule Neurons. Cell. Mol. Neurobiol. *31*, 351–356.

Washbourne, P., Dityatev, A., Scheiffele, P., Biederer, T., Weiner, J.A., Christopherson, K.S., and El-Husseini, A. (2004). Cell Adhesion Molecules in Synapse Formation. J. Neurosci. *24*, 9244–9249.

Wiencken-Barger, A.E., Mavity-Hudson, J., Bartsch, U., Schachner, M., and Casagrande, V.A. (2004). The Role of L1 in Axon Pathfinding and Fasciculation. Cereb. Cortex *14*, 121–131.

Wilson, P.M., Fryer, R.H., Fang, Y., and Hatten, M.E. (2010). Astn2, a novel member of the astrotactin gene family, regulates the trafficking of ASTN1 during glial-guided neuronal migration. J. Neurosci. Off. J. Soc. Neurosci. *30*, 8529–8540.

Xenaki, D., Martin, I.B., Yoshida, L., Ohyama, K., Gennarini, G., Grumet, M., Sakurai, T., and Furley, A.J.W. (2011). F3/contactin and TAG1 play antagonistic roles in the regulation of sonic hedgehog-induced cerebellar granule neuron progenitor proliferation. Development *138*, 519–529.

Yamamoto, M., Boyer, A.M., Crandall, J.E., Edwards, M., and Tanaka, H. (1986). Distribution of stage-specific neurite-associated proteins in the developing murine nervous system recognized by a monoclonal antibody. J. Neurosci. Off. J. Soc. Neurosci. *6*, 3576–3594.

Yamamoto, M., Hassinger, L., and Crandall, J.E. (1990). Ultrastructural localization of stage-specific neurite-associated proteins in the developing rat cerebral and cerebellar cortices. J. Neurocytol. *19*, 619–627.

Yamasaki, T., Kawaji, K., Ono, K., Bito, H., Hirano, T., Osumi, N., and Kengaku, M. (2001). Pax6 regulates granule cell polarization during parallel fiber formation in the developing cerebellum. Dev. Camb. Engl. *128*, 3133–3144.

Yoshihara, Y., Oka, S., Ikeda, J., and Mori, K. (1991). Immunoglobulin superfamily molecules in the nervous system. Neurosci. Res. *10*, 83–105.

**Figure legends**

**Fig.1. Igsf3 is expressed in the developing mouse brain.**

(A) Analysis of mRNA expression of the four EWI family members by quantitative RT-PCR at different stages of mouse cerebellar development. Data are normalized to the housekeeping gene Gapdh. Mean±SEM of 3 independent experiments.

(B) Expression of *Igsf3* mRNA in various regions of the mouse brain detected by in situ hybridization at postnatal day 0 (P0), P7 and adult stage. Scale bar = 500 µm.

(C) Expression of IGSF3 protein detected by immunohistochemistry using sections from P0, P7 and adult mouse brain. Scale bar= 500 µm.

**Fig. 2. Expression of Igsf3 in the developing cerebellum.**

(A) *Igsf3* mRNA expression detected by in situ hybridization in the mouse cerebellum at P0 and P7. Scale bar=100 µm.

(B) IGSF3 protein localization detected by immunohistochemistry in the mouse cerebellum at P0 and P7. Scale bar=100 µm.

(C) Co-immunolabeling using an antibody against calbindin (CaBP) to label Purkinje cells specifically shows that the IGSF3 protein is abundant around Purkinje cell bodies and growing dendrites in P7 mouse cerebellum. Scale bar = 10 µm. External granular layer (EGL), molecular layer (ML), Purkinje cell layer (PCL), Internal granular layer (IGL).

**Fig. 3. In the developing cerebellum, IGSF3 is expressed by a majority of granule cells and by some glial cells.**

(A) Co-immunolabeling for IGFS3 and Pax6, a marker of postmitotic granule cells, in P7 mouse brain sections. Scale bar = 50 µm.

(B) Co-immunolabeling for IGSF3 and Pax6, a marker of postmitotic granule cells, in mixed cerebellar cultures at days *in vitro* 0 (DIV0). Scale bar = 20 µm.

(C) Immunolabeling for IGSF3 (green) in cerebellar sections from a transgenic mouse expressing eGFP in astrocytes and radial glial cells (hGFAP-GFP). Scale bar =10 µm.

(D) High magnification of the region indicated in Figure 2C (white rectangle) shows that IGSF3 immunostaining overlaps partially with some glial fibers, particularly in the ML. Scale bar =10 µm.

(E) Co-immunolabeling for IGSF3 and GLAST, a marker of glial cells, and Hoechst counterstaining in mixed cerebellar cultures at DIV0. IGSF3 is expressed in some glial cells

(arrows). Scale bar = 20 μm. External granular layer (EGL), Molecular layer (ML), Purkinje cell layer (PCL), Internal granular layer (IGL).

**Fig. 4. IGSF3 is concentrated at developing granule cell axonal terminals.**

(A) Co-immunolabeling for IGSF3 and TAG-1, a marker for premigratory granule neurons, in P7 mouse brain sections. Scale bar = 50 μm.

(B) High magnification of the region defined by the white rectangle in Figure 5A shows colocalization of IGSF3 with TAG-1. Scale bar = 10 μm.

(C) Co-immunolabeling for IGSF3 and L1-CAM, a marker for granule cell axonal terminals, in P7 mouse brain sections. Scale bar = 50 μm.

(D) High magnification of the region defined by the white rectangle in Figure 5C shows extensive colocalization of IGSF3 with L1-CAM. Scale bar = 10 μm.

(E) Co-immunolabeling for IGSF3 and vGLUT-1, a marker for mature parallel fiber/Purkinje cell synapses, in P7 mouse brain sections. Scale bar = 50 μm.

(F) High magnification of the region defined by the white rectangle in Figure 5E shows only partial colocalization of IGSF3 with VGluT1. Scale bar = 10 μm. External granular layer (EGL), Molecular layer (ML), Purkinje cell layer (PCL), Internal granular layer (IGL).

**Fig. 5. IgSF3 regulates granule cell morphology.**

(A) Expression of *Igsf3*, *Igsf8* and *Bai3* mRNAs in cerebellar granule cell cultures at different days *in vitro* (DIV) was assessed by quantitative RT-PCR analysis. Data are relative to the housekeeping gene Rpl13. Mean±SEM of 3 independent experiments.

(B) Top: Total cell number in cerebellar granule cell cultures at different DIVs. siRNA treatment was started at DIV0. Accell non-targeting control siRNA (siCTR), Accell siRNA targeting mouse siIgSF3 (siIgSF3). No significant effect was detected. Unpaired T-test. Bottom: Percentage of proliferating cells expressing the proliferation marker Ki67 over the total number of Hoechst positive cells in cerebellar granule cell cultures at different DIVs. mean±SEM, 3-6 independent experiments per condition.

(C) Left: representative cerebellar granule cells transfected with membrane GFP.siRNA treatment was started at DIV0. Accell non-targeting control siRNA (siCTR), Accell siRNA targeting mouse siIgSF33 (siIgSF3). Treatment started at DIV0, analysis at DIV4. Scale bar =50 μm. Right: quantitative analysis of dendrite number, length and axonal length of granule cells. mean±SEM of 3 independent experiments, 20-25 cells, *$p<0.05$. Unpaired T-test.

(D) Left: representative granule cells transfected with mbGFP (CTR) or IgSF3 + mbGFP (IgSF3) at DIV1 and analyzed at DIV4. Scale bar =50 μm. Right: quantitative analysis of dendrite number, length and axonal length of granule cells. mean±SEM of 3 independent experiments, 20-25 cells,***p<0.001, **p<0.01, *p<0.05. Unpaired T-test.

**Fig. 6. IgSF3 is in the same molecular complex as TSPAN7.**

(A) Top: *Tspan7* mRNA expression was assessed by quantitative RT-PCR on cDNA extracts from the mouse cerebellum at different stages of development. Data are relative to the housekeeping gene *Gapdh*. Mean±SEM of 3 independent experiments. Bottom: *Tspan7* mRNA expression in the P7 cerebellum mRNA by in situ hybridization (Brain Gene Expression Map, http://www.stjudebgem.org/).

(B) IgSF3 affinity-purification from P8 cerebella shows an IgSF3/TSPAN7 complex in the mouse brain. Total input lysate (IN), flow through (FT), Immunoprecipitates (IP); control: beads coated with IgG (IP IgG), IgSF3 pull down: beads coated with IgSF3 antibody (IP IgSF3). Samples were probed for the presence of IgSF3 (upper panel), L1-CAM (middle panel), TSPAN7 (bottom panel).

(C) Co-localization of IgSF3 and TSPAN7 shown by immunofluorescent labelling of transfected HEK293H cells. Scale bar = 10 μm.

**Fig. 1 Supplementary. Specific immunodetection of mouse IgSF3.**

(A) Immunofluorescent labeling using a polyclonal antibody raised against human IGSF3 showed a specific labeling of HEK293 cells transiently transfected with a bidirectional vector co-expressing mGFP and IGSF3, but not in those transfected with the vector coding for mGFP alone. Scale bar = 50 μm. (B) Western blot analysis of protein lysates from HEK293 cells using the same antibody reveals two specific bands of molecular weight ~ 200 and 225 kDa only in extracts from HEK293 cells transfected with mGFP and IGSF3 (IGSF3 lane), but not in those not transfected (NT lane). Beta-actin was used as a loading control.

**Fig. 2 Supplementary. IgSF3 downregulation does not affect synaptogenesis.**

(A) Quantitative RT-PCR analysis of *Igsf3*, *Igsf8* and *Bai3* mRNAs in extracts from cerebellar mixed cultures at different days *in vitro* (DIV) show a similar time course for *Igsf3* as the one detected *in vivo*. Data are normalized to the housekeeping gene *Gapdh*. Mean±SEM of 3 independent experiments.

(B) Validation of specific Igsf3 knockdown by siRNAs in cerebellar mixed cultures using quantitative RT-PCR for *Igsf3*, *Igsf8* and *Bai3* mRNA. Accell non-targeting control siRNA (siCTR), Accell siRNA targeting mouse siIgsf3 (siIgsf3). Data are relative to the housekeeping gene GAPDH and normalized to the control values. Mean±SEM of 3 independent experiments. **p<0.01 Unpaired T-test.

(C) Validation of Igsf3 knockdown by siRNAs in cerebellar mixed cultures using immunofluorescent staining for IGSF3. Hoechst fluorescent nuclear staining shows the cell density. Accell non-targeting control siRNA (siCTR), Accell siRNA targeting mouse siIgsf3 (siIgsf3). Scale bar = 50 µm.

(D) Quantitative analysis of the number and size of excitatory synapses labelled using an antibody against vGLUT-1in control cerebellar mixed cultures (siCTR) or after Igsf3 downregulation (siIgsf3). Treatment starting at DIV0, analysis at DIV4. No statistical differences are observed, mean±SEM of 3 independent experiments, total of 30 cells per condition, Unpaired T-test.

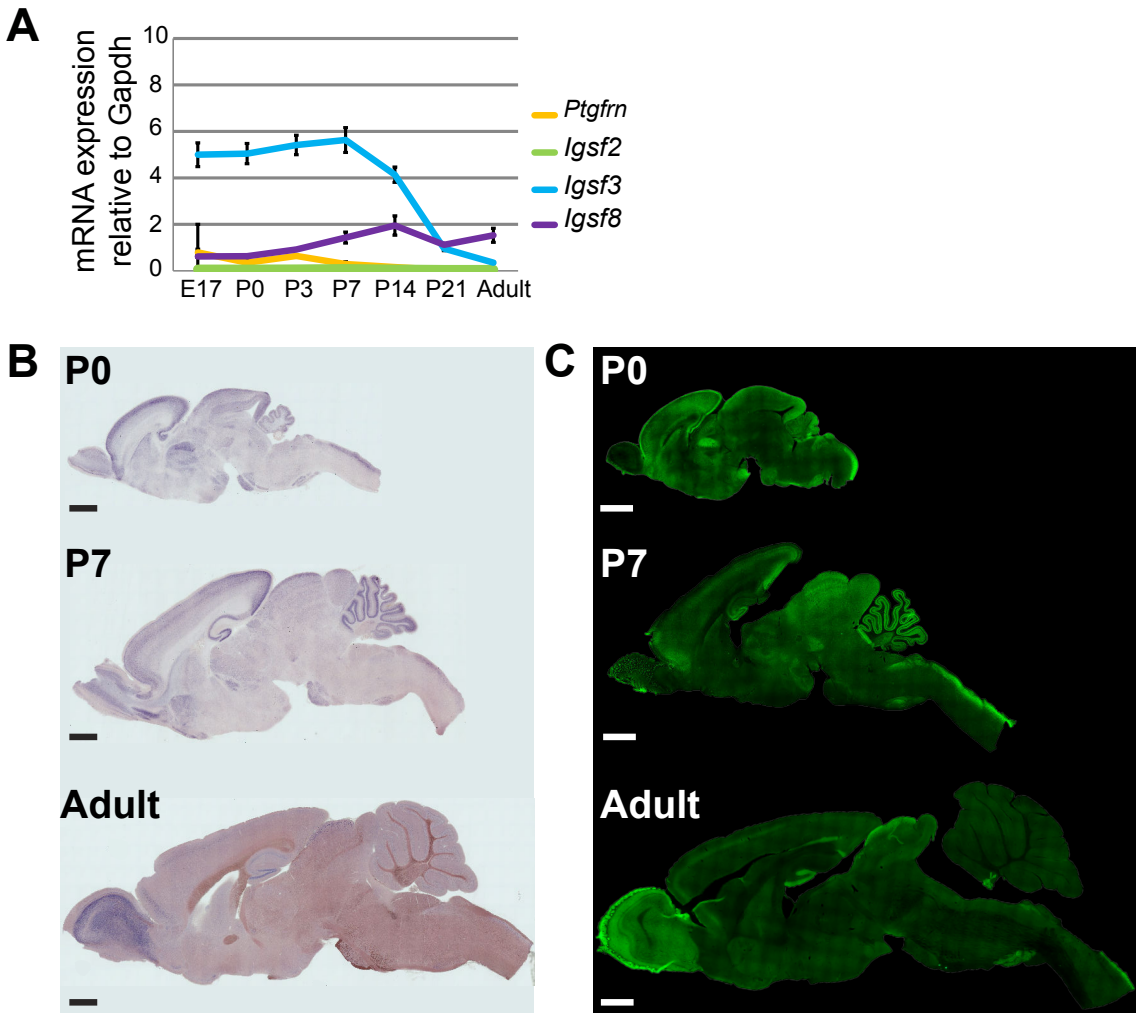
A
mRNA expression relative to Gapdh
10
8
6
4
2
0
E17 P0 P3 P7 P14 P21 Adult
Ptgfrn
Igsf2
Igsf3
Igsf8
B
P0
P7
Adult
C
P0
P7
Adult

**Figure 1**

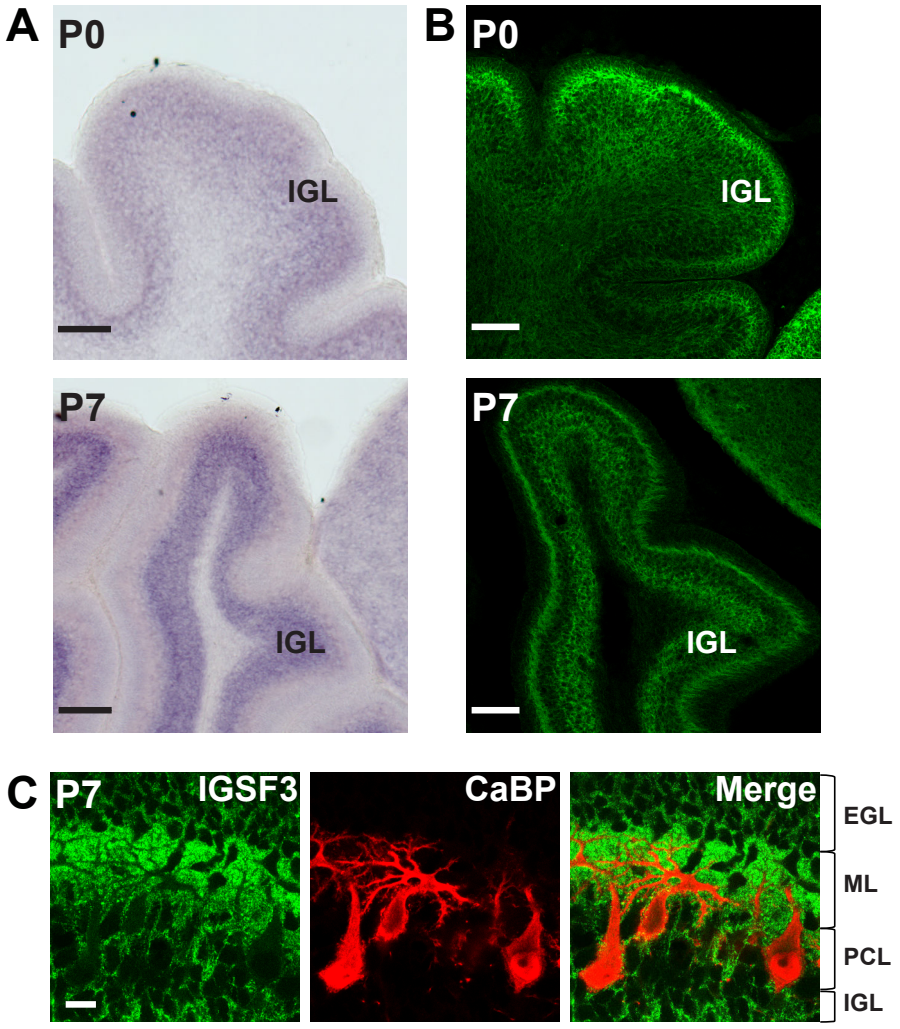
A
P0
IGL
B
P0
IGL
P7
IGL
P7
IGL
C
P7
IGSF3
CaBP
Merge
EGL
ML
PCL
IGL

**Figure 2**

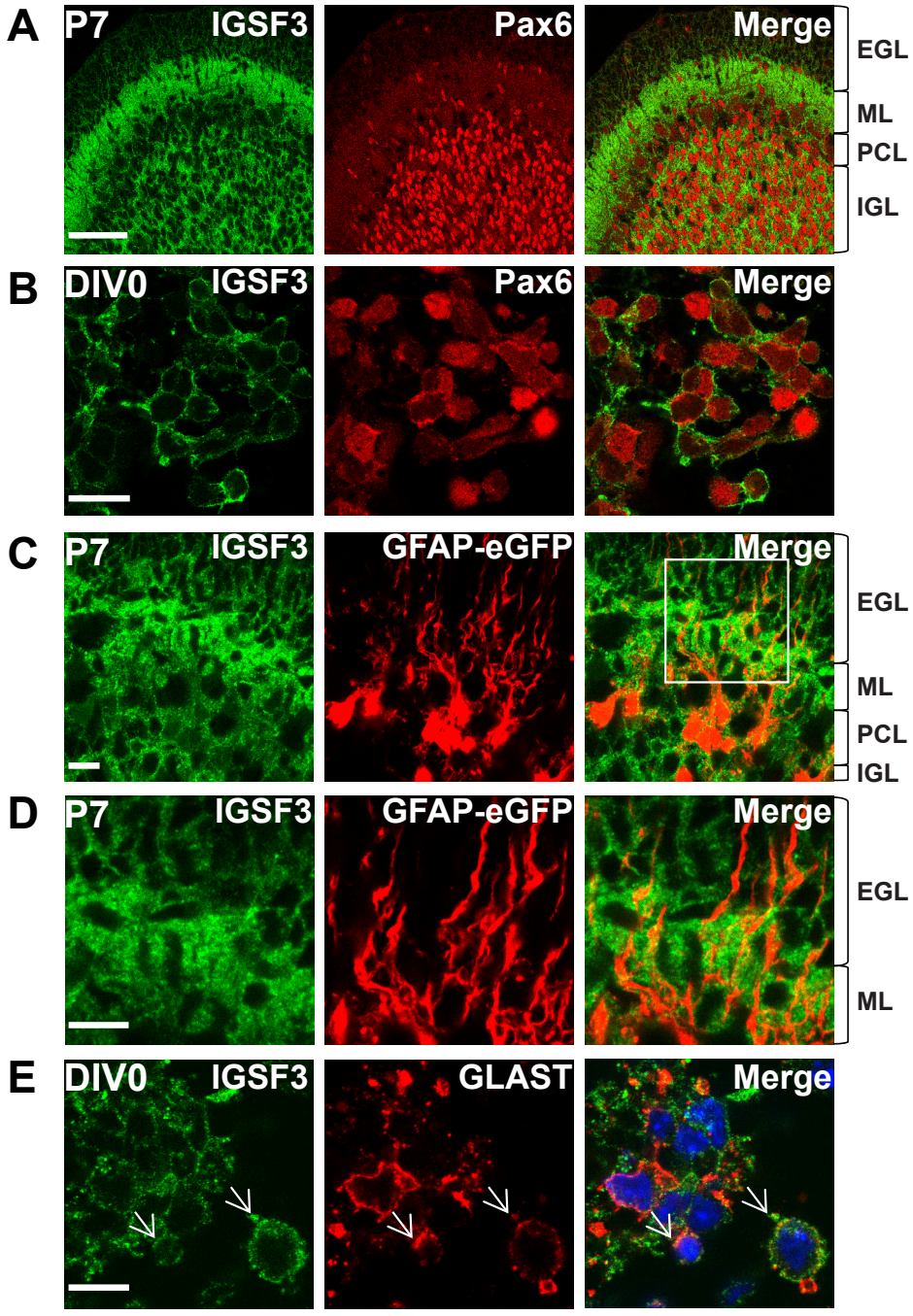
A
P7
IGSF3
Pax6
Merge
EGL
ML
PCL
IGL
B
DIV0
IGSF3
Pax6
Merge
C
P7
IGSF3
GFAP-eGFP
Merge
EGL
ML
PCL
IGL
D
P7
IGSF3
GFAP-eGFP
Merge
EGL
ML
E
DIV0
IGSF3
GLAST
Merge

**Figure 3**

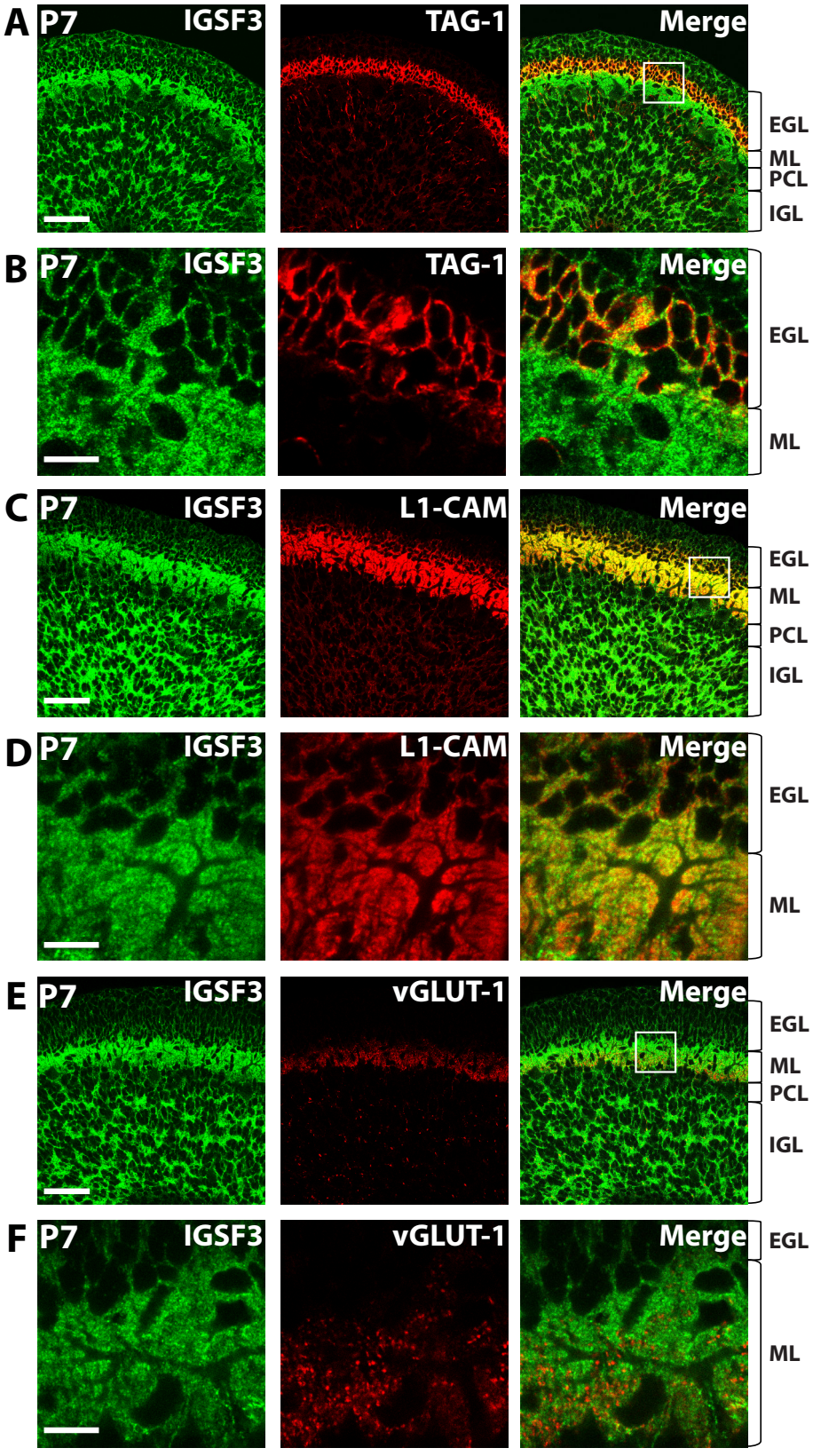
A
P7
IGSF3
TAG-1
Merge
EGL
ML
PCL
IGL
B
P7
IGSF3
TAG-1
Merge
EGL
ML
C
P7
IGSF3
L1-CAM
Merge
EGL
ML
PCL
IGL
D
P7
IGSF3
L1-CAM
Merge
EGL
ML
E
P7
IGSF3
vGLUT-1
Merge
EGL
ML
PCL
IGL
F
P7
IGSF3
vGLUT-1
Merge
EGL
ML

**Figure 4**

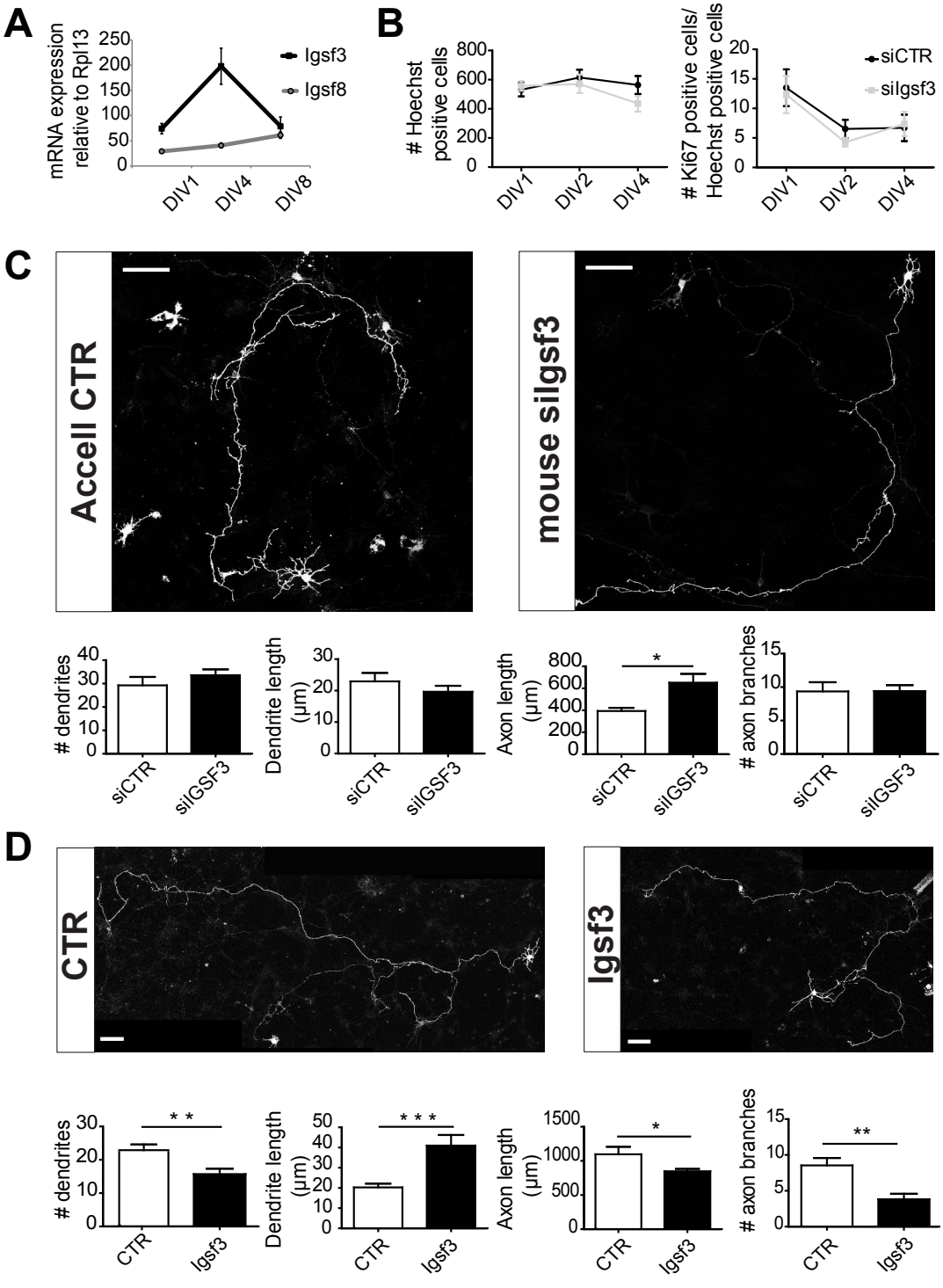
A
mRNA expression relative to Rpl13
Igsf3
Igsf8
DIV1
DIV4
DIV8
B
# Hoechst positive cells
DIV1
DIV2
DIV4
# Ki67 positive cells/ Hoechst positive cells
siCTR
siIgsf3
C
Accell CTR
mouse siIgsf3
# dendrites
Dendrite length (µm)
Axon length (µm)
# axon branches
siCTR
siIGSF3
D
CTR
Igsf3
CTR
Igsf3

**Figure 5**

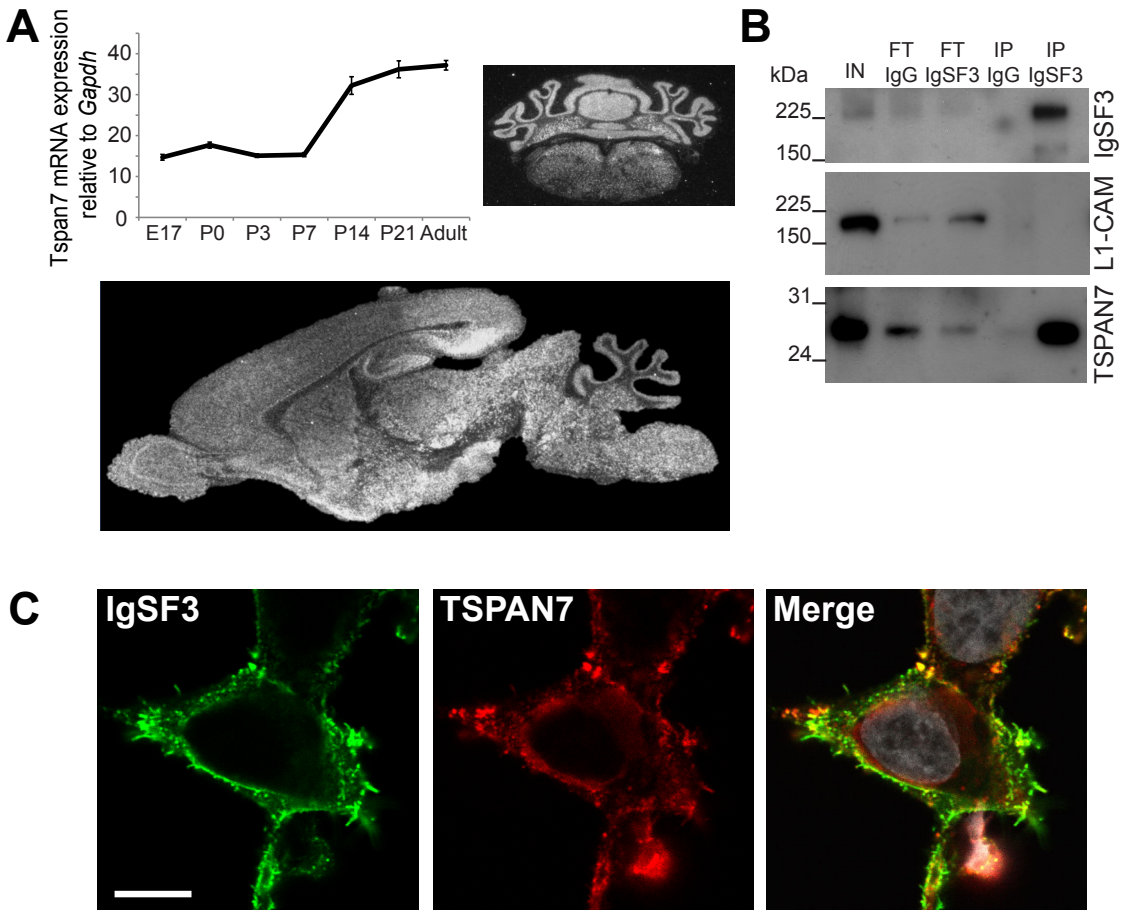
A
Tspan7 mRNA expression relative to Gapdh
40
30
20
10
0
E17
P0
P3
P7
P14
P21
Adult
B
kDa
IN
FT IgG
FT IgSF3
IP IgG
IP IgSF3
225
150
IgSF3
225
150
L1-CAM
31
24
TSPAN7
C
IgSF3
TSPAN7
Merge

**Figure 6**

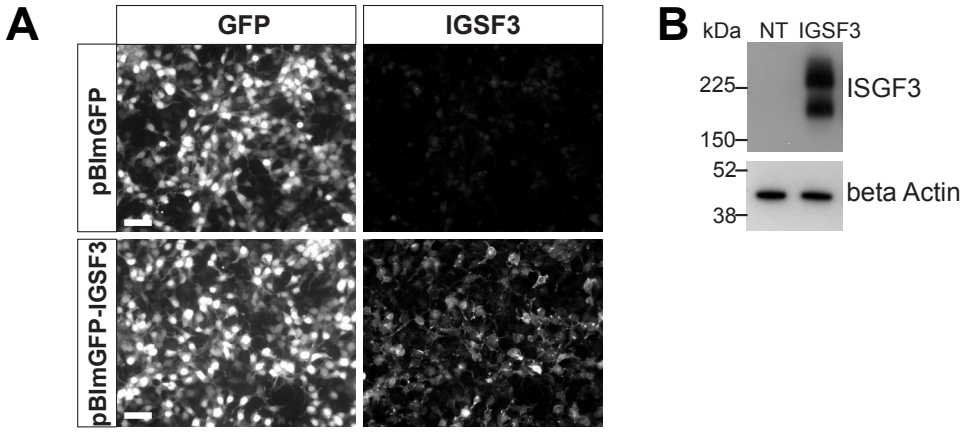


**Supplemental Figure 1**

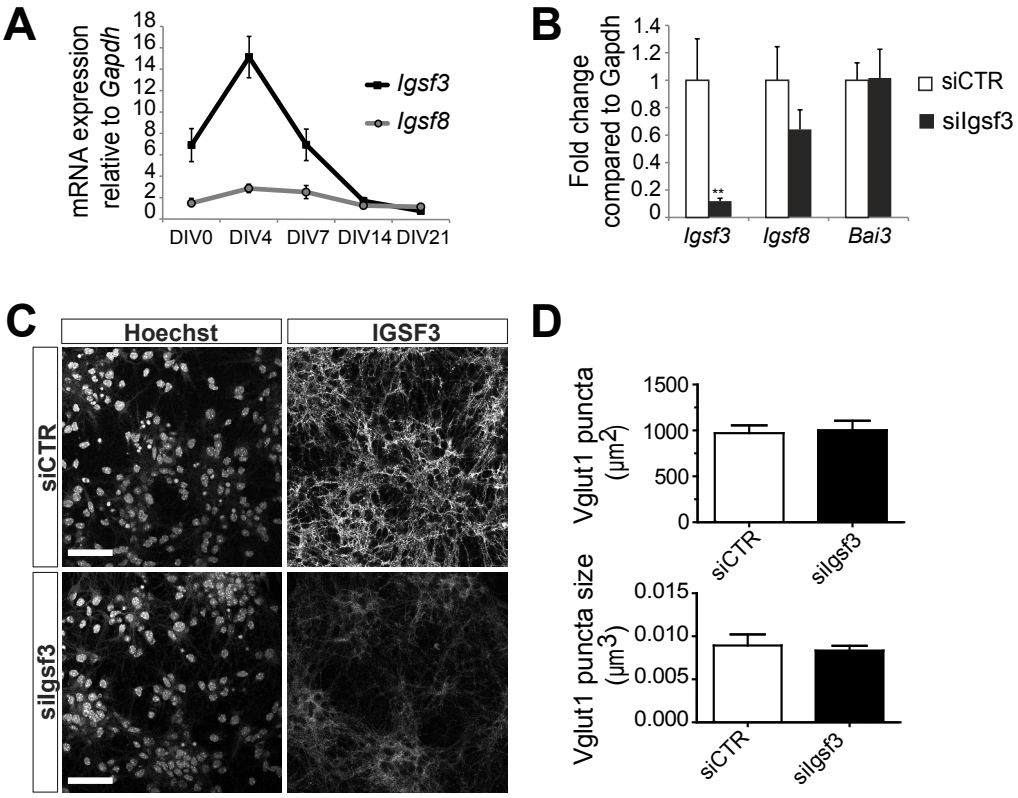


**Supplemental Figure 2**

# BIBLIOGRAPHY

**- A -**


Ahmad-Annuar, A., Ciani, L., Simeonidis, I., Herreros, J., Fredj, N B., Rosso, S B., Hall, A., Brickley, S., & Salinas, P C. (2006). Signaling across the synapse: a role for Wnt and Dishevelled in presynaptic assembly and neurotransmitter release. *The Journal of Cell Biology*, *174*(1), 127–139.

Ahmari, S. E., & Smith, S. J. (2002). Knowing a nascent synapse when you see it. *Neuron*, *34*(3), 333–336.

Akira, S., Uematsu, S., & Takeuchi, O. (2006). Pathogen Recognition and Innate Immunity. *Cell*, *124*(4), 783–801.

Alba, A., Kano, M., Chen, C., Stanton, M. E., Fox, G. D., Herrup, K., Zwingman, T. A., & Tonegawa, S. (1994). Deficient Cerebellar Long-Term Depression and Impaired Motor Learning in mGluR1 Mutant Mice. *Cell, 79*, 377-388.

Albus, J. S. (1971). A theory of cerebellar function. *Mathematical Biosciences*, 10, 25-61.

Altman, J. (1972). Postnatal development of the cerebellar cortex in the rat. II. Phases in the maturation of Purkinje cells and of the molecular layer. *Journal of Comparative Neurology*, *145*(4), 399–463.

Altman, J. (1973). Experimental reorganization of the cerebellar cortex. IV. Parallel fiber reorientation following regeneration of the external germinal layer. *Journal of Comparative Neurology*, *149*(2), 181–192.

Altman, J., & Bayer, S. A. (1985a). Embryonic development of the rat cerebellum. I. Delineation of the cerebellar primordium and early cell movements. *Journal of Comparative Neurology*, *231*(1), 1–26.

Altman, J., & Bayer, S. A. (1985b). Embryonic development of the rat cerebellum. II. Translocation and regional distribution of the deep neurons. *Journal of Comparative Neurology*, *231*(1), 27–41.

Altman, J., & Bayer, S. A. (1987). Development of the precerebellar nuclei in the rat: II. The intramural olivary migratory stream and the neurogenetic organization of the inferior olive. *Journal of Comparative Neurology*, *257*(4), 490–512.

Ango, F., di Cristo, G., Higashiyama, H., Bennett, V., Wu, P., & Huang, Z. J. (2004). Ankyrin-based subcellular gradient of neurofascin, an immunoglobulin family protein, directs GABAergic innervation at purkinje axon initial segment. *Cell*, *119*(2), 257–272.

Ango, F., Wu, C., Van der Want, J. J., Wu, P., Schachner, M., & Huang, Z. J. (2008). Bergmann Glia and the Recognition Molecule CHL1 Organize GABAergic Axons and Direct Innervation of Purkinje Cell Dendrites. *PLoS Biology*, *6*(4), 739–756.

Araki, K., Meguro, H., Kushiya, E., Takayama, C., Inoue, Y., & Mishina, M. (1993). Selective expression of the glutamate receptor channel δ2 subunit in cerebellar Purkinje cells. *Biochemical and Biophysical Research Communications*, *197*(3), 1267–1276.

Armstrong, C. L., & Hawkes, R. (2000). Pattern formation in the cerebellar cortex. *Biochemistry and Cell Biology = Biochimie Et Biologie Cellulaire*, *78*(5), 551–562.

Azizi, S. A., & Woodward, D. J. (1987). Inferior Olivary Nuclear Complex of the Rat: Morphology and Comments on the Principles of Organization Within the Olivo-cerebellar System. *The Journal of Comparative Neurology, 263*, 467-484.

**- B -**


Babbitt, B. P., Allen, P. M., Matsueda, G., Haber, E., & Unanue, E. R. (1985). Binding of immunogenic peptides to Ia histocompatibility molecules. *Nature*, *317*(6035), 359–361.

Bao, D., Pang, Z., & Morgan, J. I. (2005). The structure and proteolytic processing of Cbln1 complexes. *Journal of Neurochemistry*, *95*(3), 618–629.

Bao, D., Pang, Z., Morgan, M. A., Parris, J., Rong, Y., Li, L., & Morgan, J. I. (2006). Cbln1 Is Essential for Interaction-Dependent Secretion of Cbln3. *Molecular and Cellular Biology*, *26*(24), 9327–9337.

Barlow, P. N., Baron, M., Norman, D. G., Day, A. J., Willis, A. C., Sim, R. B., & Campbell, I. D. (1991). Secondary structure of a complement control protein module by two-dimensional 1H NMR. *Biochemistry (Washington)*, *30*(4), 997–1004.

Barnabé-Heider, F., Wasylnka, J. A., Fernandes, K. J. L., Porsche, C., Sendtner, M., Kaplan, D. R., & Miller, F. D. (2005). Evidence that Embryonic Neurons Regulate the Onset of Cortical Gliogenesis via Cardiotrophin-1. *Neuron*, *48*(2), 253–265.

Barrett, R. M., & Wood, M. A. (2008). Beyond transcription factors: The role of chromatin modifying enzymes in regulating transcription required for memory. *Learning & Memory*, *15*(7), 460–467.

Bats, C., Groc, L., & Choquet, D. (2007). The Interaction between Stargazin and PSD-95 Regulates AMPA Receptor Surface Trafficking. *Neuron*, *53*(5), 719–734.

Bauer, S., Kerr, B. J., & Patterson, P. H. (2007). The neuropoietic cytokine family in development, plasticity, disease and injury. *Nature Reviews Neuroscience*, *8*(3), 221–232.

Bauerfeind, R., Jelinek, R., Hellwig, A., & Huttner, W. B. (1995). Neurosecretory vesicles can be hybrids of synaptic vesicles and secretory granules. *Proceedings of the National Academy of Sciences*, *92*(16), 7342–7346.

Bayer, S. A. (1985). Hippocampal region. *The Rat Nervous System*.

Beattie, E. C., Stellwagen, D., Morishita, W., Bresnahan, J. C., Keun Ha, B., Zastrow, von, M., Beattie, M. S., & Malenka, R. C. (2002). Control of synaptic strength by glial TNFα. *Science,* 295(5563), 2282-2285.

Bekirov, I. H., Needleman, A., Zhang, W., & Benson, D. L. (2002). Identification and localization of multiple classic cadherins in developing rat limbic system. *Neuroscience,* 115(1), 213-227.

Benke, T. A., Luthi, A., Isaac, J., & Collingridge, G. L. (1998). Modulation of AMPA receptor unitary conductance by synaptic activity. *Nature*, *393*(6687), 793–797.

Benson, D. L., & Tanaka, H. (1998). N-cadherin redistribution during synaptogenesis in hippocampal neurons. *The Journal of Neuroscience*, *18*(17), 6892–6904.

Bettler, B. (2004). Molecular Structure and Physiological Functions of $GABA_B$ Receptors. *Physiological Reviews*, *84*(3), 835–867.

Bialas, A. R., & Stevens, B. (2013). TGF-β signaling regulates neuronal C1q expression and developmental synaptic refinement. *Nature Neuroscience*, *16*(12), 1773–1782.

Biederer, T., & Sudhof, T. C. (2000). Mints as Adaptors: Direct binding to neurexins and recruitment of Munc18. *Journal of Biological Chemistry*, *275*(51), 39803–39806.

Biederer, T., Sara, Y., Mozhayeva, M., Atasoy, D., Liu, X., Kavalali, E. T., & Sudhof, T. C. (2002).

SynCAM, a synaptic adhesion molecule that drives synapse assembly. *Science, 297,* 1525-1531.

Biermann, B., Ivankova-Susankova, K., Bradaia, A., Abdel Aziz, S., Besseyrias, V., Kapfhammer, J. P., Missler, M., Gassmann, M., & Bettler, B. (2010). The Sushi domains of $GABA_B$ receptors function as axonal targeting signals. *Journal of Neuroscience*, *30*(4), 1385–1394.

Bingol, B., & Schuman, E. M. (2006). Activity-dependent dynamics and sequestration of proteasomes in dendritic spines. *Nature Letters*, *441*(7097), 1144–1148.

Bingol, B., & Sheng, M. (2011). Deconstruction for Reconstruction: The Role of Proteolysis in Neural Plasticity and Disease. *Neuron*, *69*(1), 22–32.

Bjartmar, L., Huberman, A. D., Ullian, E. M., Renteria, R. C., Liu, X., Xu, W., Prezioso, J., Susman, M. W., et al. (2006). Neuronal Pentraxins Mediate Synaptic Refinement in the Developing Visual System. *Journal of Neuroscience*, *26*(23), 6269–6281.

Blenkinsop, T. A. (2006). Block of Inferior Olive Gap Junctional Coupling Decreases Purkinje Cell Complex Spike Synchrony and Rhythmicity. *Journal of Neuroscience*, *26*(6), 1739–1748.

Bolliger, M. F., Martinelli, D. C., & Sudhof, T. C. (2011). The cell-adhesion G protein-coupled receptor BAI3 is a high-affinity receptor for C1q-like proteins. *Proceedings of the National Academy of Sciences*, *108*(6), 2534–2539.

Bolshakov, V. Y., & Siegelbaum, S. A. (1995). Regulation of Hippocampal Transmitter Release During Development and Long-Term Potentiation. *Science*, *269*(5231), 1730–1734.

Bordelon, J. R. (2005). Differential Localization of Protein Phosphatase-1$\alpha$, $\beta$ and $\gamma$1 Isoforms in Primate Prefrontal Cortex. *Cerebral Cortex*, *15*(12), 1928–1937.

Bork, P. (1991). Complement components C1r/C1s, bone morphogenetic protein 1 and Xenopus laevis developmentally regulated protein UVS.2 share common repeats. *FEBS Letters, 282*(1), 9–12.

Bork, P., & Beckmann, G. (1993). The CUB Domain: A widespread module in developmentally regulated proteins. *Journal of Molecular Biology, 231*, 539–545.

Bottazzi, B., Doni, A., Garlanda, C., & Mantovani, A. (2010). An Integrated View of Humoral Innate Immunity: Pentraxins as a Paradigm. *Annual Review of Immunology*, *28*(1), 157–183.

Bouchard, D., Morisset, D., Bourbonnais, Y., & Tremblay, G. M. (2006). Proteins with whey-acidic-protein motifs and cancer. *The Lancet. Oncology*, *7*(2), 167–174.

Boulanger, L. M. (2009). Immune Proteins in Brain Development and Synaptic Plasticity. *Neuron*, *64*(1), 93–109.

Boulanger, L. M., & Shatz, C. J. (2004). Immune signalling in neural development, synaptic plasticity and disease. *Nature Reviews Neuroscience*, *5*(7), 521–531.

Bourne, J. N., Sorra, K. E., Hurlburt, J., & Harris, K. M. (2007). Polyribosomes are increased in spines of CA1 dendrites 2 h after the induction of LTP in mature rat hippocampal slices. *Hippocampus*, *17*(1), 1–4.

Bourrat, F., & Sotelo, C. (1986). Neuronal migration and dendritic maturation of the medial cerebellar nucleus in rat embryos: an HRP in vitro study using cerebellar slabs. *Brain Research,* 378, 69-85.

Bourrat, F., & Sotelo, C. (1988). Migratory pathways and neuritic differentiation of inferior olivary neurons in the rat embryo. Axonal tracing studyusing the in vitro slab technique. *Developmental Brain Research, 39*, 19–37.

Bourrat, F., & Sotelo, C. (1991). Relationships between neuronal birthdates and cytoarchitecture in the rat inferior olivary complex. *Journal of Comparative Neurology*, *313*(3), 509–521.

Bozdagi, O., Valcin, M., Poskanzer, K., Tanaka, H., & Benson, D. L. (2004). Temporally distinct demands for classic cadherins in synapse formation and maturation. *Molecular and Cellular Neuroscience*, *27*(4), 509–521.

Bramham, C. R., & Wells, D. G. (2007). Dendritic mRNA: transport, translation and function. *Nature Reviews Neuroscience, 8*(10), 776–789.

Bravin, M., Morando, L., Vercelli, A., Rossi, F., & Strata, P. (1999). Control of spine formation by electrical activity in the adult rat cerebellum. *Proceedings of the National Academy of Sciences*, *96*(4), 1704–1709.

Bresler, T., Shapira, M., Boeckers, T., Dresbach, T., Futter, M., Garner, C C., Rosenblum, K., Gundelfinger, E D., & Ziv, N E. (2004). Postsynaptic Density Assembly Is Fundamentally Different from Presynaptic Active Zone Assembly. *Journal of Neuroscience*, *24*(6), 1507–1520.

Bressan, G. M., Daga-Gordini, D., Colombatti, A., Castellani, I., Marigo, V., & Volpin, D. (1993). Emilin, a component of elastic fibers preferentially located at the elastin-microfibrils interface. *The Journal of Cell Biology*, *121*(1), 201–212.

Briseno-Roa, L., & Bessereau, J. L. (2014). Proteolytic Processing of the Extracellular Scaffolding Protein LEV-9 Is Required for Clustering Acetylcholine Receptors. *Journal of Biological Chemistry*, *289*(16), 10967–10974.

Brittis, P. A., Lu, Q., & Flanagan, J. G. (2002). Axonal protein synthesis provides a mechanism for localized regulation at an intermediate target. *Cell*, *110*(2), 223–235.

Brochu, G., Maler, L., & Hawkes, R. (1990). Zebrin-II: A Polypeptide Antigen Expressed Selectively by Purkinje-Cells Reveals Compartments in Rat and Fish Cerebellum. *Journal of Comparative Neurology*, *291*(4), 538–552.

Bryceson, Y. T., Foster, J. A., Kuppusamy, S. P., Herkenham, M., & Long, E. O. (2005). Expression of a killer cell receptor-like gene in plastic regions of the central nervous system. *Journal of Neuroimmunology*, *161*(1-2), 177–182.

Burkhalter, A., Gonchar, Y., Mellor, R. L., & Nerbonne, J. M. (2006). Differential Expression of IA Channel Subunits Kv4.2 and Kv4.3 in Mouse Visual Cortical Neurons and Synapses. *Journal of Neuroscience*, *26*(47), 12274–12282.

Butz, S., Okamoto, M., & Sudhof, T. C. (1998). A tripartite protein complex with the potential to couple synaptic vesicle exocytosis to cell adhesion in brain. *Cell*, 94, 773-782.

**- C -**

Cameron, D. B., Kasai, K., Jiang, Y., Hu, T., Saeki, Y., & Komuro, H. (2009). Four distinct phases of basket/stellate cell migration after entering their final destination (the molecular layer) in the developing cerebellum. *Developmental Biology*, *332*(2), 309–324.

Campbell, G., & Shatz, C. J. (1992). Synapses formed by identified retinogeniculate axons during the segregation of eye input. *The Journal of Neuroscience*, *12*(5), 1847–1858.

Caras, I. W., Davitz, M. A., Rhee, L., Weddell, G., Martin, D. W., & Nussenzweig, V. (1987). Cloning of decay-accelerating factor suggests novel use of splicing to generate two proteins. *Nature*, *325*(6104), 545–549.

Carpentier, P. A., & Palmer, T. D. (2009). Immune Influence on Adult Neural Stem Cell Regulation and Function. *Neuron*, *64*(1), 79–92.

Carrillo, J., Nishiyama, N., & Nishiyama, H. (2013). Dendritic Translocation Establishes the Winner in Cerebellar Climbing Fiber Synapse Elimination. *Journal of Neuroscience*, *33*(18), 7641–7653.

Carroll, M. C. (2004). The complement system in regulation of adaptive immunity. *Nature Immunology*, *5*(10), 981–986.

Cerpa, W., Godoy, J. A., Alfaro, I., Farías, G. G., Metcalfe, M. J., Fuentealba, R., Bonansco, C., & Inestrosa, N. C. (2008). Wnt-7a modulates the synaptic vesicle cycle and synaptic transmission in hippocampal neurons. *The Journal of Biological Chemistry*, *283*(9), 5918–5927.

Cesa, R., & Strata, P. (2009). Axonal competition in the synaptic wiring of the cerebellar cortex during development and in the mature cerebellum. *Neuroscience*, *162*(3), 624–632.

Cesa, R., Morando, L., & Strata, P. (2003). Glutamate receptor δ2 subunit in activity-dependent heterologous synaptic competition. *Journal of Neuroscience*, *23*(6), 2363–2370.

Chan-Palay, V., Palay, S. L., Brown, J. T., & Van Itallie C. (1977). Sagittal Organization of Olivo-cerebellar and Reticulocerebellar Projections: Autoradiographic studies with $^{35}$S-Methionine. *Experimental Brain Research, 30*, 561–576.

Chedotal, A., & Sotelo, C. (1993). The 'creeper stage' in cerebellar climbing fiber synaptogenesis precedes the “pericellular nest” - ultrastructural evidence with parvalbumin immunocytochemistry. *Developmental Brain Research, 76*, 207–220.

Chedotal, A., Bloch-Gallego, E., & Sotelo, C. (1997). The embryonic cerebellum contains topographic cues that guide developing inferior olivary axons. *Development*, *124*(4), 861–870.

Chen, L., Chetkovich, D. M., Petralia, R. S., Sweeney, N. T., Kawasaki, Y., Wenthold, R. J., Bredt, D. S., & Nicoll, R. A. (2000). Stargazin regulates synaptic targeting of AMPA receptors by two distinct mechanisms. *Nature,* 408, 936-943.

Chen, X., Vinade, L., Leapman, R. D., Petersen, J. D., Nakagawa, T., Phillips, T. M., Sheng, M., & Reese, T. S. (2005). Mass of the postsynaptic density and enumeration of three key molecules. *Proceedings of the National Academy of Sciences*, *102*(32), 11551–11556.

Chen, X., Winters, C., Azzam, R., Li, X., Galbraith, J. A., Leapman, R. D., & Reese, T. S. (2008). Organization of the core structure of the postsynaptic density. *Proceedings of the National Academy of Sciences*, *105*(11), 4453–4458.

Chédotal, A., & Sotelo, C. (1992). Early Development of Olivo-cerebellar Projections in the Fetal Rat Using CGRP Immunocytochemistry. *The European Journal of Neuroscience*, *4*(11), 1159–1179.

Choi, Y. B., Tenneti, L., Le, D. A., Ortiz, J., Bai, G., Chen, H., & Lipton, S. A. (2000). Molecular

basis of NMDA receptor-coupled ion channel modulation by S-nitrosylation. *Nature Neuroscience*, *3*(1), 15–21.

Chou, K. C., & Heinrikson, R. L. (1997). Prediction of the tertiary structure of the complement control protein module. *Journal of Protein Chemistry*, *16*(8), 765–773.

Christopherson, K. S., Ullian, E. M., Stokes, C. C. A., Mullowney, C. E., Hell, J. W., Agah, A., Lawler, J., Mosher, D. F., et al. (2005). Thrombospondins Are Astrocyte-Secreted Proteins that Promote CNS Synaptogenesis. *Cell*, *120*(3), 421–433.

Chubykin, A. A., Atasoy, D., Etherton, M. R., Brose, N., Kavalali, E. T., Gibson, J. R., & Südhof, T. C. (2007). Activity-Dependent Validation of Excitatory versus Inhibitory Synapses by Neuroligin-1 versus Neuroligin-2. *Neuron*, *54*(6), 919–931.

Cingolani, L. A., & Goda, Y. (2008). Actin in action: the interplay between the actin cytoskeleton and synaptic efficacy. *Nature Reviews Neuroscience*, *9*(5), 344–356.

Clayton, E. L., & Cousin, M. A. (2009). Quantitative monitoring of activity-dependent bulk endocytosis of synaptic vesicle membrane by fluorescent dextran imaging. *Journal of Neuroscience Methods*, *185*(1), 76–81.

Colledge, M., Snyder, E. M., Crozier, R. A., Soderling, J. A., Jin, Y., Langeberg, L. K., Lu, H., Bear, M. F., & Scott, J. D. (2003). Ubiquitination regulates PSD-95 degradation and AMPA receptor surface expression. *Neuron*, *40*(3), 595–607.

Collins, M. O., Husi, H., Yu, L., Brandon, J. M., Anderson, C. N. G., Blackstock, W. P., Choudhary, J. S., & Grant, S. G. N. (2006). Molecular characterization and comparison of the components and multiprotein complexes in the postsynaptic proteome. *Journal of Neurochemistry*, *97 Suppl 1*, 16–23.

Conroy, W. G., Nai, Q., Ross, B., Naughton, G., & Berg, D. K. (2007). Postsynaptic neuroligin enhances presynaptic inputs at neuronal nicotinic synapses. *Developmental Biology*, *307*(1), 79–91.

Contractor, A., Rogers, C., Maron, C., Henkemeyer, M., Swanson, G. T., & Heinemann, S. F. (2002). Trans-synaptic Eph receptor-ephrin signaling in hippocampal mossy fiber LTP. *Science*, *296*(5574), 1864–1869.

Corriveau, R. A., Huh, G. S., & Shatz, C. J. (1998). Regulation of Class I MHC gene expression in the developing and mature CNS by neural activity. *Neuron*, 21, 505-520.

Cottrell, J. R., Dube, G. R., Egles, C., & Liu, G. S. (2000). Distribution, density, and clustering of functional glutamate receptors before and after synaptogenesis in hippocampal neurons. *Journal of Neurophysiology*, *84*(3), 1573–1587.

Craig, A. M., Blackstone, C. D., Huganir, R. L., & Banker, G. (1993). The distribution of glutamate receptors in cultured rat hippocampal neurons: postsynaptic clustering of AMPA selective subunits. *Neuron*, 10, 1055-1068.

Craven, S. E., & Bredt, D. S. (1998). PDZ proteins organize synaptic signaling pathways. *Cell*, 93, 495-498.

Cremer, H., Chazal, G., Goridis, C., & Represa, A. (1997). NCAM Is Essential for Axonal Growth and Fasciculation in the Hippocampus. *Molecular and Cellular Neuroscience*, 8, 323-335.

Cremer, H., Chazal, G., Carleton, A., Goridis, C., Vincent, J. D., & Lledo, P. M. (1998). Long-term but not short-term plasticity at mossy fiber synapses is impaired in neural cell adhesion molecule-deficient mice. *Proceedings of the National Academy of Sciences*,

*95*(22), 13242–13247.

Crepel, F. (1982). Regression of functional synapses in the immature mammalian cerebellum. *Trends in Neurosciences*, *5*, 266–269.

Crepel, F., Mariani, J., & Delhaye-Bouchaud, N. (1976). Evidence for a multiple innervation of Purkinje cells by climbing fibers in the immature rat cerebellum. *Journal of Neurobiology*, *7*(6), 567–578.

Cresswell, P., Ackerman, A. L., Giodini, A., Peaper, D. R., & Wearsch, P. A. (2005). Mechanisms of MHC class I-restricted antigen processing and cross-presentation. *Immunological Reviews*, *207*, 145–157.

**- D -**

Dalva, M. B., Takasu, M. A., Lin, M. Z., Shamah, S. M., Hu, L., Gale, N. W., & Greenberg, M. E. (2000). EphB receptors interact with NMDA receptors and regulate excitatory synapse formation. *Cell*, *103*(6), 945–956.

Danglot, L., Triller, A., & Bessis, A. (2003). Association of gephyrin with synaptic and extrasynaptic $GABA_A$ receptors varies during development in cultured hippocampal neurons. *Molecular and Cellular Neuroscience*, *23*(2), 264–278.

Darstein, M., Petralia, R. S., Swanson, G. T., Wenthold, R. J., & Heinemann, S. F. (2003). Distribution of kainate receptor subunits at hippocampal mossy fiber synapses. *The Journal of Neuroscience*, *23*(22), 8013–8019.

Datwani, A., McConnell, M. J., Kanold, P. O., Micheva, K. D., Busse, B., Shamloo, M., Smith, S. J., & Shatz, C. J. (2009). Classical MHC-I Molecules Regulate Retinogeniculate Refinement and Limit Ocular Dominance Plasticity. *Neuron*, *64*(4), 463–470.

Davis, J. Q., & Bennett, V. (1994). Ankyrin binding activity shared by the neurofascin/L1/NrCAM family of Nervous System Cell Adhesion Molecules. *The Journal of Biological Chemistry*, *269*(44), 27163–27166.

Davis, J. Q., Lambert, S., & Bennett, V. (1997). Molecular Composition of the Node of Ranvier:Identification of Ankyrin- binding Cell Adhesion Molecules Neurofascin (Mucin+/Third FNIII Domain-) and NrCAM at Nodal Axon Segments, *The Journal of Cell Biology,* 135(5), 1355-1367.

De Blas, A. L. (1984). Monoclonal antibodies to specific astroglial and neuronal antigens reveal the cytoarchitecture of the Bergmann glia fibers in the cerebellum. *The Journal of Neuroscience, 4*(1), 265-273.

De Wit, J., Sylwestrak, E., Sullivan, M. L. O., Otto, S., Tiglio, K., Savas, J. N., Yates, J. R., III, Comoletti, D., et al. (2009). LRRTM2 Interacts with Neurexin1 and Regulates Excitatory Synapse Formation. *Neuron*, *64*(6), 799–806.

De Zeeuw, C. I., Hoebeek, F. E., Bosman, L. W. J., Schonewille, M., Witter, L., & Koekkoek, S. K. (2011). Spatiotemporal firing patterns in the cerebellum. *Nature Reviews Neuroscience,* 12, 327-344.

De Zeeuw, C. I., Simpson, J. I., Hoogenraad, C. C., Galjart, N., Koekkoek, S., & Ruigrok, T. J. H. (1998). Microcircuitry and function of the inferior olive. *Trends in Neurosciences, 21*, 391–400.

Dean, C., Scholl, F. G., Choih, J., DeMaria, S., Berger, J., Isacoff, E., & Scheiffele, P. (2003).

Neurexin mediates the assembly of presynaptic terminals. *Nature Neuroscience*, *6*(7), 708–716.

Desmond, J. E., & Fiez, J. A. (1998). Neuroimaging studies of the cerebellum: language, learning and memory. *Trends in Cognitive Sciences, 2*(9), 355-362.

Deverman, B. E., & Patterson, P. H. (2009). Cytokines and CNS Development. *Neuron*, *64*(1), 61–78.

Dieck, S. T., Sanmartí-Vila, L., Langnaese, K., Richter, K., Kindler, S., Soyke, A., Wex, H., Smalla, K. H., et al. (1998). Bassoon, a novel zinc-finger CAG/glutamine-repeat protein selectively localized at the active zone of presynaptic nerve terminals. *Journal of Cell Biology*, *142*(2), 499–509.

Dityatev, A., Schachner, M., & Sonderegger, P. (2010). The dual role of the extracellularmatrix in synaptic plasticityand homeostasis. *Nature Reviews Neuroscience*, 11, 735-746.

Doyle, J. P., Dougherty, J. D., Heiman, M., Schmidt, E. F., Stevens, T. R., Ma, G., Bupp, S., Shrestha, P., et al. (2008). Application of a Translational Profiling Approach for the Comparative Analysis of CNS Cell Types. *Cell*, *135*(4), 749–762.

**- E -**

Eccles, J. C. (1967). Circuits in the cerebellar control of movement. *Proceedings of the National Academy of Sciences of the United States of America*, 58, 336-343.

Edmondson, J. C., & Hatten, M. E. (1987). Glial-guided granule neuron migration in vitro: a high-resolution time-lapse video microscopic study. *The Journal of Neuroscience*, *7*(6), 1928–1934.

Edstrom, E., Kullberg, S., Ming, Y., Zheng, H., & Ulfhake, B. (2004). MHC Class I, β2 microglobulin, and the INF-γ receptor are upregulated in aged motoneurons. *Journal of Neuroscience Research*, *78*(6), 892–900.

Ehlers, M. D. (2003). Activity level controls postsynaptic composition and signaling via the ubiquitin-proteasome system. *Nature Neuroscience*, *6*(3), 231–242.

El-Husseini, A. E., Schnell, E., Dakoji, S., Sweeney, N., Zhou, Q., Prange, O., Gauthier-Campbell, C., Aguilera-Moreno, A., et al. (2002). Synaptic strength regulated by palmitate cycling on PSD-95. *Cell*, *108*(6), 849–863.

Elia, L. P., Yamamoto, M., Zang, K., & Reichardt, L. F. (2006). p120 Catenin Regulates Dendritic Spine and Synapse Development through Rho-Family GTPases and Cadherins. *Neuron*, *51*(1), 43–56.

Emes, R. D., Pocklington, A. J., Anderson, C. N. G., Bayes, A., Collins, M. O., Vickers, C. A., Croning, M. D. R., Malik, B. R., et al. (2008). Evolutionary expansion and anatomical specialization of synapse proteome complexity. *Nature Neuroscience*, *11*(7), 799–806.

Estes, M. L., & McAllister, A. K. (2015). Immune mediators in the brain and peripheral tissues in autism spectrum disorder. *Nature Reviews Neuroscience*, *16*(8), 469–486.

**- F -**

Feng, W., & Zhang, M. (2009). Organization and dynamics of PDZ-domain-related

supramodules in the postsynaptic density. *Nature Reviews Neuroscience*, *10*(2), 87–99.
Fenster, S. D., Chung, W. J., Zhai, R., Cases-Langhoff, C., Voss, B., Garner, A. M., Kaempf, U., Kindler, S., et al. (1999). Piccolo, a presynaptic zinc finger protein structurally related to bassoon. *Neuron*, *25*(1), 203–214.
Fernandez-Busnadiego, R., Zuber, B., Maurer, U. E., Cyrklaff, M., Baumeister, W., & Lucic, V. (2010). Quantitative analysis of the native presynaptic cytomatrix by cryoelectron tomography. *The Journal of Cell Biology*, *188*(1), 145–156.
Fiala, J. C., Feinberg, M., Popov, V., & Harris, K. M. (1998). Synaptogenesis via dendritic filopodia in developing hippocampal area CA1. *The Journal of Neuroscience, 18*(21), 8900–8911.
Fifkova, E., & Delay, R. J. (1982). Cytoplasmic Actin in Neuronal Processes as a Possible Mediator of Synaptic Plasticity. *The Journal of Cell Biology, 95*, 345–350.
Flanagan, J. G., & Vanderhaeghen, P. (1998). The ephrins and Eph receptors in neural development. *Annual Review of Neuroscience*, *21*, 309–345.
Fonseca, R., Vabulas, R. M., Hartl, F. U., Bonhoeffer, T., & Nägerl, U. V. (2006). A Balance of Protein Synthesis and Proteasome-Dependent Degradation Determines the Maintenance of LTP. *Neuron*, *52*(2), 239–245.
Fox, M. A., & Umemori, H. (2006). Seeking long-term relationship: axon and target communicate to organize synaptic differentiation. *Journal of Neurochemistry*, *97*(5), 1215–1231.
Fox, M. A., Sanes, J. R., Borza, D.-B., Eswarakumar, V. P., Fässler, R., Hudson, B. G., John, S. W. M., Ninomiya, Y., et al. (2007). Distinct Target-Derived Signals Organize Formation, Maturation, and Maintenance of Motor Nerve Terminals. *Cell*, *129*(1), 179–193.
Fritschy, J. M., Panzanelli, P., Kralic, J E., Vogt, K E. & Sassoe-Pognetto, M. (2006). Differential Dependence of Axo-Dendritic and Axo-Somatic GABAergic Synapses on $GABA_A$ Receptors Containing the $\alpha 1$ Subunit in Purkinje Cells. *Journal of Neuroscience*, *26*(12), 3245–3255.

**- G -**

Gaboriaud, C., Juanhuix, J., Gruez, A., Lacroix, M., Darnault, C., Pignol, D., Verger, D., Fontecilla-Camps, J. C., & Arlaud, G. J. (2003). The Crystal Structure of the Globular Head of Complement Protein C1q Provides a Basis for Its Versatile Recognition Properties. *Journal of Biological Chemistry*, *278*(47), 46974–46982.
Gallagher, E., Howell, B. W., Soriano, P., Cooper, J. A., & Hawkes, R. (1998). Cerebellar abnormalities in the disabled (mdab1-1) mouse. *Journal of Comparative Neurology*, *402*(2), 238–251.
Gally, C., Eimer, S., Richmond, J. E., & Bessereau, J.-L. (2004). A transmembrane protein required for acetylcholine receptor clustering in Caenorhabditis elegans. *Nature*, *431*(7008), 578–582.
Gao, Z., van Beugen, B. J., & De Zeeuw, C. I. (2012). Distributed synergistic plasticity and cerebellar learning. *Nature Reviews Neuroscience*, *13*(9), 619–635.
Garay, P. A., & McAllister, A. K. (2010). Novel roles for immune molecules in neural development: implications for neurodevelopmental disorders. *Frontiers in Synaptic*

*Neuroscience*, *2*, 136.

Gendrel, M., Rapti, G., Richmond, J. E., & Bessereau, J.-L. (2009). A secreted complement-control-related protein ensures acetylcholine receptor clustering. *Nature*, *461*(7266), 992–996.

Gerrow, K., Romorini, S., Nabi, S. M., Colicos, M. A., Sala, C., & El-Husseini, A. (2006). A Preformed Complex of Postsynaptic Proteins Is Involved in Excitatory Synapse Development. *Neuron*, *49*(4), 547–562.

Ghai, R., Waters, P., Roumenina, L. T., Gadjeva, M., Kojouharova, M. S., Reid, K. B. M., Sim, R. B., & Kishore, U. (2007). C1q and its growing family. *Immunobiology*, *212*(4), 253–266.

Gil, O. D., Needleman, L., & Huntley, G. W. (2002). Developmental patterns of cadherin expression and localization in relation to compartmentalized thalamocortical terminations in rat barrel cortex. *Journal of Comparative Neurology*, *453*(4), 372–388.

Gilmore, E. C., & Herrup, K. (2000). Cortical development: receiving reelin. *Current Biology*, *10*(4), R162–6.

Giulian, D., Young, D. G., Woodward, J., Brown, D. C., & Lachman, L. B. (1988). Interleukin-1 is an astroglial growth factor in the developing brain. *The Journal of Neuroscience*, *8*(2), 709–714.

Goddard, C. A., Butts, D. A., & Shatz, C. J. (2007). Regulation of CNS synapses by neuronal MHC class I. *Proceedings of the National Academy of Sciences*, *104*(16), 6828–6833.

Godement, P., Salaün, J., & Imbert, M. (1984). Prenatal and postnatal development of retinogeniculate and retinocollicular projections in the mouse. *Journal of Comparative Neurology*, *230*(4), 552–575.

Gordon, S. (2002). Pattern recognition receptors: doubling up for the innate immune response. *Cell,* 111, 927-930.

Graf, E. R., Zhang, X. Z., Jin, S. X., Linhoff, M. W., & Craig, A. M. (2004). Neurexins induce differentiation of GABA and glutamate postsynaptic specializations via neuroligins. *Cell*, *119*(7), 1013–1026.

Granit, R., & Phillips, C. G. (1956). Excitatory and inhibitory processes acting upon individual Purkinje cells of the cerebellum in cats. *Journal of Physiology,* 133, 520-547.

Gray, E. G. (1959). Axo-somatic and axo-dendritic synapses of the cerebral cortex: An electron microscope study. *Journal of Anatomy*, 420-433.

Gray, N. W., Weimer, R. M., Bureau, I., & Svoboda, K. (2006). Rapid redistribution of synaptic PSD-95 in the neocortex in vivo. *PLoS Biology*, *4*(11), 2065–2075.

Groenewegen, H. J., & Voogd, J. (1977). The parasagittal zonation within the olivo-cerebellar projection. I. Climbing fiber distribution in the vermis of cat cerebellum. *Journal of Comparative Neurology*, *174*(3), 417–488.

Grutzendler, J., Kasthuri, N., & Gan, W. (2002). Long-term dendritic spine stability in the adult cortex. *Nature*, *420*(6917), 810–812.

Gulley, R. L., & Reese, T. S. (1981). Cytoskeletal organization at the postsynaptic complex. *Journal of Cell Biology*, *91*(1), 298–302.

Gunnersen, J. M., Kim, M. H., Fuller, S. J., De Silva, M., Britto, J. M., Hammond, V. E., Davies, P. J., Petrou, S., et al. (2007). Sez-6 Proteins Affect Dendritic Arborization Patterns and Excitability of Cortical Pyramidal Neurons. *Neuron*, *56*(4), 621–639.

**- H -**


Haddick, P. C. G., Tom, I., Luis, E., Quiñones, G., Wranik, B. J., Ramani, S. R., Stephan, J.-P., Tessier-Lavigne, M., & Gonzalez, L. C. (2014). Defining the Ligand Specificity of the Deleted in Colorectal Cancer (DCC) Receptor. *PLoS ONE*, *9*(1), 1-12.

Haglerød, C., Kapic, A., Boulland, J. L., Hussain, S., Holen, T., Skare, Laake, P., Ottersen, O. P., et al. (2009). Protein interacting with C Kinase 1 (PICK1) and GluR2 are associated with presynaptic plasma membrane and vesicles in hippocampal excitatory synapses. *Neuroscience*, *158*(1), 242–252.

Hall, A. C., Lucas, F. R., & Salinas, P. C. (2000). Axonal Remodeling and Synaptic Differentiation in the Cerebellum Is Regulated by WNT-7a Signaling. *Cell, 100*, 525–535.

Hallam, S. J., Goncharov, A., McEwen, J., Baran, R., & Jin, Y. (2002). SYD-1, a presynaptic protein with PDZ, C2 and rhoGAP-like domains, specifies axon identity in C. elegans. *Nature Neuroscience*, *5*(11), 1137–1146.

Hallonet, M. E., & Le Douarin, N. M. (1993). Tracing neuroepithelial cells of the mesencephalic and metencephalic alar plates during cerebellar ontogeny in quail-chick chimaeras. *The European Journal of Neuroscience*, *5*(9), 1145–1155.

Hannan, S., Wilkins, M. E., & Smart, T. G. (2012). Sushi domains confer distinct trafficking profiles on $GABA_B$ receptors. *Proceedings of the National Academy of Sciences of the United States of America, 109*(30), 12171–12176.

Harris, K. M., & Stevens, J. K. (1988). Dendritic spines of rat cerebellar Purkinje cells: serial electron microscopy with reference to their biophysical characteristics. *The Journal of Neuroscience*, *8*(12), 4455–4469.

Harris, K. M., & Stevens, J. K. (1989). Dendritic Spines of CA1 Pyramidal Cells in the Rat Hippocampus: Serial Electron Microscopy with Reference to Their Biophysical Characteristics. *The Journal of Neuroscience, 9*(8), 2982-2997.

Harris, K. M., & Sultan, P. (1995). Variation in the number, location and size of synaptic vesicles provides an anatomical basis for the nonuniform probability of release at hippocampal CA1 synapses. *Neuropharmacology*, *34*(11), 1387–1395.

Harvey, R. J., & Napper, R. (1991). Quantitative studies on the Mammalian cerebellum. *Progress in Neurobiology, 36*, 437-463.

Hashimoto, K., & Kano, M. (2003). Functional Differentiation of Multiple Climbing Fiber Inputs during Synapse Eliminationin the Developing Cerebellum, *Neuron,* 38, 785-796.

Hashimoto, K., & Kano, M. (2005). Postnatal development and synapse elimination of climbing fiber to Purkinje cell projection in the cerebellum. *Neuroscience Research*, *53*(3), 221–228.

Hashimoto, K., Ichikawa, R., Kitamura, K., Watanabe, M., & Kano, M. (2009a). Translocation of a ‘‘Winner’’ Climbing Fiber to the Purkinje Cell Dendrite and Subsequent Eliminationof ‘‘Losers’’ from the Soma in Developing Cerebellum. *Neuron*, *63*(1), 106–118.

Hashimoto, K., Ichikawa, R., Takechi, H., Inoue, Y., Aiba, A., Sakimura, K., Mishina, M., Hashikawa, T., et al. (2001). Roles of glutamate receptor δ2 subunit (GluRδ2) and metabotropic glutamate receptor subtype 1 (mGluR1) in climbing fiber synapse elimination during postnatal cerebellar development. *Journal of Neuroscience*, *21*(24),

9701–9712.

Hashimoto, K., Yoshida, T., Sakimura, K., Mishina, M., Watanabe, M., & Kano, M. (2009b). Influence of parallel fiber–Purkinje cell synapse formation on postnatal development of climbing fiber–Purkinje cell synapses in the cerebellum. *Neuroscience*, *162*(3), 601–611.

Hashimoto, M., & Mikoshiba, K. (2003). Mediolateral compartmentalization of the cerebellum is determined on the "birth date" of Purkinje cells. *The Journal of Neuroscience*, *23*(36), 11342–11351.

Hata, Y., Butz, S., & Sudhof, T. C. (1996). CASK: a novel dlg/PSD95 homolog with an N-terminal calmodulin-dependent protein kinase domain identified by interaction with neurexins. *The Journal of Neuroscience 16*(8), 2488–2494.

Hatten, M. E., & Heintz, N. (1995). Mechanisms of neural patterning and specification in the developing cerebellum. *Annual Review of Neuroscience*, *18*, 385–408.

Hatten, M. E., Alder, J., Zimmerman, K., & Heintz, N. (1997). Genes involved in cerebellar cell specification and differentiation. *Current Opinion in Neurobiology*, *7*(1), 40–47.

Hawkes, R. (1992). Antigenic markers of cerebellar modules in the adult mouse. *Biochemical Society Transactions*, *20*(2), 391–395.

Hawkes, R., & Herrup, K. (1995). Aldolase C/zebrin II and the regionalization of the cerebellum. *Journal of Molecular Neuroscience*, *6*(3), 147–158.

Hayward, C. P., Hassell, J. A., Denomme, G. A., Rachubinski, R. A., Brown, C., & Kelton, J. G. (1995). The cDNA sequence of human endothelial cell multimerin. A unique protein with RGDS, coiled-coil, and epidermal growth factor-like domains and a carboxyl terminus similar to the globular domain of complement C1q and collagens type VIII and X. *The Journal of Biological Chemistry*, *270*(31), 18246–18251.

Håvik, B., Le Hellard, S., Rietschel, M., Lybæk, H., Djurovic, S., Mattheisen, M., Mühleisen, T. W., Degenhardt, F., et al. (2011). The Complement Control-Related Genes CSMD1 and CSMD2 Associate to Schizophrenia. *Biological Psychiatry*, *70*(1), 35–42.

Henderson, J. T., Georgiou, J., Jia, Z. P., Robertson, J., Elowe, S., Roder, J. C., & Pawson, T. (2001). The receptor tyrosine kinase EphB2 regulates NMDA-dependent synaptic function. *Neuron*, *32*(6), 1041–1056.

Hensch, T. K. (2005). Critical period plasticity in local cortical circuits. *Nature Reviews Neuroscience*, *6*(11), 877–888.

Hering, H., & Sheng, M. (2001). Dendritic spines: Structure, dynamics and regulation. *Nature Reviews Neuroscience*, *2*(12), 880–888.

Herrup, K., & Kuemerle, B. (1997). The compartmentalization of the cerebellum. *Annual Review of Neuroscience*, *20*, 61–90.

Hirai, H., Pang, Z., Bao, D., Miyazaki, T., Li, L., Miura, E., Parris, J., Rong, Y., et al. (2005). Cbln1 is essential for synaptic integrity and plasticity in the cerebellum. *Nature Neuroscience*, *8*(11), 1534–1541.

Hirano, T., Kasono, K., Araki, K., & Shinozuka, K. (1994). Involvement of the glutamate receptor δ2 subunit in the long-term depression of glutamate responsiveness in cultured rat Purkinje cells. *Neuroscience Letters*, 182, 172-176.

Hirsch, J. A., & Oertel, D. (1988). Synaptic connections in the dorsal cochlear nucleus of mice, in vitro. *Journal of Physiology,* 396, 549-562.

Holmquist, E., Okroj, M., Nodin, B., Jirstrom, K., & Blom, A. M. (2013). Sushi domain-containing protein 4 (SUSD4) inhibits complement by disrupting the formation of the classical C3 convertase. *The FASEB Journal*, *27*(6), 2355–2366.

Honda, T., Sakisaka, T., Yamada, T., Kumazawa, N., Hoshino, T., Kajita, M., Kayahara, T., Ishizaki, H., et al. (2006). Involvement of nectins in the formation of puncta adherentia junctions and the mossy fiber trajectory in the mouse hippocampus. *Molecular and Cellular Neuroscience*, *31*(2), 315–325.

Hoogland, P. V., Welker, E., & Van der Loos, H. (1987). Organization of the projections from barrel cortex to thalamus in mice studied with Phaseolus vulgaris-leucoagglutinin and HRP. *Experimental Brain Research*, *68*(1), 73–87.

Hoon, M., Soykan, T., Falkenburger, B., Hammer, M., Patrizi, A., Schmidt, K.-F., Sassoè-Pognetto, M., Löwel, S., et al. (2011). Neuroligin-4 is localized to glycinergic postsynapses and regulates inhibition in the retina. *Proceedings of the National Academy of Sciences*, *108*(7), 3053–3058.

Hoshino, M., Matsuzaki, F., Nabeshima, Y., & Hama, C. (1993). Hikaru genki, a CNS-specific gene identified by abnormal locomotion in Drosophila, encodes a novel type of protein. *Neuron*, *10*(3), 395–407.

Hoshino, M., Suzuki, E., Nabeshima, Y., & Hama, C. (1996). Hikaru genki protein is secreted into synaptic clefts from an early stage of synapse formation in Drosophila. *Development*, *122*(2), 589–597.

Howell, B. W., Hawkes, R., Soriano, P., & Cooper, J. A. (1997). Neuronal position in the developing brain isregulated by mouse disabled-1. *Nature,* 389, 733–737.

Huh, G. S., Boulanger, L. M., Du, H., Riquelme, P. A., Brotz, T. M., & Shatz, C. J. (2000). Functional requirement for Class I MHC in CNS Development and Plasticity. *Science*, *306*(5703), 1895–1895.

**- I -**

Ichikawa, R., Miyazaki, T., Kano, M., Hashikawa, T., Tatsumi, H., Sakimura, K., Mishina, M., Inoue, Y., & Watanabe, M. (2002). Distal extension of climbing fiber territory and multiple innervation caused by aberrant wiring to adjacent spiny branchlets in cerebellar Purkinje cells lacking glutamate receptor δ2. *Journal of Neuroscience*, *22*(19), 8487–8503.

Ichtchenko, K., Hata, Y., Nguyen, T., Ullrich, B., Missler, M., Moomaw, C., & Sudhof, T. C. (1995). Neuroligin 1: a splice site-specific ligand for β-neurexins. *Cell*, *81*(3), 435–443.

Ichtchenko, K., Nguyen, T., & Sudhof, T. C. (1996). Structures, alternative splicing, and neurexin binding of multiple neuroligins. *The Journal of Biological Chemistry*, *271*(5), 2676–2682.

Iijima, T., Miura, E., Matsuda, K., Kamekawa, Y., Watanabe, M., & Yuzaki, M. (2007). Characterization of a transneuronal cytokine family Cbln–regulation of secretion by heteromeric assembly. *European Journal of Neuroscience*, *25*(4), 1049–1057.

Iijima, T., Miura, E., Watanabe, M., & Yuzaki, M. (2010). Distinct expression of C1q-like family mRNAs in mouse brain and biochemical characterization of their encoded proteins. *European Journal of Neuroscience*, 31, 1606-1615.

Inoue, A., & Okabe, S. (2003). The dynamic organization of postsynaptic proteins: translocating molecules regulate synaptic function. *Current Opinion in Neurobiology*, *13*(3), 332–340.

Inoue, A., & Sanes, J. R. (1997). Lamina-specific connectivity in the brain: Regulation by N-cadherin, neurotrophins, and glycoconjugates. *Science*, *276*(5317), 1428–1431.

Irie, M., Hata, Y., Takeuchi, M., Ichtchenko, K., Toyoda, A., Hirao, K., Takai, Y., Rosahl, T. W., & Sudhof, T. C. (1997). Binding of neuroligins to PSD-95. *Science*, *277*(5331), 1511–1515.

Isope, P., & Barbour, B. (2002). Properties of unitary granule cell - Purkinje cell synapses in adult rat cerebellar slices. *The Journal of Neuroscience*, *22*(22), 9668–9678.

Ito, M. (1982). Cerebellar control of the vestibulo-ocular reflex - around the flocculus hypothesis. *Annual Review of Neuroscience*, 275–296.

Ito, M. (1998). Cerebellar learning in the vestibulo–ocular reflex. *Trends in Cognitive Sciences, 2*(9), 313–321.

Ito-Ishida, A., Miyazaki, T., Miura, E., Matsuda, K., Watanabe, M., Yuzaki, M., & Okabe, S. (2012). Presynaptically Released Cbln1 Induces Dynamic Axonal Structural Changes by Interacting with GluD2 during Cerebellar Synapse Formation. *Neuron*, *76*(3), 549–564.

**- J -**

Jackson, A. C., & Nicoll, R. A. (2011). The expanding social network of ionotropic glutamate receptors: TARPs and other transmembrane auxiliary subunits. *Neuron,* 70, 178-199.

Janeway, C. A., Jr., & Medzhitov, R. (2002). Innate immune recognition. *Annual Review of Immunology*, *20*(1), 197–216.

Jedlicka, P., Vlachos, A., Schwarzacher, S. W., & Deller, T. (2008). A role for the spine apparatus in LTP and spatial learning. *Behavioural Brain Research*, *192*(1), 12–19.

Jenkins, S. M. (2001). Ankyrin-G coordinates assembly of the spectrin-based membrane skeleton, voltage-gated sodium channels, and L1 CAMs at Purkinje neuron initial segments. *The Journal of Cell Biology*, *155*(5), 739–746.

Jiang, Y., Kumada, T., Cameron, D. B., & Komuro, H. (2008). Cerebellar Granule Cell Migration and the Effects of Alcohol. *Developmental Neuroscience*, *30*(1-3), 7–23.

Joo, J.-Y., Lee, S.-J., Uemura, T., Yoshida, T., Yasumura, M., Watanabe, M., & Mishina, M. (2011). Biochemical and Biophysical Research Communications. *Biochemical and Biophysical Research Communications*, *406*(4), 627–632.

**- K -**

Kakegawa, W., Mitakidis, N., Miura, E., Abe, M., Matsuda, K., Takeo, Y. H., Kohda, K., Motohashi, J., et al. (2015). Anterograde C1ql1 Signaling Is Required in Order to Determine and Maintain a Single-Winner Climbing Fiber in the Mouse Cerebellum. *Neuron*, *85*(2), 316–329.

Kakegawa, W., Miyazaki, T., Kohda, K., Matsuda, K., Emi, K., Motohashi, J., Watanabe, M., & Yuzaki, M. (2009). The N-Terminal Domain of GluD2 (GluRδ2) Recruits Presynaptic Terminals and Regulates Synaptogenesis in the Cerebellum In Vivo. *Journal of Neuroscience*, *29*(18), 5738–5748.

Kandel, E. (2000). Principles of Neural Science, 1–1229.

Kaneko, M., Stellwagen, D., Malenka, R. C., & Stryker, M. P. (2008). Tumor Necrosis Factor-α Mediates One Component of Competitive, Experience-Dependent Plasticity in Developing Visual Cortex. *Neuron*, *58*(5), 673–680.

Kashiwabuchi, N., Ikeda, K., Araki, K., Hirano, T., Shibuki, K., Takayama, C., Inoue, Y., Kutsuwada, T., et al. (1995). Impairment of motor coordination, Purkinje cell synapse formation, and cerebellar long-term depression in GluRδ2 mutant mice. *Cell*, *81*(2), 245–252.

Kaupmann, K., Huggel, K., Held, J., Flor, P. J., Bischoff, S., Mickel, S. J., McMaster, G., Angst, C., et al. (1997). Expression cloning of $GABA_B$ receptors uncovers similarity to metabotropic glutamate receptors. *Nature*, 386, 239-246.

Kawasaki, Y., Zhang, L., Cheng, J.-K., & Ji, R.-R. (2008). Cytokine mechanisms of central sensitization: distinct and overlapping role of interleukin-1β, interleukin-6, and tumor necrosis factor-α in regulating synaptic and neuronal activity in the superficial spinal cord. *Journal of Neuroscience*, *28*(20), 5189–5194.

Kennedy, M. B. (2000). Signal-processing machines at the postsynaptic density. *Science*, *290*(5492), 750–754.

Kim, E., & Sheng, M. (2004). PDZ domain proteins of synapses. *Nature Reviews Neuroscience*, *5*(10), 771–781.

Kim, M. J., Futai, K., Jo, J., Hayashi, Y., Cho, K., & Sheng, M. (2007). Synaptic Accumulation of PSD-95 and Synaptic Function Regulated by Phosphorylation of Serine-295 of PSD-95. *Neuron*, *56*(3), 488–502.

King, N., Hittinger, C. T., & Carroll, S. B. (2003). Evolution of Key Cell Signaling and Adhesion Protein Families Predates Animal Origins. *Science, 301*, 361–363.

Kirkitadze, M. D., & Barlow, P. N. (2001). Structure and flexibility of the multiple domain proteins that regulate complement activation. *Immunological Reviews*, *180*, 146–161.

Kishore, U., Gaboriaud, C., Waters, P., Shrive, A. K., Greenhough, T. J., Reid, K. B. M., Sim, R. B., & Arlaud, G. J. (2004). C1q and tumor necrosis factor superfamily: modularity and versatility. *Trends in Immunology*, *25*(10), 551–561.

Kishore, U., Leigh, L. E., Eggleton, P., Strong, P., Perdikoulis, M. V., Willis, A. C., & Reid, K. B. (1998). Functional characterization of a recombinant form of the C-terminal, globular head region of the B-chain of human serum complement protein, C1q. *The Biochemical Journal*, *333 ( Pt 1)*, 27–32.

Klassen, M. P., & Shen, K. (2007). Wnt signaling positions neuromuscular connectivity by inhibiting synapse formation in C. elegans. *Cell*, *130*(4), 704–716.

Kneussel, M., Helmut Brandstätter, J., Gasnier, B., Feng, G., Sanes, J. R., & Betz, H. (2001). Gephyrin-Independent Clustering of Postsynaptic $GABA_A$ Receptor Subtypes. *Molecular and Cellular Neuroscience*, *17*(6), 973–982.

Knott, G. W., Quairiaux, C., Genoud, C., & Welker, E. (2002). Formation of Dendritic Spines with GABAergic Synapses Induced by Whisker Stimulation in Adult Mice. *Neuron, 34*, 265–273.

Kohmura, N., Senzaki, K., Hamada, S., Kai, N., Yasuda, R., Watanabe, M., Ishii, H., Yasuda, M., et al. (1998). Diversity revealed by a novel family of cadherins expressed in neurons at a synaptic complex. *Neuron*, *20*(6), 1137–1151.

Komuro, H., Yacubova, E., Yacubova, E., & Rakic, P. (2001). Mode and tempo of tangential cell migration in the cerebellar external granular layer. *The Journal of Neuroscience*, *21*(2), 527–540.

Korbo, L., Andersen, B. B., Ladefoged, O., & Moller, A. (1993). Total Numbers of Various Cell-Types in Rat Cerebellar Cortex Estimated Using an Unbiased Stereological Method. *Brain Research*, *609*(1-2), 262–268.

Korobova, F., & Svitkina, T. (2010). Molecular architecture of synaptic actin cytoskeleton in hippocampal neurons reveals a mechanism of dendritic spine morphogenesis. *Molecular Biology of the Cell,* 21, 165-176.

Kralic, J. E., Criswell, H. E., Osterman, J. L., O'Buckley, T. K., Wilkie, M. E., Matthews, D. B., Hamre, K., Breese, G. R., et al. (2005). Genetic essential tremor in γ-aminobutyric $acid_A$ receptor α1 subunit knockout mice. *Journal of Clinical Investigation*, *115*(3), 774–779.

Ksiazek, I., Burkhardt, C., Lin, S., Seddik, R., Maj, M., Bezakova, G., Jucker, M., Arber, S., et al. (2007). Synapse loss in cortex of agrin-deficient mice after genetic rescue of perinatal death. *Journal of Neuroscience*, *27*(27), 7183–7195.

Kulik, A. (2006). Compartment-Dependent Colocalization of Kir3.2-Containing K+ Channels and $GABA_B$ Receptors in Hippocampal Pyramidal Cells. *Journal of Neuroscience*, *26*(16), 4289–4297.

Kumada, T., Jiang, Y., Kawanami, A., Cameron, D. B., & Komuro, H. (2009). Autonomous turning of cerebellar granule cells in vitro by intrinsic programs. *Developmental Biology*, *326*(1), 237–249.

Kusnoor, S. V., Parris, J., Muly, E. C., Morgan, J. I., & Deutch, A. Y. (2010). An extra-cerebellar role for Cerebellin1: Modulation of dendritic spine density and synapses in striatal medium spiny neurons. *Journal of Comparative Neurology*, 518(13), 2525-2537.

**- L -**

Lai, C., Fisher, S. E., Hurst, J. A., & Vargha-Khadem, F. (2001). A forkhead-domain gene is mutated in a severe speech and language disorder. *Nature*, 413, 519-523.

Landis, D. M. (1987). Initial junctions between developing parallel fibers and Purkinje cells are different from mature synaptic junctions. *Journal of Comparative Neurology*, *260*(4), 513–525.

Landis, D. M., & Reese, T. S. (1974). Differences in membrane structure between excitatory and inhibitory synapses in the cerebellar cortex. *Journal of Comparative Neurology*, *155*(1), 93–125.

Landis, D. M., & Reese, T. S. (1983). Cytoplasmic organization in cerebellar dendritic spines. *Journal of Cell Biology*, *97*(4), 1169–1178.

Landis, D. M., & Sidman, R. L. (1978). Electron microscopic analysis of postnatal histogenesis in the cerebellar cortex of staggerer mutant mice. *Journal of Comparative Neurology*, *179*(4), 831–863.

Landis, D., Hall, A. K., Weinstein, L. A., & Reese, T. S. (1988). The organization of cytoplasm at the presynaptic active zone of a central nervous system synapse. *Neuron*, 1, 201-209.

Lanoue, V., Usardi, A., Sigoillot, S. M., Talleur, M., Iyer, K., Mariani, J., Isope, P., Vodjdani, G., et al. (2013). The adhesion-GPCR BAI3, a gene linked to psychiatric disorders, regulates

dendrite morphogenesis in neurons. *Molecular Psychiatry*, *18*(8), 943–950.
Lee, C. H., Herman, T., Clandinin, T. R., Lee, R., & Zipursky, S. L. (2001). N-cadherin regulates target specificity in the Drosophila visual system. *Neuron*, *30*(2), 437–450.
Lee, H., Brott, B. K., Kirkby, L. A., Adelson, J. D., Cheng, S., Feller, M. B., Datwani, A., & Shatz, C. J. (2014). Synapse elimination and learning rules co-regulated by MHC class I H2-Db. *Nature*, *509*(7499), 195–200.
Lee, R. C., Clandinin, T. R., Lee, C.-H., Chen, P.-L., Meinertzhagen, I. A., & Zipursky, S. L. (2003). The protocadherin Flamingo is required for axon target selection in the Drosophila visual system. *Nature Neuroscience*, *6*(6), 557–563.
Lee, S. J., Uemura, T., Yoshida, T., & Mishina, M. (2012). GluR 2 Assembles Four Neurexins into Trans-Synaptic Triad to Trigger Synapse Formation. *Journal of Neuroscience*, *32*(13), 4688–4701.
Leiner, H. C., Leiner, A. L., & Dow, R. S. (2002). Cognitive and language fundions of the human cerebellum, *Trends in Neurosciences,* 16(11), 444–447.
Letellier, M., Willson, M. L., Gautheron, V., Mariani, J., & Lohof, A. M. (2008). Normal adult climbing fiber monoinnervation of cerebellar Purkinje cells in mice lacking MHC class I molecules. *Developmental Neurobiology*, *68*(8), 997–1006.
Letts, V. A., Felix, R., Biddlecome, G. H., Arikkath, J., Mahaffey, C. L., Valenzuela, A., Bartlett, F. S., Mori, Y., et al. (1998). The mouse stargazer gene encodes a neuronal $Ca^{2+}$-channel γ-subunit. *Nature Genetics*, *19*(4), 340–347.
Levi, S., Grady, R. M., Henry, M. D., Campbell, K. P., Sanes, J. R., & Craig, A. M. (2002). Dystroglycan is selectively associated with inhibitory GABAergic synapses but is dispensable for their differentiation. *The Journal of Neuroscience, 22*(11), 4274–4285.
Lewis, J. A., Wu, C. H., Berg, H., & Levine, J. H. (1980). The genetics of levamisole resistance in the nematode Caenorhabditis elegans. *Genetics*, *95*(4), 905–928.
Lichtman, J. W., & Colman, H. (2000). Synapse elimination and indelible memory. *Neuron*, *25*(2), 269–278.
Lidman, O., TT, O., & Piehl, F. (1999). Expression of nonclassical MHC class I (RT1-U) in certain neuronal populations of the central nervous system. *The European Journal of Neuroscience, 11*, 4468–4472.
Limbach, C., Laue, M. M., Wang, X., & Hu, B. (2011). Molecular in situ topology of Aczonin/Piccolo and associated proteins at the mammalian neurotransmitter release site. *Proceedings of the National Academy of Sciences*, 108(31), 392-401.
Linhoff, M. W., Laurén, J., Cassidy, R. M., Dobie, F. A., Takahashi, H., Nygaard, H. B., Airaksinen, M. S., Strittmatter, S. M., & Craig, A. M. (2009). An Unbiased Expression Screen for Synaptogenic Proteins Identifies the LRRTM Protein Family as Synaptic Organizers. *Neuron*, *61*(5), 734–749.
Liu, F.-T. (2000). Galectins: A New Family of Regulators of Inflammation. *Clinical Immunology*, *97*(2), 79–88.
Llinas, R., & Sasaki, K. (1989). The Functional Organization of the Olivo-Cerebellar System as Examined by Multiple Purkinje Cell Recordings. *European Journal of Neuroscience*, *1*(6), 587–602.
Loconto, J., Papes, F., Chang, E., Stowers, L., Jones, E. P., Takada, T., Kumánovics, A., Lindahl, K. F., & Dulac, C. (2003). Functional expression of murine V2R pheromone receptors

involves selective association with the M10 and M1 families of MHC class Ib molecules. *Cell*, *112*(5), 607–618.

Logiudice, L., Sterling, P., & Matthews, G. (2009). Vesicle recycling at ribbon synapses in the finely branched axon terminals of mouse retinal bipolar neurons. *Neuroscience*, *164*(4), 1546–1556.

Long, E. O. (2008). Negative signaling by inhibitory receptors: the NK cell paradigm. *Immunological Reviews*, *224*(1), 70–84.

Lörincz, A., Notomi, T., Tamás, G., Shigemoto, R., & Nusser, Z. (2002). Polarized and compartment-dependent distribution of HCN1 in pyramidal cell dendrites. *Nature Neuroscience*, *5*(11), 1185–1193.

Lučić, V., Yang, T., Schweikert, G., Förster, F., & Baumeister, W. (2005). Morphological Characterization of Molecular Complexes Present in the Synaptic Cleft. *Structure*, *13*(3), 423–434.

Lüscher, C., & Malenka, R. C. (2011). Drug-Evoked Synaptic Plasticity in Addiction: From Molecular Changes to Circuit Remodeling. *Neuron*, *69*(4), 650–663.

**- M -**

MacAskill, A. F., Atkin, T. A., & Kittler, J. T. (2010). Mitochondrial trafficking and the provision of energy and calcium buffering at excitatory synapses. *European Journal of Neuroscience*, *32*(2), 231–240.

Malenka, R. C. (2003). Synaptic plasticity and AMPA receptor trafficking. *Annals of the New York Academy of Sciences*, *1003*, 1–11.

Mariani, J., & Changeux, J. P. (1981). Ontogenesis of olivo-cerebellar relationships. II. Spontaneous activity of inferior olivary neurons and climbing fibermediated activity of cerebellar Purkinje cells in developing rats. *The Journal of Neuroscience*, *1*(7), 703–709.

Maro, G. S., Gao, S., Olechwier, A. M., Hung, W. L., Liu, M., Özkan, E., Zhen, M., & Shen, K. (2015). MADD-4/Punctin and Neurexin Organize C. elegans GABAergic Postsynapses through Neuroligin. *Neuron, 86*, 1–13.

Mason, C. A., Christakos, S., & Catalano, S. M. (1990). Early climbing fiber interactions with Purkinje cells in the postnatal mouse cerebellum. *Journal of Comparative Neurology*, *297*(1), 77–90.

Mataga, N., Mizuguchi, Y., & Hensch, T. K. (2004). Experience-Dependent Pruning of Dendritic Spines in Visual Cortex by Tissue Plasminogen Activator. *Neuron, 44*, 1031–1041.

Matsuda, K., Miura, E., Miyazaki, T., Kakegawa, W., Emi, K., Narumi, S., Fukazawa, Y., Ito-Ishida, A., et al. (2010). Cbln1 Is a Ligand for an Orphan Glutamate Receptor 2, a Bidirectional Synapse Organizer. *Science*, *328*(5976), 363–368.

Matus, A., Ackermann, M., Pehling, G., Byers, H. R., & Fujiwara, K. (1982). High actin concentrations in brain dendritic spines and postsynaptic densities. *Proceedings of the National Academy of Sciences*, *79*(23), 7590–7594.

Mauch, D. H., Nagler, K., Schumacher, S., Goritz, C., Muller, E. C., Otto, A., & Pfrieger, F. W. (2001). CNS synaptogenesis promoted by glia-derived cholesterol. *Science*, *294*(5545), 1354–1357.

McAllister, A. K. (2007). Dynamic Aspects of CNS Synapse Formation. *Annual Review of Neuroscience*, *30*(1), 425–450.

McConnell, M. J., Huang, Y. H., Datwani, A., & Shatz, C. J. (2009). H2-K-b and H2-D-b regulate cerebellar long-term depression and limit motor learning. *Proceedings of the National Academy of Sciences*, *106*(16), 6784–6789.

Mercep, M., Bonifacino, J. S., Garcia-Morales, P., Samelson, L. E., Klausner, R. D., & Ashwell, J. D. (1988). T cell CD3-ξη heterodimer expression and coupling to phosphoinositide hydrolysis. *Science*, *242*(4878), 571–574.

Miller, K. D., Keller, J. B., & Stryker, M. P. (1989). Ocular dominance column development: analysis and simulation. *Science*, *245*(4918), 605–615.

Milstein, A. D., & Nicoll, R. A. (2008). Regulation of AMPA receptor gating and pharmacology by TARP auxiliary subunits. *Trends in Pharmacological Sciences*, *29*(7), 333–339.

Missler, M., Hammer, R. E., & Sudhof, T. C. (1998). Neurexophilin binding to α-neurexins. A single LNS domain functions as an independently folding ligand-binding unit. *The Journal of Biological Chemistry*, *273*(52), 34716–34723.

Mitsui, S., Hidaka, C., Furihata, M., Osako, Y., & Yuri, K. (2013). A mental retardation gene, motopsin/prss12, modulates cell morphology by interaction with seizure-related gene 6. *Biochemical and Biophysical Research Communications*, *436*(4), 638–644.

Miura, E., Iijima, T., Yuzaki, M., & Watanabe, M. (2006). Distinct expression of Cbln family mRNAs in developing and adult mouse brains. *European Journal of Neuroscience*, *24*(3), 750–760.

Miura, E., Matsuda, K., Morgan, J. I., Yuzaki, M., & Watanabe, M. (2009). Cbln1 accumulates and colocalizes with Cbln3 and GluRδ2 at parallel fiber-Purkinje cell synapses in the mouse cerebellum. *European Journal of Neuroscience*, *29*(4), 693–706.

Miyahara, M., Nakanishi, H., Takahashi, K., Satoh-Horikawa, K., Tachibana, K., & Takai, Y. (2000). Interaction of nectin with afadin is necessary for its clustering at cell-cell contact sites but not for its cis dimerization or trans interaction. *The Journal of Biological Chemistry*, *275*(1), 613–618.

Mizoguchi, A., Nakanishi, H., Kimura, K., Matsubara, K., Ozaki-Kuroda, K., Katata, T., Honda, T., Kiyohara, Y., et al. (2002). Nectin: an adhesion molecule involved in formation of synapses. *The Journal of Cell Biology*, *156*(3), 555–565.

Mohrmann, R., Lessmann, V., & Gottmann, K. (2003). Developmental maturation of synaptic vesicle cycling as a distinctive feature of central glutamatergic synapses. *Neuroscience*, *117*(1), 7–18.

Mok, H., Shin, H., Kim, S., Lee, J.-R., Yoon, J., & Kim, E. (2002). Association of the kinesin superfamily motor protein KIF1Bα with postsynaptic density-95 (PSD-95), synapse-associated protein-97, and synaptic scaffolding molecule PSD-95/discs large/zona occludens-1 proteins. *The Journal of Neuroscience*, *22*(13), 5253–5258.

Monji, A., Kato, T., & Kanba, S. (2009). Cytokines and schizophrenia: Microglia hypothesis of schizophrenia. *Psychiatry and Clinical Neurosciences*, *63*(3), 257–265.

Morales, M., & Fifkova, E. (1989). In situ localization of myosin and actin in dendritic spines with the immunogold technique. *Journal of Comparative Neurology*, *279*(4), 666–674.

Morando, L., Cesa, R., Rasetti, R., Harvey, R., & Strata, P. (2001). Role of glutamate δ-2

receptors in activity-dependent competition between heterologous afferent fibers. *Proceedings of the National Academy of Sciences*, *98*(17), 9954–9959.

Morgan, J. I., Slemmon, J. R., Danho, W., Hempstead, J., Berrebi, A. S., & Mugnaini, E. (1988). Cerebellin and related postsynaptic peptides in the brain of normal and neurodevelopmentally mutant vertebrates. *Synapse (New York, N.Y.)*, *2*(2), 117–124.

Moy, I., Todorovic, V., Dubash, A. D., Coon, J. S., Parker, J. B., Buranapramest, M., Huang, C. C., Zhao, H., et al. (2014). Estrogen-dependent sushi domain containing 3 regulates cytoskeleton organization and migration in breast cancer cells, *Oncogene,* 34(3), 323–333.

Mulley, J. C., Iona, X., Hodgson, B., Heron, S. E., Berkovic, S. F., Scheffer, I. E., & Dibbens, L. M. (2011). The Role of Seizure-Related SEZ6 as a Susceptibility Gene in Febrile Seizures. *Neurology Research International*, *2011*(4), 1–4.

Muly, E. C., Smith, Y., Allen, P., & Greengard, P. (2004). Subcellular distribution of spinophilin immunolabeling in primate prefrontal cortex: Localization to and within dendritic spines. *Journal of Comparative Neurology*, *469*(2), 185–197.

Murase, S., Mosser, E., & Schuman, E. M. (2002). Depolarization drives β-catenin into neuronal spines promoting changes in synaptic structure and function. *Neuron*, *35*(1), 91–105.

**- N -**

Nadjar, Y., Triller, A., Bessereau, J.-L., & Dumoulin, A. (2015). The Susd2 protein regulates neurite growth and excitatory synaptic density in hippocampal cultures. *Molecular and Cellular Neuroscience*, *65*(C), 82–91.

Naisbitt, S., Kim, E., Tu, J. C., Xiao, B., Sala, C., Valtschanoff, J., Weinberg, R. J., Worley, P. F., & Sheng, M. (1999). Shank, a novel family of postsynaptic density proteins that binds to the NMDA receptor/PSD-95/GKAP complex and cortactin. *Neuron*, *23*(3), 569–582.

Nakayama, M., & Hama, C. (2011). Modulation of neurotransmitter receptors and synaptic differentiation by proteins containing complement-related domains. *Neuroscience Research*, *69*(2), 87–92.

Napper, R. M., & Harvey, R. J. (1988). Number of parallel fiber synapses on an individual Purkinje cell in the cerebellum of the rat. *Journal of Comparative Neurology*, *274*(2), 168–177.

Nathan, C. F., Prendergast, T. J., Wiebe, M. E., Stanley, E. R., Platzer, R., Remold, H. G., Welte, K., Rubin, B. Y., & Murray, H. W. (1985). Activation of human macrophages. *Human Immunology*, *14*(1), 11–17.

Neuhoff, H., Sassoè-Pognetto, M., Panzanelli, P., Maas, C., Witke, W., & Kneussel, M. (2005). The actin-binding protein profilin I is localized at synaptic sites in an activity-regulated manner. *European Journal of Neuroscience*, *21*(1), 15–25.

Neumann, H., Cavalie, A., Jenne, D. E., & Wekerle, H. (1995). Induction of MHC class I genes in neurons. *Science*, *269*(5223), 549–552.

Neumann, H., Schmidt, H., Cavalie, A., Jenne, D., & Wekerle, H. (1997). Major Histocompatibility Complex (MHC) Class I Gene Expression in Single Neurons of the Central Nervous System: Differential Regulation by Interferon (IFN)-γ and Tumor

Necrosis Factor (TNF)-α. *The Journal of Experimental Medicine, 185*(2), 305–316.
Niwa, S., Tanaka, Y., & Hirokawa, N. (2008). KIF1Bβ- and KIF1A-mediated axonal transport of presynaptic regulator Rab3 occurs in a GTP-dependent manner through DENN/MADD. *Nature Cell Biology*, *10*(11), 1269–1279.
Noebels, J. L., Qiao, X., Bronson, R. T., Spencer, C., & Davisson, M. T. (1990). Stargazer - a New Neurological Mutant on Chromosome-15 in the Mouse with Prolonged Cortical Seizures. *Epilepsy Research*, *7*(2), 129–135.
Notomi, T., & Shigemoto, R. (2004). Immunohistochemical localization of Ih channel subunits, HCN1-4, in the rat brain. *Journal of Comparative Neurology*, *471*(3), 241–276.
Nusser, Z. (2000). AMPA and NMDA receptors: similarities and differences in their synaptic distribution. *Current Opinion in Neurobiology*, *10*(3), 337–341.
Nusser, Z., Lujan, R., Laube, G., Roberts, J., Molnar, E., & Somogyi, P. (1998). Cell type and pathway dependence of synaptic AMPA receptor number and variability in the hippocampus. *Neuron*, *21*(3), 545–559.

**- O -**

O'Brien, R. J., Xu, D., Petralia, R. S., Steward, O., Huganir, R. L., & Worley, P. F. (1999). Synaptic clustering of AMPA receptors by the extracellular immediate-early gene product Narp. *Neuron*, *23*(2), 309–323.
O'Shea, J. J., & Murray, P. J. (2008). Cytokine Signaling Modules in Inflammatory Responses. *Immunity*, *28*(4), 477–487.
Ogawa, Y., & Rasband, M. N. (2008). The functional organization and assembly of the axon initial segment. *Current Opinion in Neurobiology*, *18*(3), 307–313.
Okajima, D., Kudo, G., & Yokota, H. (2010). Antidepressant-like behavior in brain-specific angiogenesis inhibitor 2-deficient mice. *The Journal of Physiological Sciences*, *61*(1), 47–54.
Oscarsson, O. (1979). Functional units of the cerebellum - sagittal zones and microzones. *Trends in Neurosciences*, 143-145.
Ostroff, L. E., Fiala, J. C., Allwardt, B., & Harris, K. M. (2002). Polyribosomes Redistribute from Dendritic Shafts into Spines with Enlarged Synapses during LTP in Developing Rat Hippocampal Slices. *Neuron*, *35*(3), 535–545.
Ottersen, O. P., & Landsend, A. S. (1997). Organization of glutamate receptors at the synapse. *European Journal of Neuroscience*, *9*(11), 2219–2224.
Owald, D., Fouquet, W., Schmidt, M., Wichmann, C., Mertel, S., Depner, H., Christiansen, F., Zube, C., et al. (2010). A Syd-1 homologue regulates pre- and postsynaptic maturation in Drosophila. *The Journal of Cell Biology*, *188*(4), 565–579.

**- P -**

Palay, S. L., & Chan-Palay, V. (1974). Cerebellar Cortex, 1–361.
Pang, Z., Zuo, J., & Morgan, J. I. (2000). Cbln3, a novel member of the precerebellin family that binds specifically to Cbln1. *The Journal of Neuroscience, 20*(17), 6333–6339.
Paradies, M. A., & Eisenman, L. M. (1993). Evidence of early topographic organization in the

embryonic olivo-cerebellar projection: a model system for the study of pattern formation processes in the central nervous system. *Developmental Dynamics*, *197*(2), 125–145.

Pascual, M., Pozas, E., Barallobre, M. J., Tessier-Lavigne, M., & Soriano, E. (2004). Coordinated functions of Netrin-1 and Class 3 secreted Semaphorins in the guidance of reciprocal septohippocampal connections. *Molecular and Cellular Neuroscience*, *26*(1), 24–33.

Patel, M. R., Lehrman, E. K., Poon, V. Y., Crump, J. G., Zhen, M., Bargmann, C. I., & Shen, K. (2006). Hierarchical assembly of presynaptic components in defined C. elegans synapses. *Nature Neuroscience*, *9*(12), 1488–1498.

Patrizi, A., Scelfo, B., Viltono, L., Briatore, F., Fukaya, M., Watanabe, M., Strata, P., Varoqueaux, F., et al. (2008). Synapse formation and clustering of neuroligin-2 in the absence of $GABA_A$ receptors. *Proceedings of the National Academy of Sciences*, *105*(35), 13151–13156.

Paukert, M., Huang, Y. H., Tanaka, K., Rothstein, J. D., & Bergles, D. E. (2010). Zones of Enhanced Glutamate Release from Climbing Fibers in the Mammalian Cerebellum. *Journal of Neuroscience*, *30*(21), 7290–7299.

Pelkey, K. A., Barksdale, E., Craig, M. T., Yuan, X., Sukumaran, M., Vargish, G. A., Mitchell, R. M., Wyeth, M. S., et al. (2015). Pentraxins Coordinate Excitatory Synapse Maturation and Circuit Integration of Parvalbumin Interneurons. *Neuron*, *85*(6), 1257–1272.

Perez-Alcazar, M., Daborg, J., Stokowska, A., Wasling, P., Björefeldt, A., Kalm, M., Zetterberg, H., Carlström, K. E., et al. (2014). Altered cognitive performance and synaptic function in the hippocampus of mice lacking C3. *Experimental Neurology*, *253*(C), 154–164.

Perry, V. H., & O'Connor, V. (2008). C1q: the perfect complement for a synaptic feast? *Nature Reviews Neuroscience*, *9*(11), 807–811.

Petralia, R. S., Sans, N., Wang, Y. X., & Wenthold, R. J. (2005). Ontogeny of postsynaptic density proteins at glutamatergic synapses. *Molecular and Cellular Neuroscience*, *29*(3), 436–452.

Pieraut, S., Lucas, O., Sangari, S., Sar, C., Boudes, M., Bouffi, C., Noel, D., & Scamps, F. (2011). An Autocrine Neuronal Interleukin-6 Loop Mediates Chloride Accumulation and NKCC1 Phosphorylation in Axotomized Sensory Neurons. *Journal of Neuroscience*, *31*(38), 13516–13526.

Pinan-Lucarré, B., Tu, H., Pierron, M., Cruceyra, P. I., Zhan, H., Stigloher, C., Richmond, J. E., & Bessereau, J.-L. (2014). C. elegans Punctin specifies cholinergic versus GABAergic identity of postsynaptic domains. *Nature, 511*(7510), 466–470.

Pollerberg, G. E., & Beck-Sickinger, A. (1993). A functional role for the middle extracellular region of the neural cell adhesion molecule (NCAM) in axonal fasciculation and orientation. *Developmental Biology*, *156*(2), 324–340.

Poo, M. M. (2001). Neurotrophins as synaptic modulators. *Nature Reviews Neuroscience*, *2*(1), 24–32.

Poulopoulos, A., Aramuni, G., Meyer, G., Soykan, T., Hoon, M., Papadopoulos, T., Zhang, M., Paarmann, I., et al. (2009). Neuroligin 2 Drives Postsynaptic Assembly at Perisomatic Inhibitory Synapses through Gephyrin and Collybistin. *Neuron*, *63*(5), 628–642.

Puente, N., Mendizabal-Zubiaga, J., Elezgarai, I., Reguero, L., Buceta, I., & Grandes, P. (2010).

Precise localization of the voltage-gated potassium channel subunits Kv3.1b and Kv3.3 revealed in the molecular layer of the rat cerebellar cortex by a pre-embedding immunogold method. *Histochemistry and Cell Biology*, *134*(4), 403–409.

**- R -**

Rabinovich, G. A. (2005). Galectin-1 as a potential cancer target. *British Journal of Cancer*, *92*(7), 1188–1192.

Rakic, P. (1971). Neuron-glia relationship during granule cell migration in developing cerebellar cortex. A Golgi and electronmicroscopic study in Macacus Rhesus. *Journal of Comparative Neurology*, *141*(3), 283–312.

Rakic, P., & Sidman, R. L. (1973). Sequence of Developmental Abnormalities Leading to Granule Cell Deficit in Cerebellar Cortex of Weaver Mutant. *Journal of Comparative Neurology*, 1–30.

Ransohoff, R. M., Liu, L., & Cardona, A. E. (2007). Chemokines and Chemokine Receptors: Multipurpose Players in Neuroinflammation. *International Review of Neurobiology*, 82, 187–204.

Rao, A., & Craig, A. M. (1997). Activity regulates the synaptic localization of the NMDA receptor in hippocampal neurons. *Neuron*, *19*(4), 801–812.

Raymond, J. L., Lisberger, S. G., & Mauk, M. D. (1996). The cerebellum: a neuronal learning machine? *Science*, *272*(5265), 1126–1131.

Redies, C., Neudert, F., & Lin, J. (2011). Cadherins in cerebellar development: translation of embryonic patterning into mature functional compartmentalization. *Cerebellum*, *10*(3), 393–408.

Reeber, S. L., & Sillitoe, R. V. (2011). Patterned expression of a cocaine- and amphetamine-regulated transcript peptide reveals complex circuit topography in the rodent cerebellar cortex. *Journal of Comparative Neurology*, *519*(9), 1781–1796.

Reeber, S. L., White, J. J., George-Jones, N. A., & Sillitoe, R. V. (2013). Architecture and development of olivo-cerebellar circuit topography. *Frontiers in Neural Circuits*, *6*, 1–14.

Reid, K. B. M., & Day, A. J. (1989). Structure-function relationships of the complement components, *Immunology Today,* 10 (6), 177–180.

Reid, K. B. M., & Porter, R. R. (1976). Subunit Composition and Structure of Subcomponent Clq of the First Component of Human Complement. *The Biochemical Journal, 155*, 19–23.

Ressl, S., Vu, B. K., Vivona, S., Martinelli, D. C., Südhof, T. C., & Brunger, A. T. (2015). Structures of C1q-like Proteins Reveal Unique Features among the C1q/TNF Superfamily. *Structure*, *23*(4), 688–699.

Ricklin, D., Hajishengallis, G., Yang, K., & Lambris, J. D. (2010). Complement: a key system for immunesurveillance and homeostasis. *Nature Immunology*, *11*(9), 785–797.

Roll, P., Rudolf, G., Pereira, S., Royer, B., Scheffer, I E., Massacrier, A., Valenti, M-P., Roeckel-Trevisiol, N., Jamali, S., Beclin, C., Seegmuller, C., Metz-Lutz, M-N., Lemainque, A., Delepine, M., Caloustian, C., Martin, A., Bruneau, N., Depetris, D., Mattei, M-G., Flori, E., Robaglia-Schlupp, A., Levy, N., Neubauer, B A., Ravid, R., Marescaux, C., Berkovic, S F.,

Hirsch, E., Lathrop, M., Cau, P., & Szepetowski, P. (2006). SRPX2 mutations in disorders of language cortex and cognition. *Human Molecular Genetics*, *15*(7), 1195–1207.

Roll, P., Vernes, S. C., Bruneau, N., Cillario, J., Ponsole-Lenfant, M., Massacrier, A., Rudolf, G., Khalife, M., et al. (2010). Molecular networks implicated in speech-related disorders: FOXP2 regulates the SRPX2/uPAR complex. *Human Molecular Genetics*, *19*(24), 4848–4860.

Rossi, F., & Strata, P. (1995). Reciprocal trophic interactions in the adult climbing fiber-Purkinje cell system. *Progress in Neurobiology*, 47, 341-369.

Royer-Zemmour, B., Ponsole-Lenfant, M., Gara, H., Roll, P., Leveque, C., Massacrier, A., Ferracci, G., Cillario, J., et al. (2008). Epileptic and developmental disorders of the speech cortex: ligand/receptor interaction of wild-type and mutant SRPX2 with the plasminogen activator receptor uPAR. *Human Molecular Genetics*, *17*(23), 3617–3630.

Ruigrok, T. J., & Voogd, J. (2000). Organization of projections from the inferior olive to the cerebellar nuclei in the rat. *Journal of Comparative Neurology*, *426*(2), 209–228.

**- S -**

Sabo, S. L., Gomes, R. A., & McAllister, A. K. (2006). Formation of Presynaptic Terminals at Predefined Sites along Axons. *Journal of Neuroscience*, *26*(42), 10813–10825.

Sahay, A., Molliver, M. E., Ginty, D. D., & Kolodkin, A. L. (2003). Semaphorin 3F is critical for development of limbic system circuitry and is required in neurons for selective CNS axon guidance events. *The Journal of Neuroscience*, *23*(17), 6671–6680.

Salmi, M., Bruneau, N., Cillario, J., Lozovaya, N., Massacrier, A., Buhler, E., Cloarec, R., Tsintsadze, T., et al. (2013). Tubacin prevents neuronal migration defects and epileptic activity caused by rat Srpx2 silencing in utero. *Brain*, *136*(8), 2457–2473.

Samuels, B. A., Hsueh, Y.-P., Shu, T., Liang, H., Tseng, H.-C., Hong, C.-J., Su, S. C., Volker, J., et al. (2007). Cdk5 Promotes Synaptogenesis by Regulating the Subcellular Distribution of the MAGUK Family Member CASK. *Neuron*, *56*(5), 823–837.

Sanes, J. R., & Yamagata, M. (2009). Many Paths to Synaptic Specificity. *Annual Review of Cell and Developmental Biology*, *25*(1), 161–195.

Sankaranarayanan, S., Atluri, P. P., & Ryan, T. A. (2003). Actin has a molecular scaffolding, not propulsive, role in presynaptic function. *Nature Neuroscience*, *6*(2), 127–135.

Sans, N., Petralia, R. S., Wang, Y. X., Blahos, J., Hell, J. W., & Wenthold, R. J. (2000). A developmental change in NMDA receptor-associated proteins at hippocampal synapses. *The Journal of Neuroscience, 20*(3), 1260–1271.

Sassoè-Pognetto, M., Frola, E., Pregno, G., Briatore, F., & Patrizi, A. (2011). Understanding the Molecular Diversity of GABAergic Synapses. *Frontiers in Cellular Neuroscience*, *5*, 1-12.

Satoh-Horikawa, K., Nakanashi, H., Takahashi, K., Miyahara, M., Nishimura, M., Tachibana, K., Mizoguchi, A., & Takai, Y. (2000). Nectin-3, a New Member of Immunoglobulin-like Cell Adhesion Molecules That Shows Homophilic and Heterophilic Cell-Cell Adhesion Activities. *The Journal of Biological Chemistry, 275*(14), 10291-10299.

Sawada, K., Fukui, Y., & Hawkes, R. (2008). Spatial distribution of corticotropin-releasing factor immunopositive climbing fibers in the mouse cerebellum: Analysis by whole

mount immunohistochemistry. *Brain Research*, *1222*, 106–117.
Schafer, D. P., Lehrman, E. K., Kautzman, A. G., Koyama, R., Mardinly, A. R., Yamasaki, R., Ransohoff, R. M., Greenberg, M. E., et al. (2012). Microglia Sculpt Postnatal Neural Circuits in an Activity and Complement-Dependent Manner. *Neuron*, *74*(4), 691–705.
Scheiffele, P. (2003). Cell-cell signaling during synapse formation in the CNS. *Annual Review of Neuroscience*, *26*, 485–508.
Scheiffele, P., Fan, J., Choih, J., Fetter, R., & Serafini, T. (2000). Neuroligin expressed in nonneuronal cells triggers presynaptic development in contacting axons. *Cell*, *101*(6), 657–669.
Schikorski, T., & Stevens, C. F. (1997). Quantitative ultrastructural analysis of hippocampal excitatory synapses. *The Journal of Neuroscience*, *17*(15), 5858–5867.
Schild, R. F. (1970). On the Inferior Olive of the Albino Rat. *Journal of Comparative Neurology,* 140, 255-260.
Schlimgen, A. K., Helms, J. A., Vogel, H., & Perin, M. S. (1995). Neuronal pentraxin, a secreted protein with homology to acute phase proteins of the immune system. *Neuron*, *14*(3), 519–526.
Schmahmann, J. D. (1998). Dysmetria of thought: clinical consequences of cerebellar dysfunction on cognition and affect. *Trends in Cognitive Sciences, 2*(9), 362–371.
Schmid, R. S., Pruitt, W. M., & Maness, P. F. (2000). A MAP kinase-signaling pathway mediates neurite outgrowth on L1 and requires Src-dependent endocytosis. *The Journal of Neuroscience*, *20*(11), 4177–4188.
Schuster, T., Krug, M., Stalder, M., Hackel, N., Gerardy-Schahn, R., & Schachner, M. (2001). Immunoelectron microscopic localization of the neural recognition molecules L1, NCAM, and its isoform NCAM180, the NCAM-associated polysialic acid, β1 integrin and the extracellular matrix molecule tenascin-R in synapses of the adult rat hippocampus. *Journal of Neurobiology*, *49*(2), 142–158.
Schwenk, J., Metz, M., Zolles, G., Turecek, R., Fritzius, T., Bildl, W., Tarusawa, E., Kulik, A., et al. (2010). Native $GABA_B$ receptors are heteromultimers with a family of auxiliary subunits. *Nature*, *465*(7295), 231–235.
Scott, T. G. (1963). A Unique Pattern of Localization within the Cerebellum. *Nature,* 200, 793.
Selimi, F., Cristea, I. M., Heller, E., Chait, B. T., & Heintz, N. (2009). Proteomic Studies of a Single CNS Synapse Type: The Parallel Fiber/Purkinje Cell Synapse. *PLoS Biology*, *7*(4), 948-957.
Sellar, G. C., Blake, D. J., & Reid, K. B. M. (1991). Characterization and organization of the genes encoding the A-, B- and C-chains of human complement component C1q. *The Biochemical Journal, 274,* 481-490.
Serafini, T., Colamarino, S. A., Leonardo, E. D., Wang, H., Beddington, R., Skarnes, W. C., & TessierLavigne, M. (1996). Netrin-1 is required for commissural axon guidance in the developing vertebrate nervous system. *Cell*, *87*(6), 1001–1014.
Serra-Pages, C., Medley, Q. G., Tang, M., Hart, A., & Streuli, M. (1998). Liprins, a family of LAR transmembrane protein-tyrosine phosphatase-interacting proteins. *The Journal of Biological Chemistry*, *273*(25), 15611–15620.
Setou, M., Seog, D.-H., Tanaka, Y., Kanal, Y., Takel, Y., Kawagishi, M., & Nobutaka, H. (2002).

Glutamate-receptor-interacting protein GRIP1 directly steers kinesin to dendrites. *Nature, 417*, 83-87.

Shaffer, L. G., Theisen, A., Bejjani, B. A., Ballif, B. C., Aylsworth, A. S., Lim, C., McDonald, M., Ellison, J. W., et al. (2007). The discovery of microdeletion syndromes in the post-genomic era: review of the methodology and characterization of a new 1q41q42 microdeletion syndrome. *Genetics in Medicine*, *9*(9), 607–616.

Shapira, M., Zhai, R. G., Dresbach, T., Bresler, T., Torres, V. I., Gundelfinger, E. D., Ziv, N. E., & Garner, C. C. (2003). Unitary assembly of presynaptic active zones from Piccolo-Bassoon transport vesicles. *Neuron*, *38*(2), 237–252.

Shapiro, L., & Colman, D. R. (1999). The diversity of cadherins and implications for a synaptic adhesive code in the CNS. *Neuron*, 23, 427-430.

Shapiro, L., & Scherer, P. E. (1998). The crystal structure of a complement-1q family protein suggests an evolutionary link to tumor necrosis factor. *Current Biology*, *8*(6), 335–338.

Shatz, C. J. (2009). MHC Class I: An unexpected role in neuronal plasticity. *Neuron*, *64*(1), 40–45.

Shatz, C. J., & Sretavan, D. W. (1986). Interactions between retinal ganglion cells during the development of the mammalian visual system. *Annual Review of Neuroscience, 9,* 171-207.

Shatz, C. J., & Stryker, M. P. (1978). Ocular dominance in layer IV of the cat's visual cortex and the effects of monocular deprivation. *The Journal of Physiology*, *281*, 267–283.

Sheng, M., & Hoogenraad, C. C. (2007). The Postsynaptic Architecture of Excitatory Synapses: A More Quantitative View. *Annual Review of Biochemistry*, *76*(1), 823–847.

Sheng, M., & Kim, E. (2011). The Postsynaptic Organization of Synapses. *Cold Spring Harbor Perspectives in Biology*, *3*(12), a005678.

Shepherd, J. D., & Huganir, R. L. (2007). The Cell Biology of Synaptic Plasticity: AMPA Receptor Trafficking. *Annual Review of Cell and Developmental Biology*, *23*(1), 613–643.

Shimizu-Nishikawa, K., Kajiwara, K., & Sugaya, E. (1995a). Cloning and characterization of seizure-related gene, SEZ-6. *Biochemical and Biophysical Research Communications*, *216*(1), 382–389.

Shimizu-Nishikawa, K., Kajiwara, K., Kimura, M., Katsuki, M., & Sugaya, E. (1995b). Cloning and expression of SEZ-6, a brain-specific and seizure-related cDNA. *Molecular Brain Research*, *28*(2), 201–210.

Sia, G. M., Clem, R. L., & Huganir, R. L. (2013). The human language-associated gene SRPX2 regulates synapse formation and vocalization in mice. *Science*, 342, 987-991.

Sia, G.-M., Béïque, J.-C., Rumbaugh, G., Cho, R., Worley, P. F., & Huganir, R. L. (2007). Interaction of the N-Terminal Domain of the AMPA Receptor GluR4 Subunit with the Neuronal Pentraxin NP1 Mediates GluR4 Synaptic Recruitment. *Neuron*, *55*(1), 87–102.

Siddiqui, T. J., Pancaroglu, R., Kang, Y., Rooyakkers, A., & Craig, A. M. (2010). LRRTMs and Neuroligins Bind Neurexins with a Differential Code to Cooperate in Glutamate Synapse Development. *Journal of Neuroscience*, *30*(22), 7495–7506.

Siegelman, M. H., & Weissman, I. L. (1989). Human homologue of mouse lymph node homing receptor: evolutionary conservation at tandem cell interaction domains. *Proceedings of the National Academy of Sciences,* 86, 5562-5566.

Sigoillot, S. M., Iyer, K., Binda, F., González-Calvo, I., Talleur, M., Vodjdani, G., Isope, P., &

Selimi, F. (2015). The Secreted Protein C1QL1 and Its Receptor BAI3 Control the Synaptic Connectivity of Excitatory Inputs Converging on Cerebellar Purkinje Cells. *Cell Reports*, *10*(5), 820–832.

Slemmon, J. R., Blacher, R., Danho, W., Hempstead, J. L., & Morgan, J. I. (1984). Isolation and sequencing of two cerebellum-specific peptides. *Proceedings of the National Academy of Sciences*, *81*(21), 6866–6870.

Somogyi, P., & Hámori, J. (1975). A quantitative electron microscopic study of the Purkinje cell axon initial segment. *Neuroscience*, *1*(5), 361–365.

Song, I., & Huganir, R. L. (2002). Regulation of AMPA receptors during synaptic plasticity. *Trends in Neurosciences*, *25*(11), 578–588.

Song, J. Y., Ichtchenko, K., Sudhof, T. C., & Brose, N. (1999). Neuroligin 1 is a postsynaptic cell-adhesion molecule of excitatory synapses. *Proceedings of the National Academy of Sciences*, *96*(3), 1100–1105.

Sorra, K. E., Mishra, A., Kirov, S. A., & Harris, K. M. (2006). Dense core vesicles resemble active-zone transport vesicles and are diminished following synaptogenesis in mature hippocampal slices. *Neuroscience*, *141*(4), 2097–2106.

Sotelo, C. (1990). Cerebellar synaptogenesis: what we can learn from mutant mice. *The Journal of Experimental Biology,* 153, 225-249.

Sotelo, C. (2007). Development of "Pinceaux" formations and dendritic translocation of climbing fibers during the acquisition of the balance between glutamatergic and γ-aminobutyric acidergic inputs in developing Purkinje cells. *Journal of Comparative Neurology*, *506*(2), 240–262.

Sotelo, C., & Chedotal, A. (2005). Development of the olivo-cerebellar system: migration and formation of cerebellar maps. *Progress in Brain Research, 148*, 1–20.

Srivastava, S., Osten, P., Vilim, F. S., Khatri, L., Inman, G., States, B., Daly, C., DeSouza, S., et al. (1998). Novel anchorage of GluR2/3 to the postsynaptic density by the AMPA receptor-binding protein ABP. *Neuron*, *21*(3), 581–591.

Steiner, P., Higley, M. J., Xu, W., Czervionke, B. L., Malenka, R. C., & Sabatini, B. L. (2008). Destabilization of the Postsynaptic Density by PSD-95 Serine 73 Phosphorylation Inhibits Spine Growth and Synaptic Plasticity. *Neuron*, *60*(5), 788–802.

Stellwagen, D., & Malenka, R. C. (2006). Synaptic scaling mediated by glial TNF-α. *Nature Cell Biology*, *440*(7087), 1054–1059.

Stephan, A. H., Barres, B. A., & Stevens, B. (2012). The Complement System: An Unexpected Role in Synaptic Pruning During Development and Disease. *Annual Review of Neuroscience*, *35*(1), 369–389.

Stephan, A. H., Madison, D. V., Mateos, J. M., Fraser, D. A., Lovelett, E. A., Coutellier, L., Kim, L., Tsai, H. H., et al. (2013). A Dramatic Increase of C1q Protein in the CNS during Normal Aging. *Journal of Neuroscience*, *33*(33), 13460–13474.

Stephan, A., Mateos, J. M., Kozloy, S. V., Cinelli, P., Kistler, A. D., Hettwer, S., Rulicke, T., Streit, P., et al. (2008). Neurotrypsin cleaves agrin locally at the synapse. *The FASEB Journal,* 22, 1861-1873.

Stevens, B., Allen, N. J., Vazquez, L. E., Howell, G. R., Christopherson, K. S., Nouri, N., Micheva, K. D., Mehalow, A. K., et al. (2007). The Classical Complement Cascade Mediates CNS Synapse Elimination. *Cell*, *131*(6), 1164–1178.

Steward, O., & Schuman, E. M. (2003). Compartmentalized synthesis and degradation of proteins in neurons. *Neuron*, 40, 347-359.

Sudhof, T. C. (1995). The synaptic vesicle cycle: a cascade of protein-protein interactions. *Nature, 375*, 645–653.

Sugahara, T., Yamashita, Y., Shinomi, M., Yamanoha, B., Iseki, H., Takeda, A., Okazaki, Y., Hayashizaki, Y., et al. (2007). Isolation of a novel mouse gene, mSVS-1/SUSD2, reversing tumorigenic phenotypes of cancer cells in vitro. *Cancer Science*, *98*(6), 900–908.

Sugihara, I. (2004). Molecular, Topographic, and Functional Organization of the Cerebellar Cortex: A Study with Combined Aldolase C and Olivo-cerebellar Labeling. *Journal of Neuroscience*, *24*(40), 8771–8785.

Sugihara, I. (2005). Microzonal projection and climbing fiber remodeling in single olivo-cerebellar axons of newborn rats at postnatal days 4-7. *Journal of Comparative Neurology*, *487*(1), 93–106.

Sugihara, I., Wu, H. S., & Shinoda, Y. (2001). The entire trajectories of single olivo-cerebellar axons in the cerebellar cortex and their contribution to Cerebellar compartmentalization. *The Journal of Neuroscience*, *21*(19), 7715–7723.

Sugita, S., Saito, F., Tang, J., Satz, J., Campbell, K., & Sudhof, T C. (2001). A stoichiometric complex of neurexins and dystroglycan in brain. *The Journal of Cell Biology*, *154*(2), 435–446.

Sun, Q., & Turrigiano, G. G. (2011). PSD-95 and PSD-93 Play Critical But Distinct Roles in Synaptic Scaling Up and Down. *Journal of Neuroscience*, *31*(18), 6800–6808.

Suto, F., Tsuboi, M., Kamiya, H., Mizuno, H., Kiyama, Y., Komai, S., Shimizu, M., Sanbo, M., et al. (2007). Interactions between Plexin-A2, Plexin-A4, and Semaphorin 6A Control Lamina-Restricted Projection of Hippocampal Mossy Fibers. *Neuron*, *53*(4), 535–547.

Südhof, T. C., & Rothman, J. E. (2009). Membrane fusion: grappling with SNARE and SM proteins. *Science*, *323*(5913), 474–477.

Syken, J., & Shatz, C. J. (2003). Expression of T cell receptor β locus in central nervous system neurons. *Proceedings of the National Academy of Sciences*, *100*(22), 13048–13053.

Syken, J., GrandPre, T., Kanold, P. O., & Shatz, C. J. (2006). PirB restricts ocular-dominance plasticity in visual cortex. *Science*, *313*(5794), 1795–1800.

**- T -**

Takai, Y., Shimizu, K., & Ohtsuka, T. (2003). The roles of cadherins and nectins in interneuronal synapse formation. *Current Opinion in Neurobiology*, 13, 520-526.

Takai, Y., Irie, K., Shimizu, K., Sakisaka, T., & Ikeda, W. (2003a). Nectins and nectin-like molecules: Roles in cell adhesion, migration and polarization. *Cancer Science,* 94: 655-667.

Takasu, M. A., Dalva, M. B., Zigmond, R. E., & Greenberg, M. E. (2002). Modulation of NMDA receptor-dependent calcium influx and gene expression through EphB receptors. *Science*, *295*(5554), 491–495.

Takeuchi, T., Miyazaki, T., Watanabe, M., Mori, H., Sakimura, K., & Mishina, M. (2005).

Control of Synaptic Connection by Glutamate Receptor 2 in the Adult Cerebellum. *Journal of Neuroscience*, *25*(8), 2146–2156.

Takeuchi, Y., Asano, H., Katayama, Y., Muragaki, Y., Imoto, K., & Miyata, M. (2014). Large-Scale Somatotopic Refinement via Functional Synapse Elimination in the Sensory Thalamus of Developing Mice. *Journal of Neuroscience*, *34*(4), 1258–1270.

Tanaka, H., Shan, W. S., Phillips, G. R., Arndt, K., Bozdagi, O., Shapiro, L., Huntley, G. W., Benson, D. L., & Colman, D. R. (2000). Molecular modification of N-cadherin in response to synaptic activity. *Neuron*, *25*(1), 93–107.

Tang, L., Hung, C. P., & Schuman, E. M. (1998). A Role for the Cadherin Family of Cell Adhesion Molecules in Hippocampal Long-Term Potentiation. *Neuron, 20*, 1165–1175.

Terauchi, A., Johnson-Venkatesh, E. M., Toth, A. B., Javed, D., Sutton, M. A., & Umemori, H. (2010). Distinct FGFs promote differentiation of excitatory and inhibitory synapses. *Nature*, *465*(7299), 783–787.

Tessier-Lavigne, M. (1995). Eph Receptor Tyrosine Kinases, Axon Repulsion, and the Developmentof Topographic Maps. *Cell, 82*, 345-348.

Thach, W. T., Goodkin, H. P., & Keating, J. G. (1992). The cerebellum and the adaptive coordination of movement. *Annual Review of Neuroscience*, *15*, 403–442.

Togashi, H., Abe, K., Mizoguchi, A., Takaoka, K., Chisaka, O., & Takeichi, M. (2002). Cadherin regulates dendritic spine morphogenesis. *Neuron*, *35*(1), 77–89.

Togashi, H., Miyoshi, J., Honda, T., Sakisaka, T., Takai, Y., & Takeichi, M. (2006). Interneurite affinity is regulated by heterophilic nectin interactions in concert with the cadherin machinery. *The Journal of Cell Biology*, *174*(1), 141–151.

Tomita, S., Chen, L., Kawasaki, Y., Petralia, R. S., Wenthold, R. J., Nicoll, R. A., & Bredt, D. S. (2003). Functional studies and distribution define a family of transmembrane AMPA receptor regulatory proteins. *The Journal of Cell Biology*, *161*(4), 805–816.

Tovar, K. R., & Westbrook, G. L. (1999). The incorporation of NMDA receptors with a distinct subunit composition at nascent hippocampal synapses in vitro. *The Journal of Neuroscience*, *19*(10), 4180–4188.

Trachtenberg, J. T., Chen, B. E., Knott, G. W., Feng, G. P., Sanes, J. R., Welker, E., & Svoboda, K. (2002). Long-term in vivo imaging of experience-dependent synaptic plasticity in adult cortex. *Nature*, *420*(6917), 788–794.

Tsui, C. C., Copeland, N. G., Gilbert, D. J., Jenkins, N. A., Barnes, C., & Worley, P. F. (1996). Narp, a novel member of the pentraxin family, promotes neurite outgrowth and is dynamically regulated by neuronal activity. *The Journal of Neuroscience*, *16*(8), 2463–2478.

Tu, H., Pinan-Lucarré, B., Ji, T., Jospin, M., & Bessereau, J.-L. (2015). C. elegans Punctin Clusters $GABA_A$ receptors via Neuroligin binding and UNC-40/DCC recruitment. *Neuron, 86*(6), 1407–1419.

Turrigiano, G. G. (2008). The Self-Tuning Neuron: Synaptic Scaling of Excitatory Synapses. *Cell*, *135*(3), 422–435.

**- U -**

Uemura, T., Kakizawa, S., Yamasaki, M., Sakimura, K., Watanabe, M., Iino, M., & Mishina, M.

(2007). Regulation of Long-Term Depression and Climbing Fiber Territory by Glutamate Receptor 2 at Parallel Fiber Synapses through its C-Terminal Domain in Cerebellar Purkinje Cells. *Journal of Neuroscience*, *27*(44), 12096–12108.

Uemura, T., Lee, S.-J., Yasumura, M., Takeuchi, T., Yoshida, T., Ra, M., Taguchi, R., Sakimura, K., & Mishina, M. (2010). Trans-Synaptic Interaction of GluRd2 and Neurexin through Cbln1 Mediates Synapse Formation in the Cerebellum. *Cell*, *141*(6), 1068–1079.

Ullian, E. M., Harris, B. T., Wu, A., Chan, J. R., & Barres, B. A. (2004). Schwann cells and astrocytes induce synapse formation by spinal motor neurons in culture. *Molecular and Cellular Neuroscience*, *25*(2), 241–251.

Umemori, H., Linhoff, M. W., Ornitz, D. M., & Sanes, J. R. (2004). FGF22 and its close relatives are presynaptic organizing molecules in the mammalian brain. *Cell*, *118*(2), 257–270.

Ushkaryov, Y. A., Petrenko, A., Geppert, M., & Sudhof, T. C. (1992). Neurexins: Synaptic cell surface proteins related to the α-latrotoxin receptor and laminin. *Science, 257*, 50–56.

Uzman, L. L. (1960). The histogenesis of the mouse cerebellum as studied by its tritiated thymidine uptake. *Journal of Comparative Neurology,* 137-159.

**- V -**

Valtschanoff, J. G., Burette, A., Davare, M. A., Leonard, A. S., Hell, J. W., & Weinberg, R. J. (2000). SAP97 concentrates at the postsynaptic density in cerebral cortex. *European Journal of Neuroscience*, *12*(10), 3605–3614.

Varoqueaux, F., Aramuni, G., Rawson, R. L., Mohrmann, R., Missler, M., Gottmann, K., Zhang, W., Südhof, T. C., & Brose, N. (2006). Neuroligins Determine Synapse Maturation and Function. *Neuron*, *51*(6), 741–754.

Varoqueaux, F., Jamain, S., & Brose, N. (2004). Neuroligin 2 is exclusively localized to inhibitory synapses. *European Journal of Cell Biology*, *83*(9), 449–456.

Verhage, M., Maia, A. S., Plomp, J. J., Brussaard, A. B., Heeroma, J. H., Vermeer, H., Toonen, R. F., Hammer, R. E., et al. (2000). Synaptic assembly of the brain in the absence of neurotransmitter secretion. *Science*, *287*(5454), 864–869.

Victório, S. C., Cartarozzi, L. P., Hell, R. C., & Oliveira, A. L. (2012). Decreased MHC I expression in IFN-γ mutant mice alters synaptic elimination in the spinal cord after peripheral injury. *Journal of Neuroinflammation, 9*(88), 1–14.

Vikman, K., Robertson, B., Grant, G., & Liljeborg, A. (1998). Interferon-γ receptors are expressed at synapses in the rat superficial dorsal horn and lateral spinal nucleus. *Journal of Neurocytology, 27*, 749–760.

Vivier, E., & Malissen, B. (2005). Innate and adaptive immunity: specificities and signaling hierarchies revisited. *Nature Immunology*, *6*(1), 17–21.

**- W -**

Waites, C. L., Craig, A. M., & Garner, C. C. (2005). Mechanisms of vertebrate synaptogenesis. *Annual Review of Neuroscience*, *28*, 251–274.

Wang, V. Y., & Zoghbi, H. Y. (2001). Genetic regulation of cerebellar development. *Nature Reviews Neuroscience*, *2*(7), 484–491.

Washbourne, P., Bennett, J. E., & McAllister, A. K. (2002). Rapid recruitment of NMDA receptor transport packets to nascent synapses. *Nature Neuroscience*, 5(8),751-759.

Washbourne, P., Liu, X., Jones, E G., & McAllister, A K. (2004). Cycling of NMDA Receptors during Trafficking in Neurons before Synapse Formation. *Journal of Neuroscience*, *24*(38), 8253–8264.

Wassef, M., Chedotal, A., Cholley, B., Thomasset, M., Heizmann, C. W., & Sotelo, C. (1992). Development of the olivo-cerebellar projection in the rat: I. Transient biochemical compartmentation of the inferior olive. *Journal of Comparative Neurology*, *323*(4), 519–536.

Wassef, M., Zanetta, J. P., Brehier, A., & Sotelo, C. (1985). Transient biochemical compartmentalization of Purkinje cells during early cerebellar development. *Developmental Biology*, *111*(1), 129–137.

Watanabe, M., & Kano, M. (2011). Climbing fiber synapse elimination in cerebellar Purkinje cells. *European Journal of Neuroscience*, *34*(10), 1697–1710.

Watson, A. P., Evans, R. L., & Egland, K. A. (2013). Multiple Functions of Sushi Domain Containing 2 (SUSD2) in Breast Tumorigenesis. *Molecular Cancer Research*, *11*(1), 74–85.

Wei, P., Pattarini, R., Rong, Y., Guo, H., Bansal, P. K., Kusnoor, S. V., Deutch, A. Y., Parris, J., & Morgan, J. I. (2012). The Cbln family of proteins interact with multiple signaling pathways. *Journal of Neurochemistry*, *121*(5), 717–729.

Wei, P., Rong, Y., Li, L., Bao, D., & Morgan, J. I. (2009). Characterization of trans-neuronal trafficking of Cbln1. *Molecular and Cellular Neuroscience*, *41*(2), 258–273.

Wei, P., Smeyne, R. J., Bao, D., Parris, J., & Morgan, J. I. (2007). Mapping of Cbln1-like immunoreactivity in adult and developing mouse brain and its localization to the endolysosomal compartment of neurons. *European Journal of Neuroscience*, *26*(10), 2962–2978.

Weisheit, G., Gliem, M., Endl, E., Pfeffer, P. L., Busslinger, M., & Schilling, K. (2006). Postnatal development of the murine cerebellar cortex: formation and early dispersal of basket, stellate and Golgi neurons. *European Journal of Neuroscience*, *24*(2), 466–478.

Welsh, J. P. (1998). Systemic harmaline blocks associative and motor learning by the actions of the inferior olive. *The European Journal of Neuroscience*, *10*(11), 3307–3320.

Whitehead, A. S., Zahedi, K., Rits, M., Mortensen, R. F., & Lelias, J. M. (1990). Mouse C-reactive protein. Generation of cDNA clones, structural analysis, and induction of mRNA during inflammation. *The Biochemical Journal, 266*, 283-290.

Wilson, C. J., Groves, P. M., Kitai, S. T., & Linder, J. C. (1983). Three-dimensional structure of dendritic spines in the rat neostriatum. *The Journal of Neuroscience*, *3*(2), 383–388.

Wong, G. H., Bartlett, P. F., Clark-Lewis, I., Battye, F., & Schrader, J. W. (1984). Inducible expression of H-2 and Ia antigens on brain cells. *Nature*, *310*(5979), 688–691.

Wyszynski, M., Kim, E., Dunah, A. W., Passafaro, M., Valtschanoff, J. G., Serra-Pages, C., Streuli, M., Weinberg, R. J., & Sheng, M. (2002). Interaction between GRIP and liprin-α/SYD2 is required for AMPA receptor targeting. *Neuron*, *34*(1), 39–52.

Wyszynski, M., Valtschanoff, J. G., Naisbitt, S., Dunah, A. W., Kim, E., Standaert, D. G., Weinberg, R., & Sheng, M. (1999). Association of AMPA receptors with a subset of glutamate receptor-interacting protein in vivo. *The Journal of Neuroscience*, *19*(15),

6528–6537.

**- X -**

Xu, D., Hopf, C., Reddy, R., Cho, R. W., Guo, L., Lanahan, A., Petralia, R. S., Wenthold, R. J., et al. (2003). Narp and NP1 form heterocomplexes that function in developmental and activity-dependent synaptic plasticity. *Neuron*, *39*(3), 513–528.

Xu-Friedman, M. A., Harris, K. M., & Regehr, W. G. (2001). Three-dimensional comparison of ultrastructural characteristics at depressing and facilitating synapses onto cerebellar Purkinje cells. *Journal of Neuroscience*, *21*(17), 6666–6672.

**- Y -**

Yamagata, M., & Sanes, J. R. (2008). Dscam and Sidekick proteins direct lamina-specific synaptic connections in vertebrate retina. *Nature*, *451*(7177), 465–469.

Yamagata, M., Weiner, J. A., & Sanes, J. R. (2002). Sidekicks: Synaptic adhesion molecules that promote lamina-specific connectivity in the retina. *Cell*, *110*(5), 649–660.

Yamauchi, T., Kamon, J., Waki, H., Terauchi, Y., Kubota, N., Hara, K., Mori, Y., Ide, T., et al. (2001). The fat-derived hormone adiponectin reverses insulin resistance associated with both lipoatrophy and obesity. *Nature Medicine*, *7*(8), 941–946.

Yan, X. X., & Ribak, C. E. (1998). Developmental expression of γ-aminobutyric acid transporters (GAT-1 and GAT-3) in the rat cerebellum: evidence for a transient presence of GAT-1 in Purkinje cells. *Developmental Brain Research*, *111*(2), 253–269.

Yu, Z.-L., Jiang, J.-M., Wu, D.-H., Xie, H.-J., Jiang, J.-J., Zhou, L., Peng, L., & Bao, G.-S. (2006). Febrile seizures are associated with mutation of seizure-related (SEZ) 6, a brain-specific gene. *Journal of Neuroscience Research*, *85*(1), 166–172.

Yuste, R., & Bonhoeffer, T. (2004). Genesis of dendritic spines: insights from ultrastructural and imaging studies. *Nature Reviews Neuroscience*, *5*(1), 24–34.

Yuzaki, M. (2003). The δ2 glutamate receptor: 10 years later. *Neuroscience Research*, *46*(1), 11–22.

Yuzaki, M. (2008). Cbln and C1q family proteins – New transneuronal cytokines. *Cellular and Molecular Life Sciences*, *65*(11), 1698–1705.

**- Z -**

Zhai, R. G., Vardinon-Friedman, H., Cases-Langhoff, C., Becker, B., Gundelfinger, E. D., Ziv, N. E., & Garner, C. C. (2001). Assembling the presynaptic active zone: A characterization of an active zone precursor vesicle. *Neuron*, *29*(1), 131–143.

Zhang, L., & Goldman, J. E. (1996). Generation of cerebellar interneurons from dividing progenitors in white matter. *Neuron*, *16*(1), 47–54.

Zhang, W. D., & Benson, D. L. (2001). Stages of synapse development defined by dependence on F-actin. *The Journal of Neuroscience*, *21*(14), 5169–5181.

Zhang, W., & Benson, D. L. (2002). Developmentally regulated changes in cellular compartmentation and synaptic distribution of actin in hippocampal neurons. *Journal*

*of Neuroscience Research*, *69*(4), 427–436.
Zhao, H. M., Wenthold, R. J., & Petralia, R. S. (1998). Glutamate receptor targeting to synaptic populations on Purkinje cells is developmentally regulated. *The Journal of Neuroscience, 18*(14), 5517–5528.
Zipfel, P. F., & Skerka, C. (2009). Complement regulators and inhibitory proteins. *Nature Reviews Immunology*, *9*(10), 729–740.
Ziv, N. E., & Smith, S. J. (1996). Evidence for a role of dendritic filopodia in synaptogenesis and spine formation. *Neuron*, *17*(1), 91–102.
Zou, Y.-R., Kottmann, A. H., Kuroda, M., Taniuchi, I., & Littman, D. R. (1998). Function of the chemokine receptor CXCR4 in haematopoiesis and in cerebellar development. *Nature, 393*, 595–599.
Zuber, B., Nikonenko, I., Klauser, P., Muller, D., & Dubochet, J. (2005). The mammalian central nervous synaptic cleft contains a high density of periodically organized complexes. *Proceedings of the National Academy of Sciences*, *102*(52), 19192–19197.